

Development and Evaluation of an Acylating Agent
Detector Using Surface Acoustic Wave Devices

by

Glen David Wollenberg

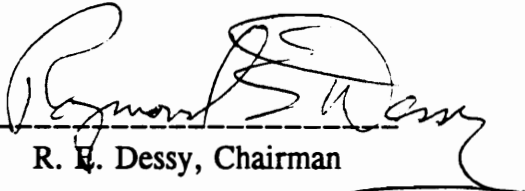
Dissertation submitted to the Faculty of the
Virginia Polytechnic Institute and State University
in partial fulfillment of the requirements for the degree of

DOCTOR OF PHILOSOPHY

in

Chemistry

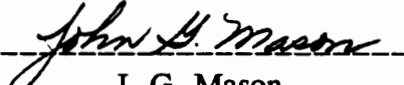
Approved:



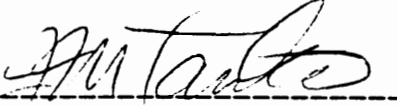
R. E. Dessy, Chairman



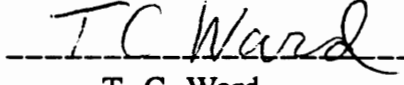
M. R. Anderson



J. G. Mason



J. M. Tanko



T. C. Ward

February, 1992

Blacksburg, Virginia

c.2

LD

5655

V856

1992

W644

C.2

**The Development and Evaluation of an Acylating Agent
Detector Using Surface Acoustic Wave Devices**

by

Glen D. Wollenberg

Committee Chairman: Raymond E. Dessy

Analytical Chemistry

(ABSTRACT)

The monitoring of harmful ambient vapors is of major concern in the industrial environment. To this end, the development of systems which detect and respond in real time to specific vapors is a highly desirable goal.

Surface Acoustic Wave (SAW) devices have been used for chemical analysis since 1978. While sensitive to mass changes occurring on their surfaces, they are not selective to the mass they will detect. Their use as chemical sensors requires the development of specificity for a vapor (or class of vapors) using selective chemical reagents suspended in film media that can have their permeability easily changed.

This dissertation presents the development of an automated dosimeter for the detection of phosgene using SAW devices. By changing the film media from a very permeable material to a film exhibiting less permeability, the analytical range of the device using the same suspended selective chemical reagent is expanded to concentrations which the very permeable film is incapable of accurately measuring.

Acknowledgements

Looking back on the road I have traveled it seems impossible to identify all of the individuals who made that journey possible. I am thankful to those who helped me along the way.

It was my pleasure to be a part of the Laboratory Automation and Instrument Design (LAID) group and be associated with past and present members of this group. This environment for professional growth and maturity was provided by Dr. Raymond Dessy and Lee Dessy. I am forever grateful for the experiences I take with me.

I would like to thank Dr. Henry Wohltjen for his expertise and support. His infectious enthusiasm, insight and willingness to discuss results and observations obtained from his own investigations were a major factor in the completion of this work. It was very reassuring to know that a vital resource was only a phone call away.

I would like to thank Fred Blair, Bob Ross and Melvin Shaver of the physics machine shop for their expertise but more importantly for their friendship. In the chemistry electronics shop, Jim Hall and Larry Jackson were always willing to help solve my problems and equipment needs. Thank you goes to Greg Lyle for his friendship and his attempts to turn me into a polymer chemist. To Al and Kelley Wagner, thank you for more than you'll ever know.

In a different vein, the retention of a portion of my sanity is due to the opportunity to play with the Virginia Lancers, the Virginia Tech Hockey club, the Roanoke Valley Adult Hockey Association and especially Jim Fisher, who can still give me fits with his backhand shot. When frustration sets in and things just will not work, I

know of very few competitive positions in which the sole reason for being is to continuously frustrate someone else. A wonderful and refreshing catharsis.

Finally, words cannot do justice to describe the love and support I have received from Kelly Sanderson Wollenberg. If it is true that we unconsciously search the earth looking for that special someone to make us whole, I need look no further because I have found myself in her.

TABLE OF CONTENTS

Abstract	ii
Acknowledgments	iii
Table of Contents	v
List of Figures	viii
List of Tables	xv
Introduction	1
Historical	4
A) Surface Acoustic Wave Detectors	4
B) Alkylating and Acylating Agent Monitoring Methods	8
Theoretical	18
A) Surface Acoustic Waves	18
1) Scaling Laws	27
B) Chemistry of Alkylating and Acylating agents and 4-(4'-nitrobenzyl)pyridine	28
C) SAW sensor design	33
1) Film permeability	34
2) Reagent reaction rate	41
a) Kinetic responses	43
b) Fixed time exposure responses	55
D) SAW Device Response	76
E) Model Experimental Response	79
1) Long term response model	79
2) Short term response model	84

Instrumental	89
A) Detector and associated apparatus.	89
B) Permeation tubes and mixing manifold	95
C) Frequency Meter	102
D) The Frequency interface board.	103
E) LSI-11	108
Experimental	110
A) Preparation	110
1) Preparation of SAW films	110
2) Preparation of materials	113
3) Preparation of Phosgene Concentrations	114
4) SAW Device Response and Acquisition Rate	114
B) Exposure	124
1) Long Term Exposure	125
a) Ethylene Oxide	125
b) Phosgene	131
1) 100% 4-(4'-nitrobenzyl)pyridine	131
2) 4-(4'-nitrobenzyl)pyridine in poly(ethylene glycol) MW 400	133
a) High Phosgene Concentrations	133
b) Low Phosgene Concentrations	148
3) 4-(4'-nitrobenzyl)pyridine in poly(ethylene glycol) MW 1500	158
4) 4-(4'-nitrobenzyl)pyridine in polystyrene MW 280,000	166

5) Background Exposures to Neat poly(ethylene glycol)	
MW 400	174
c) Thionyl Chloride	176
d) Long Term Exposure Summary	182
2) Short Term Exposure	187
a) Phosgene	188
1) Poly(ethylene glycol) Exposures	188
a) 40 KHz film load exposures	188
b) 20 KHz film load exposures	189
c) Reduced 4-(4'-nitrobenzyl)pyridine film concentration	199
d) Response to High Exposure Levels	206
e) Minimum Detectable Quantities	210
2) Flow Rate Effects on Poly(ethylene glycol) Films	217
3) Polystyrene Films	223
b) Thionyl Chloride	229
C) Infrared and Visible Results	234
Conclusions and future investigations	236
References	239
Appendix A - Forth software listings.	248
Appendix B - Reversible detector using cobalt schiff base complexes.	257

LIST OF FIGURES

Figure 1.	Potassium dichromate colorimetric reaction for ethylene oxide detection.	16
Figure 2.	Acid hydrolysis of ethylene oxide.	17
Figure 3.	Rayleigh wave crystal deformation.	19
Figure 4.	Sinusoidal wave generation by an interdigitized transducer array.	20
Figure 5.	Interdigitized array.	23
Figure 6.	Alkylation and acylation products of 4-(4'-nitrobenzyl)pyridine.	30
Figure 7.	Reaction product of phosgene and 4-(4'-nitrobenzyl)pyridine.	31
Figure 8.	Reaction product possibilities for 4-(4'-nitrobenzyl)pyridine and ethylene oxide.	32
Figure 9.	Vapor distribution for Dt product of $5 \cdot 10^{-10}$ cm ² /sec.	37
Figure 10.	Vapor distribution for Dt product of $5 \cdot 10^{-9}$ cm ² /sec.	38
Figure 11.	Kinetic response curve for $d[C]/dt = k[A][B]$.	45
Figure 12.	Normalized kinetic response curve for $d[C]/dt = k[A][B]$.	46
Figure 13.	Kinetic response curve for $d[C]/dt = k[A][B]^2$.	48
Figure 14.	Kinetic response curve for $d[C]/dt = k[A]^2[B]$.	49
Figure 15.	Kinetic response curve for $d[C]/dt = k[A]^2[B]^2$.	50
Figure 16.	Normalized kinetic response curve for $d[C]/dt = k[A][B]^2$.	52
Figure 17.	Normalized kinetic response curve for $d[C]/dt = k[A]^2[B]$.	53
Figure 18.	Normalized kinetic response curve for $d[C]/dt = k[A]^2[B]^2$.	54
Figure 19.	Fixed time exposure response curve for $d[C]/dt = k[A][B]$.	57
Figure 20.	Fixed time exposure response curve for $d[C]/dt = k[A][B]$.	58
Figure 21.	Fixed time exposure response curve for $d[C]/dt = k[A][B]^2$.	59

Figure 22.	Fixed time exposure response curve for $d[C]/dt = k[A][B]^2$.	60
Figure 23.	Fixed time exposure response curve for $d[C]/dt = k[A]^2[B]$.	61
Figure 24.	Fixed time exposure response curve for $d[C]/dt = k[A]^2[B]$.	62
Figure 25.	Fixed time exposure response curve for $d[C]/dt = k[A]^2[B]^2$.	63
Figure 26.	Fixed time exposure response curve for $d[C]/dt = k[A]^2[B]^2$.	64
Figure 27.	Normalized fixed time exposure response curve for $d[C]/dt = k[A][B]$.	67
Figure 28.	Normalized fixed time exposure response curve for $d[C]/dt = k[A][B]$.	68
Figure 29.	Normalized fixed time exposure response curve for $d[C]/dt = k[A][B]^2$.	69
Figure 30.	Normalized fixed time exposure response curve for $d[C]/dt = k[A][B]^2$.	70
Figure 31.	Normalized fixed time exposure response curve for $d[C]/dt = k[A]^2[B]$.	71
Figure 32.	Normalized fixed time exposure response curve for $d[C]/dt = k[A]^2[B]$.	72
Figure 33.	Normalized fixed time exposure response curve for $d[C]/dt = k[A]^2[B]^2$.	73
Figure 34.	Normalized fixed time exposure response curve for $d[C]/dt = k[A]^2[B]^2$.	74
Figure 35.	Permeation rate limiting curve.	80
Figure 36.	Film consumption by permeating vapor.	82
Figure 37.	Steady state film loading.	83
Figure 38.	Multiple fixed time exposures.	86

Figure 39.	Frequency and frequency change rate.	88
Figure 40.	Schematic for dual SAW device detector.	90
Figure 41.	Frequency mixer outputs.	92
Figure 42.	Dual SAW device detector cell.	93
Figure 43.	Permeation tube chamber.	97
Figure 44.	Permeation tube vapor generation manifold.	98
Figure 45.	Fluke BCD interface board.	104
Figure 46.	Frequency to parallel port interface board.	105
Figure 47.	Box schematic of instrumental configuration for data acquisition.	109
Figure 48.	Beat and individual frequencies from reversible solvation.	117
Figure 49.	Irreversible mass loading frequency shift - lower sample frequency.	118
Figure 50.	Irreversible mass loading frequency shift - higher sample frequency.	119
Figure 51.	Irreversible mass loading frequency shift - sample frequency passes through reference frequency.	120
Figure 52.	Determination of differential data.	121
Figure 53.	50.46% NBP in poly(ethylene glycol), MW 400 - 248 ppm ethylene oxide exposure.	126
Figure 54.	50.46% NBP in poly(ethylene glycol), MW 400 - 248 ppm ethylene oxide exposure.	127
Figure 55.	50.46% NBP in poly(ethylene glycol), MW 400 - 2.48 ppm phosgene exposure.	128
Figure 56.	50.46% NBP in poly(ethylene glycol), MW 400 - 2.48 ppm phosgene exposure.	129

Figure 57.	50.05% NBP in poly(ethylene glycol), MW 400 - 24.8 ppm phosgene exposure.	135
Figure 58.	50.05% NBP in poly(ethylene glycol), MW 400 - 24.8 ppm phosgene exposure - frequency change rate.	136
Figure 59.	50.05% NBP in poly(ethylene glycol), MW 400 - 12.4 ppm phosgene exposure.	137
Figure 60.	50.05% NBP in poly(ethylene glycol), MW 400 - 12.4 ppm phosgene exposure - frequency change rate.	138
Figure 61.	50.05% NBP in poly(ethylene glycol), MW 400 - 4.96 ppm phosgene exposure.	139
Figure 62.	50.05% NBP in poly(ethylene glycol), MW 400 - 4.96 ppm phosgene exposure - frequency change rate.	140
Figure 63.	25.47% NBP in poly(ethylene glycol), MW 400 - 4.96 ppm phosgene exposure.	143
Figure 64.	25.47% NBP in poly(ethylene glycol), MW 400 - 4.96 ppm phosgene exposure - frequency change rate.	144
Figure 65.	50.47% NBP in poly(ethylene glycol), MW 400 - 2.48 ppm phosgene exposure.	149
Figure 66.	50.47% NBP in poly(ethylene glycol), MW 400 - 2.48 ppm phosgene exposure - frequency change rate.	150
Figure 67.	50.47% NBP in poly(ethylene glycol), MW 400 - 2.48 ppm phosgene exposure.	151
Figure 68.	50.47% NBP in poly(ethylene glycol), MW 400 - 2.48 ppm phosgene exposure - frequency change rate.	152

Figure 69.	50.47% NBP in poly(ethylene glycol), MW 400 - 1.24 ppm phosgene exposure.	153
Figure 70.	50.47% NBP in poly(ethylene glycol), MW 400 - 1.24 ppm phosgene exposure - frequency change rate.	154
Figure 71.	50.47% NBP in poly(ethylene glycol), MW 400 - 0.496 ppm phosgene exposure.	155
Figure 72.	50.47% NBP in poly(ethylene glycol), MW 400 - 0.496 ppm phosgene exposure - frequency change rate.	156
Figure 73.	50.00% NBP in poly(ethylene glycol), MW 1500 - 24.8 ppm phosgene exposure.	159
Figure 74.	50.00% NBP in poly(ethylene glycol), MW 1500 - 24.8 ppm phosgene exposure - frequency change rate.	160
Figure 75.	50.00% NBP in poly(ethylene glycol), MW 1500 - 12.4 ppm phosgene exposure.	161
Figure 76.	50.00% NBP in poly(ethylene glycol), MW 1500 - 12.4 ppm phosgene exposure - frequency change rate.	162
Figure 77.	50.00% NBP in poly(ethylene glycol), MW 1500 - 4.96 ppm phosgene exposure.	163
Figure 78.	50.00% NBP in poly(ethylene glycol), MW 1500 - 4.96 ppm phosgene exposure - frequency change rate.	164
Figure 79.	49.90% NBP in polystyrene, MW 280,000 - 24.8 ppm phosgene exposure.	169
Figure 80.	49.90% NBP in polystyrene, MW 280,000 - 24.8 ppm phosgene exposure - frequency change rate.	170

Figure 81.	49.90% NBP in polystyrene, MW 280,000 - 12.4 ppm phosgene exposure.	171
Figure 82.	49.90% NBP in polystyrene, MW 280,000 - 12.4 ppm phosgene exposure - frequency change rate.	172
Figure 83.	50.47% NBP in poly(ethylene glycol), MW 400 - 5.25 ppm thionyl chloride exposure.	177
Figure 84.	50.47% NBP in poly(ethylene glycol), MW 400 - 5.25 ppm thionyl chloride exposure - frequency change rate.	178
Figure 85.	50.47% NBP in poly(ethylene glycol), MW 400 - 5.25 ppm thionyl chloride exposure continued.	179
Figure 86.	50.47% NBP in poly(ethylene glycol), MW 400 - 5.25 ppm thionyl chloride exposure continued - frequency change rate.	180
Figure 87.	Calibration curve for phosgene exposure of 50.46% 4-(4'-nitrobenzyl)pyridine in poly(ethylene glycol), MW 400 - 40 KHz film loads.	191
Figure 88.	Calibration curve for phosgene exposure of 50.46% 4-(4'-nitrobenzyl)pyridine in poly(ethylene glycol), MW 400 - 20 KHz film loads.	193
Figure 89.	Calibration curves for phosgene exposure of 50.46% 4-(4'-nitrobenzyl)pyridine in poly(ethylene glycol), MW 400 - 20 KHz and 40 KHz film loads.	194
Figure 90.	Calibration curve for phosgene exposure of 26.14% 4-(4'-nitrobenzyl)pyridine in poly(ethylene glycol), MW 400 - 40 KHz film loads.	201
Figure 91.	Calibration curves for phosgene exposure.	203

Figure 92.	Normalized calibration curves for phosgene exposure.	204
Figure 93.	Exposure to high phosgene concentrations of 50.46% 4-(4'-nitrobenzyl)pyridine in poly(ethylene glycol) MW 400 - 40 KHz film loads.	208
Figure 94.	Exposure to high phosgene concentrations of 26.14% 4-(4'-nitrobenzyl)pyridine in poly(ethylene glycol) MW 400 - 40 KHz film loads.	209
Figure 95.	Short term baseline and long term frequency drift noise components.	211
Figure 96.	Calibration curves for phosgene exposure - flow rate effects.	219
Figure 97.	Calibration curve for phosgene exposure of 50.22% 4-(4'-nitrobenzyl)pyridine in polystyrene, MW 280,000 - 40 KHz film loads.	225
Figure 98.	Normalized calibration curves for 4-(4'-nitrobenzyl)pyridine in poly(ethylene glycol), MW 400.	226
Figure 99.	Normalized calibration curve for 4-(4'-nitrobenzyl)pyridine in polystyrene, MW 280,000.	227
Figure 101.	Calibration curve for thionyl chloride exposure of 50.46% 4-(4'-nitrobenzyl)pyridine in poly(ethylene glycol), MW 400 - 40 KHz film loads.	232
Figure 102.	Normalized calibration curve for thionyl chloride exposure of 4-(4'-nitrobenzyl)pyridine in poly(ethylene glycol), MW 400.	233
Figure 103.	Copolymer of p-chloromethylstyrene and n-hexyl methacrylate incorporating oxygenated Co(salDPT).	258

LIST OF TABLES

Table 1.	Theoretical fixed time exposure responses for $d[C]/dt = k[A]^2[B]$.	65
Table 2.	Film exposure constants for 4-(4'-nitrobenzyl)pyridine in poly(ethylene glycol) MW 400 films.	141
Table 3.	Phosgene exposure to neat poly(ethylene glycol) MW 400.	175
Table 4.	50.46% NBP in poly(ethylene glycol), MW 400 - Concentration-time products and responses for phosgene exposure - 40 KHz film loadings.	190
Table 5.	50.46% NBP in poly(ethylene glycol), MW 400 - Concentration-time products and responses for phosgene exposure - 20 KHz film loadings.	192
Table 6.	Equations of the lines for 50.46% 4-(4'-nitrobenzyl)pyridine in poly(ethylene glycol), MW 400 films - 20 KHz and 40 KHz film loads.	195
Table 7.	26.14% NBP in poly(ethylene glycol), MW 400 - Concentration-time products and responses for phosgene exposure - 40 KHz film loadings.	200
Table 8.	Equations of the lines for phosgene exposure.-	202
Table 9.	Normalized equations of the lines for phosgene exposure.	205
Table 10.	Background run stability tests - long term frequency drifts.	214
Table 11.	Minimum detectable quantities.	215

Table 12.	50.46% NBP in poly(ethylene glycol), MW 400 - Concentration-time products and responses for phosgene exposure - flow rate effects.	218
Table 13.	Equations of the lines - flow rate effects.	220
Table 14.	Concentration-time products and responses for phosgene exposure of 50.22% 4-(4'-nitrobenzyl)pyridine in polystyrene, MW 280,000 - 40 KHz film loads.	224
Table 15.	Concentration-time products and responses for thionyl chloride exposure of 50.46% 4-(4'-nitrobenzyl)pyridine in poly(ethylene glycol), MW 400 - 40 KHz film loads.	231

INTRODUCTION

The development of chemical sensors continues to be a challenging and expanding area in the field of analytical chemistry. While new sensors are being developed, work continues on the utilization of sensors previously developed. Chemfets, fiber optic transducers, ISFETS, and tin oxide semiconductors continue to be investigated for use today. Two areas of continuing research are associated with developed sensors.

The first area is to improve the sensor itself. This may involve the miniaturizations of the device, improvements in sensitivity and ruggedness, elimination of hysteresis effects, and improvement in response times. The goal of this research is to explore the operating principles for the devices or improve the devices themselves.

The second area is to apply these devices to a particular chemical environment. This research area is concerned with the fact that many of the sensors which have been developed or are being developed are usually incapable of distinguishing between different chemical species. While the transducer will produce a signal that is related to a change in its environment, the signal produced may not represent a change due to a specific agent. The sensors are not selective. Although it is true that a separation method could be employed in front of the sensor, this type of sensor configuration becomes just another chromatographic detector. Though inherently this may be a useful avenue of pursuit, the reality is that detectors already developed for the separation methods will usually be more reliable, sensitive, and possess larger dynamic ranges. Since the separation has already been performed on the analyte, the goal for these detectors is to be universal, since the burden of distinguishing different chemical species has been removed.

The research efforts in this dissertation are to develop chemical systems that impart selectivity to one class of the new microelectronic chemical sensors.

Two approaches to the problem of selectivity have been investigated for use with surface acoustic wave (SAW) devices. The first is to develop a film which will display a high degree of specificity to the particular chemical species that is to be monitored. The second approach is to create an array of SAW devices each coated with a different film. Each device in the array will generate a different signal output for each vapor mixture introduced into the array cell. Each possible individual component of a mixture will first be introduced by itself into the array cell, generating a response from each SAW device. A response surface can then be described. Using this library and measuring the response of the array to a vapor mixture allows concentration and composition of the unknown to be determined statistically¹.

Each approach has its inherent advantages and disadvantages. With the array approach, the difficulty of developing a film with high specificity is eliminated but the problem of species outside the original matrix is introduced. Since the surface map is determined for a particular group of vapors, any vapor which is not in the experimental set will introduce responses that will be attributed to components in the set. Since the objective of the array is to produce a response for a series of vapors with the least number of devices possible, this presents a serious concern for sensor application development. An immediate remedy is to either generate a new map for each application that has introduced a new environmental factor or to ensure by other means that the environment to be monitored contains only vapors which are a subset of the vapors used to create the original response surface map. In response to this problem, rank annihilation methods are being investigated for use in performing quantitative analysis in the presence of interferences not accounted for in the original model².

On the other hand, the development of a film which shows high specificity minimizes the problem posed by new vapor species being introduced into the matrix. However the researcher is challenged with the problem of developing such a film. The ideal film would exhibit a fast response to only one chemical species or class of species in the range that the application requires, a not so trivial problem. Many films that have been developed have attempted to incorporate these ideals and are successful to one degree or another. Most applications that have been developed measure the particular species at a part per million or lower level. This is due to the fact that most species which are investigated are either regulated by a governmental agency or are a hazard that needs to be measured at a low level. It is not sacrosanct that all sensor work be concerned with low level monitoring. The measurement of oxygen concentrations could be performed at ppm (glove box monitoring), low percent (air mixture preparations) or high percent (pure oxygen cylinder filling stations) concentrations depending upon the particular requirements of the environment.

To the investigator interested in chemical sensor development and applications, the essence of the matter is what are the needs and in what direction should efforts be invested. If the problem is approached from an array perspective, efforts will be invested on generation of the statistical analyses necessary to determine the concentration and composition of a vapor matrix. If the problem is approached from a specific film perspective, efforts will be invested in the development of these films and their associated chemistry.

With this analysis of the overall problem the reader of this dissertation may pursue the development of a highly selective film for the monitoring of the alkylating agents phosgene, thionyl chloride and ethylene oxide.

HISTORICAL

A) Surface Acoustic Wave Detectors

The development of acoustic detectors as chemical sensors was first investigated by King in 1964³ using a bulk acoustic wave detector. Many uses of bulk acoustic wave detectors have been described^{4,5}. The Sauerbrey fundamental frequency response equation for a quartz bulk acoustic wave device is:

$$\Delta f = -2.3 * 10^6 f_0^2 \Delta M/A \quad (1)$$

where Δf is the frequency shift in Megahertz associated with a given mass change, f_0 is the fundamental operating frequency of the device in Megahertz, ΔM is the change in mass on the surface of the crystal in grams, and A is the surface area of the device in square centimeters³.

The development of the surface acoustic wave detector was made possible by the development of the interdigitized transducer array (IDT) by White and Voltmer in 1965⁶. This allowed for a very convenient way to generate surface waves in piezoelectric solids. This breakthrough led to a considerable amount of investigation in the application of surface acoustic wave devices for radio frequency signal processing. The small size, high performance and simplicity of SAW filters, delay lines and convolvers found many applications including electronic countermeasure systems for aerospace use.

However one problem did exist with these devices. The acoustic wave was constrained to the surface of the crystal and the devices displayed a high sensitivity to their surroundings, requiring developers of these devices to encapsulate them under vacuum or inert atmospheres⁷ to prevent drifting of the devices due to ambient effects.

As it turned out, this deleterious effect of ambient surroundings upon the stability of SAW devices proved to be a boon to chemists and engineers who would pursue their use in chemical and physical sensor development. It became truly a case of one man's noise becoming another man's signal.

In 1979, the first reported use of SAW devices as chemical sensors appeared⁸. The use of a SAW device as a chemical sensor relies on the sensitivity of the surface wave to changes occurring in the thin surface film. With the advent of the SAW chemical vapor sensor, many investigators explored the further development of SAW devices using either quartz or lithium niobate as the substrate material. SAW devices have been used for the detection of hydrogen⁹, nitric oxides¹⁰, water¹¹ and ammonia¹². These detectors showed high sensitivity to the gases that were being measured using mass changes occurring upon the surface of the SAW device and the selectivity of a surface film to specifically adsorb or absorb the vapors being monitored.

Most of the work done with SAW devices as chemical sensors has been in the area of developing selective films for particular applications. Since the acoustic wave is confined to the surface of the substrate and interacts with the film deposited upon the device, any changes in the film such as density, viscosity, modulus¹³ or film conductivity¹⁴ will affect the velocity and amplitude of the surface wave travelling across the device. Therefore the sensitivity and selectivity of the SAW sensor is a function of the physicochemical properties of the film itself.

The use of SAW devices as chemical sensors can be segregated into two major response categories, electric potential wave interactions (dielectric constant, conductivity) and mechanical wave interactions (mass, density and modulus).

Electrical potential wave interactions occur because the propagation of the surface acoustic wave results in the physical displacement of the piezoelectric crystal

lattice, creating an electric potential wave that interacts with the dielectric and conductivity properties of the surface film. The presence of a conductive film will cause a fractional change in the wave velocity as well as a reduction in its amplitude. If the conductivity of the film is sensitive to the presence of certain vapors, then a chemical sensor can be developed based on these velocity changes. An example of such a system has been described by Ricco and co-workers for the determination of NO_2 ¹⁴. Using lead phthalocyanine on a lithium niobate SAW delay line oscillator, the authors were able to demonstrate that the change in velocity, and therefore the change in the oscillation frequency, was due to the chemically induced conductivity changes in the lead phthalocyanine film in the presence of NO_2 at the ppm level.

The limitation of using this method for chemical sensor development is that the sheet conductivity of the film must be in the range of the surface conductivity of the device for interaction to take place. This condition severely limits the applicability of this technique.

Mechanical wave interactions represent the method most utilized in the development of SAW based chemical sensors due to the fact that mass loading and density changes in films are not as constrained as those based on electrical effects. Vapor sensors that have been developed in this category use either metallic films (to detect H_2 or NH_3)^{15,16}, ceramic films (for H_2S)¹⁷ or organic films which greatly increases the number of possible films available.

In the case of organic films, selectivity is a key concern. The choices that have been made previously were to attempt to develop a selective, reversible film for one species or to use a SAW device array to determine the concentrations of the intended species. This is no longer the only approach to the problem.

An irreversible dosimeter based on the gas phase Diels-Alder reaction of cyclopentadiene with poly(ethylene maleate) was developed by Wohltjen and Snow¹⁸. This proved to be highly selective. One limitation might be its irreversibility, but, depending upon the application and expected analytical lifetime, this may not be a limitation at all. Recently Zellers has introduced a semiselective polymeric film supporting a platinum organometallic complex which will undergo a substitution reaction to dosimetrically detect styrene and vinyl acetate¹⁹. The advantage of this system is that after the film is exposed to styrene or vinyl acetate, the original complex can be regenerated.

The use of SAW devices as liquid phase sensors has been reported. The development of an immunoassay detector based on an antibody/antigen binding reaction on the surface of a SAW device is an example²⁰. The use of SAW devices as liquid phase detector systems is a highly controversial subject due to the problems associated with the propagation of leaky Rayleigh waves in a dense fluid media²¹. The argument proposed is that if a liquid media capable of propagating a compressional wave and having a lower acoustic velocity is placed in contact with the surface of a SAW device, the acoustic energy of the device will be coupled out of the crystal and into the surrounding media. The experiments conducted shows that for a device similar to the one used in the development of the immunoassay detector, wave modes other than Rayleigh waves were responsible for the acoustic motion between the interdigitized transducer arrays. Devices utilizing plate mode or Lamb waves however offer the possibility of developing liquid phase sensors^{22,23}.

B) Alkylating and Acylating Agent Monitoring Methods

The development of phosgene monitoring and detection methods have been of keen interest since the introduction of this highly poisonous gas as a chemical weapon in World War I. While one of the most sensitive methods for the detection of phosgene involves the use of an electron capture detector/gas chromatographic system, the development of a real time portable personal monitoring device for low level detection of phosgene has remained an elusive goal.

In 1945, Brown, Wilzbach and Ballweber suggested the use of papers impregnated with a mixture of 4-(4'-nitrobenzyl)pyridine, N-benzylaniline and sodium carbonate for detecting phosgene, the intensity of the color being determined by optical transmittance²⁴. Liddell, sensitive to the disadvantages of the standard method of phosgene detection at that time, incorporated a mixture of p-dimethylaminobenzaldehyde, N-ethyl-N-2-hydroxyethyl-aniline and diethyl phthalate into a filter paper that would detect a level of 5 ppm in air by means of a chemical coupling reaction producing a change of color from white to blue. This method was found to be insensitive to "any reasonable concentration of mineral-acid vapor". This is in contrast to the method in use at the time which consisted of a chemical reaction mixture of diphenylamine and p-dimethylaminobenzaldehyde which produced a color change from white to yellow and was also sensitive to acid vapors²⁵.

Witten and Prostack in 1957 investigated the use of 4-(4'-nitrobenzyl)pyridine in a colorimetric crayon detector for the analysis of low concentrations of cyanogen chloride, cyanogen bromide, hydrogen cyanide, phosgene, lewisite, and ethyl dichloroarsine. Using the concept of a concentration-time value, defined as the exposure in time of a concentration of vapor generating a response in the crayon, an atmospheric level of 7.5 ppb of phosgene at 90 degrees Fahrenheit turned a crayon red

in one minute (7.5 ppb-min) of exposure. The use of the ppb-minute term is appropriate since the intensity of the color is dependent upon both the concentration and length of exposure of the device to phosgene. The crayon contained 2% NPB, 5% N-phenylbenzylamine, 5% sodium carbonate and 88% blanc fixé as the support medium²⁶.

Dixon and Hands, utilizing the work of Liddell, Witten and Prostack, developed a field method for the detection of phosgene utilizing a filter paper impregnated with a mixture of 4-(4'-nitrobenzyl)pyridine and N-benzylalanine. The paper was allowed to dry after impregnation and exposure to phosgene generated a red stain. This stain could then be compared to a calibrated set of paper exposures or glass color standards to determine the concentration of the unknown vapor. This method was found to be sensitive to a phosgene level of 0.25 ppm and showed no sensitivity to hydrogen chloride up to a concentration of 500 ppm²⁷.

Linch examined colorimetric detectors utilizing liquid reagents, impregnated paper or granular solids in order to improve the detection procedure for the analysis of phosgene in air. Physical methods of analysis (Ultraviolet, Infrared) proved to suffer from either a lack of sensitivity or selectivity. Hydrolysis, argentometric and iodometric procedures for the detection of phosgene also suffered from a lack of selectivity. The findings presented showed that for continuous automatic monitoring of airborne phosgene, colorimetric detectors in a liquid reagent system proved to be the most reliable. 4,4'-bis(diethylamino)benzophenone dissolved in o-dichlorobenzene proved to be the best liquid reagent system for phosgene detection in concentrations as low as 0.1 ppm. Paper supported dry reagents were noted as being capable of a high degree of selectivity, specificity and reliability but were not applicable to continuous monitoring instrumentation. Of the chemical systems evaluated,

4-(4'-nitrobenzyl)pyridine gave the best results. Gas titration (the volume of air required to produce a perceptible color change related to the phosgene concentration) delivered greater sensitivity and precision than visual color standard stain matching and was recommended as an alternative procedure for field analysis²⁸.

Noweir and Pfitzer, utilizing a gas bubbling system similar to the one employed by Linch, demonstrated that a reagent solution composed of 0.25 gram 4-(4'-nitrobenzyl)pyridine and 0.5 gram N-benzylaniline dissolved in 100 ml of diethylphthalate could spectrophotometrically determine concentrations under 0.1 ppm of phosgene in air²⁹.

Tuggle and associates conducted field evaluations of selected monitoring methods for phosgene in air. The methods investigated were manual and automated colorimetry using the reagent scheme employed by Nowier and Pfitzer, gas chromatography using an electron capture detector, infrared spectroscopy, and a paper tape monitor. Using phosgene permeation tubes to generate the vapor concentrations, lower detection limits for the various techniques ranged from 0.05 ppm for the manual colorimetric method to 0.0001 ppm for the gas chromatographic system. Portability and required operator expertise and attention were also evaluated, with the chromatographic system requiring the most skill and attention. It was noted that the manual colorimetric method employing 4-(4'-nitrobenzyl)pyridine, due to its time proven validity, was recommended as a reliable backup or confirmatory procedure for other instrumental methods of phosgene analysis. The main drawback to its use is the lack of real time capability, being only useful for time weighted average and short time exposures³⁰.

A passive dosimeter for immediate assessment of phosgene vapors was developed by Matherne, Lubs and Kerfoot. A paper tape that was impregnated with

4-(4'-nitrobenzyl)pyridine was attached to a badge worn by personnel. The upper and lower exposure limits of the device were 100 and 2 ppm-minutes respectively. While the authors concede that their device does not approach the current OSHA permissible exposure concentration of 0.1 ppm, their aim was to provide a personal, simple device to inform the user when a serious exposure level arose. With the cited lethal exposure dose for man being 400 to 500 ppm-minutes, their device is intended to prevent critical exposures from occurring³¹.

The detection of phosgene is not confined to air monitoring. An invention describing the use of 4-(4'-nitrobenzyl)pyridine to monitor the phosgene concentration in the preparation of polycarbonate resins in organic solutions was reported by Dick, Ham and Gross. Using dihydric phenols and phosgene, the phosgene concentration was monitored since the use of too small or too large an amount of phosgene has disastrous effects upon the color and properties of the generated polycarbonate resin³².

A coated bulk wave piezoelectric detector was described by Suleiman and Guilbault. The coating, methyltrioctylphosphonium dimethylphosphate, was applied to the device using a syringe. The range for detection of the system was 0 to 140 ug/l. It was noted that the system was sensitive to hydrogen chloride, hydrogen sulfide and ammonia. A prefiltering column composed of phosphorus pentoxide was used to remove these interferences before they reached the device³³.

The use of 4-(4'-nitrobenzyl)pyridine is not limited to the detection of phosgene and cyanide related compounds. 4-(4'-nitrobenzyl)pyridine has been used for the detection of a wide variety of alkylating agents in both vapor and solution states. Friedman and Boger in 1961 demonstrated the ability of 4-(4'-nitrobenzyl)pyridine to be used as the active ingredient in the detection of nitrogen mustards in aqueous media³⁴. In 1963, Sawicki developed a spectrophotometric method using

4-(4'-nitrobenzyl)pyridine for the determination of over 90 alkylating agents. The method employed involved the addition of the alkylating agent to a solution containing 4-(4'-nitrobenzyl)pyridine and cyclohexylamine for the development of the color that was monitored by a spectrometer. The resulting solution was heated for 3 to 15 minutes to develop the color and then immediately measured. Microgram quantities of alkylating agents could be detected by this method. Agree and Meeker examined the use of 4-(4'-nitrobenzyl)pyridine in solution for the quantitative determination of acid chlorides at room temperature. For the 34 compounds investigated, a 10 minute standing time between introduction of the chemical agent into the 4-(4'-nitrobenzyl)pyridine solution and the subsequent absorbance measurements was sufficient for completion of the reaction and stabilization of the chromophore for most agents. Heating and longer reactions times were necessary for a few compounds. The pseudo first order rate constant for phosgene was measured as $1.5 * 10^{-1} \text{ l.mole.}^{-1}\text{sec}^{-1}$. by monitoring the increasing absorbance in the solution as a function of time³⁵.

One use of 4-(4'-nitrobenzyl)pyridine that has been investigated greatly is in the monitoring of vaporous ethylene oxide. This alkylating agent is used extensively as a sterilizing gas because of its ability to alkylate the amine nitrogen of bacterial DNA, thereby destroying the spores without affecting the material being sterilized. The major concerns from a material point of view are twofold: has the material been exposed for a sufficient length of time for destruction of the spores to have taken place and has the material been aerated for a sufficient time to remove any residual ethylene oxide solubilized in the material. While the ethylene oxide has no effect on materials which are normally sterilized, the effects of ethylene oxide exposure to human beings is a

major problem. The recommended exposure limit for ethylene oxide is 1 part per million TLV³⁶.

Brewer and Arnsberger examined the use of 4-(4'-nitrobenzyl)pyridine as an agent for determining the completeness of a sterilization cycle as compared to biological spore strips. Paper strips impregnated with 4-(4'-nitrobenzyl)pyridine and sodium carbonate placed into objects to be sterilized will produce a blue color when ethylene oxide has permeated the object material. The advantages of the system is that an immediate evaluation of the completeness of sterilization can be ascertained by the chromophoric development on the paper rather than by evaluation of the residual spore count on a biological spore strip³⁷.

Cheng devised a method for determining residual ethylene oxide in sterilized materials. A sealed package contains ampules which themselves contain substituted pyridines (one being 4-(4'-nitrobenzyl)pyridine). After sterilization and aeration, one of the ampules is fractured and a color development indicates the presence of ethylene oxide. Aeration of the material continues until the fracture of an ampule does not generate a color³⁸.

Whitbourne and Eastman developed a device that would both monitor the extent of sterilization and aeration. They employed 4-(4'-nitrobenzyl)pyridine and low molecular weight poly(ethylene glycol) (molecular weights of 200 and 400) on an impregnated paper strip. This was inserted into a gas permeable envelope and long exposures to ethylene oxide resulted in a bluish hue. When the envelope was allowed to aerate, the color of the strip would fade to a gray-green. Poly(ethylene glycol)s were chosen because they are good solvents for 4-(4'-nitrobenzyl)pyridine and produced good color changes. Polyethylene glycol, molecular weight 1500, has been used as the support medium in an attempt to monitor the sterilization and aeration cycle for

polyvinyl chloride materials which have a high solubility for ethylene oxide. The differences in permeation of the gas through the support medium effectively change the range of analysis of the sensor³⁹.

Other dosimeters for monitoring the extent of ethylene oxide sterilization have been developed. The main differences are in the support matrix that is used^{40,41}. Manning utilized a layered approach to monitoring ethylene oxide exposure by "sandwiching" the dosimetric film containing 4-(4'-nitrobenzyl)pyridine between two transport limiting layers (such as polyesters or polyolefins) or an impermeable layer and a permeable layer (aluminum and polyolefin). Ensuring that the dosimetric layer is composed of a material having a higher diffusion constant than the laminating layers, the laminating layers will effectively control the response and color development of the dosimetric film.

Passive dosimeters for monitoring part per million levels of ethylene oxide have been developed. Gonzalez and Sefton used a solution of 0.108 M potassium dichromate in 0.650 M sulfuric acid immobilized onto a 1 millimeter wide silica gel coated plastic strip. Exposure to ethylene oxide generated a green stain whose length was proportional to the concentration of, and exposure duration to, ethylene oxide⁴² (Figure 1).

Another ppm level ethylene oxide passive dosimeter relies on the use of sulfuric acid solutions absorbed onto support media, such as silica gel, to hydrolyze ethylene oxide into ethylene glycol (Figure 2). Ethylene glycol is then oxidized to formaldehyde by sodium periodate which can be treated with chromotropic acid (4,5-Dihydroxy-2,7-naphthalenedisulfonic acid), phenylhydrazine, or Schiff's reagent to generate a chromophore for colorimetric detection⁴³. The development of the Dupont Pro-Tek monitoring badge for ethylene oxide utilizes this same analytical scenario. Using a detector badge designed for formaldehyde, a chamber containing 2.4 milliliters

of 0.05 N sulfuric acid is exposed to ethylene oxide. After exposure, 1 milliliter samples of the sulfuric acid solution are removed and developed using sodium paraperiodate, 3-methyl-2-benzothiazolinone hydrazone hydrochloride and ferric chloride solutions. The chromophore developed is measured spectroscopically at 632 nanometers⁴⁴.

The inherent disadvantages of these methods are that they are labor intensive and do not permit the immediate detection of and response to ethylene oxide because the exposed dosimeter must be developed. They cannot be called true "real-time" monitors for ethylene oxide vapor.

Based on the wide use of 4-(4'-nitrobenzyl)pyridine in solution and in solid phase for monitoring vaporous alkylating agents at low levels, the application of this material with a surface acoustic wave detector system offered interesting possibilities.

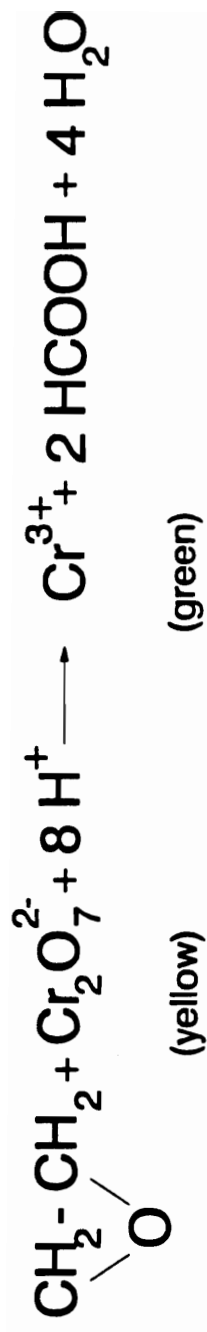


Figure 1. Potassium dichromate colorimetric reaction for ethylene oxide detection.

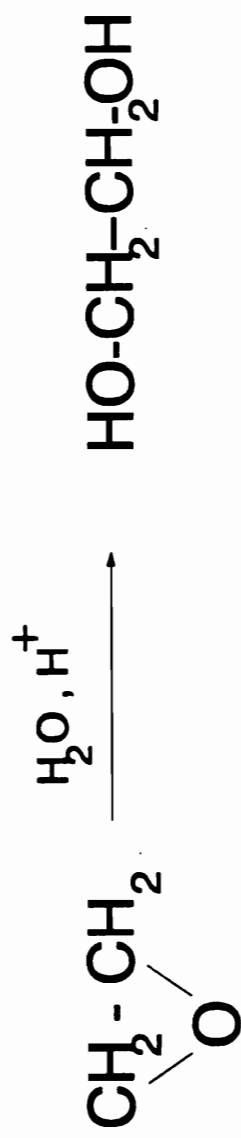


Figure 2. Acid hydrolysis of ethylene oxide.

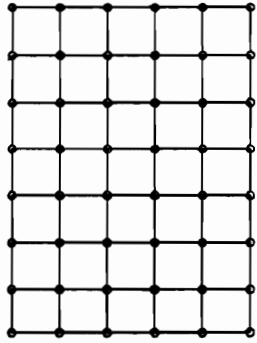
THEORETICAL

A) Surface Acoustic Waves

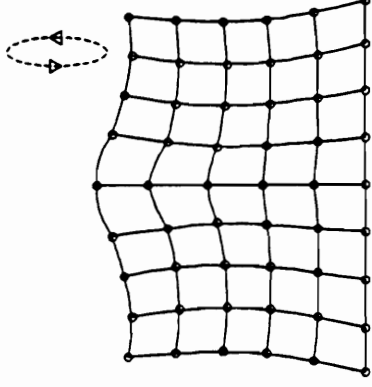
The basic physics of waves which occur on the surfaces of solids was first described by Lord Rayleigh in 1885⁴⁵. He first described the mathematical basis for a surface wave travelling on the earth's crust. While the analysis of Rayleigh waves was of importance to seismologists, it was not until the development of the interdigital transducer by White and Voltmer in 1965⁴⁶ that a convenient generation of surface waves in piezoelectric solids was achieved.

The propagation of a Rayleigh wave across a solid surface is in the form of a retrograde ellipse normal to the surface of propagation whose amplitude decays with depth into the crystal until there is no wave propagation in the bulk crystal (Figure 3). This amplitude attenuation occurs within a few wavelengths of the surface. The wavefront motion is due to the fact that a Rayleigh wave consists of two waves of equal phase velocity, a longitudinal compressional wave and a shear wave whose displacement is normal to the surface. The generation of this wave requires the presence of an interdigital transducer on the surface of the crystal.

The interdigital transducer array on the surface of the crystal is composed of metal electrodes in the form of overlapping fingers. Alternating fingers are connected to two different bus bars. When a time varying RF potential is applied to the interdigitized transducer array on the surface of the piezoelectric crystal, the crystal undergoes a physical deformation. If the substrate crystal is cut along the proper crystallographic axis, a surface wave will be generated. The wave is then detected by a second interdigitized transducer array in the reverse manner (Figure 4).



Unstressed



Rayleigh Wave

Figure 3. Rayleigh wave crystal deformation.

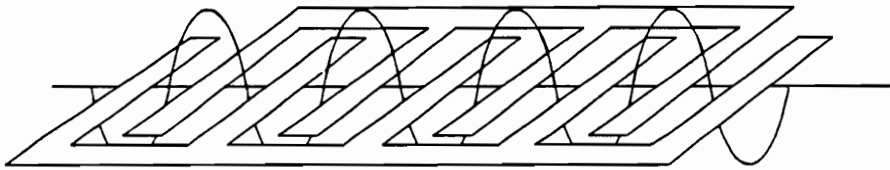


Figure 4. Sinusoidal wave generation by an interdigitized transducer array.

The choice of materials and crystal axes for the propagation of surface acoustic waves have been investigated extensively. Two factors that must be considered when developing a surface acoustic wave device are the temperature coefficient of delay and piezoelectric coupling constant for the materials. The two most popular materials used today, lithium niobate and quartz, will be compared to elucidate this situation.

The piezoelectric coupling constant determines the efficiency of the piezoelectric material to convert a radio frequency signal into an acoustic wave. The higher the efficiency, the lower the losses and the lower the number of finger pairs required in the interdigitized transducer array. The coupling constant, k^2 , is evaluated from the change in wave velocity, Δv , caused by depositing a highly conducting thin metal film on the surface. This change has been shown to be

$$k^2 \approx \frac{2 |\Delta v|}{v} \quad (2)$$

where v is the acoustic surface wave velocity of the free surface.

For lithium niobate, the coupling constant is 0.043. For ST-quartz the value is 0.002⁴⁷.

The most important consideration for the use of an acoustic oscillator is the stability of the oscillator frequency. The frequency that is measured is a reflection of the acoustic surface wave velocity of the crystal. The fundamental relationship between surface velocity and frequency is

$$c = \lambda * \xi \quad (3)$$

where c is the acoustic velocity, λ is the wavelength and ξ is the frequency. This can be rewritten as

$$V_R = \lambda * f \quad (4)$$

where V_R is the Rayleigh surface wave velocity, λ is the wavelength and f is the oscillating frequency. Because λ is constant, since the interdigitized transducer array finger width is fixed, any physical phenomena that affects the wave velocity will be reflected as a change in the oscillator frequency. In essence, the use of an oscillator circuit to generate a particular frequency and monitoring changes in this frequency is a very sensitive means for measuring small changes in the surface wave velocity.

To ensure that changes in surface velocity are attributable to changes occurring on the surface of the crystal and not to changes in the crystal itself, ST-quartz has been the material of choice for the development of surface acoustic wave oscillators. ST-quartz has been chosen because of the zero temperature coefficient of delay at room temperature. While lithium niobate and other piezoelectric crystalline materials have higher coupling efficiencies, the temperature coefficient of delay is the most important parameter to consider.

Since the acoustic wave velocity of the substrate is determined by the choice of crystal material and axis of propagation, the interdigital transducer finger pattern will determine the acoustic wavelength and by default the oscillation frequency. The finger width and space between alternating fingers are $1/4$ wavelength (Figure 5). The width of the fingers therefore determines the acoustic wavelength:

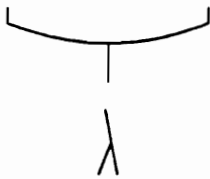
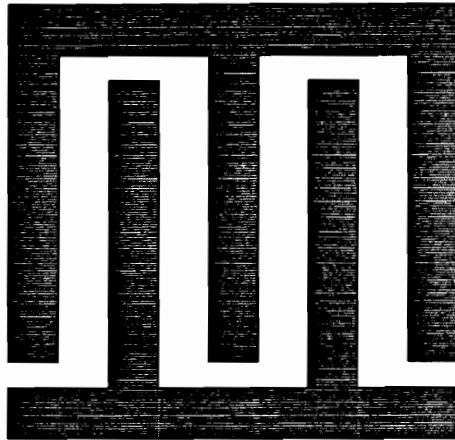
$$\lambda = 4 * (\text{finger width}) \quad (5)$$

with the oscillation frequency being:

$$f = V_R / \lambda \quad (6)$$

where V_R is the Rayleigh surface wave velocity and λ is the wavelength. For a ST-Quartz Surface Acoustic Wave Device having a $25 \mu\text{m}$ finger width and a surface wave velocity of 3158 meters/second, the acoustic wavelength is $100 \mu\text{m}$ and the fundamental oscillating frequency is 31.58 Megahertz. The transfer function of the

$\lambda/4$



Interdigitized Array

Figure 5. Interdigitized array.

interdigitized transducer array is a $(\sin x)/x$ curve having a bandwidth related to the number of finger pairs, N . Dieulesaint⁴⁸ has expressed the bandwidth as

$$\Delta f/f = 1.77/(N-1) \quad (7)$$

In many applications, nonconducting polymer films are applied to the surface of the device. The response for a SAW device having a thin, isotropic, nonconducting film is :

$$\Delta f = (k_1 + k_2)f_0^2 hp - k_2 hf_0^2 (4\mu/V_R^2)[(\lambda + \mu)/(\lambda + 2\mu)] \quad (8)$$

where k_1 and k_2 are material constants for the quartz substrate, V_R is the Rayleigh surface wave velocity, f_0 is the fundamental frequency of the device in Hertz, p is the film density, h is the film thickness, μ is the shear modulus of the film material, and λ is the Lamé constant^{49,50}. The first half of the equation describes the shift in frequency due to mass loading and is independent of the mechanical properties of the film. The second half of the equation describes the frequency shift due to changes in the elastic properties of the film. If the coating is a soft, rubbery material such that $4\mu/V_R^2$ is less than 100, the changes in frequency attributable to modulus changes are minimal and the second term can be ignored. Inserting the values for the material constants for an ST-Quartz device ($k_1 = -9.33 \cdot 10^{-8} \text{ m}^2 \text{sec/kg}$, $k_2 = -4.16 \cdot 10^{-8} \text{ m}^2 \text{sec/kg}$), the wave equation becomes:

$$\Delta f = (-1.3 \cdot 10^{-7} \text{ m}^2 \text{sec/kg}) f_0^2 (10^6 \text{ Hz/MHz})^2 hp \quad (9)$$

$$* (10^2 \text{ cm/m})^2 (10^{-3} \text{ kg/g})$$

$$\Delta f = -1.3 \cdot 10^6 f_0^2 hp$$

This is equivalent in form to the Sauerbrey equation for mass loading on a bulk wave quartz crystal microbalance since the quantity hp is simply a mass per unit area term.

Remembering that the Sauerbrey equation for quartz is:

$$\Delta f = -2.3 \cdot 10^6 f_0^2 M/A \quad (10)$$

on first examination it would appear that a bulk wave detector offers a greater sensitivity to mass changes than a surface wave detector. However, it must be remembered that the upper frequency limit for a bulk device is about 10 Megahertz, due to the fact that higher frequencies require thinner crystals, a situation which leads to a very fragile device. With surface wave devices, base frequencies of 158 Megahertz are presently available. The upper limit is determined by the finger width available using microlithographic techniques which at present are capable of generating devices in the low gigahertz region.

Changes in surface wave velocities which are reflected as frequency shifts in the SAW oscillator are not the only concern. Even though most vapor phase monitoring investigations using SAW devices rely on measuring changes in an oscillator frequency, surface acoustic wave amplitude attenuation is a concern. When a film is deposited upon a SAW device, the energy content of the wave can be diminished from lossy interactions of the wave with the film. If these interactions are large enough, the attenuation losses can be greater than the amplifier gain for the circuit. At this point the circuit will cease to oscillate⁵¹. Amplitude attenuation then becomes the limiting factor for the film thickness that a SAW oscillating circuit can support.

The presence of a thin organic film on the surface of a SAW device will cause attenuation of the wave through interactions with the longitudinal and vertical shear components of the Rayleigh wave. Dransfeld and Salzman discussed the mechanism of energy loss from the longitudinal component⁵². A medium in intimate contact with a SAW surface will undergo periodic compression and expansion by the longitudinal wave component at the operating frequency of the device. Since the velocity of sound in the surface coating will be different (lower for gases, organic films and water) than the velocity for the SAW substrate, radiation of compressional wave energy away from

the SAW device surface into the slower adjacent film will occur. This energy loss absorption coefficient is

$$\alpha_L = \frac{4.3 \rho_F V_F}{\rho_R V_R \tau} \text{ dB/cm} \quad (11)$$

where ρ_F and V_F are the density and velocity of sound in the adjacent film and ρ_R , V_R and τ are the density, Rayleigh wave velocity and wavelength of the SAW device. The implications of this equation is that attenuation increases with length of the SAW device and inversely with the wavelength. It must be understood that this equation is applicable only for films thick enough to support a compressional wave (thickness greater than λ). This mode of attenuation is not applicable to films deposited on the device for vapor phase analysis since these films possess thicknesses on the order of 1% of the acoustic wavelength. Compressional waves cannot exist in this thin a medium and can therefore be neglected.

This amplitude attenuation is important in the application of SAW devices to solution phase chemistry. When inserted into a solution, the surrounding medium is capable of supporting a compressional wave, which results in a large attenuation of the Rayleigh wave energy. Wohltjen's analysis of various SAW substrate thicknesses and their response when water is placed on their surfaces is a seminal investigation of this effect⁵³.

Since compressional waves do not exist in very thin films, where the film thickness is significantly less than one acoustic wavelength, the only interaction available is with the shear wave component of the Rayleigh wave.

Snider, Fredrickson and Schneider have developed a model for the investigation of the effect of thin metal films on Rayleigh wave attenuation⁵⁴. While this is not

explicitly correct for a thin viscoelastic polymer film, a qualitative understanding for thin films of low viscosity can be attained.

For a thin film of low viscosity, the following relationship exists:

$$\alpha = \dot{A}w^2\bar{\eta}h \quad (12)$$

where α is the observed attenuation per unit length of delay line, \dot{A} is a constant dependent upon the film material, w is the angular frequency of the Rayleigh wave, $\bar{\eta}$ is the film viscosity and h is its thickness. SAW attenuation should therefore be linearly dependent upon film thickness and viscosity and have a square dependence upon the frequency.

1) Scaling Laws

Wohltjen, Snow and Ballantine have applied scaling concepts to the use of Surface Acoustic Wave devices in chemical sensing applications⁵⁵. Based upon the fundamental equation describing the mass loading of a SAW device and the effect on the parameters of a SAW device with a change in the base oscillating frequency, the following characteristics were noted:

1) If a transducer impedance and delay path are kept constant, the device's analytical area is inversely proportional to the square of the operating frequency.

2) The signal produced by a given mass per unit area load is proportional to the square of the operating frequency.

3) The noise, or frequency fluctuation, of a SAW device was experimentally measured and found to be linearly dependent with the frequency. This indicates that the signal to noise ratio should increase linearly with increasing frequency.

4) The mass loading detection limit is a function of the signal and noise. Since the noise is linearly dependent on the frequency and the signal is proportional to the

square of the frequency, at a constant signal to noise ratio the minimum detectable quantity improves linearly with frequency.

5) The actual mass of a chemical species required to produce a given signal decreases with the cube of the frequency. This is because the minimum mass detectable by a SAW device is related to the mass loading detection limit (which improves proportional to frequency) times the device area (decreases proportional to the square of the frequency).

6) The response time is inversely related to the fourth power of the frequency. This occurs because the Fickian vapor diffusion time is related to the square of the film thickness. For a given frequency change the film thickness necessarily decreases with the square of the frequency.

What is apparent from this discussion is that for a reversible chemical system, the higher the frequency, the better the sensitivity, response time and limit of detection. In a dosimetric application, it is not immediately apparent that a higher frequency device may be appropriate. The reason for this hesitation is that in dosimetric work, reactive sites in the film will be consumed during sensing of the vapor. Therefore a conflict of choice may develop; should the highest frequency device be utilized to obtain the maximum sensitivity and lowest response time it must be done with the understanding that the effective lifetime of such a device will be less that of a corresponding low frequency device.

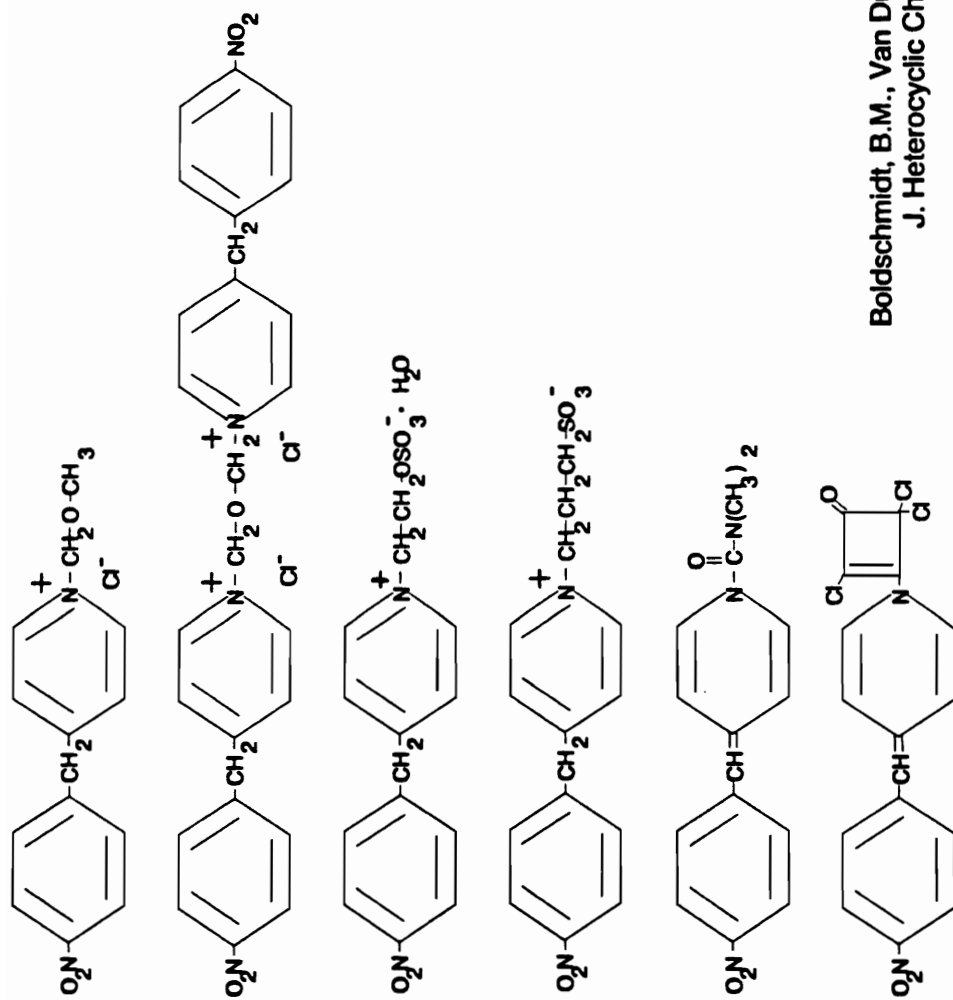
B) Chemistry of Alkylating and Acylating agents and 4-(4'-nitrobenzyl)pyridine

The detection of alkylating agents using 4-(4'-nitrobenzyl)pyridine is due to 4-(4'-nitrobenzyl)pyridine being a relatively strong nucleophile that readily forms a covalent bond with a variety of electrophiles. Work conducted on the reaction products

of 4-(4'-nitrobenzyl)pyridine with some electrophiles (chloromethyl methyl ether, bis(chloromethyl) ether, glycol sulfate, propane sultone, N,N-Dimethylcarbonyl chloride and perchlorocyclobutenone) shows that the major products formed are either substituted pyridinium salts or 1,4-dihydropyridines⁵⁶ (Figure 6). The pyridinium salts were white or yellow in color whereas the 1,4-dihydropyridine complexes were scarlet red. The elimination of the benzylic hydrogen is believed to be responsible for the red shift of the reaction products due to conjugation extension in the nitrobenzylpyridine backbone.

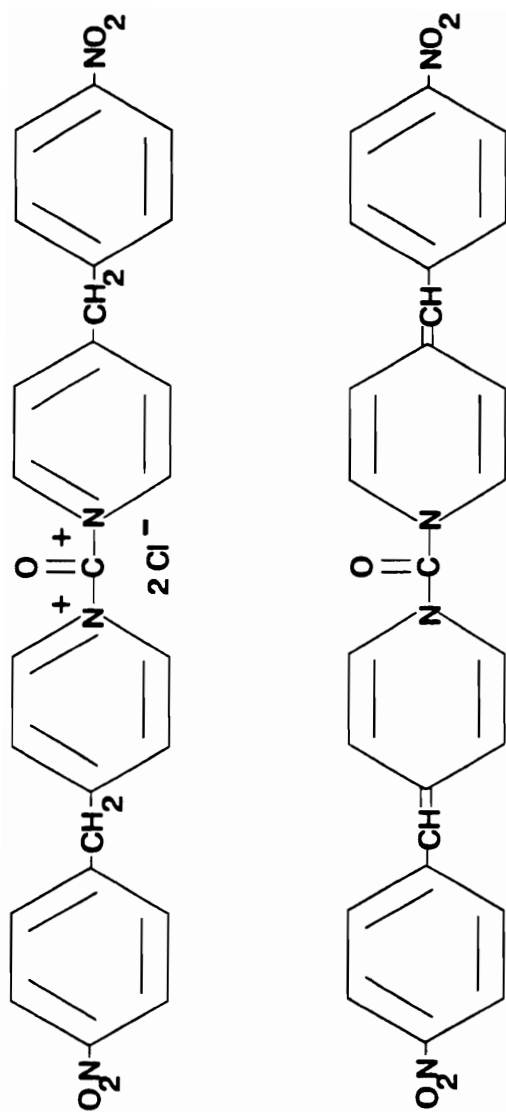
The reaction product of phosgene and 4-(4'-nitrobenzyl)pyridine is more controversial. Lamouroux proposed the pyridium chloride salt structure but Cockerill proposed that the product must contain the 1,4-dihydropyridine structure⁵⁷ (Figure 7). The reddish hue of the resultant product is indicative of the extended conjugation of the product.

To demonstrate that the 1,4-dihydropyridine structure is the chromophore necessary for the development of optically based alkylating agent detection schemes, the alkylation product of 4-(4'-nitrobenzyl)pyridine and ethylene oxide was investigated⁵⁸. ¹³C and ¹H NMR data indicates that the chromophore possesses the 1,4-dihydropyridine structure IV rather than the pyridinium structure II (Figure 8). Addition of acid to the chromophore converts it to a colorless compound, presumably the pyridinium complex III. Treatment of this compound with base regenerates the chromophore. Since the alkylating or acylating agent does not affect the extent of π conjugation, the development of a visible chromophore for any of the agents to be detected seems dependent upon the generation of the 1,4-dihydropyridine structure. This indicates the reason for the use of and need for basic materials impregnated in



Boldschmidt, B.M., Van Duuren, B.L., Goldstein, R.C.,
 J. Heterocyclic Chem., 13, 517 (1976)

Figure 6. Alkylation and acylation products of 4-(4'-nitrobenzyl)pyridine.



Cockerill, A.F., Davies, G.L.O., Rackham, D.M.
 Tetrahedron Letters, 1, 27 (1972)

Figure 7.. Reaction product of phosgene and 4-(4'-nitrobenzyl)pyridine.

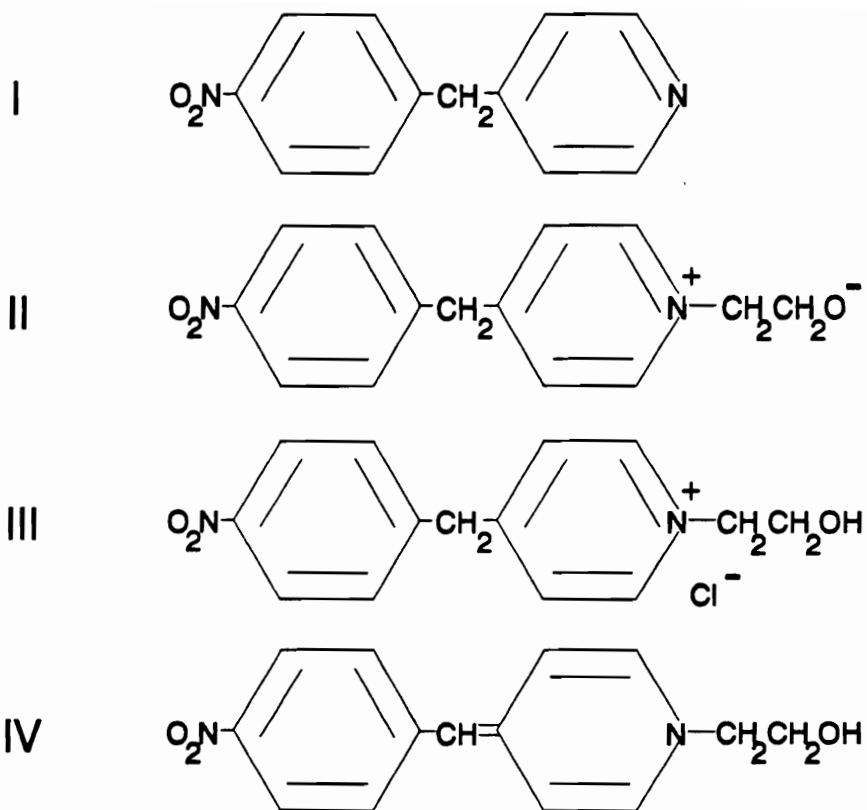


Figure 8. Reaction product possibilities for 4-(4'-nitrobenzyl)pyridine and ethylene oxide.

crayons, indicator papers and detector ampules for optical detection of alkylating and acylating agents.

Kinetic studies of the reaction between 4-(4'-nitrobenzyl)pyridine and alkylating agents in solution suggests that the reaction is S_N2 in nature, being first order in 4-(4'-nitrobenzyl)pyridine and first order in the alkylating agent⁵⁹.

C) SAW sensor design

The development of a chemical sensor designed around a surface acoustic wave device requires that major emphasis be given to the chemistry of the film involved in the monitoring of the vapor. The reason for this emphasis is that a SAW device is a non-selective, highly sensitive microbalance, able to determine very small weight changes that occur on its surface. What is attractive about using SAW devices as sensor elements is that they produce an output which can easily be monitored in real time (as the event occurs) and are sensitive to picogram quantities of mass change upon their surfaces⁶⁰.

Since SAW devices are non-selective and measure mass changes upon their surfaces, the design of a chemical system for the determination of a particular compound or class of compounds requires answers to the following questions:

1) Can a film be prepared that will interact by physisorption or chemisorption processes with only one vapor or class of vapors? This film, which can be either homogeneous or heterogeneous, must show selectivity for the target vapor.

2) Will the target vapor interact in a timeframe and at a concentration that will be useful to the user? For example, if a SAW detector is developed for the determination of nerve gas agents, it would be useless if the user succumbs to exposure before the detector responds to the concentration present.

3) Can the concentration of the vapor being monitored be determined from the response of the detector?

4) Can the composition of the film be varied so that the response of the film to the target vapor is varied. This may not appear to be of great concern initially.

However a situation can exist where the device may be needed to monitor a concentration which is beyond the films initial analytical capabilities. For example, analysis of ethylene oxide by a SAW device may have an analytical range of 0 to 100 ppm. Anything above 100 ppm does not generate an appreciable additional response change. For certain environments and applications, it may be necessary to extend the analytical range beyond 100 ppm.

With these questions in mind, the factors important in the development of a chemically sensitive film for use with SAW devices can be discussed.

1) Film permeability

When a film is deposited upon a SAW device, one factor affecting the response of the device is the permeability of the film to the vapor. Since permeability is defined as the transmission of molecules through a film, the rate with which a target vapor will enter and propagate through the film will affect the response and response time of the device.

Simple Fickian diffusion calculations show that for a film 0.5 μm thick, deposited on an impermeable boundary material with a diffusion coefficient of 10^{-7} cm^2/sec , the diffusion time is on the order of milliseconds⁶¹. If permeability were dependent solely upon diffusion and a material's diffusion coefficient, then there would be no appreciable difference in the response of different films to vapors for a film thickness of 0.5 μm .

The basis for this conclusion is that a review of the diffusion coefficients for various polymers as listed in the Polymer Handbook⁶² shows that most diffusion coefficients reside in the 10^{-6} to 10^{-9} cm^2/sec range. Analysis of the equation used in reference 61 to determine the vapor concentration at particular film depths:

$$C = C_0 \left(1 - \frac{4}{\pi} \sum_0^{\infty} \frac{1}{(2n+1)} \sin\left(\frac{(2n+1)\pi x}{2l}\right) \exp(-K) \right) \quad (13)$$

$$K = \frac{(2n+1)^2 \pi^2 D t}{4l^2}$$

where D = diffusion coefficient (cm^2/sec)

l = film thickness (cm)

C = concentration of vapor at depth x and time t

C_0 = vapor phase concentration

shows that for films of the same thickness, the concentration of vapor at a particular depth is exponentially related to the (diffusion coefficient)(time) product. Therefore, a concentration depth profile for a $0.5 \mu\text{m}$ thick film will be identical for a film coefficient of 10^{-6} cm^2/sec at 0.5 milliseconds and a film coefficient of 10^{-9} cm^2/sec at 0.5 seconds (Figure 9).

If the timeframe is increased by one order of magnitude, 5 milliseconds for 10^{-6} cm^2/sec and 5 seconds for 10^{-9} cm^2/sec , the concentration at the impermeable polymer/SAW device interface is 99% of the concentration at the surface of the polymer film. Therefore, response times will appear to either be instantaneous (10^{-6} cm^2/sec) or nearly so (10^{-9} cm^2/sec) (Figure 10).

Diffusion, however, is not the entire story. The permeation of molecules through a polymer film occurs by the solution of the vapor into the polymer and then diffusion of the dissolved vapor. The product of the diffusion coefficient D and the solubility coefficient S is defined as the permeability coefficient.

$$P = D * S \quad (14)$$

One of the predominant factors affecting the permeability coefficient is the chemical structure of the polymer with its associated intermolecular and intramolecular interactions. The chemical structure of the polymer will determine the solubility of the permeant in the polymer and therefore the permeability coefficient. If the vapor cannot get into the film due to it being insoluble in the polymer, it cannot diffuse through the film. Therefore the molecular interactions between the vapor and polymer (such as dipole-dipole interactions, ionic interactions, induction forces, and London forces) will determine the eventual solubility of the vapor with the polymer.

Of equal importance in the permeability of a vapor into a polymer is the state in which the polymer exists, namely whether it is a glass (below the glass transition temperature or T_g), an elastomer or rubber (above the T_g but below the crystalline melting temperature, T_m , if the polymer possesses any crystallinity) or a viscous or liquid material (above the T_m for crystalline or further above the T_g for amorphous materials). In general, a vapor will be able to permeate the least to most in a glass, a crystalline polymer, an elastomer and a viscous or liquid material.

In a glass, there is no polymer backbone motion and only possible side chain motion. The lack of motion reduces free volume as compared to that occurring above the T_g , thereby reducing the number of sites available for a penetrant vapor molecule to enter the polymer matrix. In a crystalline material, the compactness of the polymer chains to each other leads to the same situation. It then becomes a matter of the affinity of the polymer to another chain versus the affinity to that of the penetrant vapor.

In a rubbery state, the molecular motion of the polymer chain ensures a large free volume into which the penetrant vapor can solubilize and diffuse.

Simple Fickian Diffusion for Thin Films

Impermeable Lower Boundary

Diffusion Coefficient - Time product $5 \times 10^{-10} \text{ cm}^2$

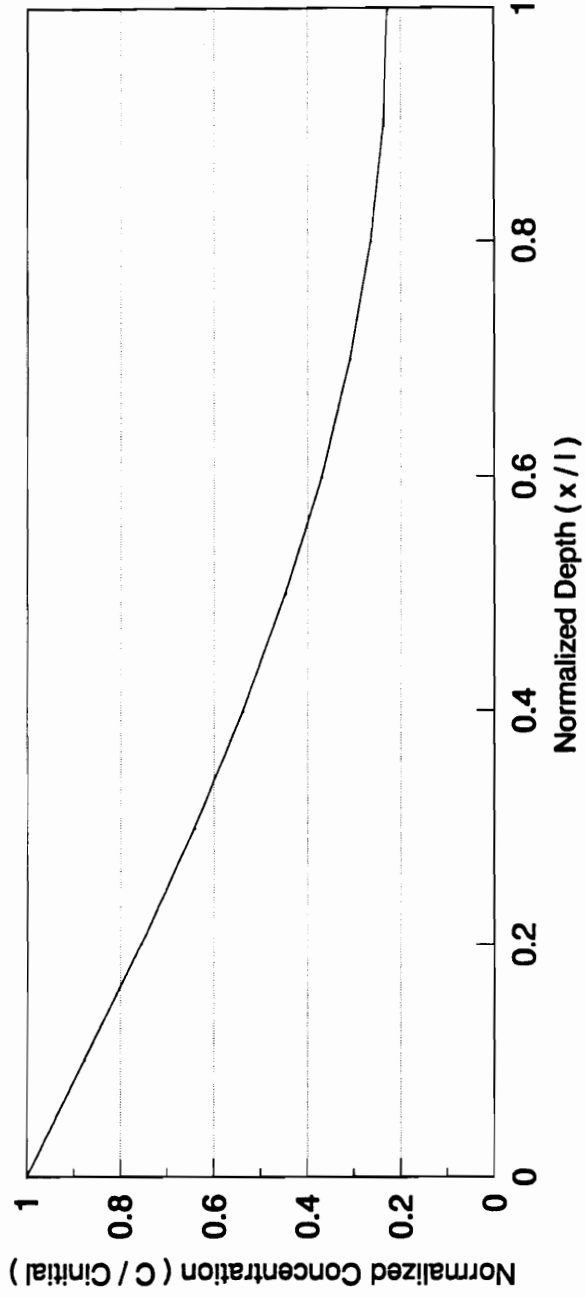


Figure 9. Vapor distribution for Dt product of $5 \times 10^{-10} \text{ cm}^2/\text{sec}$.

Simple Fickian Diffusion for Thin Films

Impermeable Lower Boundary

Diffusion Coefficient - Time product $5 \times 10^{-9} \text{ cm}^2$

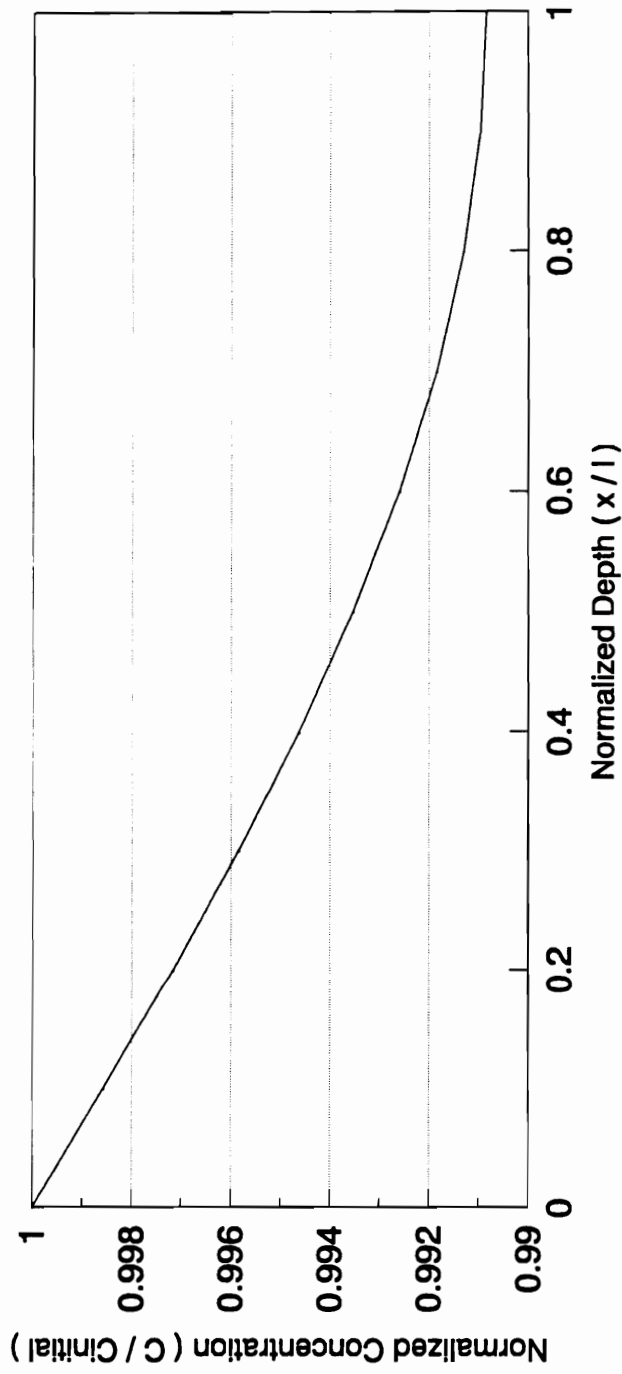


Figure 10. Vapor distribution for Dt product of $5 \times 10^{-9} \text{ cm}^2/\text{sec}$.

Unfortunately, available data for specific permeability coefficients of vapor/polymer interactions is not vast. Literature searches conducted on diffusion and permeability of phosgene and thionyl chloride yielded only one reference, that describing the development of permeation devices for phosgene, hydrocyanic acid and cyanogen chloride⁶³.

An approach to the determination of film permeability uses the partition coefficient as implemented in separation sciences. The partition coefficient, defined as

$$k = \frac{\text{(amount of solute per unit volume of stationary phase)}}{\text{(amount of solute per unit volume of vapor phase)}} \quad (15)$$

is a chromatographer's approach to determining the solubility of a permeant or solute into a film and therefore the permeability of the film⁶⁴. While absolute partition coefficient values for specific systems are unavailable, tables recommending stationary phases for different sample types will prove useful for selecting films compatible with the vapor of interest⁶⁵.

One attempt to determine partition coefficients for vapor/polymer interactions is the use of inverse gas chromatography. This method, using either packed, fiber or coated capillary columns, investigates the interaction of a vapor propagating in the mobile phase, usually hydrogen or helium, with a polymer or polymer blend composing the stationary phase. With the measurement of the retention volume for the vapor/polymer system, the partition coefficient can be calculated. From the partition coefficient, the Gibb's free energy of sorption, total partial molar enthalpy of sorption, total partial molar entropy of sorption and diffusion coefficient can be calculated, thereby determining the thermodynamic properties of the particular system investigated⁶⁶.

Determination of partition coefficients from surface acoustic wave responses have been correlated to gas-liquid chromatographic partition coefficients⁶⁷. The use of solvatochromic equations⁶⁸ to predict solubilities have been applied to vapor/coating interactions, most notably the development of a "universal" equation for the determination of vapor/polymer interactions^{69,70}.

An improvement in the solvatochromic equation approach has been the development of the linear solvation energy relationship as introduced by Grate and Abraham⁷¹. In this approach, partition coefficients from the interaction of a large number of neat vapors with the support phase are determined. Based upon a multiple linear regression analysis of these results, five particular solute-solvent interactions and their relative importance can be attributed to the support phase. These interactions (polarizability, dipole stabilization, hydrogen bond acidity and basicity, and dispersion) and their magnitude characterize the particular film studied for use as a stationary phase.

The goal of these linear solvation energy relationships is to develop a method for maximizing the interaction of a target vapor with a particular stationary phase by the careful selection of a phase whose solute-solvent interaction parameters are optimal for the vapor of interest. The better the match, the higher the partition coefficient. For a mass detector such as a SAW device, the higher the partition coefficient, the higher the dissolved vapor concentration in the film for a particular vapor concentration, leading to a greater sensitivity of the device to that vapor.

This assumes that the highest sensitivity is what is desired. For low level sensing, this is indeed the case. However, the situation may develop in which a lower sensitivity is needed for a particular vapor. As introduced in the previous section, a high sensitivity film may possess an analytical range which is capable of measuring a

concentration of a vapor from zero to 100 ppm but is incapable of measuring accurately a 1000 ppm concentration. In this case, the linear solvation energy relationship parameters could be deliberately mismatched for a vapor/polymer system to ensure that a less sensitive film is used to measure the higher concentration. If this should prove insufficient, a polymer in the glass state (below the glass transition temperature) could be chosen to further reduce the ability of the vapor to permeate the film, thereby reducing the response of the film and decreasing its sensitivity to the vapor.

While the development of a database of linear solvation energy relationship parameters will prove useful for the optimization of vapor/film systems, for an evaluation of a possible detection system the use of polymer support matrices of different states and polarities should prove sufficient.

2) Reagent reaction rate

The development of a SAW chemical sensor requires that the signal generated by the device represents the concentration of the vapor being monitored. For an irreversible dosimeter, the generation of a signal is a measure of the overall rate of reaction between the vapor that permeates into the film and the reagent contained in the film. Since the signal generated by a SAW device is a measure of the increase in mass created upon its surface by this reaction, a thorough analysis of the overall kinetics of the reaction with respect to different orders for both the vapor and the trapping agent is necessary for a correct interpretation of the signal produced by a SAW device.

The next two subsections will contain an analysis of the kinetic effect from two different perspectives, long term continuous exposure and short term fixed time exposure. In the former, the rate of product production is the parameter being examined while in the latter, the amount of product produced for the fixed exposure

time period is the parameter being examined. However, both methods of analysis and their associated outputs are dependent upon the overall reaction rate of the vapor and the trapping agent. Therefore, regardless of the method used, a thorough understanding of the kinetics of the reaction between vapor and trapping agent is necessary for the correct interpretation of the signal generated by the surface acoustic wave detector used in this study. This generic discussion is applicable to any dosimetric system that can be envisioned for use with these detectors.

With this understanding, those possessing a well founded knowledge of kinetics may wish to pass over the following two subsections. Those who wish to pursue these sections may read them now or find it helpful to read at least the following sections of this dissertation in the following order before reading these kinetic subsections:

Theoretical:

D) SAW Device Responses

E) Model Experimental Responses

1) Long term response model

2) Short term response model

Experimental

B) Exposure

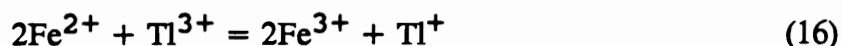
1) Long term exposure

2) Short term exposure

Once these sections have been read, it will be up to the reader's discretion as to what amount of reading of these kinetic subsections is necessary for an understanding of the experimental responses obtained in the studies and their analyses.

a) Kinetic responses

The reaction rate between two components cannot be described by a simple examination of the stoichiometry of the overall reaction. As a case in point, the following net reaction



has been experimentally determined to have an initial reaction rate which can be expressed as⁷²

$$-d[\text{Tl}^{3+}]/dt = k[\text{Tl}^{3+}][\text{Fe}^{2+}] \quad (17)$$

For the sake of simplicity, let us assume that the reaction rate for the following irreversible reaction



can be expressed as

$$-d[\text{A}]/dt = -d[\text{B}]/dt = d[\text{C}]/dt = k[\text{A}][\text{B}] \quad (19)$$

In this example, if the concentration being monitored over time is [C], then the measured rate of production of [C] will be first order with respect to both [A] and [B], the overall rate being second order.

If the initial concentrations of [A] and [B] are fixed with no further additions of reagent during the reaction, the rate of [C] production will decrease with time as both the concentration of [A] and [B] decrease. If the technique of flooding is utilized, in which the concentration of one reagent is increased to a level such that its concentration does not appreciably change during the course of the experiment, the reaction rate can be expressed as

$$d[\text{C}]/dt = k_1[\text{A}] \quad (20)$$

where [B] is the reagent that is flooded and $k_1 = k[\text{B}]$.

The effect of flooding is to reduce the dependence of the rate of production of [C] to one reagent, in this case [A]. In this example, the rate of production of [C] would be linearly dependent upon the concentration of [A].

If this analysis is taken one step further, where the concentration of [B] is flooded and the concentration of [A] is constant throughout the lifetime of the experiment, then the reaction rate can be expressed as

$$d[C]/dt = k_2 \quad (21)$$

where k_2 is equal to $k[A][B]$.

Here the rate of production of [C] is constant over the lifetime of the experiment. The value of this constant is a function of the unchanging concentrations of [A] and [B]. If the same experiment is performed with either of these two concentrations being changed, a new constant is determined. In fact a calibration curve using different concentrations of [A] can be constructed with the rate of production of [C] being dependent upon the constant concentration of [A] for an experiment at a particular concentration of [B], assuming that reagent [B] is indeed flooded for the lifetime of the experiment.

With this particular system, a linear calibration curve would be obtained, relating the rate of production of [C] to the maintained concentrations of [A]. The slope of the line would be $k[B]$. If the concentration of [B] could be changed to [B]', still maintaining a flooded condition, the curve would still be linear but with a slope of $k[B]'$ (Figure 11). To arrive at the true rate constant, the data can be normalized by dividing the slope of the line by the concentration of [B] that was utilized, leaving the slope equal to k , or by plotting (rate of production of [C])/(concentration of [B]) versus the concentration of [A]. This again yields the true rate constant k since

$$(d[C]/dt)/[B] = k[A] \quad (22)$$

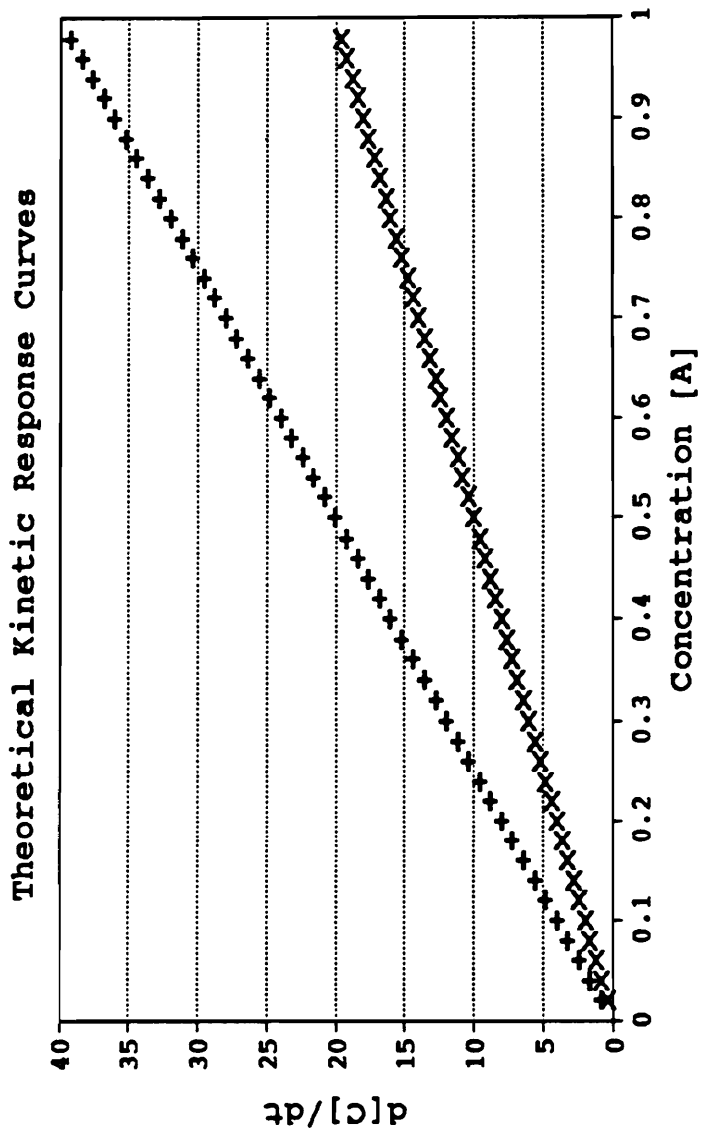


Figure 11. Kinetic response curve for $d[C]/dt = k[A][B]$.

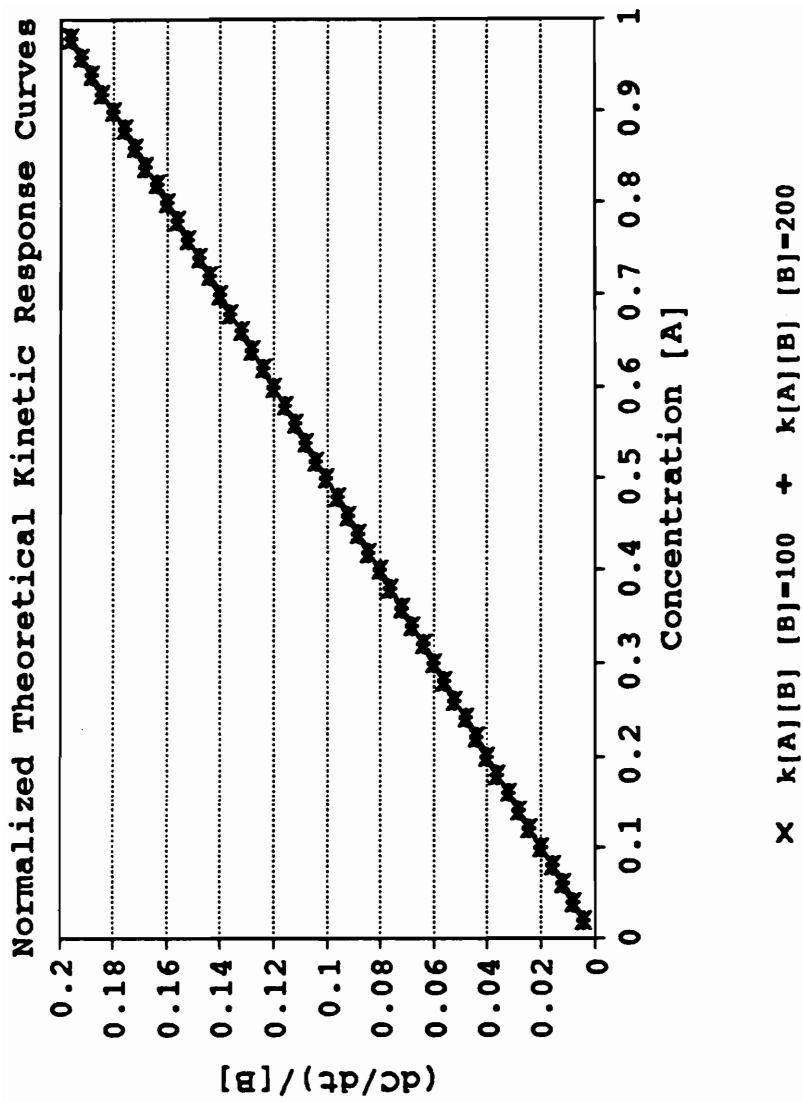


Figure 12. Normalized kinetic response curve for $d[C]/dt = k[A][B]$.

For this particular system, the normalized calibration curves for different flooding concentrations will be identical (Figure 12).

What would happen if the concentration of [B] does not remain flooded and does change during the experiment just concluded? If [A] is maintained at a constant concentration, the reaction rate will decrease as [B] decreases. In fact the rate of production of [C] at time t will be dependent upon the concentration of, and order of, the reaction with respect to [B] since

$$d[C]/dt = k_3[B] \quad \text{where } k_3 = k[A] \quad (23)$$

for the reaction being examined. If the experiment is conducted to infinite time, the reaction rate will approach zero as [B] is entirely consumed.

Finally consider the effect of increasing the concentration of [A] during the experiment with [B] remaining flooded. As [A] increases, the rate of reaction will also increase since

$$d[C]/dt = k_1[A] \quad \text{where } k_1 = k[B] \quad (24)$$

If this experiment is allowed to continue until the point where [B] is no longer flooded but diminishes with time, the rate of production of [C] will reach a maximum as [A] continues to increase and then decrease toward zero as [B] decreases to zero.

The same analysis can be used to determine the reaction rates for the production of [C] if

$$d[C]/dt = k[A][B]^2 \quad (25)$$

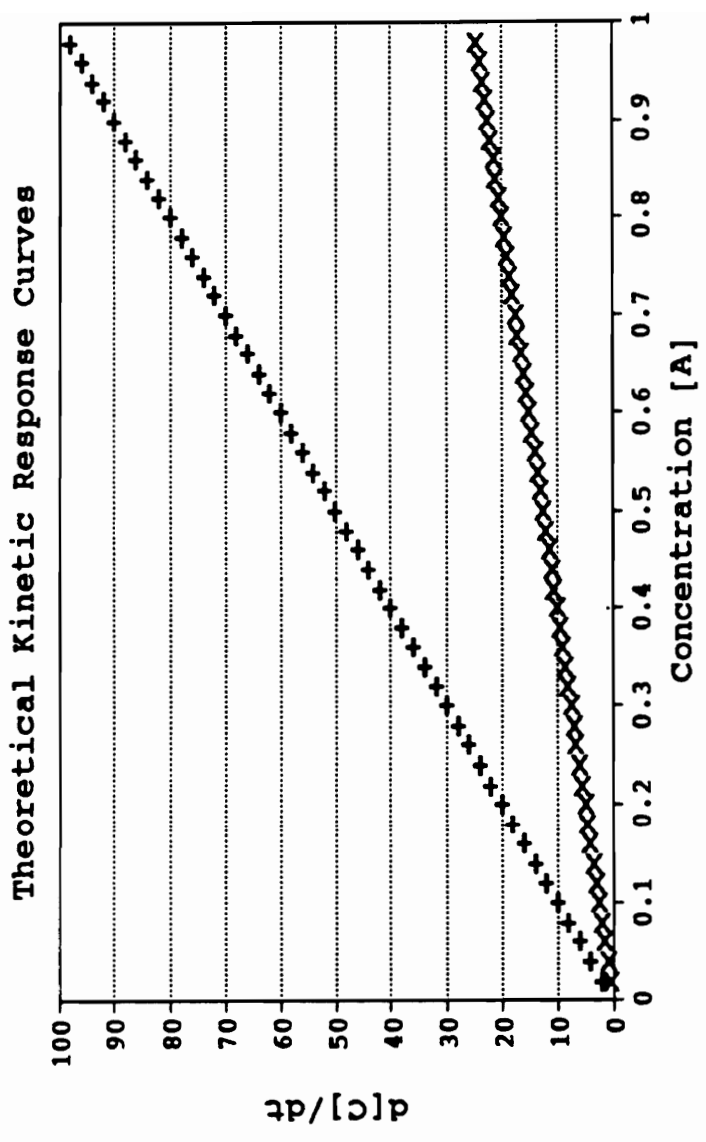
$$d[C]/dt = k[A]^2[B] \quad (26)$$

or

$$d[C]/dt = k[A]^2[B]^2 \quad (27)$$

If [B] is flooded, the reaction rates reduce to

$$d[C]/dt = k_4[A] \quad \text{where } k_4 = k[B]^2 \quad (28)$$



\times $k[A][B]^2$ [B]=100 $+$ $k[A][B]^2$ [B]=200

Figure 13. Kinetic response curve for $d[C]/dt = k[A][B]^2$.

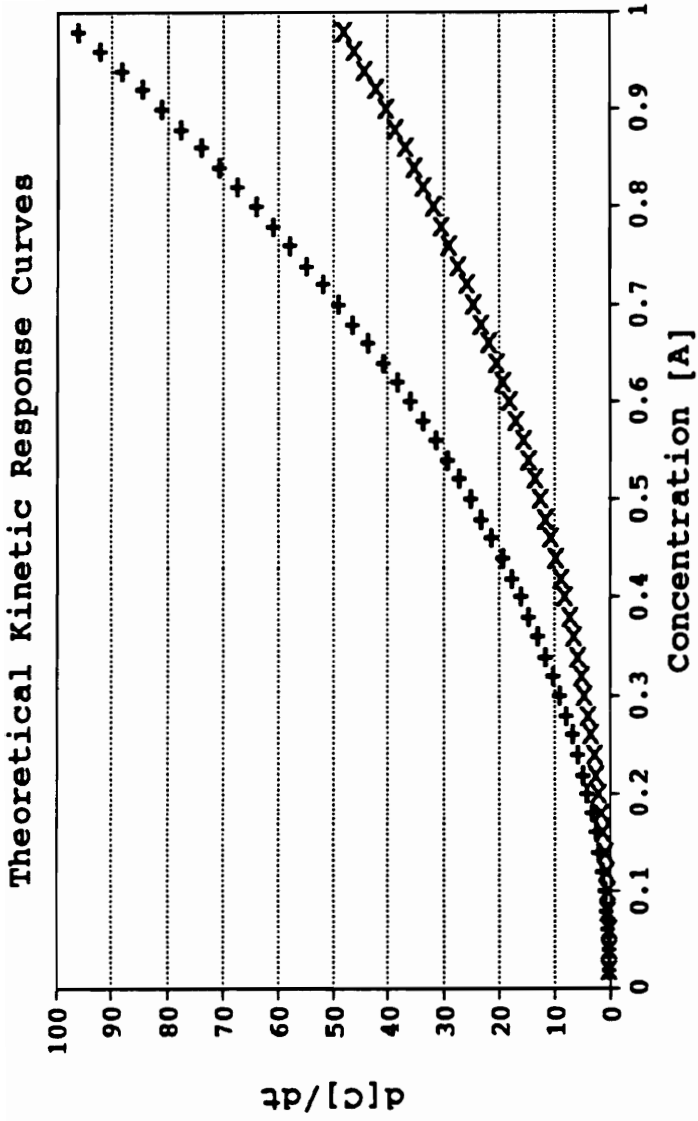
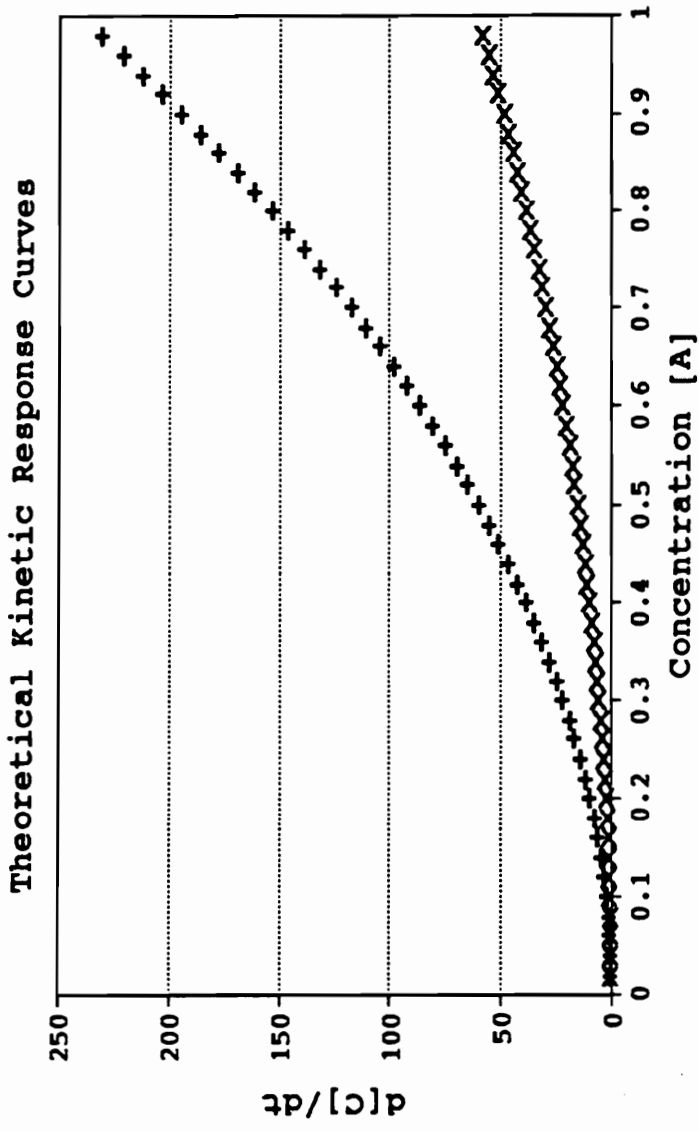


Figure 14. Kinetic response curve for $d[C]/dt = k[A]^2[B]$.



x $k[A]**2[B]**2 [B]=100$ + $k[A]**2[B]**2 [B]=200$

Figure 15. Kinetic response curve for $d[C]/dt = k[A]^2[B]^2$.

$$d[C]/dt = k_5[A]^2 \quad \text{where } k_5 = k[B] \quad (29)$$

$$d[C]/dt = k_6[A]^2 \quad \text{where } k_6 = k[B]^2 \quad (30)$$

The first reduced rate equation analysis is equivalent to

$$d[C]/dt = k[A][B]^2 \quad (31)$$

if [B] is maintained at a particular concentration. The calibration curve will be linear since the slope of the curve, $k[B]^2$, is constant and independent of [A] (Figure 13).

The second and third equations, where [B] and $[B]^2$ are constants, result in the rate of production of [C] having a square dependence upon [A].

If the concentration of [B] is flooded and [A] is maintained at a constant concentration throughout the lifetime of the experiment, the second and third reaction rates reduce to

$$d[C]/dt = k_7 \quad \text{where } k_7 = k[A]^2[B] \quad (32)$$

$$d[C]/dt = k_8 \quad \text{where } k_8 = k[A]^2[B]^2 \quad (33)$$

As before, the rate of production of [C] is constant during the experiment for these conditions. If [B] is flooded at a particular concentration, a calibration curve can be developed for the rate of production of [C] as a function of the concentration of [A]. In this case, instead of a linear relationship between the rate of production of [C] and the concentration of [A], a square relationship exists due to the second order dependence of the rate on [A]. The slope at any point on this curve will be $k[A][B]$ for $d[C]/dt = k[A]^2[B]$ (Figure 14) and $k[A][B]^2$ for $d[C]/dt = k[A]^2[B]^2$ (Figure 15).

Using different flooding concentrations of [B] and attempting to normalize the data by dividing the rate of production of [C] by [B], $(dC/dt)/[B]$, and plotting versus [A], two possible outcomes are possible for the three alternate reaction rates. They are

$$(d[C]/dt)/[B] = k[A][B] \quad \text{slope} = k[B] \quad (\text{Figure 16}) \quad (34)$$

$$(d[C]/dt)/[B] = k[A]^2 \quad \text{slope} = k[A] \quad (\text{Figure 17}) \quad (35)$$

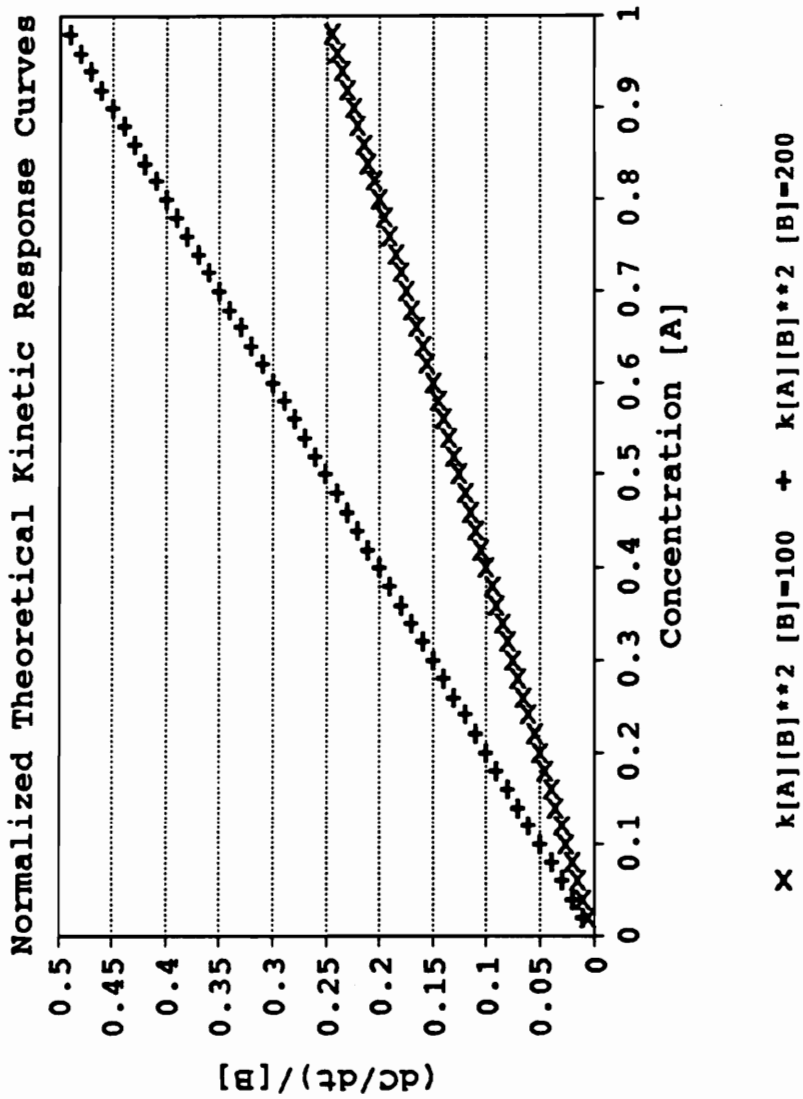


Figure 16. Normalized kinetic response curve for $d[C]/dt = k[A][B]^2$.

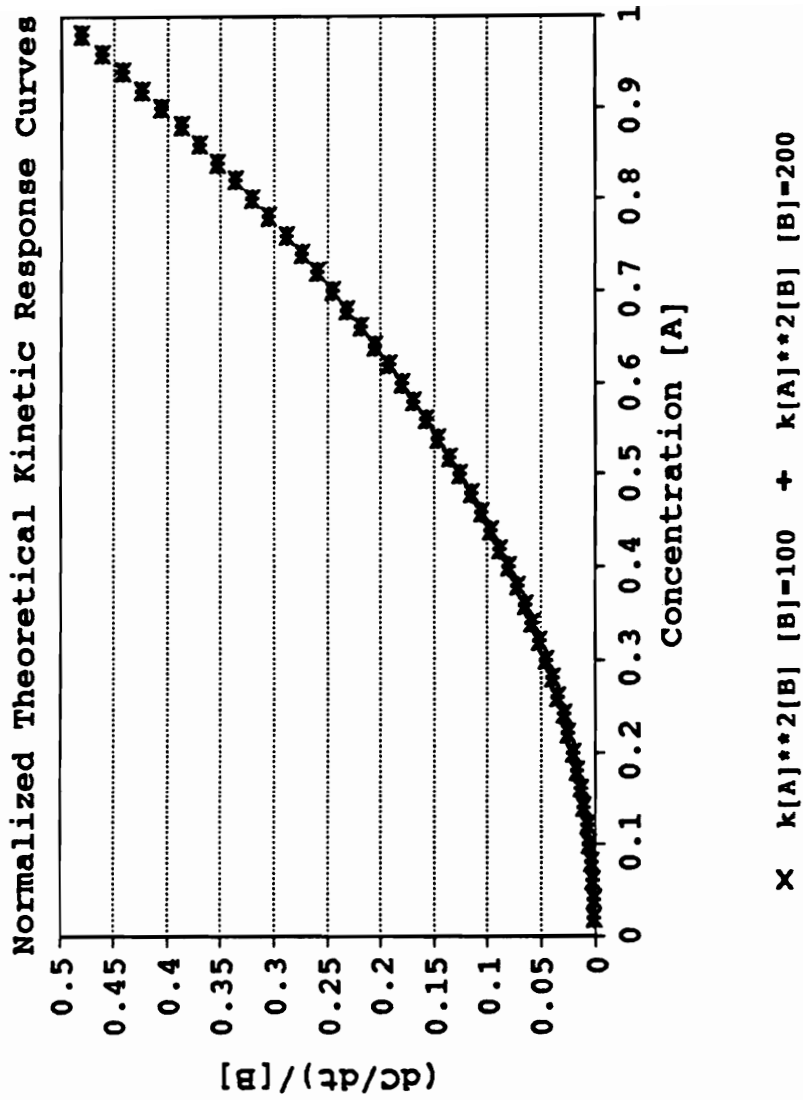
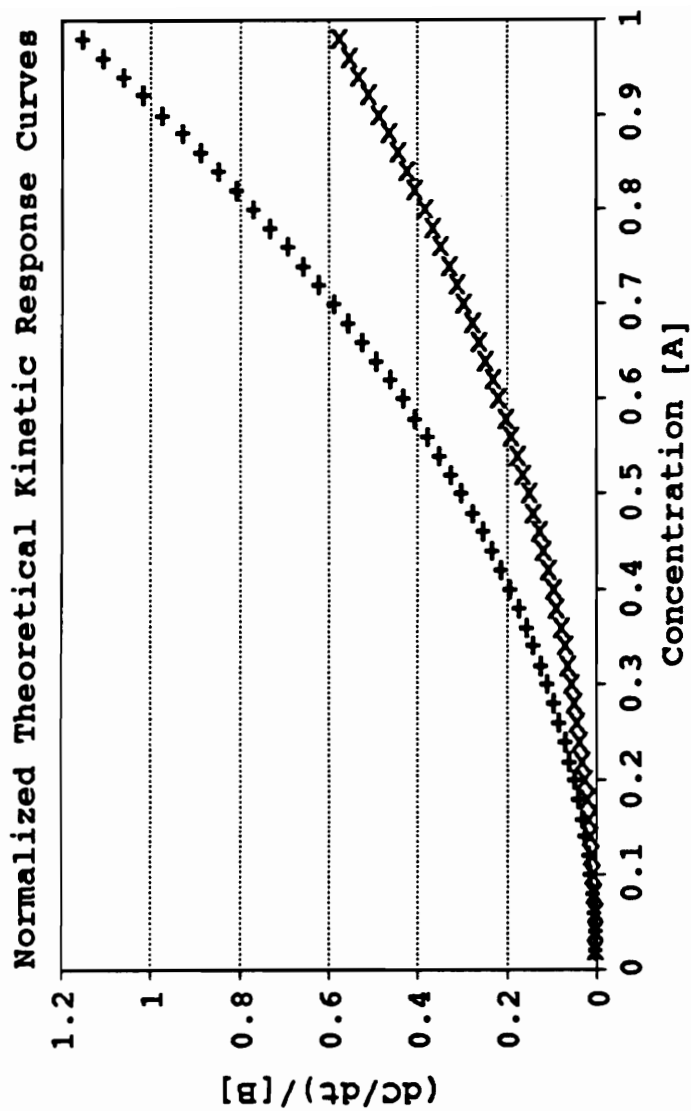


Figure 17. Normalized kinetic response curve for $d[C]/dt = k[A]^2[B]$.



\times $k[A]^2[B]^2$ [B]=100 $+$ $k[A]^2[B]^2$ [B]=200

Figure 18. Normalized kinetic response curve for $d[C]/dt = k[A]^2[B]^2$.

$$(d[C]/dt)/[B] = k[A]^2[B] \quad \text{slope} = k[A][B] \text{ (Figure 18)} \quad (36)$$

In only one case will the normalized calibration curve be identical for different flooding concentrations of [B] since the slope for the second condition is independent of [B]. The other two will show a dependence upon the concentration of [B].

b) Fixed time exposure responses

Most dosimeters developed rely on measured time of exposure and analysis of the resultant trapped agent, as in the case of charcoal collection tubes; or resultant product produced, as used by colorimetric vapor detection tubes.

Fixed time responses can be discussed using the kinetic rate responses discussed previously. Using the four basic rate equations previously discussed,

$$d[C]/dt = k[A][B] \quad (37)$$

$$d[C]/dt = k[A][B]^2 \quad (38)$$

$$d[C]/dt = k[A]^2[B] \quad (39)$$

and

$$d[C]/dt = k[A]^2[B]^2 \quad (40)$$

integration of these equations will determine the amount of [C] produced for a fixed period of time. Experimental parameters can be chosen to reduce the complexities of the problem. These parameters are:

- 1) [A] remains constant for the exposure period.

$$t_i = \text{initial point of exposure}$$

$$t_f = \text{cease exposure}$$

- 2) [B] is flooded and remains constant during the exposure period.

- 3) For times other than the exposure period, the vapor concentration above the film is zero.

With these conditions introduced, the rate equations upon integration become,

$$[C] = k[A][B](t_f - t_i) \quad (41)$$

$$[C] = k[A][B]^2(t_f - t_i) \quad (42)$$

$$[C] = k[A]^2[B](t_f - t_i) \quad (43)$$

and

$$[C] = k[A]^2[B]^2(t_f - t_i) \quad (44)$$

The development of a calibration curve for vapor exposure is based upon the concept of the concentration-time product as utilized by Witten and Prostack for a colorimetric dosimeter to detect phosgene⁷³. The calibration curve will then be the amount of [C] produced versus the concentration-time product ($[A] * (t_f - t_i)$). The slopes of the calibration curve for the four rates are

$$\text{slope} = k[B] \quad \text{for } [C] = k[A][B](t_f - t_i) \quad (\text{Figure 19}) \quad (45)$$

$$\text{slope} = k[B]^2 \quad \text{for } [C] = k[A][B]^2(t_f - t_i) \quad (\text{Figure 21}) \quad (46)$$

$$\text{slope} = k[A][B] \quad \text{for } [C] = k[A]^2[B](t_f - t_i) \quad (\text{Figure 23}) \quad (47)$$

and

$$\text{slope} = k[A][B]^2 \quad \text{for } [C] = k[A]^2[B]^2(t_f - t_i) \quad (\text{Figure 26}) \quad (48)$$

The first two equations describe a case where the slope is independent of the concentration of [A]. Since for a given set of experiments the concentration of [B] can be fixed, the calibration curves for these cases are linear. In these cases, it is true that 100 seconds exposure of 100 ppm of vapor is equivalent to 1000 seconds exposure of 10 ppm.

The last two equations are not as straightforward as the first. Since the X axis of the calibration curve is in concentration-time units, this implies that the response for a 10 second exposure of 100 ppm is the same as a 100 second exposure of 10 ppm. This is not the case. To demonstrate this, the amount of [C] generated for the following

Theoretical Fixed Time Exposure Response Curves

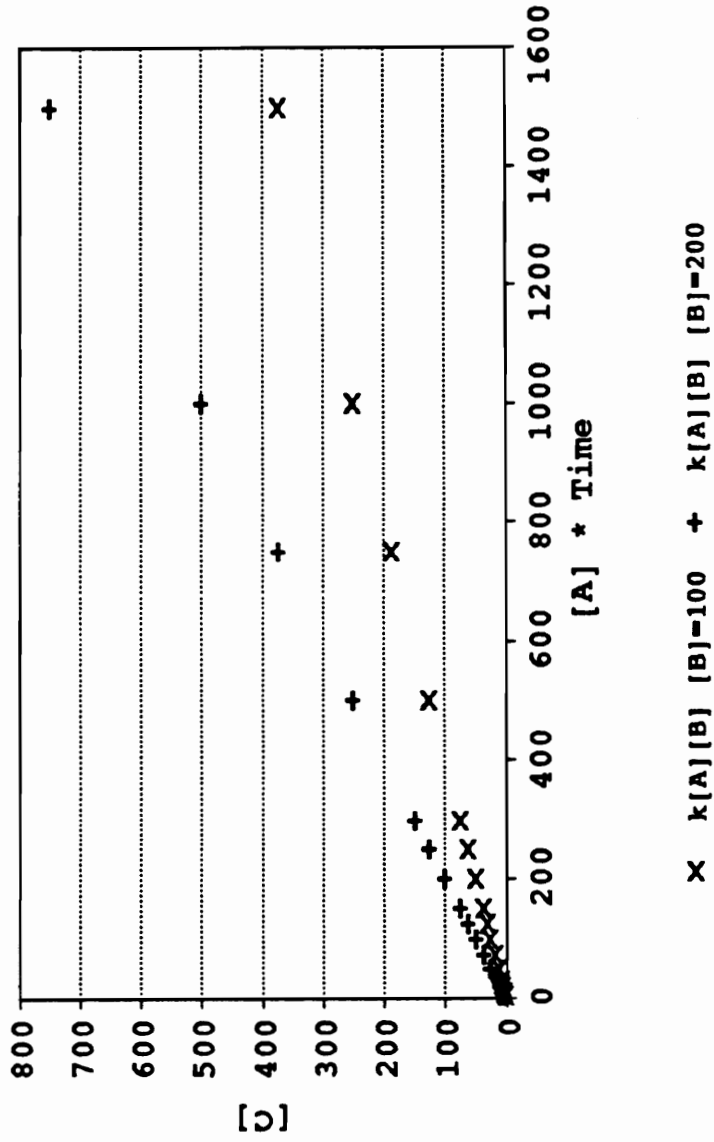
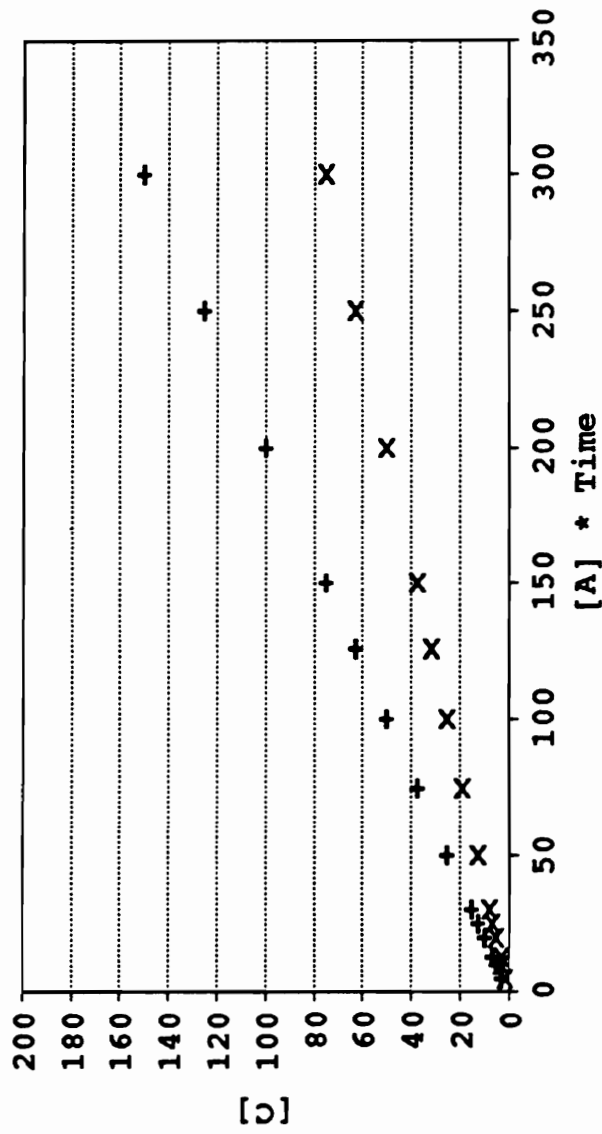


Figure 19. Fixed time exposure response curve for $d[C]/dt = k[A][B]$.

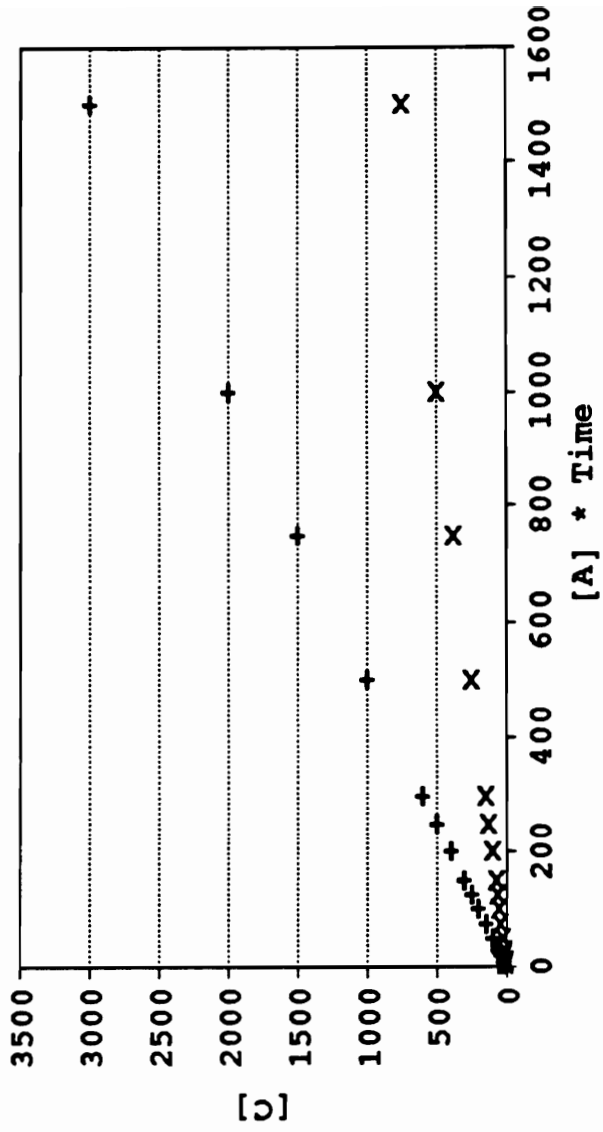
Theoretical Fixed Time Exposure Response Curves



x k[A][B] [B]=100 + k[A][B] [B]=200

Figure 20. Fixed time exposure response curve for $d[C]/dt = k[A][B]$.

Theoretical Fixed Time Exposure Response Curves



x $k[A][B]^2 [B]=100$ + $k[A][B]^2 [B]=200$

Figure 21. Fixed time exposure response curve for $d[C]/dt = k[A][B]^2$.

Theoretical Fixed Time Exposure Response Curves

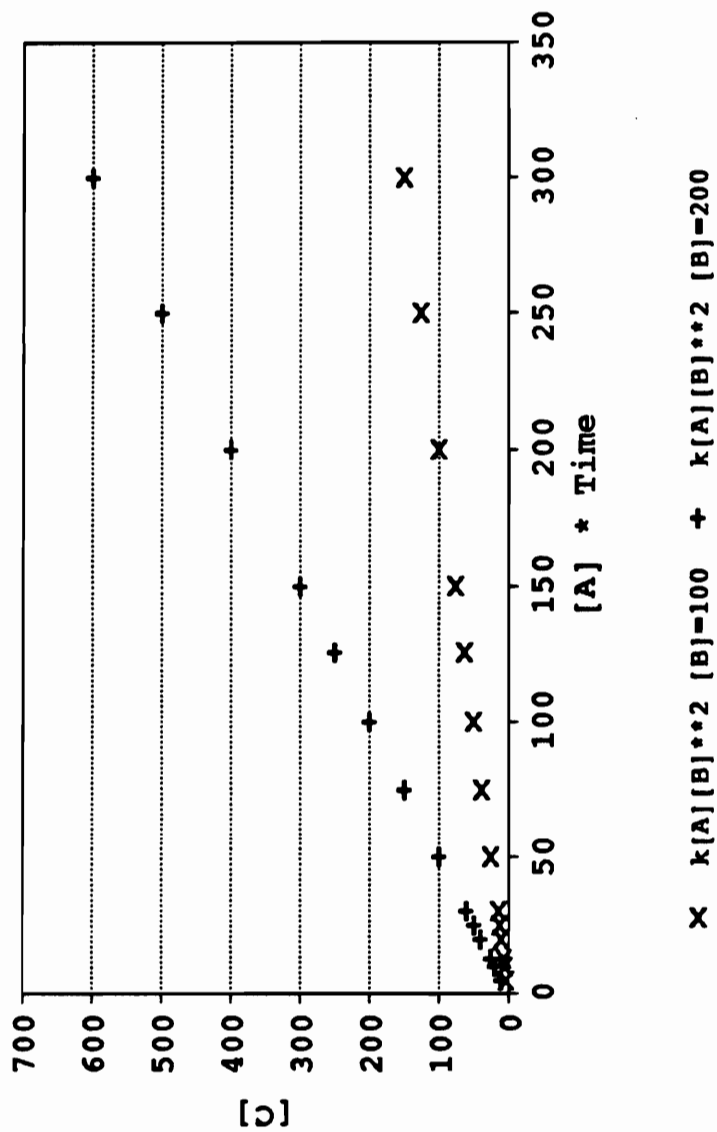
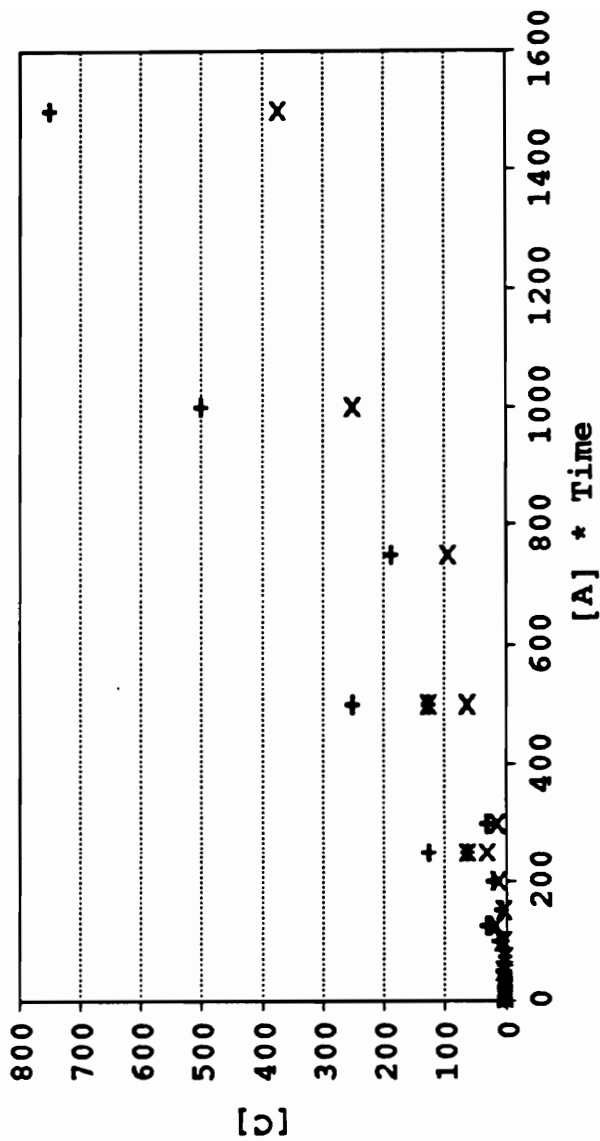


Figure 22. Fixed time exposure response curve for $d[C]/dt = k[A][B]^2$.

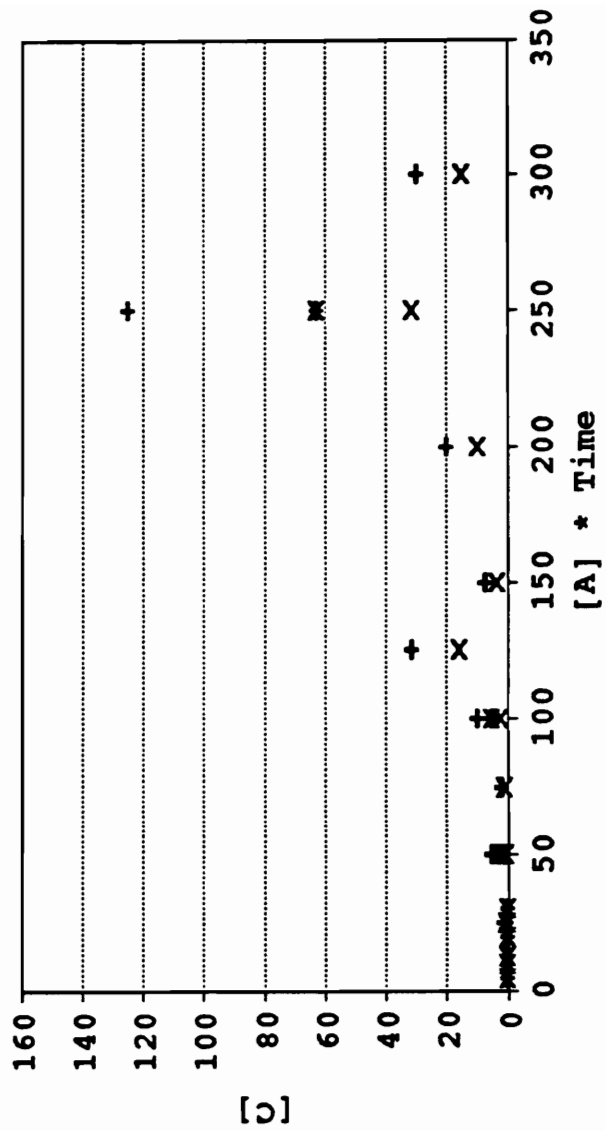
Theoretical Fixed Time Exposure Response Curves



x $k[A]^2[B]$ [B]=100 + $k[A]^2[B]$ [B]=200

Figure 23. Fixed time exposure response curve for $d[C]/dt = k[A]^2[B]$.

Theoretical Fixed Time Exposure Response Curves



x $k[A]**2[B]$ [B]=100 + $k[A]**2[B]$ [B]=200

Figure 24. Fixed time exposure response curve for $d[C]/dt = k[A]^2[B]$.

Theoretical Fixed Time Exposure Response Curves

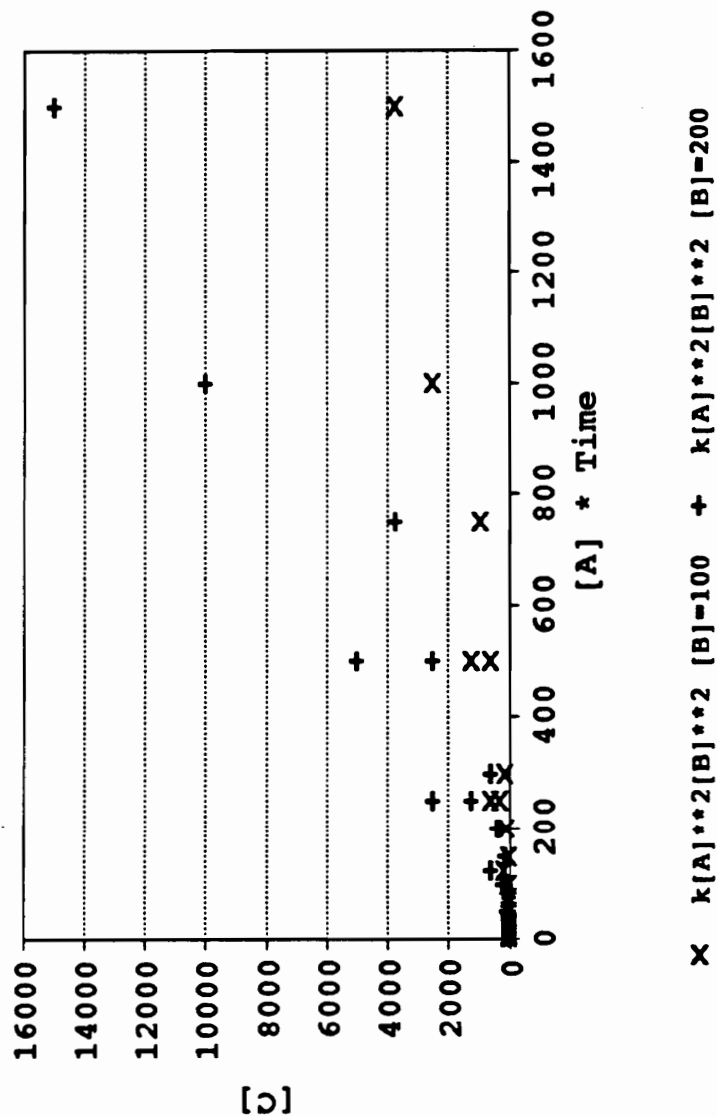
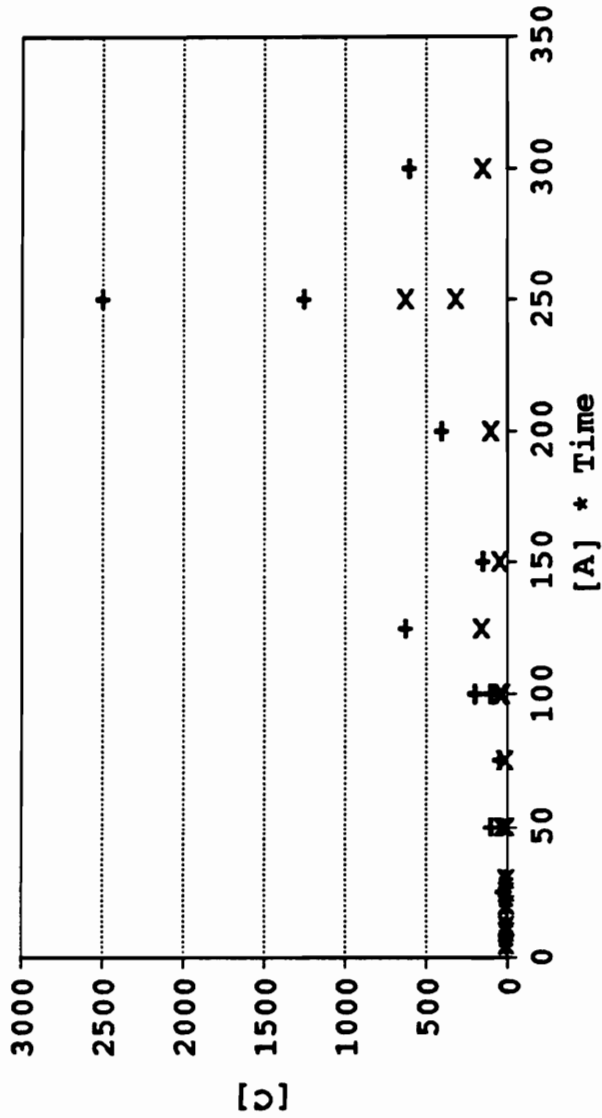


Figure 25. Fixed time exposure response curve for $d[C]/dt = k[A]^2[B]^2$.

Theoretical Fixed Time Exposure Response Curves



$$\times \quad k[A]**2[B]**2 \quad [B]=100 \quad + \quad k[A]**2[B]**2 \quad [B]=200$$

Figure 26. Fixed time exposure response curve for $d[C]/dt = k[A]^2[B]^2$.

Table 1. Theoretical fixed time exposure responses for $d[C]/dt = k[A]^2[B]$.

Theoretical Fixed Time Exposure Responses

Time(sec)	[A]	[A](time)	[B] = 100 k = 0.0001		[B] = 200 k = 0.0001	
			dC/dt = k[A] ² [B]	k[A] ²	dC/dt = k[A] ² [B]	k[A] ²
10	0.5	5	2.50E-02	2.50E-04	5.00E-02	2.50E-04
20		10	5.00E-02	5.00E-04	1.00E-01	5.00E-04
40	60	20	1.00E-01	1.00E-03	2.00E-01	1.00E-03
		30	1.50E-01	1.50E-03	3.00E-01	1.50E-03
	1.25	12.5	1.56E-01	1.56E-03	3.13E-01	1.56E-03
		25	3.13E-01	3.13E-03	6.25E-01	3.13E-03
		50	6.25E-01	6.25E-03	1.25E+00	6.25E-03
	2.5	75	9.38E-01	9.38E-03	1.88E+00	9.38E-03
		25	6.25E-01	6.25E-03	1.25E+00	6.25E-03
		50	1.25E+00	1.25E-02	2.50E+00	1.25E-02
	5	100	2.50E+00	2.50E-02	5.00E+00	2.50E-02
		150	3.75E+00	3.75E-02	7.50E+00	3.75E-02
		50	2.50E+00	2.50E-02	5.00E+00	2.50E-02
	12.5	100	5.00E+00	5.00E-02	1.00E+01	5.00E-02
		200	1.00E+01	1.00E-01	2.00E+01	1.00E-01
		300	1.50E+01	1.50E-01	3.00E+01	1.50E-01
	25	125	1.56E+01	1.56E-01	3.13E+01	1.56E-01
		250	3.13E+01	3.13E-01	6.25E+01	3.13E-01
		500	6.25E+01	6.25E-01	1.25E+02	6.25E-01
	25	750	9.38E+01	9.38E-01	1.88E+02	9.38E-01
		250	6.25E+01	6.25E-01	1.25E+02	6.25E-01
		500	1.25E+02	1.25E+00	2.50E+02	1.25E+00
	25	1000	2.50E+02	2.50E+00	5.00E+02	2.50E+00
		1500	3.75E+02	3.75E+00	7.50E+02	3.75E+00

concentrations and times is

$$[C] = k[10]^2[B](100) = 10000(k[B]) \quad (49)$$

$$[C] = k[100]^2[B](10) = 100000(k[B]) \quad (50)$$

Although the concentration-time product is the same for these two cases, the amounts of [C] generated are different by an order of magnitude.

The implication of this analysis is that an attempt to generate a calibration curve using a concentration-time axis will generate a plot that is scattered. This is due to the second order dependence of [C] on [A]. Using the calculated information found in Table 1 to generate the calibration curve in figures 23 and 26, it is apparent why this scattering occurs.

Normalizing the information for different fixed concentrations of [B], the graph of ([C]/[B]) versus ([A]*time) yields a slope for the associated equations, as shown

$$\text{slope} = k \quad \text{for } [C] = k[A][B](t_f - t_i) \quad (\text{Figure 27}) \quad (51)$$

$$\text{slope} = k[B] \quad \text{for } [C] = k[A][B]^2(t_f - t_i) \quad (\text{Figure 29}) \quad (52)$$

$$\text{slope} = k[A] \quad \text{for } [C] = k[A]^2[B](t_f - t_i) \quad (\text{Figure 31}) \quad (53)$$

and

$$\text{slope} = k[A][B] \quad \text{for } [C] = k[A]^2[B]^2(t_f - t_i) \quad (\text{Figure 33}) \quad (54)$$

In the first case, normalized curves for two different concentrations of [B] will be the same, overlapping each other, and will be the rate constant for the reaction.

The second equation will show two different curves due to second order dependence of the reaction rate upon [B]. Each curve will be linear since the concentration of [B] is fixed for each calibration curve.

The third equation will still have a scatter appearance due to the second order dependence of the reaction rate upon [A]. The two curves will overlap since the slope is now independent of [B].

Normalized Theoretical Fixed Time Exposure Response Curves

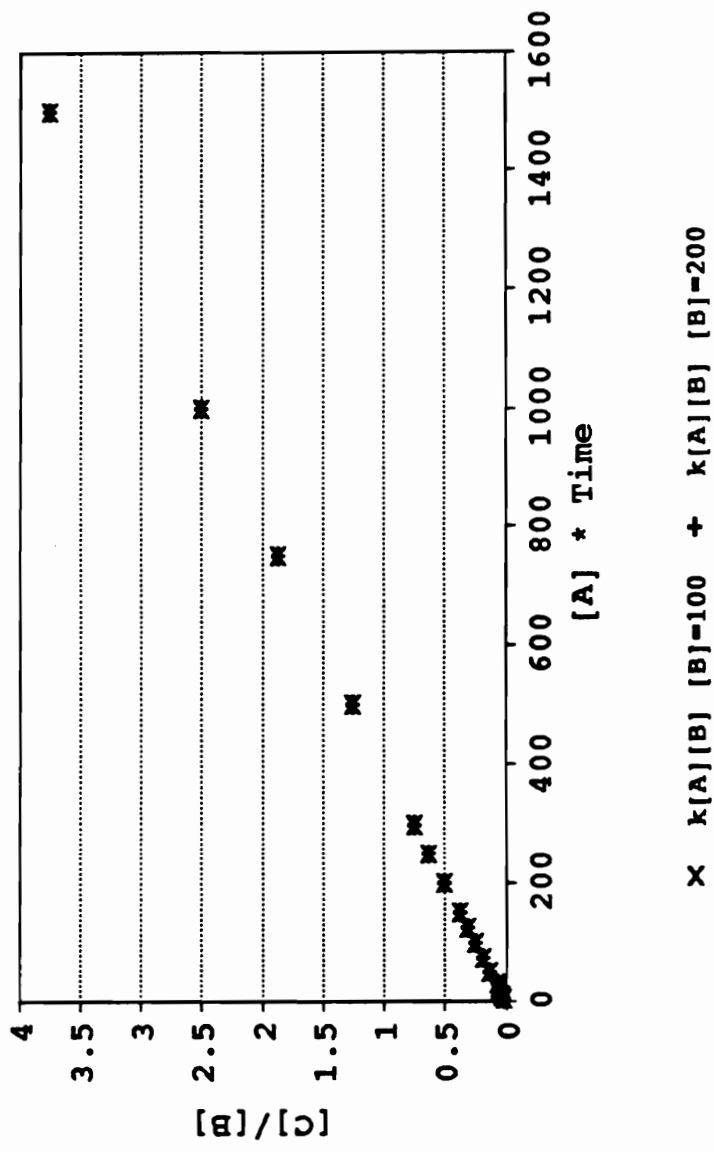


Figure 27. Normalized fixed time exposure response curve for $d[C]/dt = k[A][B]$.

Normalized Theoretical Fixed Time Exposure Response Curves

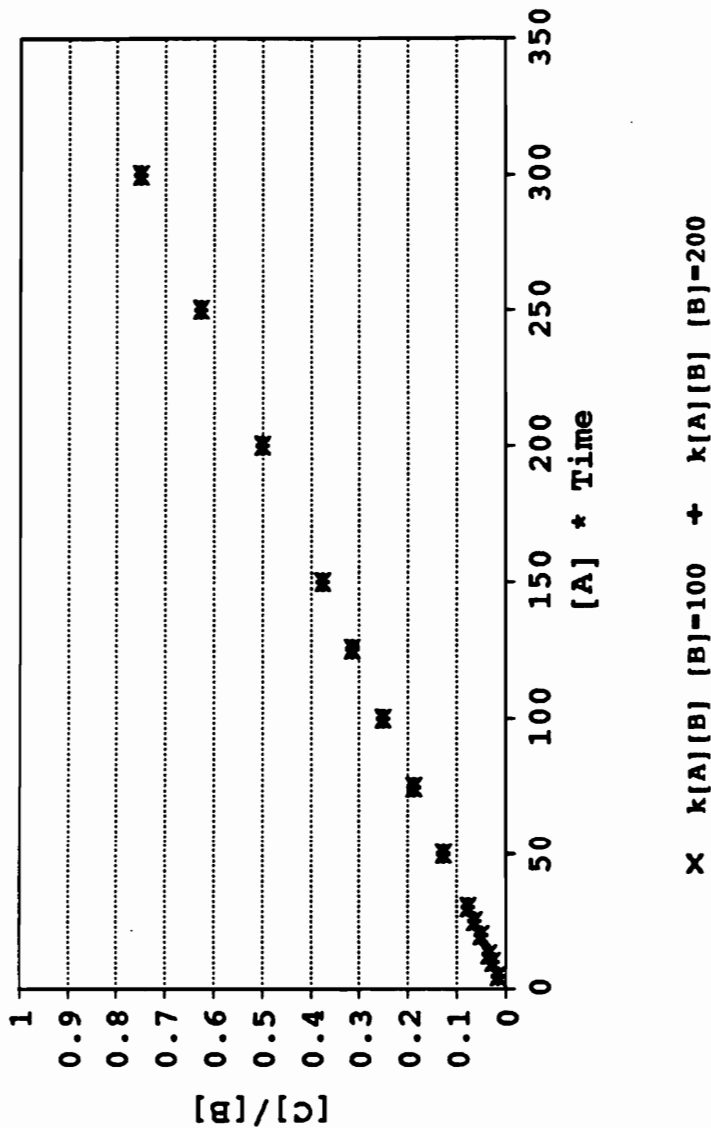


Figure 28. Normalized fixed time exposure response curve for $d[C]/dt = k[A][B]$.

Normalized Theoretical Fixed Time Exposure Response Curves

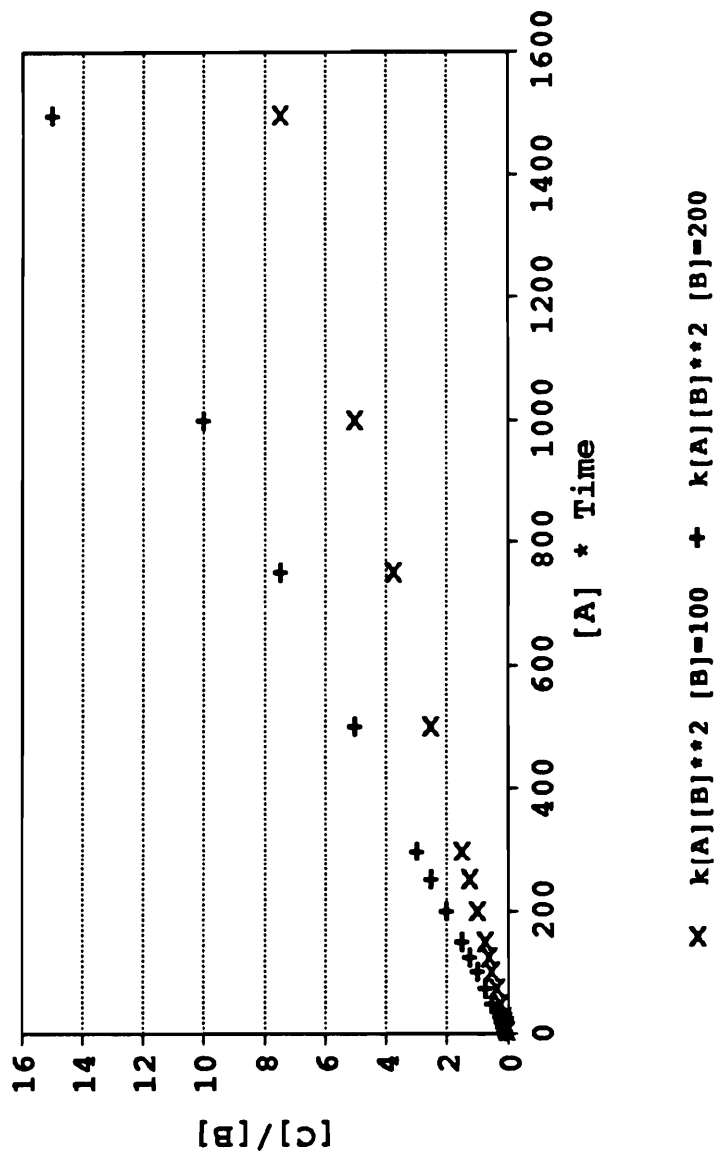
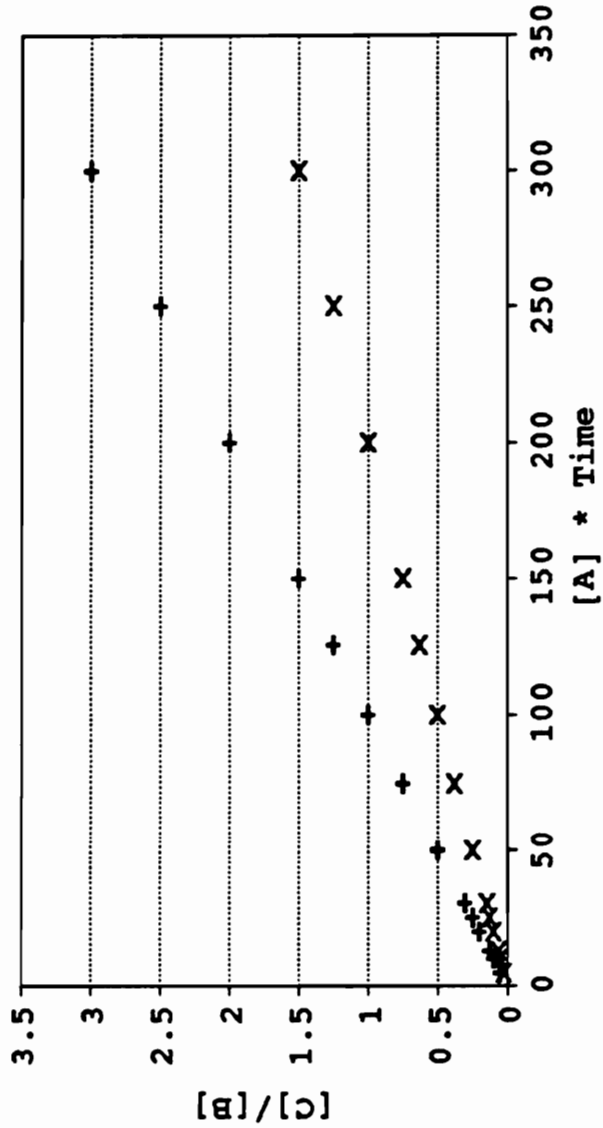


Figure 29. Normalized fixed time exposure response curve for $d[C]/dt = k[A][B]^2$.

Normalized Theoretical Fixed Time Exposure Response Curves



x $k[A][B]**2 [B]=100$ + $k[A][B]**2 [B]=200$

Figure 30. Normalized fixed time exposure response curve for $d[C]/dt = k[A][B]^2$.

Normalized Theoretical Fixed Time Exposure Response Curves

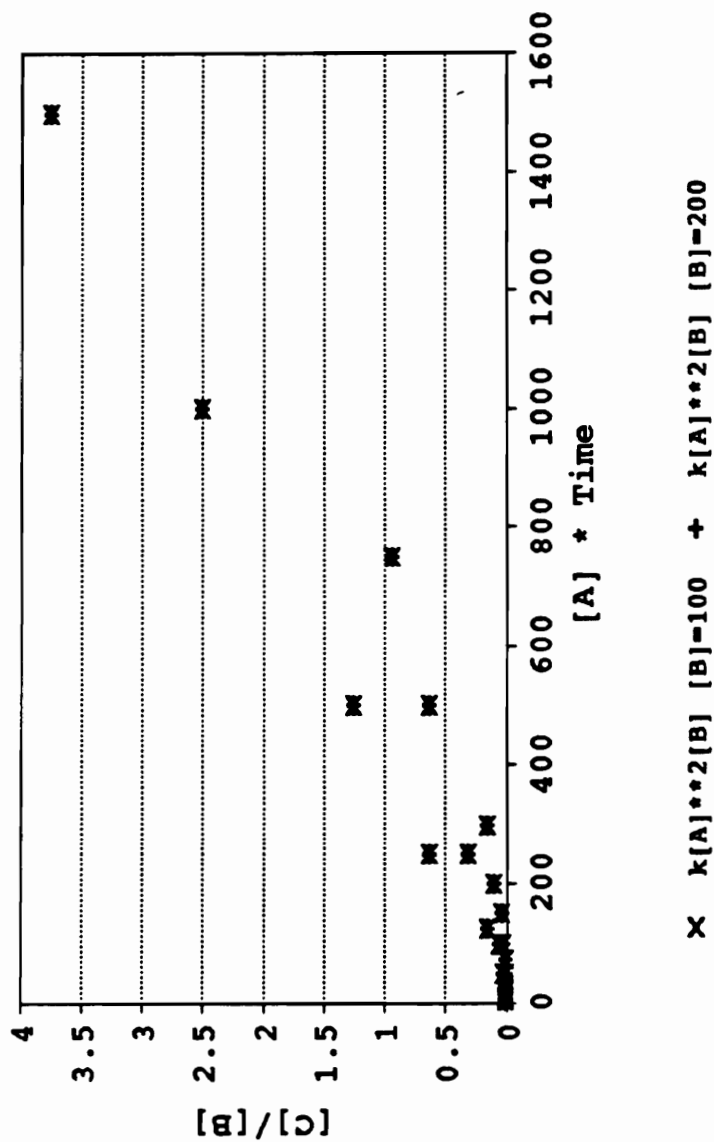


Figure 31. Normalized fixed time exposure response curve for $d[C]/dt = k[A]^2[B]$.

Normalized Theoretical Fixed Time Exposure Response Curves

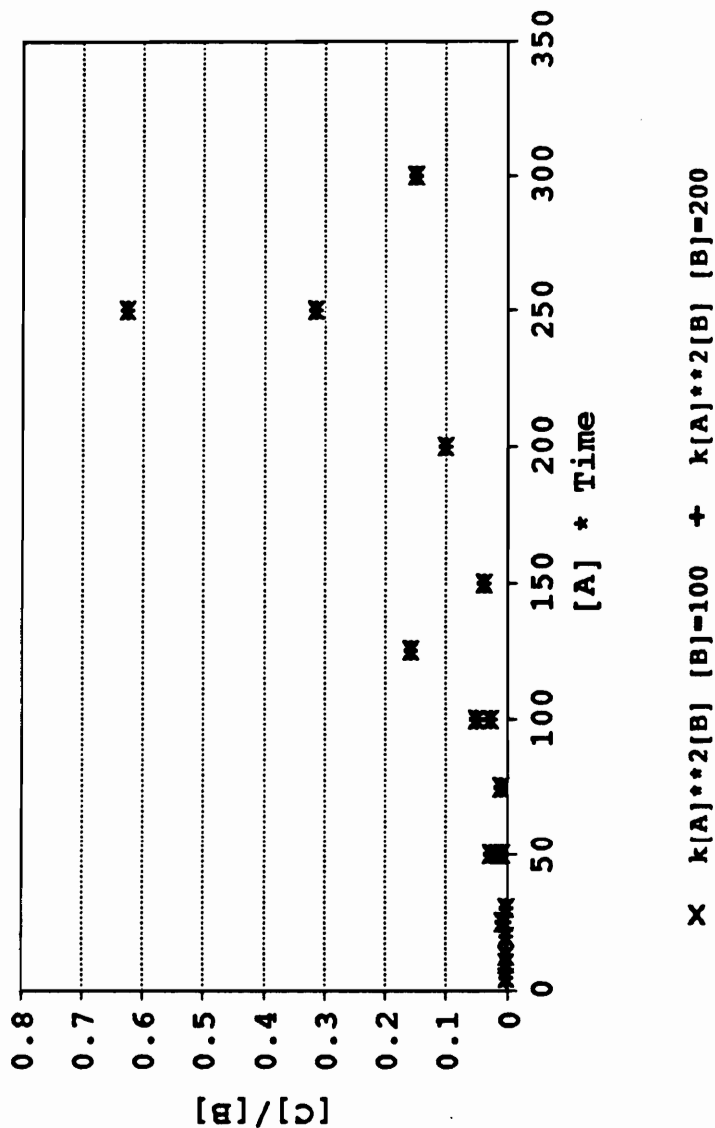


Figure 32. Normalized fixed time exposure response curve for $d[C]/dt = k[A]^2[B]$.

Normalized Theoretical Fixed Time Exposure Response Curves

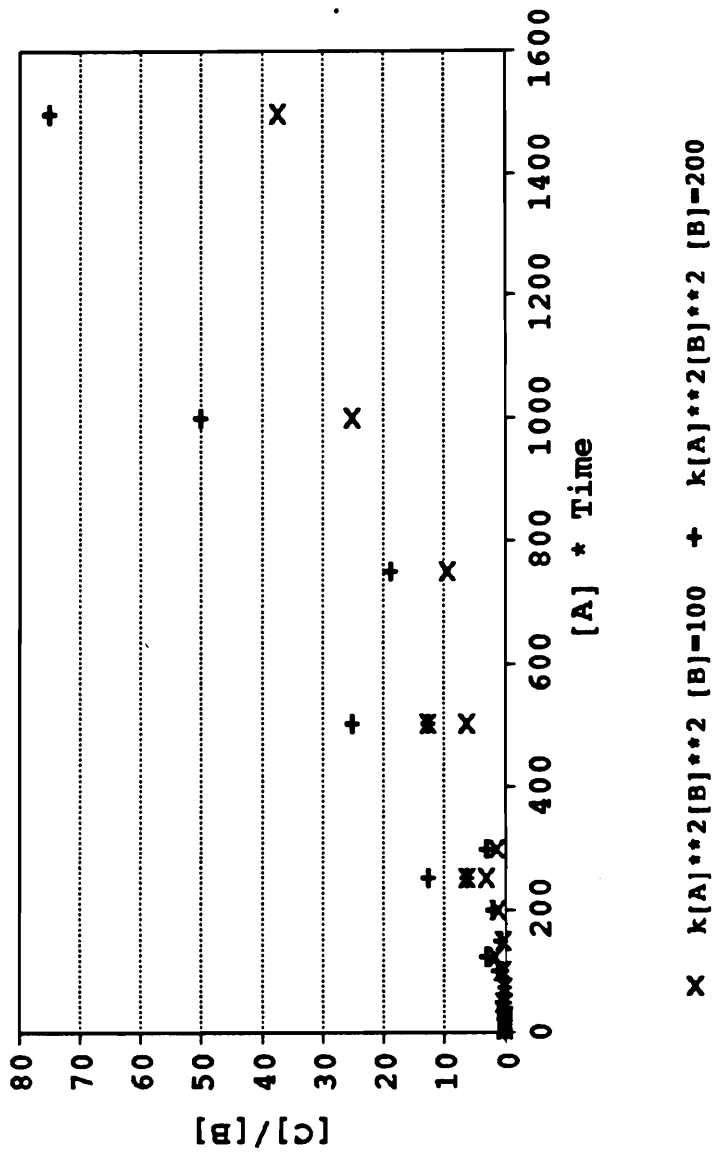
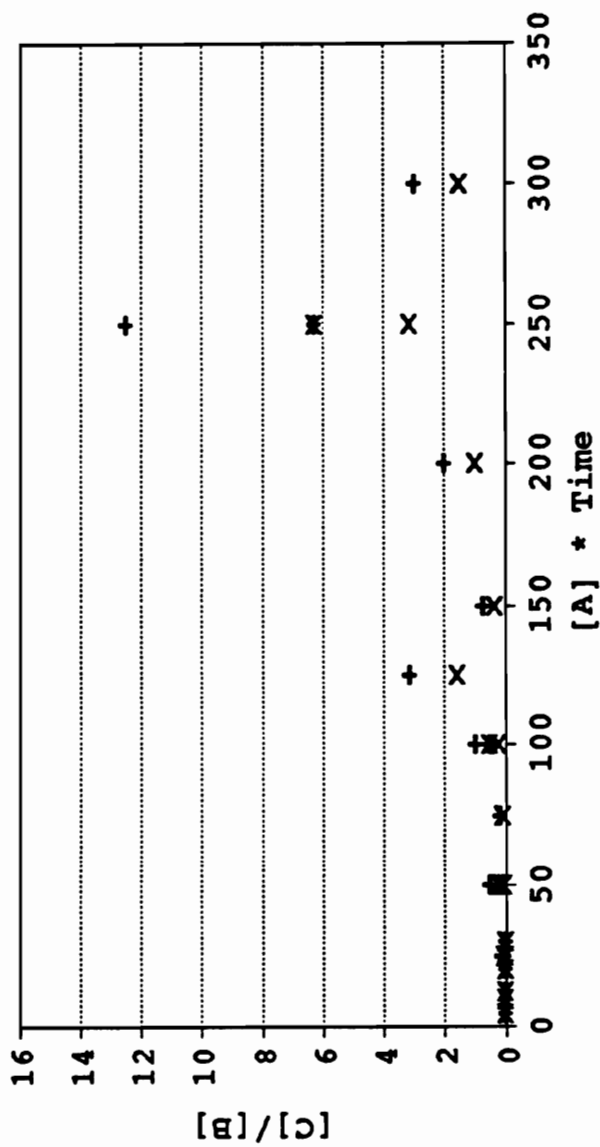


Figure 33. Normalized fixed time exposure response curve for $d[C]/dt = k[A]^2[B]^2$.

Normalized Theoretical Fixed Time Exposure Response Curves



$$x \quad k[A]**2[B]**2 \quad [B]=100 \quad + \quad k[A]**2[B]**2 \quad [B]=200$$

Figure 34. Normalized fixed time exposure response curve for $d[C]/dt = k[A]^2[B]^2$.

Finally the fourth equation will be scattered due to the second order dependence on [A] and will show two curves due to the second order dependence on [B].

In conclusion, when the data is analyzed appropriately in the form of rate of production, or the amount of product produced for a fixed exposure time, the generation of calibration curves and normalized calibration curves will display the effect of each reactant in the kinetics of the reaction.

The reason that this detailed analysis has been introduced is that it is fundamental to an understanding of data generated by a SAW device used in dosimetric applications. The device is covered by a film that reacts with a vapor. If it is irreversible, the film, containing a concentration of [B] large enough to ensure flooding, is exposed to vapor of concentration [A] producing a product [C]. The rate of production and amount produced of [C] is what generates the signal obtained from a SAW device.

In the specific case for phosgene monitoring, as stated earlier, reactions of 4-(4'-nitrobenzyl)pyridine and phosgene in solution occur by an S_N2 mechanism, thereby showing first order dependence upon the rate of reaction for both the concentration of 4-(4'-nitrobenzyl)pyridine and phosgene⁵⁸. As used in solid dosimeter crayons, Witten and Prosak developed a calibration curve using the ppm-minute exposure value, implying first order dependence of the reaction with respect to the phosgene concentration. Analysis of the responses generated and the calibration curves developed from these responses will indicate if the results from this study are consistent with these previously cited studies.

D) SAW Device Response

From the previous discussion, the physical events occurring on the surface of a SAW device are controlled by the permeability of the vapor in the film and the subsequent reaction of the vapor with a flooded reagent contained in the film. How the SAW device measures these events is dealt with in this section.

A film in intimate contact with a SAW device will create a frequency change based upon the following relationship

$$\Delta f = \Delta f_m - \Delta f_s \quad (55)$$

$$\Delta f = (k_1 + k_2)f_o^2 hp - k_2 f_o^2 h(4\mu/V_R^2)[(\lambda + \mu)/(\lambda + 2\mu)] \quad (56)$$

For films of a low shear modulus (above the glass transition temperature), the equation reduces to

$$\Delta f = (k_1 + k_2)f_o^2 hp \quad (57)$$

The equation describes the change in frequency due to mass loading on the surface, since hp is a mass per unit area term. The change in mass will generate a linear change in frequency.

The equation can be reduced to mass loading effects because the shear modulus of a film above the glass transition temperature is on the order of 10^6 N/m^2 ⁷⁴.

Evaluation of an ST-quartz SAW device with a free surface oscillation frequency of 31 MHz and a film thickness of 1 μm yields

$$\Delta f_s = -(-4.16 * 10^{-8} \text{ m}^2 \text{ sec/kg})(31*10^6/\text{sec})^2 (10^{-6} \text{ m}) \quad (58)$$
$$*(4(10^6 \text{ N/m}^2)/(3159 \text{ m/sec})^2)[(\lambda + \mu)/(\lambda + 2\mu)]$$

$$\Delta f_s = 16 \text{ Hz} \quad \text{where } [(\lambda + \mu)/(\lambda + 2\mu)] = 1$$

The evaluation of the mass loading effect for the same film (with density of 1 g/cc) is

$$\Delta f_m = (-9.33 * 10^{-8} \text{ m}^2 \text{ sec/kg} + -4.16 * 10^{-8} \text{ m}^2 \text{ sec/kg}) \quad (59)$$

$$* (31 * 10^6 / \text{sec})^2 (10^{-6} \text{ m}) (1000 \text{ kg/m}^3)$$

$$\Delta f_m = -129.6 * 10^3 \text{ Hz}$$

The frequency shift due to polymer modulus effects for polymers above their glass transition temperature is negligible. It should also be noted that a mass increase on the surface of the SAW device generates a decrease in the oscillation frequency.

In the case of a dosimeter, the reagent contained in the film will undergo an irreversible reaction with the target vapor producing a new compound of a different molecular weight. The change in molecular weight creates an increase in the mass of the film leading to a decrease in the oscillating frequency of the SAW device.

An example of this relationship should prove to be enlightening. Using the simple system examined kinetically,



assume that a 50 percent by weight mixture containing reagent [B], having a molecular weight of 200, is applied to the surface of a SAW device. The frequency shift produced by this sensing film is 40 KHz. The molecular weight of reagent [A] contained in the vapor is assumed to be 200. The net reaction produces product [C] with a molecular weight of 400. If this reaction is allowed to go to completion, then the maximum increase in mass of the film would be 50 percent due to the change in molecular weight of reacting [B] into product [C]. This would appear as a further change of 20 KHz in the oscillating frequency, generating a total frequency shift of 60 KHz from the free surface oscillation frequency. If the molecular weight of reagent [A] contained in the vapor had only been 50 atomic mass units resulting in product [C] having a molecular weight of 250, the maximum increase in mass would only be 12.5 percent, leading to a frequency shift of only 5 KHz.

Since SAW device frequency shifts are linearly related to mass changes on the surface of the film, the amount of [C] produced will be linearly related to the frequency shift encountered at the output of a SAW device. Therefore the amount of frequency shift indicates a particular amount of [C] produced. The rate at which the frequency changes with time during vapor sensing, df/dt , is proportional with the rate of production of [C] with time, $d[C]/dt$. This effect was noted in a previously reported irreversible dosimeter for the detection of cyclopentadiene⁷⁵ and for a reversible dosimeter for styrene vapor⁷⁶. Therefore frequency measurements and the first derivative of these measurements (df/dt) are a direct reflection of the film response to the vapor and will be used in this work as the response factor for evaluating these films.

In order to maximize the frequency response of the device, the ratio of the molecular weights of the vapor reagent [A], and flooded reagent [B] needs to be considered. In theory, to maximize response, the target vapor molecular weight [A] should be greater than that of the trapping agent [B], since this would lead to greater mass changes in the film for each molecule of trapping agent. Theoretical systems are sometimes unattainable in reality so the chemical system that is investigated will dictate the molecular weight ratios for the vapor and trapping agents.

The calculated frequency shifts are based upon total consumption of reagent [B] in the film. As an analytical device used to monitor the concentration of vapor [A], the goal is to have the SAW device response be representative of the concentration of [A]. Total consumption of the film cannot occur in the useable lifetime of the film. As the flooding reagent [B] is consumed, the rate of production of [C],

$$d[C]/dt = k'[A] \quad (61)$$

where $k' = k[B]$ and $[B]$ is constant, will no longer be a reflection of the concentration of $[A]$ but will be

$$d[C]/dt = k[A][B]. \quad (62)$$

As $[B]$ is consumed, the flooded condition of the film is no longer maintained. The rate of production of $[C]$ and the amount of $[C]$ produced will be a function of both the concentration of $[A]$ and $[B]$, since the concentration of $[B]$ will no longer be constant during the time of analysis. At this point, the SAW device response is a function of the concentrations of both $[A]$ and $[B]$ and not just $[A]$.

E) Model Experimental Response

Polymeric films containing flooded reagent $[B]$ can be used for long term or short term exposure monitoring of vapor $[A]$. Each of these cases will be evaluated separately.

1) Long term response model

In the long term exposure experiments, the film will be exposed to a constant concentration of vapor containing $[A]$ for an extended time period (minutes to hours). The production of product $[C]$ will depend upon two parameters, the amount of vapor $[A]$ that will permeate into the film and the rate at which $[A]$ will react with $[B]$ to produce $[C]$.

The rate of production of $[C]$ will follow two possible patterns depending upon whether permeation or reactivity is the rate determining step.

If permeation is rate limiting, what is expected is that the rate of production of $[C]$ will be a constant, the value dependent upon the concentration of $[A]$ in the vapor phase. This conclusion is reached because the system will function like a permeation

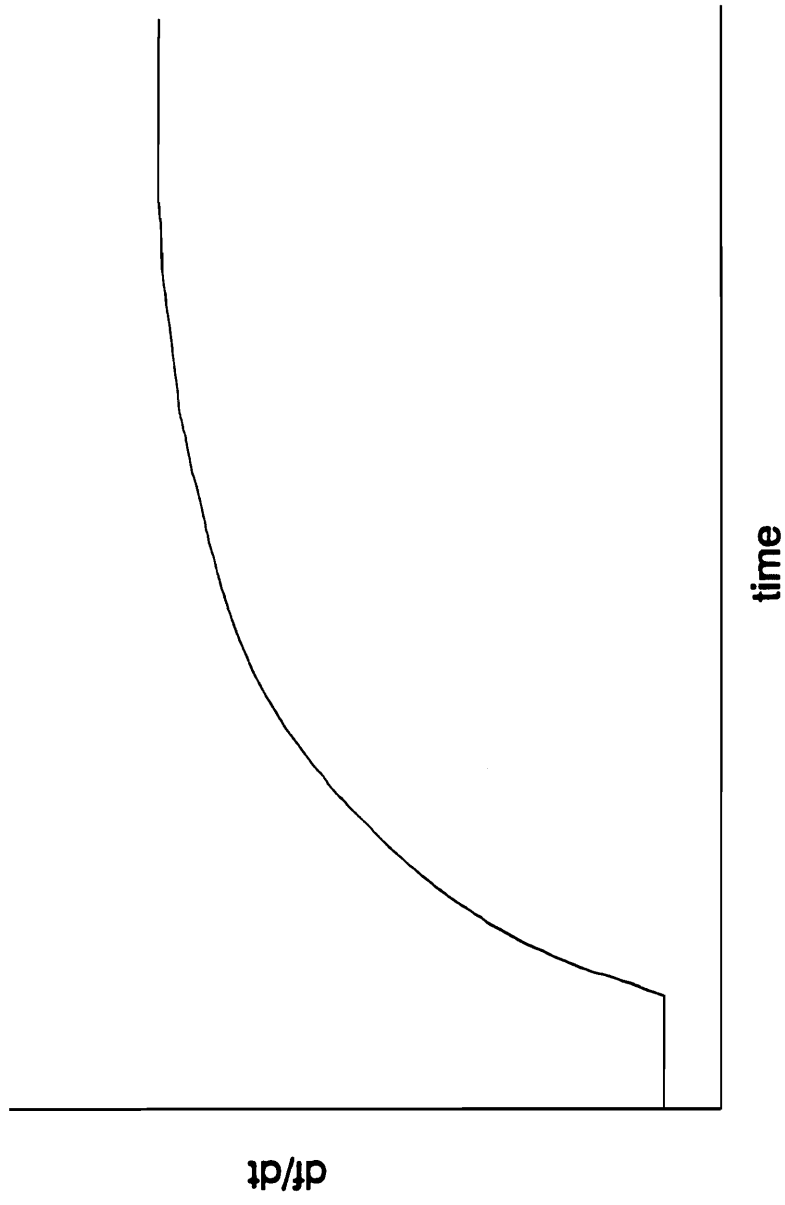


Figure 35. Permeation rate limiting curve.

tube. If the permeation rate is less than the reaction rate, the effective concentration of [A] in the film will approach zero. Since the concentration of [A] in the vapor phase above the film is constant, the rate of permeation of [A] into the film will be constant (Figure 35).

If the chemical reaction is rate limiting, then an increasing rate of production of [C] will be the result. As a constant concentration of vapor [A] flows across the film, the concentration of [A] in the film will increase with time. Since the permeability of the film to [A] is greater than the reaction rate for the production of [C], this will ensure that the concentration of [A] in the film will increase with time. Since

$$d[C]/dt = k'[A]^x \quad (x = \text{either } 1, 2, \dots) \quad (63)$$

where $k' = k[B]^y$ ($y = \text{either } 1, 2, \dots$) with $[B]^y$ constant, increasing [A] will increase $d[C]/dt$.

Two outcomes from this scenario are possible. If [A] continues to increase until the concentration of [B] is no longer in a flooded state, the rate of production of [C] will increase to a maximum and then decrease as the concentration of [B] becomes dominant in the rate of production of [C] (Figure 36).

The graph of this particular experiment will yield information describing the expected film lifetime. At the point at which the maximum rate of production of [C] is obtained, the concentration of [B] will no longer be flooded. At this point the film response is no longer dependent upon the concentration of [A] alone and is therefore considered consumed. A film constant can be calculated based upon four factors; the film thickness, the concentration of reagent [B] in the film, the concentration of vapor [A] and the time necessary to reach this rate maximum at the concentration of [A] used (i.e. film lifetime). This film exposure constant will have the units of

$$\text{Exposure} = (\text{ppm-second})/(\text{KHz-\%}[B]) \quad (64)$$

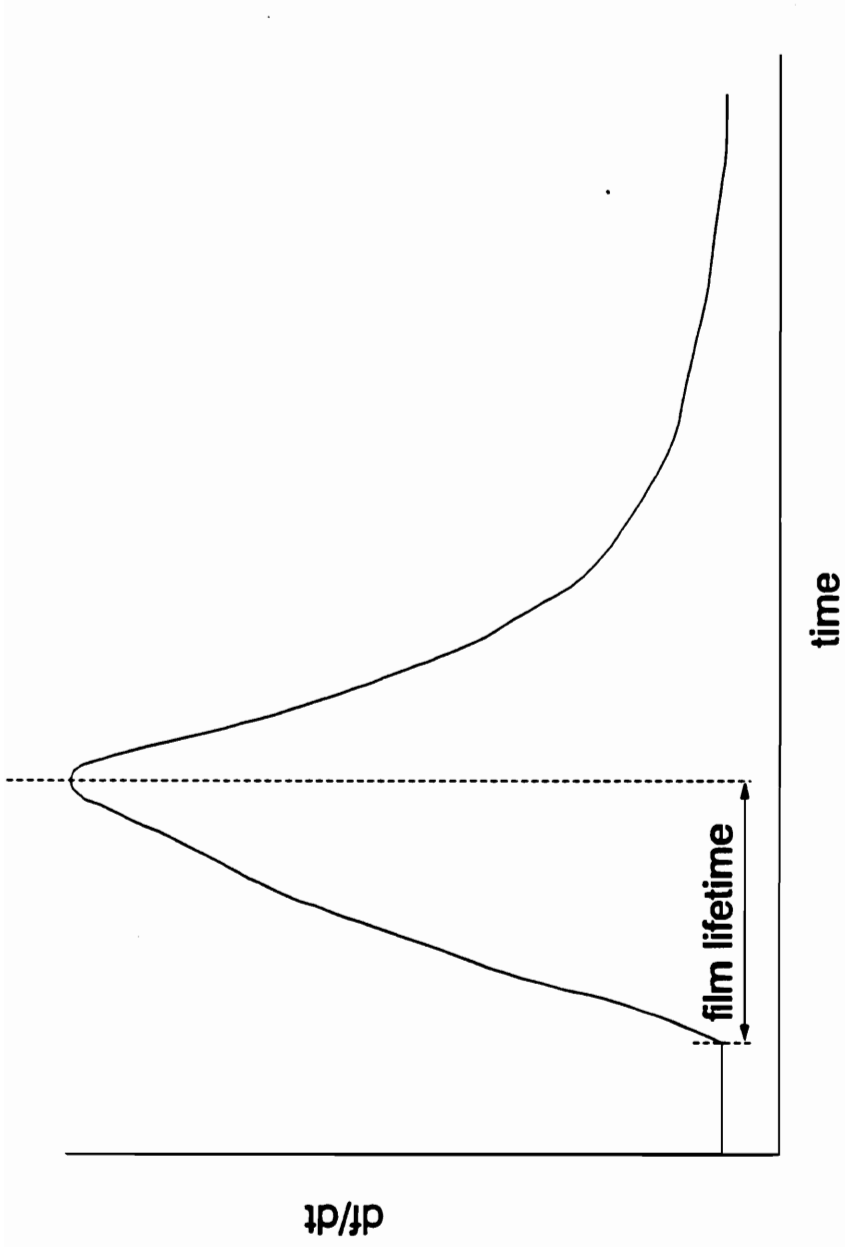


Figure 36. Film consumption by permeating vapor.

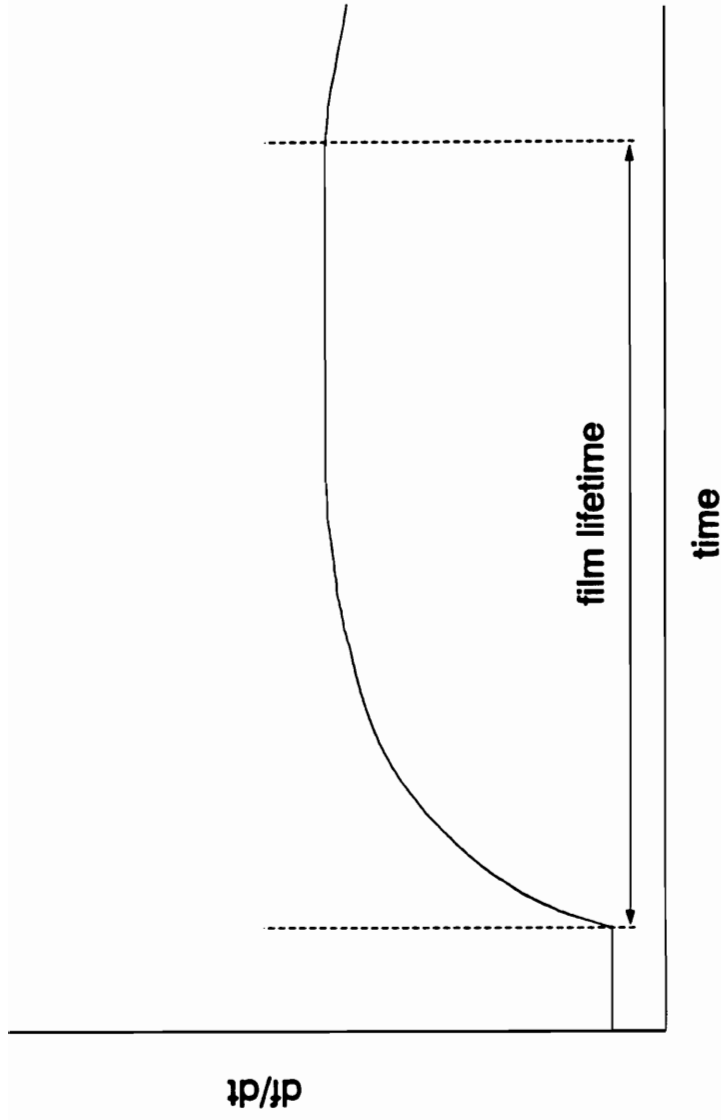


Figure 37. Steady state film loading.

if the concentration of [B] is measured in weight percentage of the film, the exposure level of [A] in parts per million, the film lifetime in seconds and the film thickness in kilohertz of frequency shift of the SAW from the clean surface oscillating frequency. These film exposure constants can be calculated for different vapor concentrations of [A], the use of different vapors for exposure, different film thicknesses, different weight percentages of [B] in the film and different polymer supports. The film exposure constants will serve as a convenient reference number with which to rate and compare films, their responses and expected lifetimes.

The other scenario is that a steady state concentration of [A] will be reached in which the amount of [A] to permeate into the film will be balanced with the amount of [A] consumed in the reaction. At this point, the rate of production of [C] will become constant. This will continue until the concentration of [B] is no longer flooded. At this point the rate of production of [C] will start to decrease with time as the concentration of [B] decreases in the film. As stated before, film exposure constants can be calculated for these cases from the point at which the concentration of [B] appears to affect the rate of production of [C] (Figure 37).

2) Short term response model

Short term exposure experiments to reagent [A] can consist of exposure times which amount to seconds or minutes to a constant concentration of reagent [A] for the duration of the exposure period. The choice of particular time segments is usually based upon a few considerations.

The detector volume may determine the minimum sample size that can be accommodated. To make this more concrete, let us use a few numbers. At a flow rate of 100 cc/min, a 10 second increment (0.17 minutes) corresponds to 17 cc of volume.

The detector cell volume for this particular experimental setup is 12 cc. Therefore an exposure period of six seconds or less would render a sample size that is equal to or less than the cell volume.

For extremely low level detection, the amount of material necessary to generate a signal may require a sample size that, at a particular flow rate, will require an extended exposure time. Conversely, monitoring high concentrations will usually require short exposures due either to the signal that can be generated in the exposure time or to the toxic nature of the vapor. For example, it would be ill-advised to require 60 seconds of exposure of 400 ppm phosgene as the analysis time necessary for the detector to generate a signal. The simple fact is that a concentration of 400 ppm phosgene for one minute is sufficient to cause death. In this instance the user of the device would be a better dosimeter for high concentrations of phosgene exposure than the device itself.

The response characteristics for sequentially timed exposures of reagent [A] will be a change in the frequency output of the SAW device detector for each exposure to reagent [A]. A time versus frequency graph for these sequential exposures will result in a staircase output (Figure 38) as exposures are introduced. The amount of mass loading, and therefore frequency shift, will be dependent upon the irreversible chemisorption of reagent [A] into the film, which manifests itself as the production of product [C].

The overall kinetics of permeation and reaction will determine the amount of mass loading that the SAW device will undergo. As discussed for long term exposures, the rate of production of [C] will either be dependent upon whether permeability or the rate of reaction between [A] and [B] is rate limiting.

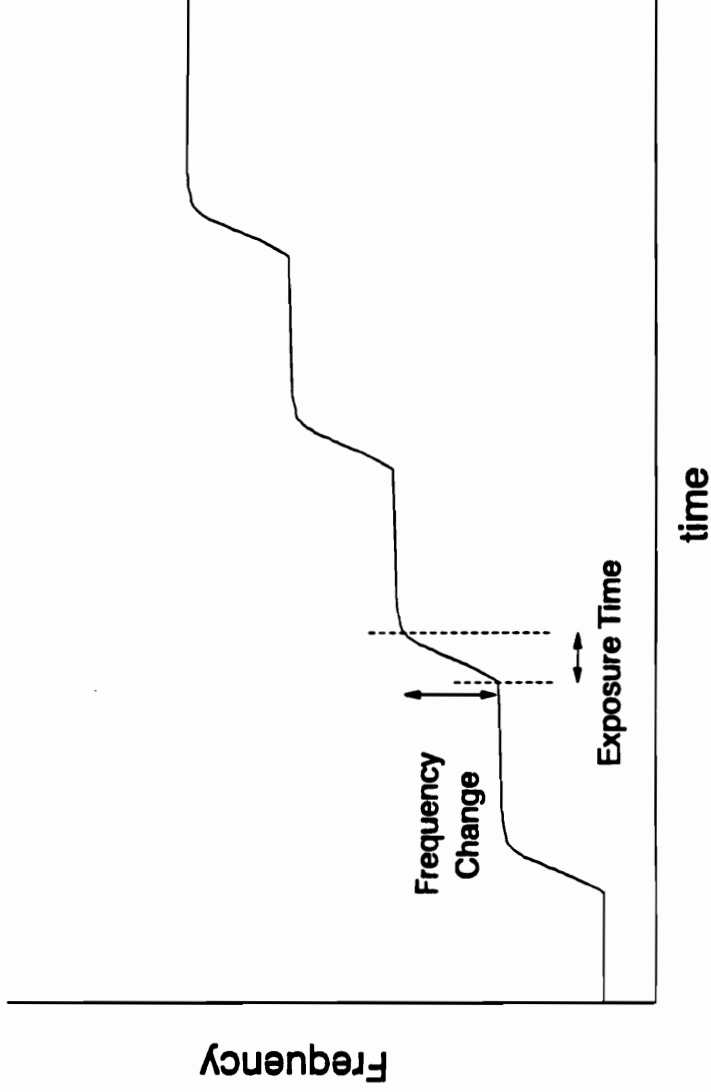


Figure 38. Multiple fixed time exposures.

If the reaction is rate limiting, the situation can become complicated. If the permeability of the film to [A] is greater than the rate of reaction of [A] with [B], the concentration of [A] will increase within the film. This will correspond to an increase in the reaction rate since

$$d[C]/dt = k'[A]^x \quad (x = 1,2,..) \quad (65)$$

where $k' = k[B]^y$ ($y = 1,2,..$) with $[B]^y$ constant. Increasing the concentration of reagent [A] in the film will increase $d[C]/dt$.

The consequences of this result is that a calibration curve of frequency change versus exposure time for a fixed concentration of [A] will not necessarily be linear. Since $d[C]/dt$ is increasing with time, the change in frequency at an early time in the exposure will be less than that at a later time (Figure 39). If the area under the curve generated from a plot of the rate of change of [C] versus time for the time periods of 0 to 20 seconds, 20 to 40 second, and 40 to 60 seconds are measured, it will be determined that the 0 to 20 second area is less than the 20 to 40 second area which is less than the 40 to 60 second area.

If permeability is the rate limiting step, the response will be dependent solely on the vapor concentration of [A]. This conclusion is reached based upon the permeation tube analogy. As the vapor permeates the film, it is consumed at a rate which is faster than that at which it permeates. Therefore the effective concentration in the film approaches zero. The calibration curve generated for this condition will be dependent upon whether the permeability of the film is or is not linearly dependent upon the vapor concentration above it.

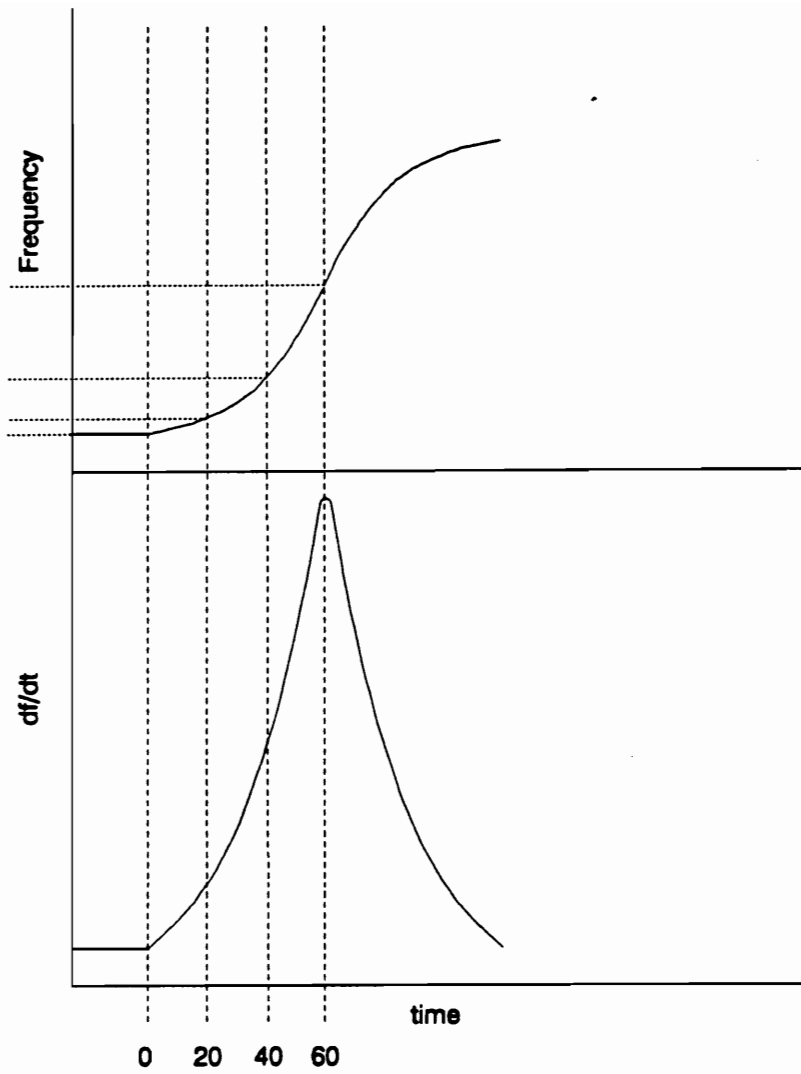


Figure 39. Frequency and frequency change rate.

INSTRUMENTAL

A) Detector and associated apparatus.

The detector used for phosgene, thionyl chloride and ethylene oxide sensitive films is based on a Surface Acoustic Wave device designed by Wohltjen and is available from Microsensor Systems, Inc. (6800 Versar Center, Springfield, Virginia 22151, 703-642-6919). The device is a 31 Megahertz acoustic delay line fabricated on an ST Quartz substrate (1/2 inch wide and 2 inches long). The interdigital electrodes consist of 50 finger pairs of 2000 angstrom gold on 200 angstroms of chromium. Each finger is 25 microns wide and is spaced 25 microns from the adjacent finger. The finger overlap length is 7250 microns. The center to center spacing between the interdigital transducer (IDT) electrodes is 2.0 centimeters.

The SAW device is configured to operate as an oscillator. Two separate oscillator circuits are used in the detector cell, one containing a sample SAW device which is coated with the vapor sensitive film and the other containing a SAW device which is coated with the support matrix acting as a reference device.

The actual circuit utilizes a TRW CA2820 wide bandwidth linear hybrid amplifier to drive the circuit into oscillation. The CA2820 has a bandwidth of 1 to 520 Megahertz with a 30 db gain and 25 to 75 ohm impedance. The amplifier output drives the SAW delay line to oscillate at its particular resonant frequency by being configured in a feedback loop with the SAW device (Figure 40). The 1.0 microhenry coils on the input and output of the SAW device is to facilitate impedance matching and to prevent power reflections between the amplifier and SAW device. The system is configured to have an impedance of 50 ohms, since the input impedance of a SAW transducer is

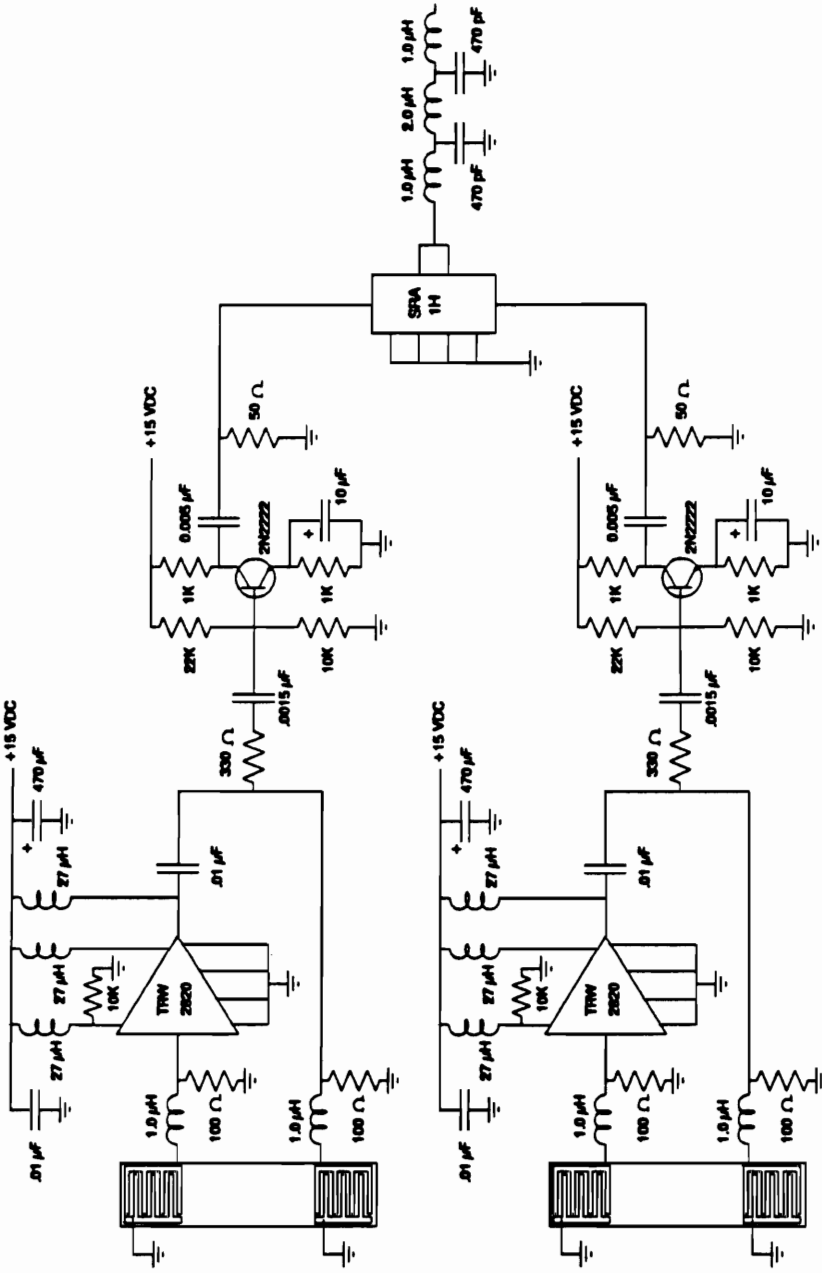


Figure 40. Schematic for dual SAW device detector.

determined by the finger width of the interdigitized transducer array.

The output of the CA2820 amplifier is fed to a 2N2222 transistor that is configured as an amplifier. The amplified output signal is then routed to a Mini-Circuits SRA-1H frequency mixer.

The purpose of the frequency mixer is to take the outputs of the two SAW oscillators and "beat" them together. When these signals are combined in the mixer, the output will contain the sum of the two input frequencies, the two individual frequencies and the difference of the two frequencies. The frequency difference signal is referred to as the beat frequency (Figure 41). When a coating is applied to only one of the SAW devices, the beat frequency generated from a coated and uncoated device will be no greater than 200 kilohertz. Since the sum of the frequencies and the frequencies of the individual devices are 62 Megahertz and 31 Megahertz respectively, a simple Chebyshev low pass LC filter on the output of the frequency mixer eliminates the high Megahertz frequencies and allows the beat frequency to pass to the frequency meter. Utilizing the LC filter connected to the output of the SRA-1H frequency mixer, the frequency cutoff for this filter was measured to be 20 Megahertz with a 3 db point of 14.5 Megahertz.

To minimize fixed offsets and noise, the circuitry for both devices is mounted on one circuit board. However in developing this board it became apparent that in order to eliminate a low noise ripple in the output of each device, separate power supplies with a common ground were needed. The circuit board layout is therefore symmetrical with each SAW circuit occupying one half of the board with separate regulated 15 volt DC sources. This layout facilitated the incorporation of the mixer circuit on the PC board directly, making it convenient to direct the three signals

Frequency Mixing

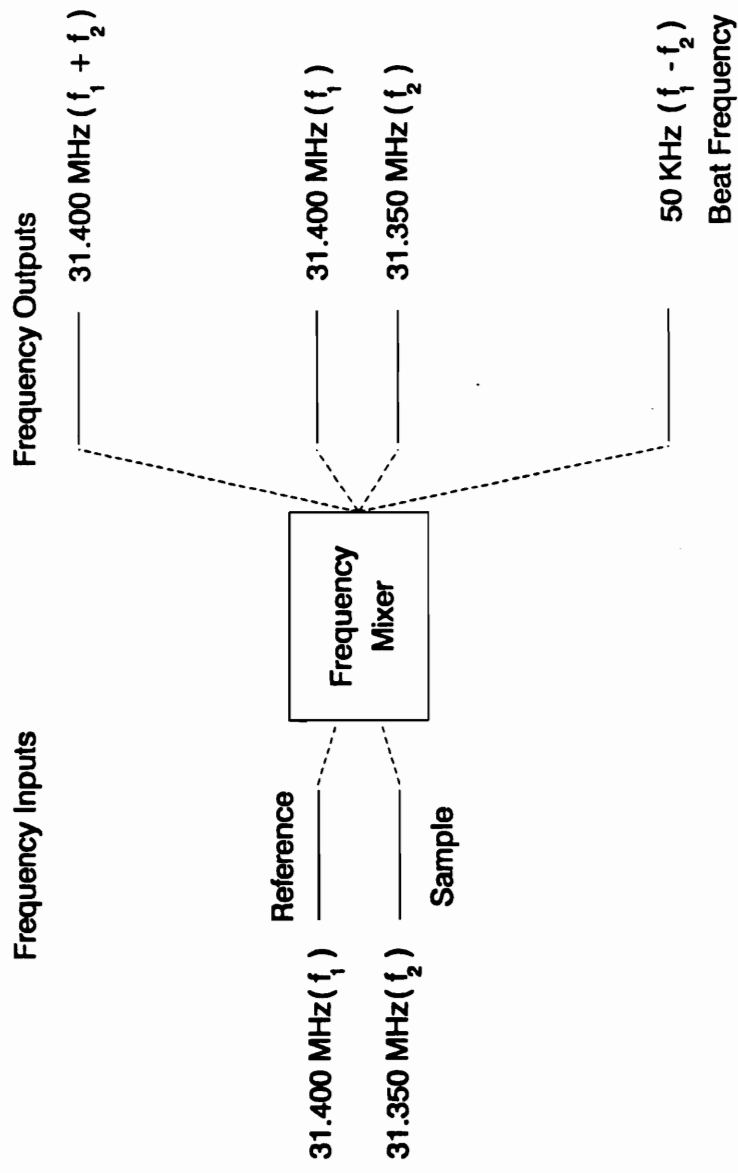


Figure 41. Frequency mixer outputs.

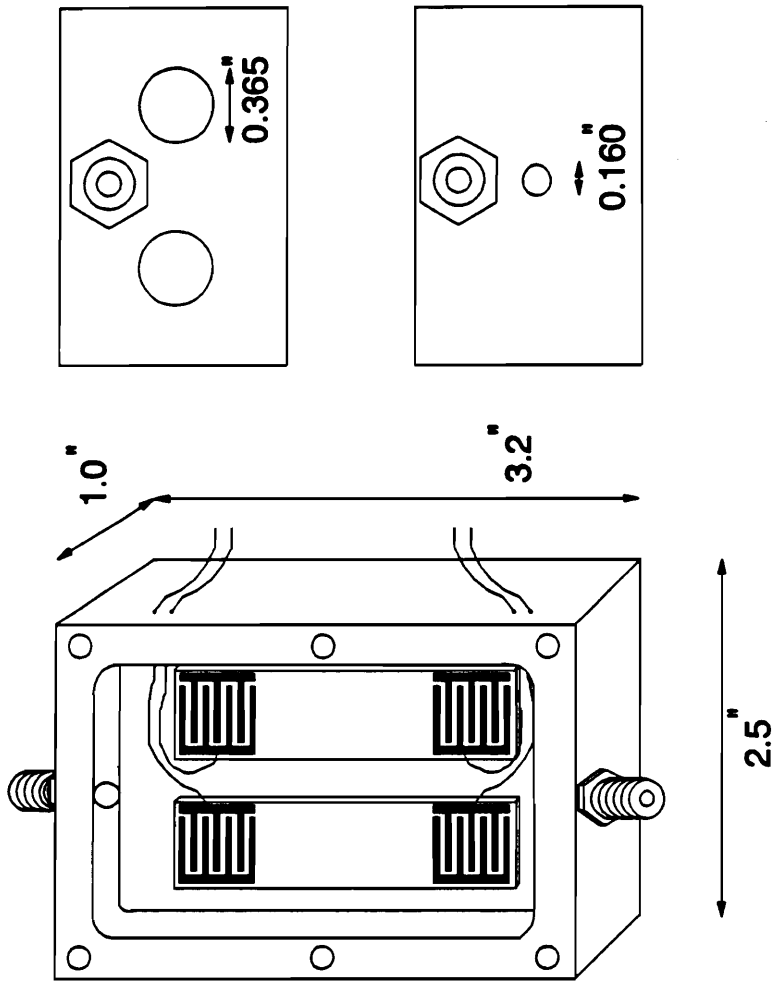


Figure 42. Dual SAW device detector cell.

generated by the SAW devices (two SAW frequencies and the beat frequency) to the front of the chassis for measurement purposes.

The detector chamber is made from a square block of aluminum (3.2" x 2.5" x 1.0") with a cell volume of 12 cc. Its dimensions are 1.85" x 3.50" x 0.28" (Figure 42). The wires from the PC board are passed through the side wall of the detector cell block and sealed to the cell wall with epoxy. The wires are soldered to metal connectors which are held in contact with the connection pads of the interdigitized transducer arrays of the SAW devices with nylon screws. The other pad of the array is connected to ground by contact with a metal connector that is screwed into the cell chamber with a steel screw. The cell is grounded to an aluminum plate which acts as a ground plane for the oscillator circuits and power supplies. The gas inlets to the detector chamber are 1/4" OD tubing to 1/8" NPT pipe Swagelok connectors threaded into the detector block and sealed with Teflon tape.

The detector block is designed to accept two cartridge heaters and a temperature probe to conduct elevated temperature experiments. The cartridge heater ports are 0.365" in diameter and 2.46" deep. The heaters used are Thermal Model 900F-2 50 watt 120 volt cartridges. The Temperature Controller and Sensing Unit are from RFL Industries, Inc. and are used for feedback control of the temperature of the block. The temperature of the detector block is measured by using a RTD temperature element which is inserted into a port in the block.

Finally, the cover of the detector cell is fitted with a quartz window (2.00" x 0.50" x 0.04") which is located above the sample SAW device. This window was originally used for early Ultraviolet radiation experiments that were discontinued. The window continues to serve as a means of visually inspecting the phosgene sensitive film when exposed. A chromophore develops as a result of the reaction product of

nitrobenzylpyridine and phosgene. The cell cover is held in place with six hex head 1/2" long 4/40 screws.

B) Permeation tubes and mixing manifold

The ability to generate a wide range of vapor concentrations for different vapors led to the conclusion that the use of permeation tubes for vapor generation was the most ideal solution available. The other choice required that gas mixtures be prepared and then diluted to the concentrations required. The ease of use and ability to quickly change the vapor to be analyzed made the permeation tube system a more reasonable choice.

Permeation tubes used in this investigation were obtained from Vici-Metronics (2991 Corvin Drive, Santa Clara, CA 95051, 408-737-0550). Permeation tubes function on the premise that a Teflon tube containing a liquid sample will be permeated by the sample at a known constant rate. This is accomplished because the vapor pressure of the liquid in the tube will remain constant at fixed temperature for as long as the tube contains liquid. If a gas stream is allowed to flow across the outside of this sealed tube, the concentration of the vapor at the outer surface of the tube will approach zero. Therefore a constant concentration gradient is established across the tube wall and the amount of material that will diffuse from the tube will be a constant amount at a given temperature for a given tube length.

To generate a specific concentration of the vapor in a flowing gas stream, the flow rate or the temperature of the tube chamber can be changed. The recommended method involves adjusting the flow rate of the gas stream to generate the concentration required.

For example, with a phosgene permeation tube whose length is 1.5 cm, the concentration of phosgene in air at 100 cc/min flow rates can be calculated from the following equation:

$$C = \frac{P L K_m}{F} \quad (66)$$

where

C = concentration in part per million (vol)

P = permeation rate in nanograms/(minute-centimeter)

L = length of tube in centimeters

F = flow rate of air in centimeters/minute

K_m = molar constant (0.247 for phosgene at 30° C)

Using this equation with the following parameters (1.5 cm tube, permeation rate of 670 ng/min/cm, K_m of 0.247 and flow rate of 100 cc/min), the concentration of phosgene generated in the stream is 2.48 ppm.

Examination of equation 66 reveals that the concentration of the vapor in the gas stream can be easily changed by varying the flow rate used. The recommended maximum flow rate that can be used with a permeation tube device is 1 liter per minute. If the minimum flow rate required by the system is 100 cc/min, the permeation tube can generate a concentration range of one order of magnitude. In practice, the maximum flow rate that was ever used was 500 cc/min, halving the range of concentrations for the system.

To extend the phosgene concentration range used in the experiments, two different phosgene permeation tubes were used. The first was 1.5 cm. in length while the second was 15 cm. in length. By using these tubes separately in the vapor

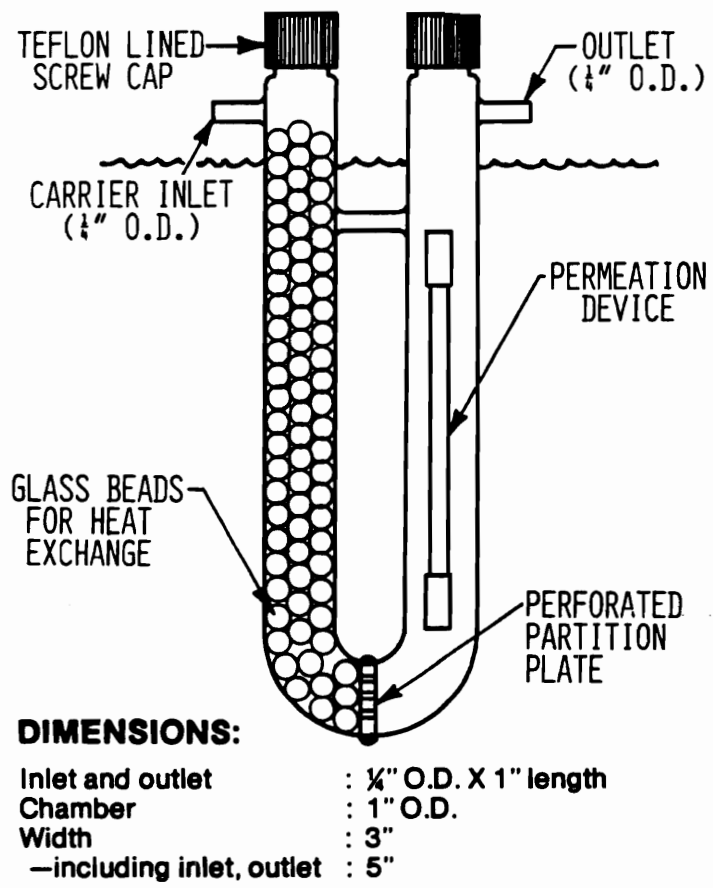


Figure 43. Permeation tube chamber.

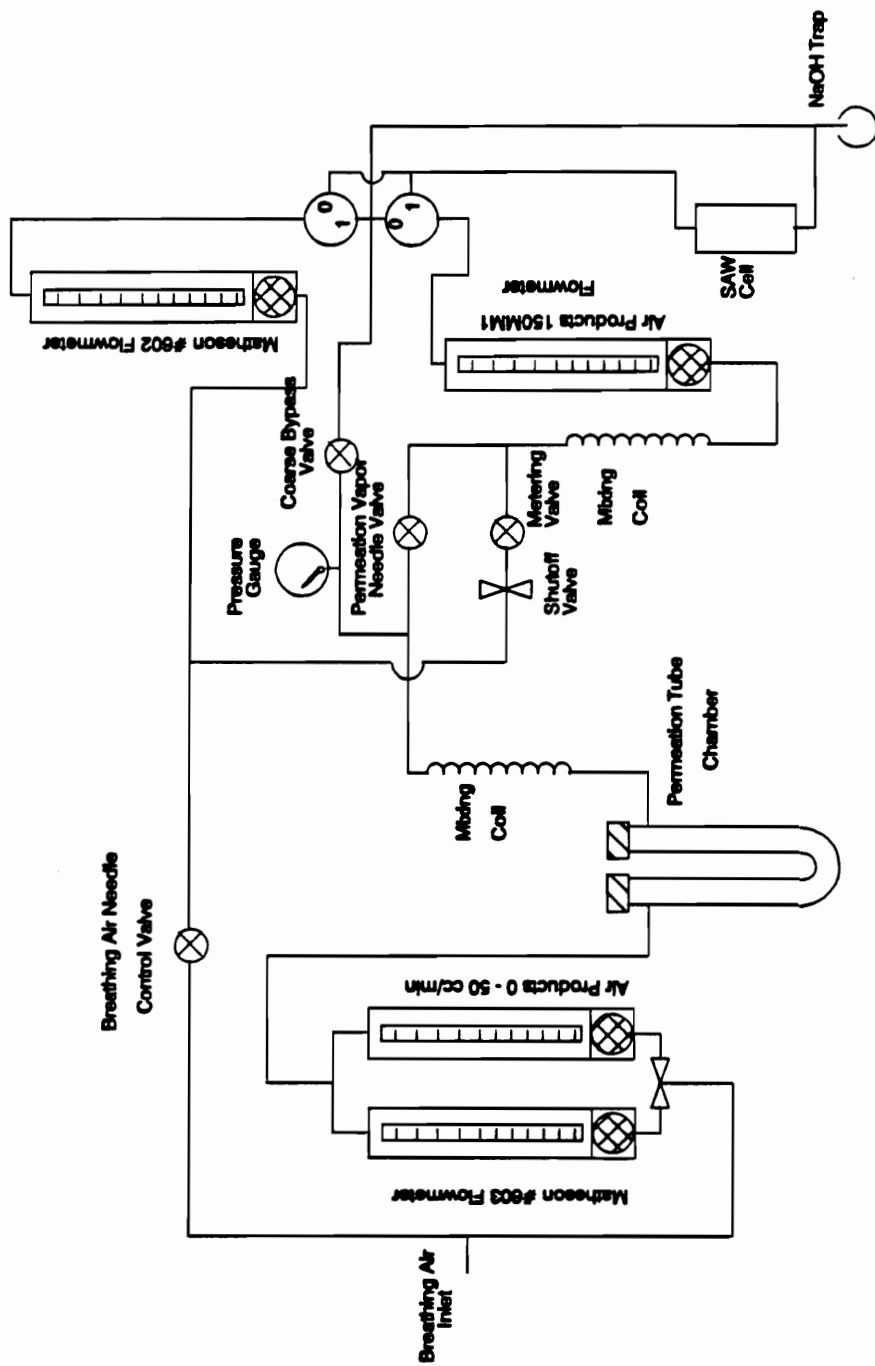


Figure 44. Permeation tube vapor generation manifold.

generating apparatus, the phosgene concentration range generated was 0.496 to 24.8 ppm.

To ensure that the temperature of the permeation tube would remain constant, a permeation tube holder and heat exchanger device was purchased from Vici-Metronics (part number 19X-415-000). The device is a large glass U-tube with screw tops and 1/4" OD glass carrier gas inlets and outlets (Figure 43). One side of the tube contains glass beads which act as heat exchangers for the carrier gas. The other side of the tube is for placement of the permeation tube. At the bottom of the "U" a perforated partition plate is integrated into the tube to prevent the glass beads from entering the permeation tube chamber. This holder can then be inserted into a constant temperature bath to ensure a stable gas concentration.

The temperature bath chosen utilizes a four liter beaker and an aquarium tank heater and aerator. The four liter beaker was found to be an ideal size for the immersion of the permeation tube holder. The aerator is employed to ensure uniform mixing of the water bath since convection currents alone are not sufficient.

The manifold system that was designed to deliver a safe and controllable flow of cylinder compressed breathing air and permeation tube air to the detector cell utilizes the components already mentioned. The goal was to enable computer control of the manifold, using a control line from the Digital Equipment Corporation LSI-11 microcomputer to turn on and off the valves selecting whether sample or breathing air was being sent to the detector cell.

Figure 44 represents the flow schematics for the manifold design.

The inlet from the breathing air cylinder is divided into two lines. One of these lines proceeds to the permeation chamber side of the manifold. The other line is used as the uncontaminated breathing air line, now referred to as zero air.

The permeation tube line enters a selection valve which directs flow to either a Air Products Model 65MM direct reading 0 to 50 cc/min flowmeter (603 Center Ave., N.W., Roanoke, VA. 24016) or a Matheson Model R7630 Gas Flowmeter (East Rutherford, NJ) with type 602 tube. The Matheson flowmeter provides the ability to change the tube and thereby change the range of measured flow rates available. The output of the flowmeters are "teed" together and enter the permeation tube holder and heat exchanger. This gas passes through a 4 foot length of coiled 1/4" OD copper tubing to ensure adequate mixing of the permeation tube vapor with the carrier gas. After mixing occurs, the permeation tube gas line is divided into a bypass and sample line.

The bypass line contains a 0 to 30 PSIG pressure gauge followed by a coarse gas bypass valve. The sample line contains a needle valve. This configuration allows for the generation of a variety of different vapor concentrations while maintaining a constant flow rate through the detector cell. With a 1.5 cm phosgene permeation tube, a flow rate of 100 cc/min across the tube will generate a concentration of 2.48 ppm. A flow rate of 500 cc/min will generate a concentration of 0.496 ppm. If the flow rate through the detector cell is to remain at 100 cc/min, the excess flow must be stripped off and vented. Adjusting the coarse bypass valve and the sample needle valve ensures that the required flow rate necessary is directed into the detector cell while the excess is directed to the vent line. The purpose of the pressure gauge ensures that a back pressure does not develop in the permeation chamber which will affect the permeation rate of the tube.

The output of the sample line needle valve connects to another coiled mixing tube and into an Air Products Model 150MM1 Flowmeter having a flow range of 4.9 to 147.8 cc/min air. This flowmeter, like the Matheson, can also accept different flow

tubes, changing the measured flow rate if desired. The output of this flowmeter is directed into a Galtek Model 203-3414-41-5 solenoid operated three way diaphragm valve (Jonathan Industrial Center, Chaska, MN 55318).

The zero air line is connected to a splitting "tee" which directs part of the zero air to a shutoff and metering valve connected in series. The purpose of this line is to enable the introduction of "fill" or dilution gas to the permeation chamber gas line. Since the maximum flow rate across a permeation tube is one liter per minute, dilution gas can be added to the sample line after it has passed through the permeation tube holder to further reduce the concentration by means of an increase in the overall flow rate. The remainder of the zero air is connected to a Matheson Model R7630 Gas Flowmeter equipped with a type 602 flow rate tube having a usable range from 20 to 860 cc/min air. The output of this flowmeter is directed into another Galtek Model 203-3414-41-5 valve.

The two Galtek solenoid valves used on both the zero air and sample air sides of the manifold are identical. These three way solenoid valves are operated by 115 volts AC and have 1/4" NPT female orifices. All wetted parts are composed of Teflon with a Kalrez seal. The two valves are connected to a Crydom optical isolated switch. The switch enables a 115 volt AC line to be controlled by a TTL compatible signal of 0 to 5 volts DC with optical isolation, preventing possible interconnection of the AC and DC voltages which would have dire consequences for the control instrumentation. In the configuration used, the valves are plumbed so that in their deactivated state, zero gas flows through the detector cell and sample gas is vented. The application of a logic 1 signal (5 volts DC) to the optoisolated switch passes 115 volt AC to the valves. The activated valves direct sample gas flow to the detector cell and zero gas to vent for as long as the valves are activated.

The vent line and detector cell lines are joined downstream from the detector cell and are directed into a base bath to eliminate phosgene. The lines were joined to eliminate any pulsation and flow fluctuations that were experienced when each line was separately run into a base bath, a problem which was encountered when a sample was injected into the detector cell. A check valve was originally placed in the detector cell line downstream from the detector to prevent possible backflow of vent line gas into the cell, but the pressure drop required to drive the check valve was too large. A shutoff valve was inserted in its place so that when film loaded SAW devices were removed and inserted into the detector cell, backflow of sample gas would not reach the detector cell leading to premature loading. No problems were encountered with this arrangement.

The base bath is composed of sodium hydroxide in water, reducing the remaining phosgene to carbon dioxide. An aquarium aeration stone disperses the air flow into the base bath to assure entire consumption of the phosgene.

C) Frequency Meter

The meter used to measure the frequency output of the SAW detector is a Fluke Model 1953A Counter/Timer (John Fluke, Ltd. Inc., Buffalo, NY). The Fluke 1953A is a DC to 125 Megahertz digital counter/timer capable of measuring frequency, frequency ratio, period, time interval and total events. Each measurement function is switch selectable and uses six different sampling ranges. Measurement results are displayed using a nine digit LED readout with overflow indication and leading zero suppression. Frequency is displayed in units of either Kilohertz or Megahertz while time units are either microseconds, milliseconds or seconds. Signal input is accomplished by BNC connectors.

The Fluke 1953A is capable of transmitting data in a Binary Coded Decimal (BCD) format when a separate Data Output Unit printed circuit board assembly (Model 1953A-02K) is installed. By constructing a wirewrap facsimile of this Data Output Unit board (Figure 45), the Fluke makes accessible to a computer interface all nine digits of measurement data, units indication, decimal point, and positioning and control signals.

D) The Frequency interface board.

The frequency information from the Fluke frequency meter is imported into the LSI-11/03 computer through the parallel port using a custom designed interface board (Figure 46). The output of the Fluke meter presents the nine BCD digits corresponding to the front LCD display. Since the SAW devices being used require only eight digits for the output of a single device (approximately 31 Megahertz), the interface board allows eight of these BCD digits to be parsed from the Fluke meter to the LSI-11 parallel port. Since each BCD digit is composed of four bits, the four bit sequence is segregated and each bit is routed into one of the four TTL74151 1-of-8 selectors. Each of the eight BCD digits is segregated and routed into the four 74151 selectors.

The selectors operate by forwarding one of the eight input lines directly to the output line by using a three bit selection code (0 through 7). By wiring the least significant BCD digit's bits to position 0 of the four selectors, the input of selection code 0 into each selector will output the BCD value for the least significant digit. These four bits from the selectors are wired to the first four bits of the LSI-11 input parallel port where they can be recorded. To reach each of the eight BCD digits, the selection code can be decremented from 7 to 0 successively and a parallel input read can be performed by the LSI-11 for each of the selector states.

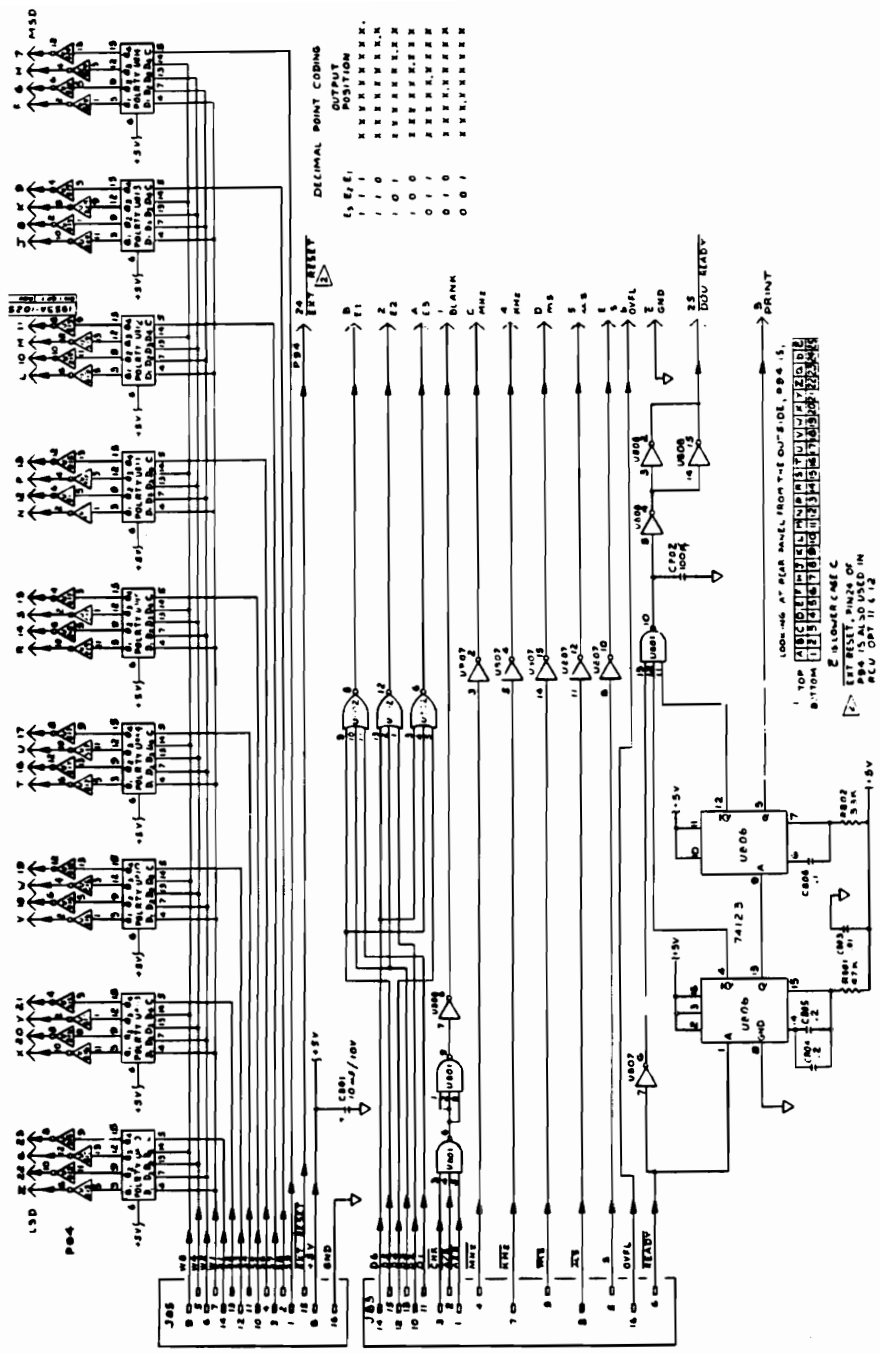


Figure 45. Fluke BCD interface board.

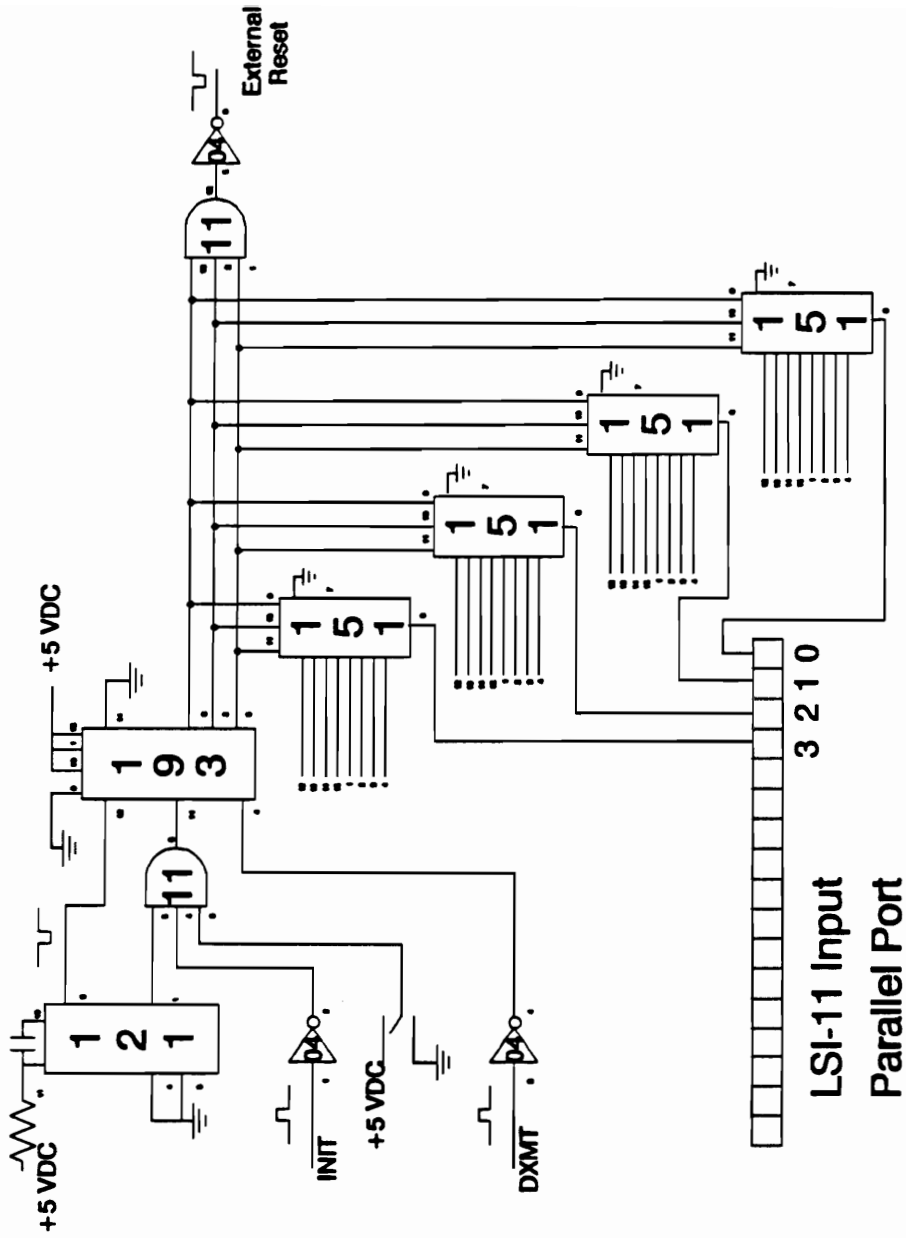


Figure 46. Frequency to parallel port interface board.

In order to generate the decrementing selection code for the selectors, a 74193 synchronous up/down binary counter is used. The 74193 counter is configured to be used in decrement mode. Since the application requires only a countdown from 7 to 0, a TTL signal (logic 0) is used to load the upper limit into the counter through four data lines which are hard wired to generate a value of seven (0111). The countdown signal is provided by DXMT (data transmitted), a signal which is generated every time the LSI-11 input parallel port is read.

The basic circuit is composed of a countdown counter which generates a selection code between seven and zero. This selection code is used by the eight to one selectors to pass the correct four bit BCD digit to the LSI-11 input parallel port. When the port is read, the DXMT signal causes the counter to decrement by one, which generates the next selection code, allowing the next BCD digit to be forwarded to the input parallel port. This pattern continues until all eight BCD digits are read into the LSI-11.

Only two items remain to be addressed. The first is that the BCD output of the Fluke meter must be "locked" while the digits are read. The second is that once the eight BCD digits are read, the counter needs to be reset to its initial state.

The ability to lock the output of the Fluke meter until all of the BCD digits are read by the input parallel port is relatively straightforward. An EXTERNAL RESET line which is TTL compatible is available as an input into the Fluke meter. When a logic one is applied to this input, the BCD output of the meter is locked and no further samplings can be performed by the meter until it is unlocked. By routing the selection code generated by the counter through a 7411 three input AND gate and a 7404 inverter, the only time the meter will be unlocked is when the selection code of seven is generated by the counter. This state is the initial state of the system.

The ability of the system to generate or regenerate this initial state is the next concern. The initial state can be generated in three ways.

The first method is instituted when the LSI-11 and frequency meter are turned on. When the LSI-11 is powered up, a front panel button is depressed on the LSI-11 to activate the Octal Debugging Technique (ODT) code used to load software necessary for the control of the experimental equipment. Depressing this button generates an INIT signal which is available on the parallel input port. This signal is passed through a 7404 inverter and is used as one of three inputs into a 7411 three input AND gate. When one of the inputs is a logic zero, the output of the AND gate will be a logic zero. This logic zero is used as a LOAD signal into the 74193 counter, loading the initial value of seven into the counter. The inverted INIT signal will be in a momentary logic zero state, thereby causing the counter to be initialized.

The second method is encountered when the input parallel port has been read for the eighth time, inputting the entire frequency value into the LSI-11. When the last read is executed, the DXMT signal generated will cause an underflow condition in the counter as a decrement to zero occurs. The underflow condition generates a BORROW signal output from the counter. This signal is input into a 74121 monostable multivibrator which is used to extend the length of this momentary logic zero BORROW signal. The output of the monostable is the second input into the three input AND gate. When a BORROW signal is generated, this AND input line will go to a logic zero, causing the output of the AND gate to go to a logic zero. This will again cause the 74193 counter to LOAD the initial value of seven into the counter.

The final method of initializing the counter is by using a push button installed on the interface board. This is strictly a fail-safe option. The switch output is the third input to the three input AND gate. The switch is configured so that it is normally

closed, allowing a logic one (+5 volts) to be applied to the input line of the AND gate. When the switch is depressed, a logic zero is applied to the input of the AND gate, generating a LOAD signal to reinitialize the counter to a value of seven.

E) LSI-11

The computer system used to acquire the frequency output of the Dual SAW device detector is a Digital Equipment Corporation LSI-11 running PolyForth. The LSI-11 configuration included 16 kilobytes of memory, two serial ports, one parallel port, a real time clock , and an Analog to Digital/Digital to Analog convertor board. The frequency information generated by the detector and the measured by the Fluke frequency meter was acquired through the parallel port. A complete listing of the Forth software that was written to control the experimental setup can be found in Appendix A. A schematic of the entire experimental setup and the LSI-11 control of the experiment can be found in figure 47.

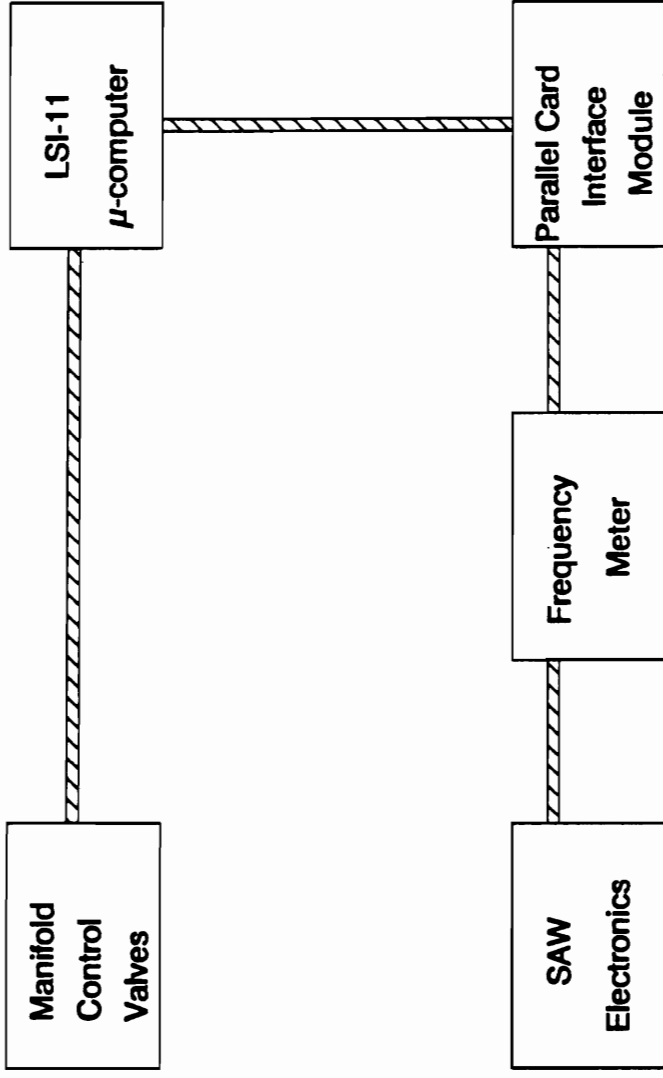


Figure 47. Box schematic of instrumental configuration for data acquisition.

EXPERIMENTAL

A) Preparation

1) Preparation of SAW films

The preparation and deposition of films upon SAW devices was accomplished by using a Badger Model 200 air brush (Badger Air Brush Co., Franklin Park, IL, 60131). This method is just one of many available for the preparation and deposition of films. Q-Tip, syringe deposition, Langmuir-Blodgett, surface flooding and spin coating are other methods available. However, air brushing was chosen because of the ease in depositing a reproducible film thickness, and therefore frequency shift, on a device⁷⁷.

Since the frequency shift is a function of the thickness and density of a film upon a SAW device, frequency shift measurements were used as the basis for measuring the average film thickness on a device. Previous studies have shown that the average film thickness can be calculated using the density of the material and the frequency shift produced with the SAW oscillator⁷⁷. Using the SAW frequency shift equation for polymeric films above the glass transition temperature, the frequency shift produced by the deposition of a 1 μm thick film with a density of 1.2 g/cc is:

$$\Delta f = (-1.3 \times 10^{-7} \text{ m}^2 \text{ sec/kg})(31.4 \times 10^6 \text{ Hz})^2 (1.2 \times 10^3 \text{ kg/m}^3)(10^{-6} \text{ m}) \quad (67)$$

$$\Delta f = -154 \text{ KHz}$$

Based on this result, frequency shifts of 60 KHz, 40 KHz and 20 KHz will result from average film thicknesses of 0.39, 0.26 and 0.13 μm .

The term film load, defined as the frequency shift from the free surface oscillation frequency that is generated with the application of a film onto a clean

device, will be used as the film thickness benchmark. The units are in KHz. Rather than convert frequency shift into average film thickness, film loads will be compared directly. Since the relationship between frequency shift and film thickness is linear, a 40 KHz film load is twice the thickness of a 20 KHz film load.

Ellipsometry was attempted for the determination of the thickness of poly(ethylene glycol) films. This proved to be impossible due to the refractive indices of the quartz SAW device (1.4585) and poly(ethylene glycol) (1.4650). Ellipsometry requires a material difference in refractive indices for the interface of two materials to be detected. The minute difference between the materials used results in the polymer acting as an index matching fluid. The interface cannot be determined and therefore the film thickness cannot be measured.

A new SAW device installed in the oscillator circuit is capable of handling a film load of 60 KHz. After 60 KHz, the attenuation of the surface wave is greater than the amplification provided by the amplifier circuit and the device ceases to oscillate. As a device is used and cleaned, the efficiency of coupling decreases due mainly to deterioration of the interdigitized transducer array electrodes. Placed under a microscope, the sharp rectangular shape of the fingers is etched leaving a distorted rectangle. This reduction in coupling efficiency means less energy is transferred to the surface wave. With less energy, the film thickness necessary to cause oscillation to cease decreases. Instead of a 60 KHz film load capacity on a new SAW device, maximums of 50 and 40 KHz film load capacities have been encountered on used devices.

To ensure that a film thickness could be chosen that would still allow SAW oscillation as the device is used again and again, most experiments were conducted

using a 40 to 50 KHz film load. It should be noted that the selection of a particular film thickness was not considered overly critical for dosimetric determinations of phosgene. Studies of 20 and 40 KHz film loads will yield the necessary information indicating if film thickness is a parameter which affects the response of the detector.

After a film was air brushed onto a SAW device, the coated device was placed into an oven at 65 to 70° C for five minutes to remove any remaining solvent. The device was then allowed to cool, installed into the detector cell and the frequency was measured. The resulting frequency value after cooling was used to determine the total frequency shift for the device. This short heating at a low temperature was determined experimentally to be optimum. At a higher temperature, evaporation of 4-(4'-nitrobenzyl)pyridine occurred (melting point 70-72°) resulting in films that either showed little or no response to phosgene vapor. Five minutes was sufficient to ensure removal of most, if not all, solvent residue. This can be determined from monitoring the SAW frequency. If solvent vapor remained in the film, as it evaporated from the film the mass would change. This would be detected as a change in the SAW oscillator frequency. Films on SAW devices heated for five minutes showed minimal frequency changes when the device was placed into the detector cell. Unheated films required an extended period of time before desolvation ceased and stable background runs could be obtained.

One note of caution needs to be mentioned concerning the polystyrene based films. In order to totally remove the solvent from these films, the material should be heated to above the glass transition temperature of 100° C. When this was attempted, evaporation of 4-(4'-nitrobenzyl)pyridine occurred along with removal of the solvent. Therefore these films were also heated at 65 to 70° C for five minutes. It is understood that all the solvent was not removed from the glassy film. However when the device

frequency was monitored, a stable frequency was obtained. Therefore the remaining solvent was interpreted as not outgassing from the film and the films were used in this state in the experiments discussed later in this work.

2) Preparation of materials

4-(4'-nitrobenzyl)pyridine/polymer mixtures were prepared using materials obtained from Aldrich Chemical Co. (Milwaukee, WI) and Scientific Polymer Products (Ontario, NY). Methanol (Certified ACS Spectroanalyzed Grade) was obtained from Fisher Scientific while toluene and methylene chloride (Baker Analyzed Reagent Grades) were obtained from J. T. Baker. Cylinder breathing air was obtained from AIRCO (Industrial Gas and Supply Company, Fairlawn, VA). Ethylene oxide, phosgene and thionyl chloride permeation tubes were obtained from Vici-Metronics (Santa Clara, CA 95051).

Mixtures prepared using poly(ethylene glycol) were dissolved in methanol with a total solids to solvent ratio of 10 grams/liter. This ratio was found to be convenient for use with air brush application. With a larger gram/liter ratio, the frequency shift produced from one pass of the air brush was excessive. Under these conditions, as the amount of frequency shift approached the target value, it proved to be very difficult to generate films in the required frequency shift range without overloading the device or overshooting the desired shift. Too much solvent required excessive air brushing before a film of adequate thickness could be obtained. The 10 grams/liter ratio was also used in the dissolution of pure poly(ethylene glycol) for the preparation of reference device films.

Mixtures containing 4-(4'-nitrobenzyl)pyridine and polystyrene were dissolved in methylene chloride with a solids to solvent ratio of 2 grams/liter. As with the

polyethylene glycol experiments, this same ratio was used for the dissolution of pure polystyrene.

3) Preparation of Phosgene Concentrations

Phosgene concentrations of 0.50, 1.24, 2.48, 4.96, 12.4 and 24.8 ppm were generated using two separate phosgene permeation tubes of 1.5 cm and 15 cm lengths.

Utilizing the equation

$$C = \frac{P L K_m}{F} \quad (68)$$

as defined earlier for determining the concentration of phosgene for different flow rates at 30° C, the flow rates necessary to generate the concentrations examined were as follows:

Flow rate (cc/min)	1.5 cm tube	15 cm tube
500	0.496 ppm	4.96 ppm
200	1.24 ppm	12.4 ppm
100	2.48 ppm	24.8 ppm

The temperature bath was monitored using a thermometer. To ensure that the temperature bath apparatus did not drift or cycle during experimental runs, an Omega Model 872 Digital Thermometer was used to measure the temperature bath for one hour at 30 second intervals. The average deviation around the norm was $\pm 0.2^\circ$ C.

The gas manifold system was configured to deliver the appropriate flow rate (100, 150 or 200 cc/min) to the detector cell as required for the experiment.

4) SAW Device Response and Acquisition Rate

The detector is a dual "beam" instrument, measuring the difference in response of two SAW devices, a sample and reference device, to the vapor being detected. As

stated earlier, the use of a dual beam instrument involves the mixing, or "beating", of the two separate SAW device frequency outputs, with the signal that is monitored being the beat frequency.

One advantage of a dual beam instrument using a beat frequency output is in minimizing temperature effects which may cause variation in the SAW device oscillation frequencies. Even though, in theory, ST-Quartz SAW devices have a zero temperature coefficient at room temperature (<3 ppm/ $^{\circ}\text{C}$ for the range -20 to $+80$ $^{\circ}\text{C}$; zero at -28 $^{\circ}\text{C}$)⁷⁸, changes of a few degrees will cause a change in the frequency. For example, the change of 1 $^{\circ}\text{C}$ using a 31 MHz SAW device will change the frequency

$$(31 \cdot 10^6 \text{ Hz})(3 \cdot 10^{-6}) = 96 \text{ Hz.}$$

By using two devices, the changes that occur to the beat frequency will be minimized since both devices undergo the same effect in the same direction.

This configuration is analogous with common mode rejection for operational amplifiers. Identical changes that occur on both inputs into an operational amplifier cancel each other out. The only signal that will be amplified by an operational amplifier is the difference between the two inputs. By taking the outputs of two SAW devices and mixing them together, common mode rejection manifests itself in the beat frequency. This beat frequency is the signal that is measured by the frequency meter.

One advantage that this particular chemical system being investigated has over previous SAW reversible adsorption and irreversible dosimeters is the use of a film coated reference device. Most configurations, other than those using multiple devices with different coatings as implemented by Carey⁷⁹ and the reversible dosimeter for styrene by Zellers⁸⁰, use an uncoated reference device due to the fact that the sensing film is a homogeneous material. It is impossible to have a reference film which will possess the same solubility for all possible interferences and still be sufficiently

different for the vapor species that is to be monitored. The system being investigated uses the same polymer support, thereby having both devices possessing the same solubility characteristics for reversible absorption and adsorption of unreactive vapors. The experimental configuration leads to a common mode rejection of the frequency shift that would be attributed to reversible solvation of the support matrix by unreactive vapors (Figure 48). The irreversible reaction of the target vapor with the active agent contained in the sample SAW device film will generate an increase in mass only on this device. This increase in mass leads to a decrease in the sample SAW oscillating frequency with the resulting frequency shift being indicative of the concentration and length of exposure of the sensing film to the vapor.

If the frequency of the reference device is greater than that of the sample device initially, the increase in mass on the sample SAW device will appear as an increase in the beat frequency (Figure 49). However, if the frequency of the reference device is smaller than that of the sample device initially, the increase in mass on the sample SAW device will appear as a decrease in the beat frequency (Figure 50). The former configuration is preferred, although there is no difference in the measurement capabilities between the two configurations. The reason for the preference is due to the situation which may develop in which the sample SAW device is initially at a frequency greater than that of the reference device but after exposure becomes less than that of the reference device (Figure 51). The problem becomes one of data analysis, since the beat frequency upon exposure first decreases to zero and then increases from zero. Therefore, in an effort to ease data analysis, sample SAW devices were either initially maintained at a lower frequency than that of the reference device or they were initially maintained at a sufficiently higher frequency than that of the reference device to ensure that this transition through a zero Hz beat frequency did not occur during the

Beat Frequency Measurement

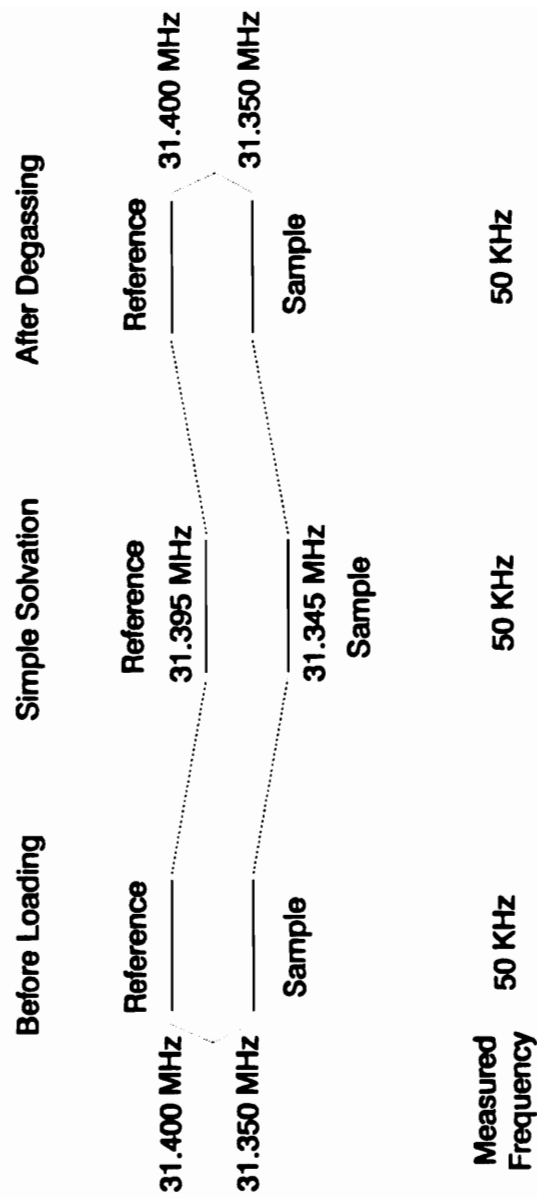


Figure 48. Beat and individual frequencies from reversible solvation.

Beat Frequency Measurement

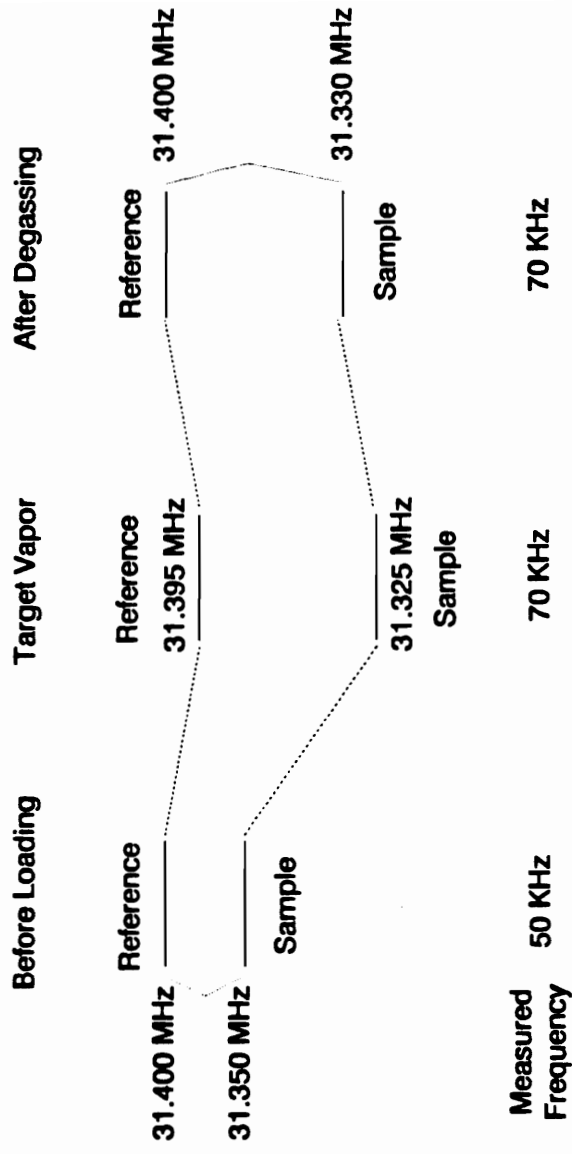


Figure 49. Irreversible mass loading frequency shift - lower sample frequency.

Beat Frequency Measurement

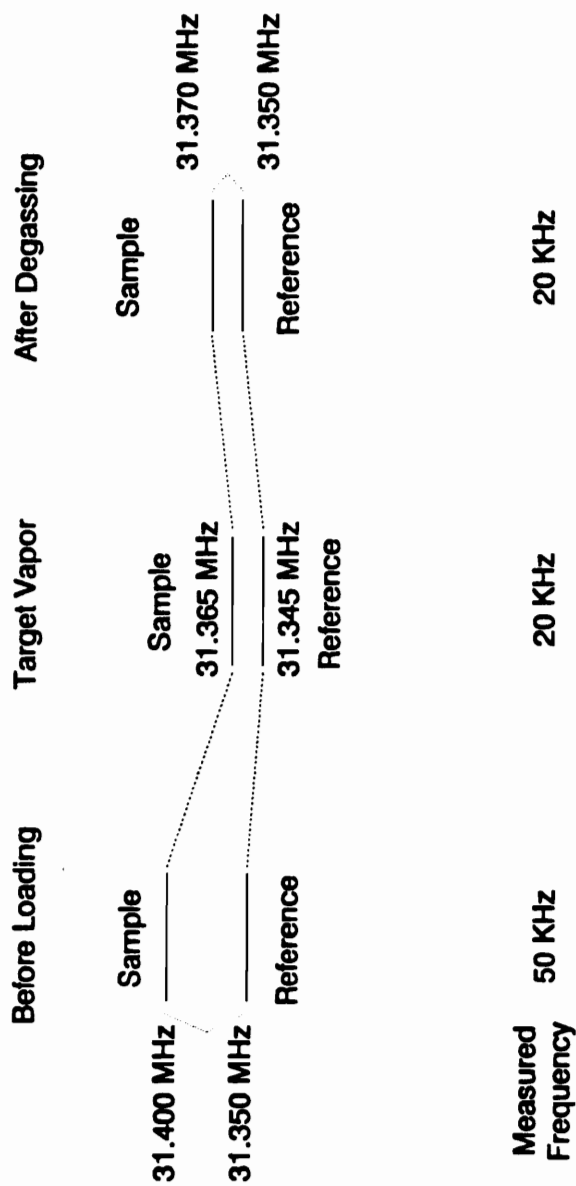


Figure 50. Irreversible mass loading frequency shift - higher sample frequency.

Beat Frequency Measurement

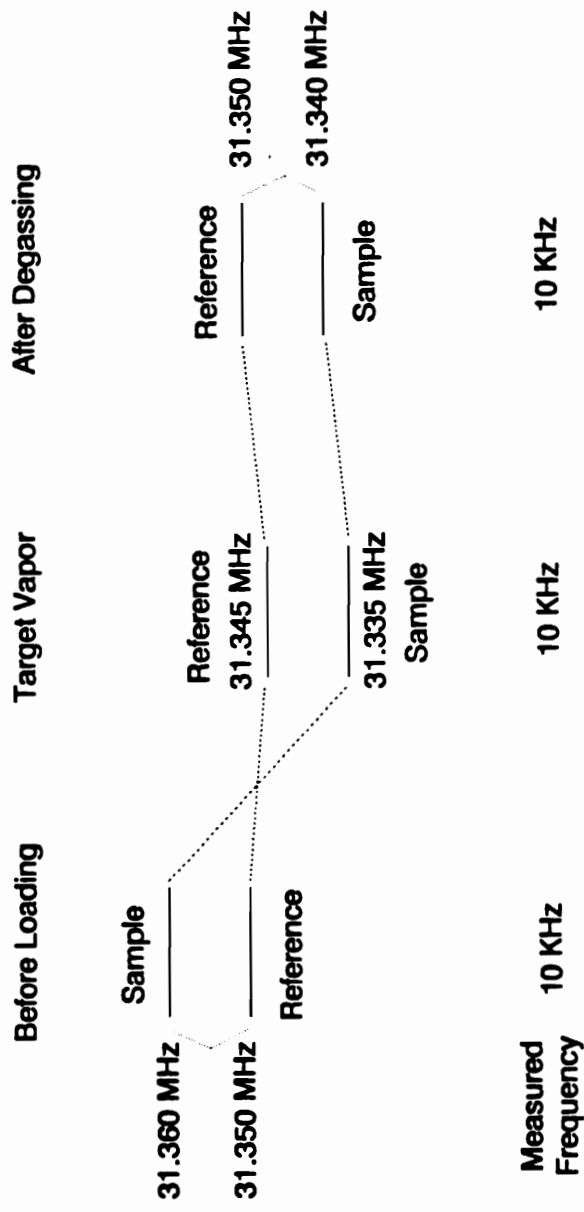


Figure 51. Irreversible mass loading frequency shift - sample frequency passes through reference frequency.

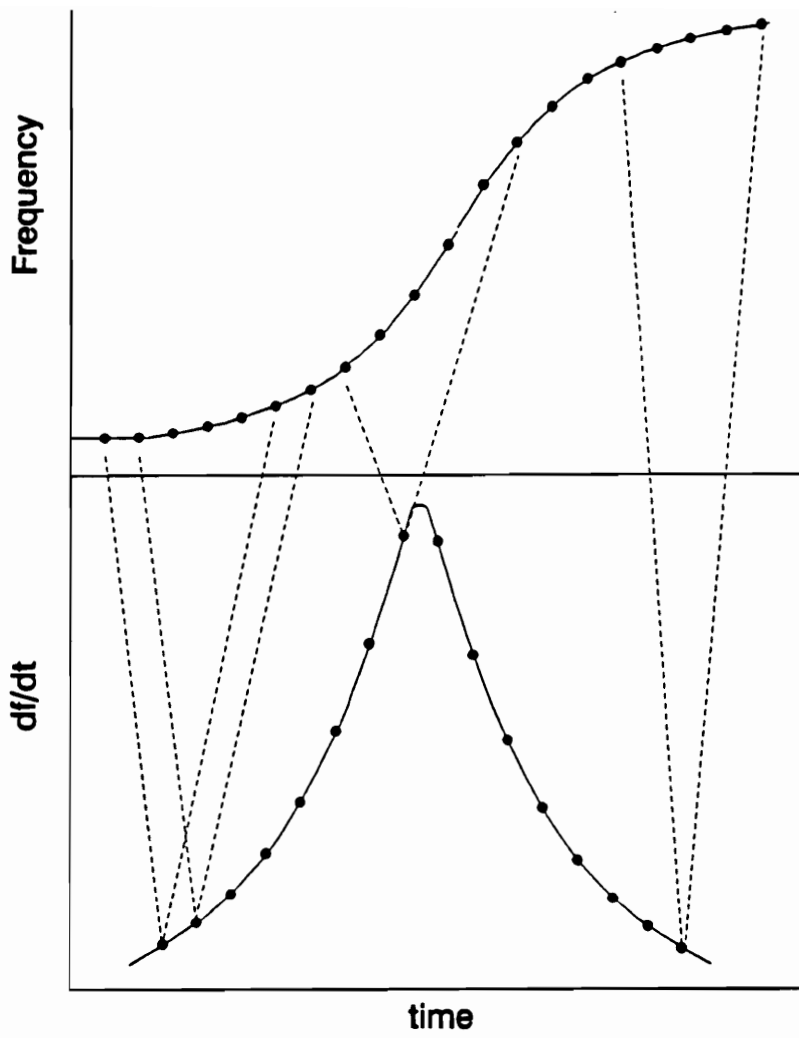


Figure 52. Determination of differential data.

experiment.

The maximum sampling rate for the experimental setup is one point every two seconds. The limiting factor is the Fluke meter acquisition rate. In order to measure frequencies with a resolution of one hertz, the frequency meter requires one second for acquisition. To ensure that the frequency meter correctly sampled the output of the dual SAW device detector, the LSI-11 can only import data from the frequency meter at a maximum rate of one point every two seconds.

Data obtained for both long term and short term exposures of vapor will be in the form of frequency versus time. For long term studies, the rate at which the frequency changes will be indicative of the rate of reaction of the vapor with 4-(4'-nitrobenzyl)pyridine. In order to obtain this frequency change rate (df/dt), the frequency difference between data points ten seconds apart was calculated and this difference was plotted against time (Figure 52). Ten seconds was selected empirically. The frequency change occurring due to exposure for the concentrations selected was sufficiently greater than that due to normal noise which appears as frequency fluctuations around a baseline value (3 Hz peak to peak).

For the short term exposure experiments, the data was analyzed as acquired. The frequency change rate was also calculated for the short term exposure experiments. This information was used to determine if the film had been consumed past its analytical lifetime. Exposures of the film to the same fixed concentration of vapor for the same time increment should yield the same frequency shifts. The derivative of this data (df/dt) generates a plot whose peak heights should be the same. If the peak height decreases with further exposures of the same concentration and exposure time, an indication that the frequency shift was diminishing with succeeding exposures, the interpretation of this observation is that the concentration of 4-(4'-nitrobenzyl)pyridine

is no longer flooded but is now affecting the overall rate of reaction. At this point the film is considered consumed and is replaced.

B) Exposure

Films containing 4-(4'-nitrobenzyl)pyridine (NBP) were exposed to phosgene, ethylene oxide and thionyl chloride of various concentrations. Exposure experiments were conducted in two different modes.

The first, known as long term exposure, involved the continuous exposure of the film to a set of different concentrations of alkylating or acylating vapor for an extended period of time, usually greater than 200 seconds. The goal of these experiments was to determine the response characteristics of the SAW device to these long term exposures and analyze the data generated as a function of observed frequency change rate. This analysis would yield fundamental information about the relationship, whether it be synergistic or competitive, between vapor phase and absorbed vapor equilibrium, permeability of the vapor into the film, and reactivity of the absorbed vapor with the trapping reagent, 4-(4'-nitrobenzyl)pyridine. From this analysis, a calibration curve measuring the frequency change rate as a function of the vapor concentration could be developed.

The second, known as short term fixed time exposure, involved the exposure of the film to fixed time (10, 20, 40 and 60 seconds) exposures of a set of concentrations of the same vapors used in the long term studies. The goal of these experiments was to determine if a calibration curve could be developed measuring the amount of frequency change as a function of ppm-seconds of vapor exposure. Based upon the calibration curves generated, the apparent order of the overall reaction can be determined for both the alkylating or acylating agent and 4-(4'-nitrobenzyl)pyridine.

Experimental conditions for each set of experiments and a brief synopsis of the goals of the experiment will introduce each particular section.

1) Long Term Exposure

a) Ethylene Oxide

Experimental Synopsis: Determination of the effect of ethylene oxide exposure upon the amount of frequency change and frequency change rate of the dual SAW device detector.

Experimental conditions:

Sample Film Composition: 50.46% 4-(4'-nitrobenzyl)pyridine in poly(ethylene glycol) MW 400

Reference Film Composition: 100% poly(ethylene glycol), MW 400, T_m 6°C

Film Thickness: approximately 40 KHz

Flow Rate: 100 cc/min

Vapors being determined: ethylene oxide, phosgene

Concentrations: 248 ppm ethylene oxide, 2.48 ppm phosgene

Ethylene oxide exposure for a period of 1102 seconds generated a small, reversible change in frequency of only 16 to 18 hertz (Figures 53, 54). Exposure of this same film to 2.48 ppm phosgene for a period of 998 seconds generated an irreversible frequency shift of approximately 6150 hertz, indicating that the film was not defective (Figures 55, 56).

Since no dosimetric mass loading occurred with a very high ethylene oxide concentration for long durations, the result of this experiment indicates that this particular system is inappropriate for low level detection of ethylene oxide. Although this particular chemical system had been used for ethylene oxide monitoring in a different matrix, the implication of these results is that the reaction rate of ethylene

50.46% NBP in poly(ethylene glycol) MW400
 248 ppm Ethylene Oxide Exposure

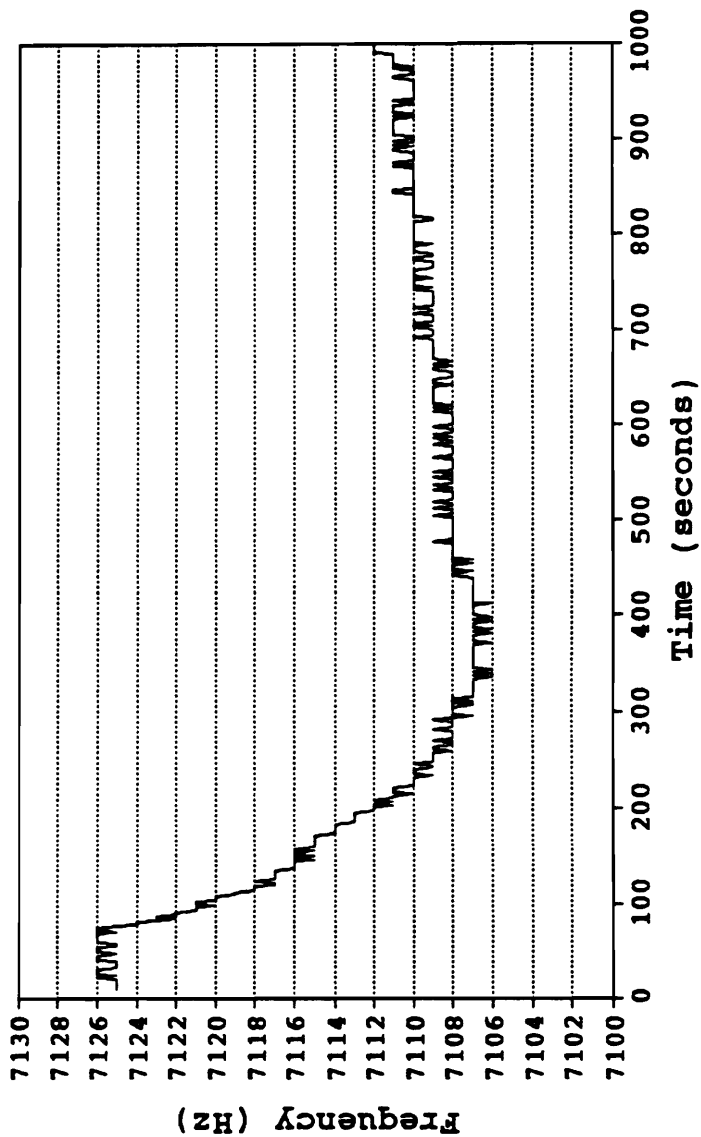


Figure 53. 248 ppm ethylene oxide exposure.

50.46% NBP in poly(ethylene glycol) MW400
248 ppm Ethylene Oxide Exposure

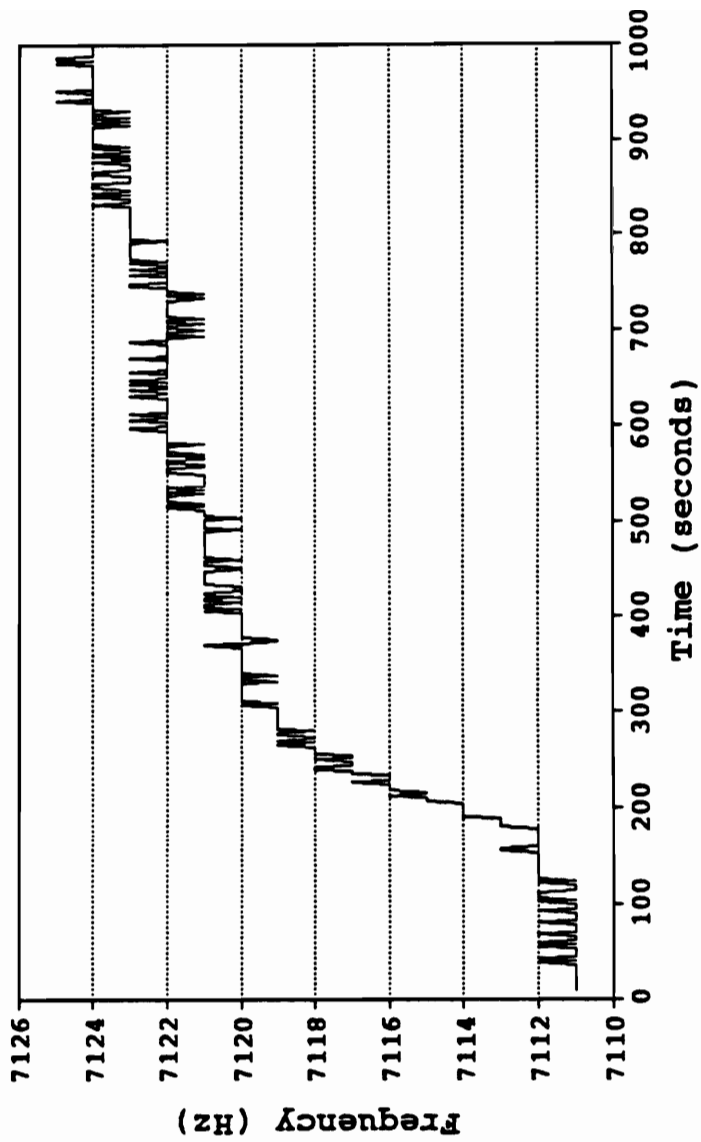


Figure 54. 248 ppm ethylene oxide exposure.

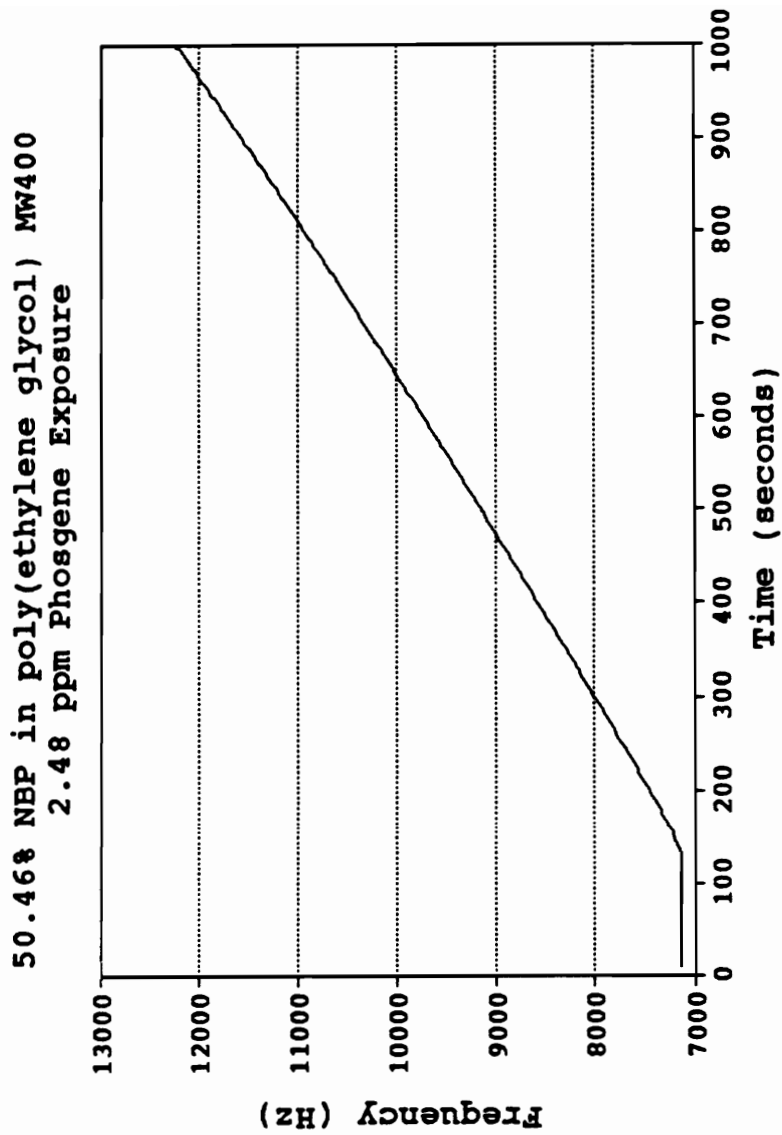


Figure 55. 2.48 ppm phosgene exposure.

50.468 NBP in poly(ethylene glycol) MW400
2.48 ppm Phosgene Exposure

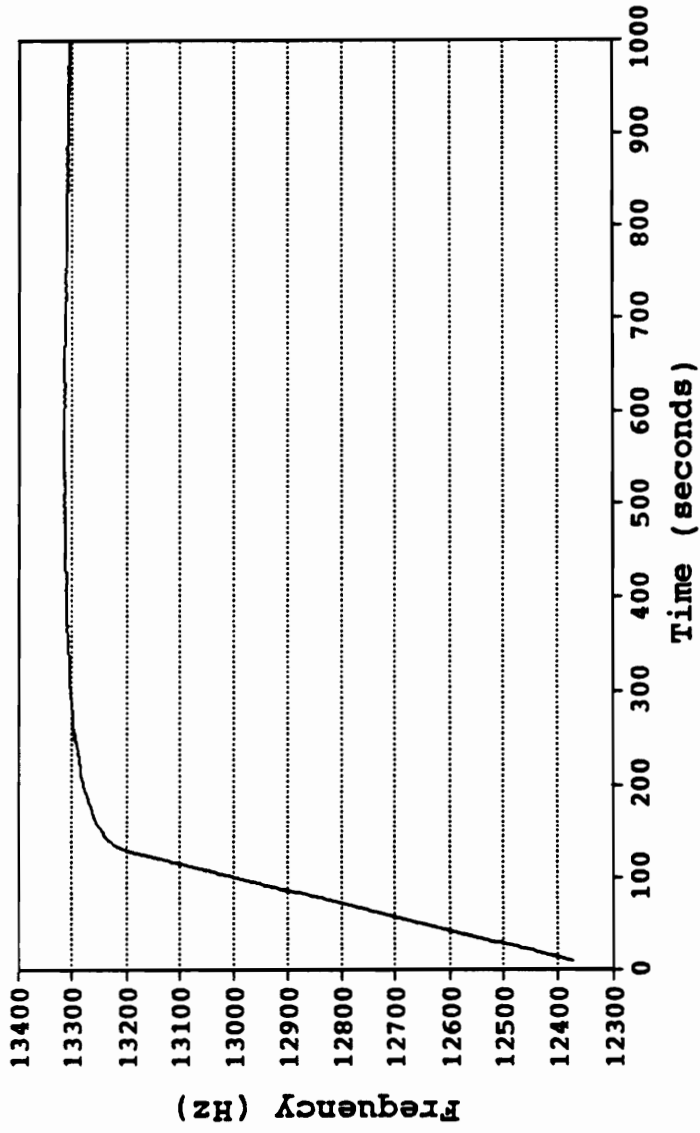


Figure 56. 2.48 ppm phosgene exposure.

oxide with 4-(4'-nitrobenzyl)pyridine in this film configuration is too slow for use as a real time dosimetric system.

This conclusion can be reached from the response of the dual detector. Before exposure, the beat frequency of the dual device was 7126 Hz. Upon exposure, the frequency changed to approximately 7106 Hz. After exposure, the frequency returns to 7124 Hz. If a reaction with the sample film had occurred, the beat frequency would not have returned to the original frequency when exposure was terminated. With exposure to phosgene, the frequency does not return to the original beat frequency, but remains at the frequency reached when exposure was terminated. It can be stated that the only affect of ethylene oxide upon the sample film is one of simple reversible solvation.

The amount of frequency change observed by this solvation is minimized by the fact that ethylene oxide dissolves into the support matrix, poly(ethylene glycol), that is used to coat both the sample and reference devices. As shown previously in Figure 48 on page 117, this dual coated device configuration ensures that both devices undergo reversible mass loading due to solvation from ethylene oxide, with the net effect being that the beat frequency remains relatively unchanged.

With the exposure of the same films to phosgene, reversible adsorption will take place in the reference film of neat poly(ethylene glycol) but irreversible absorption occurs in the sample film, due to the reaction of phosgene with 4-(4'-nitrobenzyl)pyridine contained in the film. This results in the measured net change in the beat frequency (Figure 49, page 118).

b) Phosgene

1) 100% 4-(4'-nitrobenzyl)pyridine

Experimental Synopsis: Determination of the effect of phosgene exposure upon the frequency change rate of the dual SAW device detector utilizing only 4-(4'-nitrobenzyl)pyridine.

Experimental conditions:

Sample Film Composition: 100% 4-(4'-nitrobenzyl)pyridine

Reference Film Composition: none

Film Thickness: approximately 40 KHz

Flow Rate: 100 cc/min

Vapor being determined: phosgene

Concentrations: 24.8, 12.4 and 4.96 ppm

By using neat 4-(4'-nitrobenzyl)pyridine, the maximum amount of trapping reagent could be deposited upon the sample SAW device. The exposure of these films to phosgene generated data that was erratic. The frequency change rate for these films was inconsistent from run to run. Examination of films deposited on a SAW device showed a patchy deposition of material on the device. This same problem was encountered by Zellers when applying Pt complexes for the analysis of styrene vapor⁸⁰. Zeller's solution was to mix the active organoplatinum complex in a polymer matrix to ensure uniform surface coverage.

These erratic results can be interpreted based upon an analysis of the method with which a SAW device operates. The SAW device is a mass per unit area detector. In areas where mass is deposited upon the surface of the device, the velocity of the acoustic wave is reduced linearly with mass loading. If no mass is deposited upon that

particular area of the surface the acoustic wave velocity is not reduced. With spotty and incomplete film deposition, the wave velocity will fluctuate from fast velocities in uncoated areas to slower velocities in coated areas. The overall effect is that a particular time will be required for a wavefront to traverse the area between the interdigitized transducers and this will be reflected as an average wave velocity. Since the wavelength is fixed by the spacings of the interdigitized electrodes of the transducer, the frequency changes observed reflect the overall change in this velocity.

As the material deposited upon the surface of the SAW device undergoes reaction with phosgene, the areas of the device coated with a film will increase in mass while uncoated areas undergo relatively little or no mass loading. The observed erratic frequency response may therefore be due to the wide variation in local velocities changes that generate an average velocity response for the device. Since different "films" will cover the device in different patterns, reproducibility between films will be poor. The use of a more uniform film would alleviate this response.

To this end, the active agent 4-(4'-nitrobenzyl)pyridine was mixed in two different average molecular weights of poly(ethylene glycol), molecular weight 400 and 1500, at concentrations of approximately 25 and 50 percent by weight and in polystyrene, molecular weight 280,000, at a concentration of approximately 50 percent by weight. The choice of these high mixture concentrations was made using Zeller's 1:1 weight ratio of organoplatinum/polymer mixture as a guide⁸⁰, and with the knowledge available from our pilot studies of phosgene/4-(4'-nitrobenzyl)pyridine that the reaction was rapid. Lower amounts of the reactive agent (4-(4'-nitrobenzyl)pyridine) in the film would lead to an excessively rapid consumption of the film.

2) 4-(4'-nitrobenzyl)pyridine in poly(ethylene glycol) MW 400

a) High Phosgene Concentrations

Experimental Synopsis: Determination of the effect of phosgene exposure upon the frequency change rate of the dual SAW device detector for concentrations of 24.8, 12.4 and 4.96 ppm.

Experimental conditions:

Sample Film Composition: 50.05% 4-(4'-nitrobenzyl)pyridine in poly(ethylene glycol) MW 400

Reference Film Composition: 100% poly(ethylene glycol) MW 400, T_m 6°C.

Film Thickness: approximately 50 KHz

Flow Rate: 100 cc/min

Vapor being determined: phosgene

Concentrations: 24.8, 12.4 and 4.96 ppm

Exposure to these phosgene concentrations generated a response that did not lead to a constant frequency change rate (df/dt) (Figures 57, 58, 59, 60, 61, and 62). The problem encountered in attempting to measure these high concentrations was rapid mass loading of the sample SAW device and consumption of the 4-(4'-nitrobenzyl)pyridine before the frequency change rate could reach a constant value.

This response pattern is indicative of the scenario discussed in the model responses of a film in which the concentration of the vapor increases with time in the film. The frequency change rate could, (A) become constant if [B] remained flooded, or (B) the rate could reach a maximum and then decrease as [B] is consumed to the

point where it is no longer flooded. The latter case is observed for these concentrations of phosgene.

This fact can be used to determine the analytical film lifetime and film exposure constant for each film. The frequency change maximum for these film exposures indicates the point at which the 4-(4'-nitrobenzyl)pyridine concentration is no longer flooded and affects the overall rate of reaction. With continued phosgene exposure, the frequency change rate decreases due to the depleting concentration of 4-(4'-nitrobenzyl)pyridine in the film. The point at which the 4-(4'-nitrobenzyl)pyridine concentration starts to affect the response of the detector (ie. the frequency change maximum) is the point at which the film is no longer analytically useful since the response is now dependent upon both the phosgene exposure concentration and the 4-(4'-nitrobenzyl)pyridine film concentration.

In the case of exposure to 24.8 ppm phosgene shown in Figures 57 and 58, the frequency change rate for a 54.1 KHz film load reaches a maximum of (511 Hz/10 seconds) before decreasing. The total continuous exposure time necessary to reach this maximum rate of change was 242 seconds. This is the film lifetime for this particular film composition exposed at the aforementioned concentration.

The information can be used to calculate the film exposure constant, defined previously as:

$$\text{Exposure} = (\text{ppm-second})/(\text{KHz} \cdot \%[\text{B}]) \quad (69)$$

The film exposure constant for this particular film is

$$\text{Exposure} = (24.8 \text{ ppm} \cdot 242 \text{ seconds})/(54.1 \text{ KHz} \cdot 50.05 \% \text{NBP}) \quad (70)$$

$$\text{Exposure} = 2.22 (\text{ppm-seconds})/(\text{KHz} \cdot \% \text{NBP})$$

By determining the film lifetime (the time from initial exposure to maximum frequency rate change as demonstrated in Figures 58 and 60), this same method of

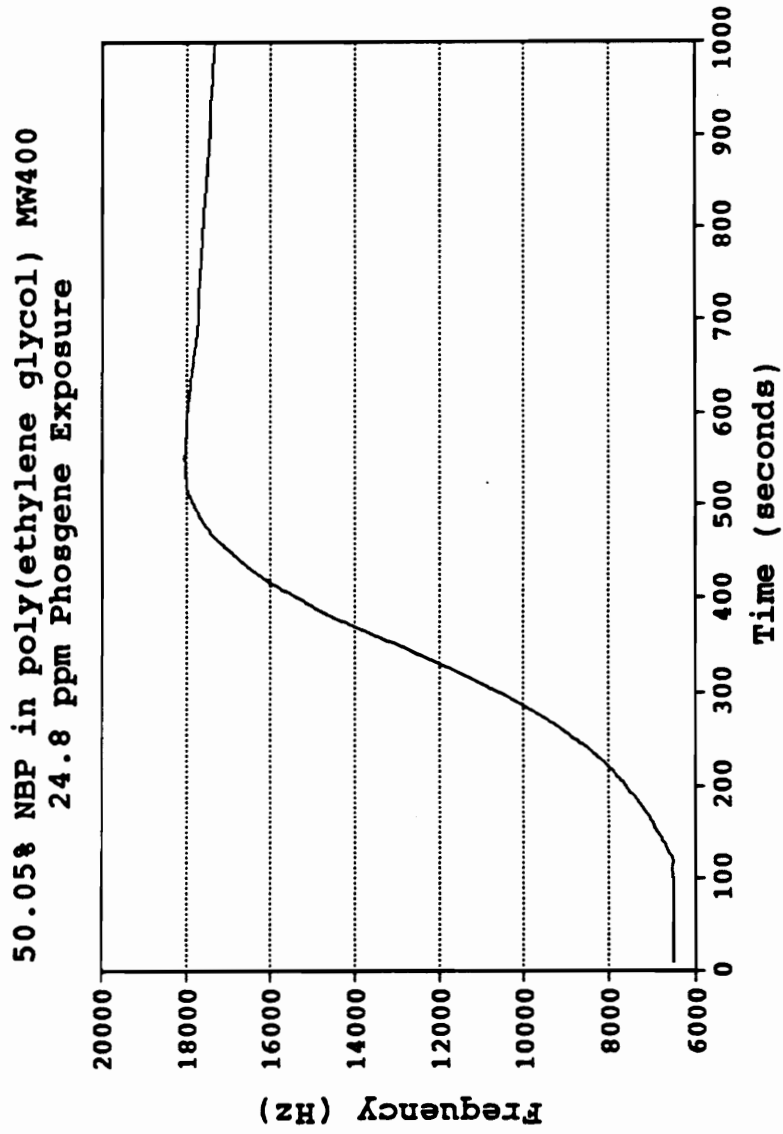


Figure 57. 24.8 ppm phosgene exposure.

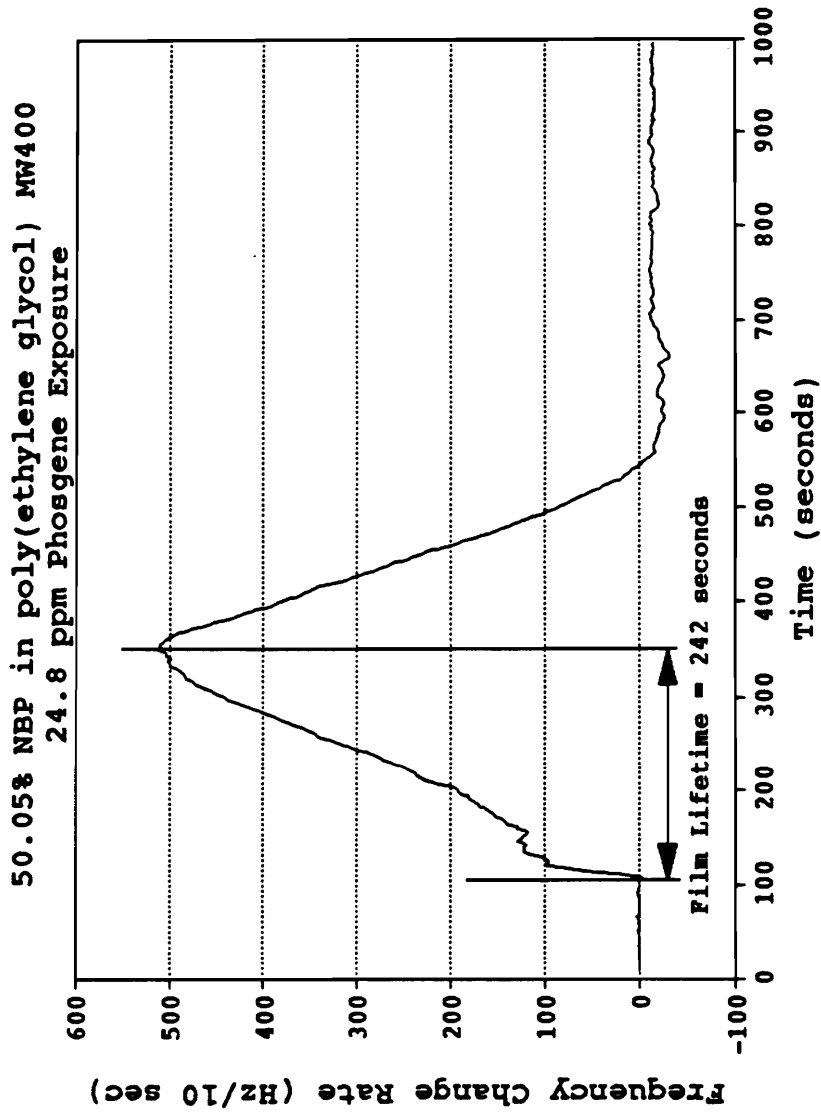


Figure 58. 24.8 ppm phosgene exposure - frequency change rate.

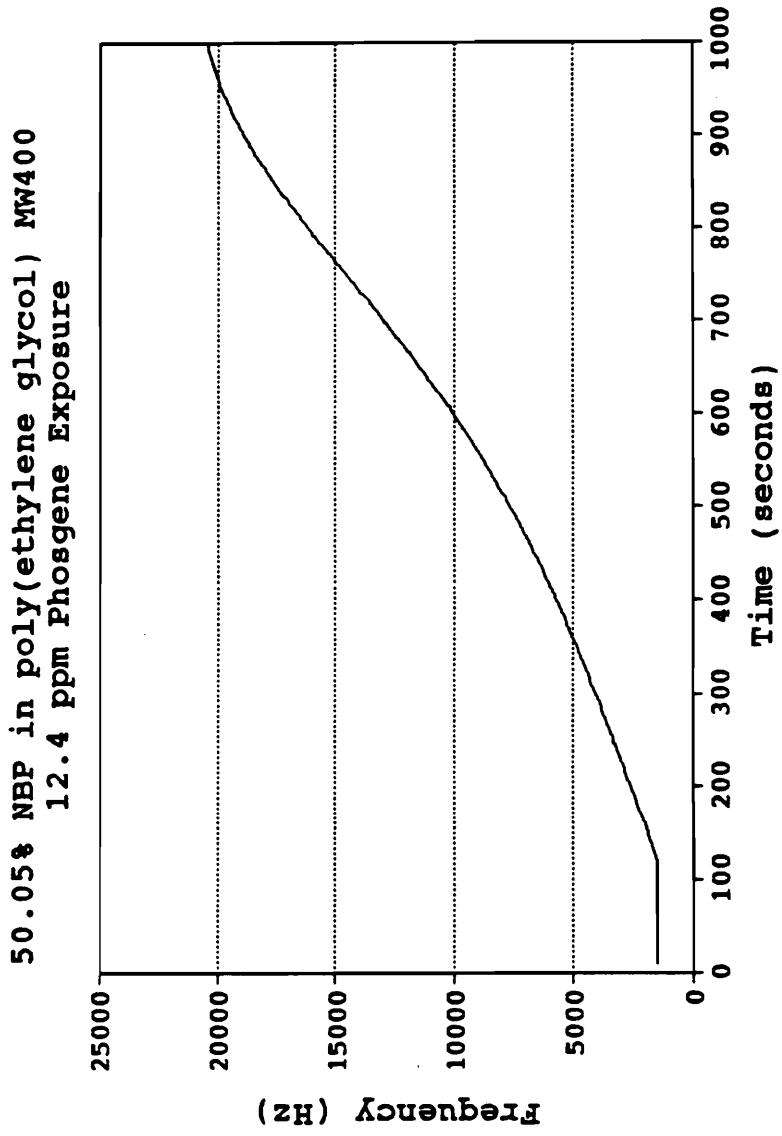


Figure 59. 12.4 ppm phosgene exposure.

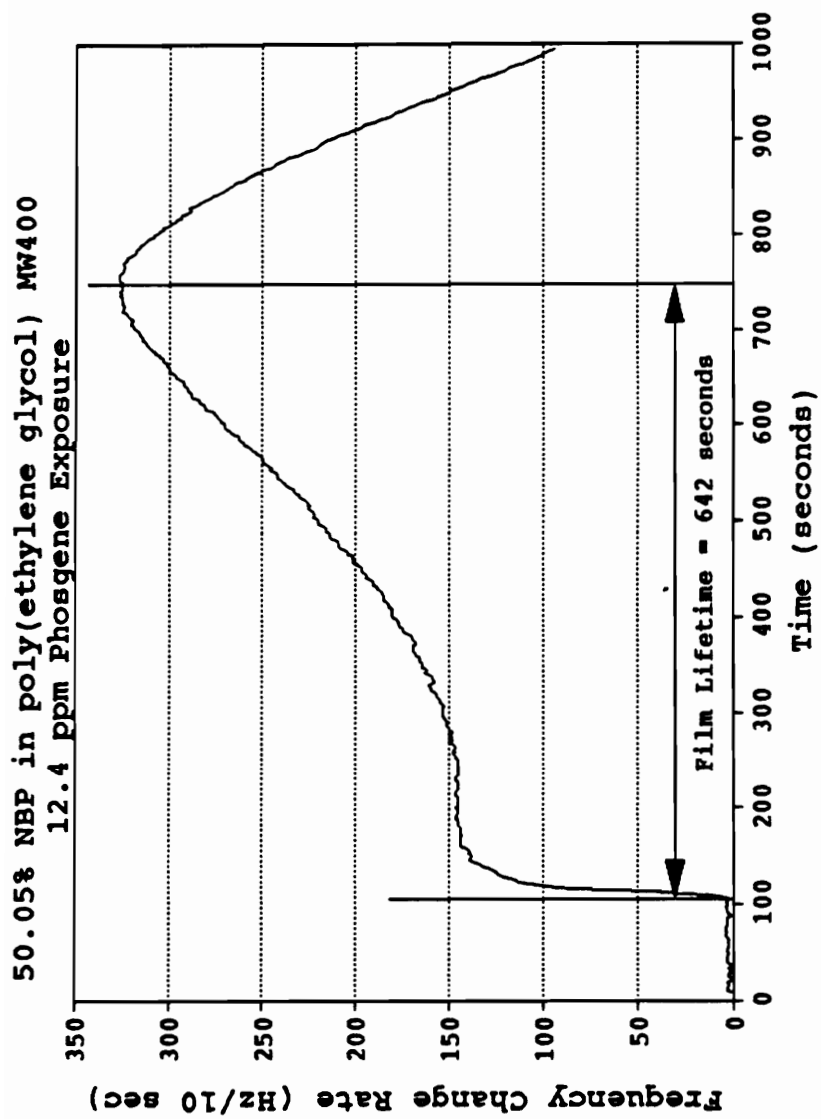


Figure 60. 12.4 ppm phosgene exposure - frequency change rate.

50.05% NBP in poly(ethylene glycol) MW400
4.96 ppm Phosgene Exposure

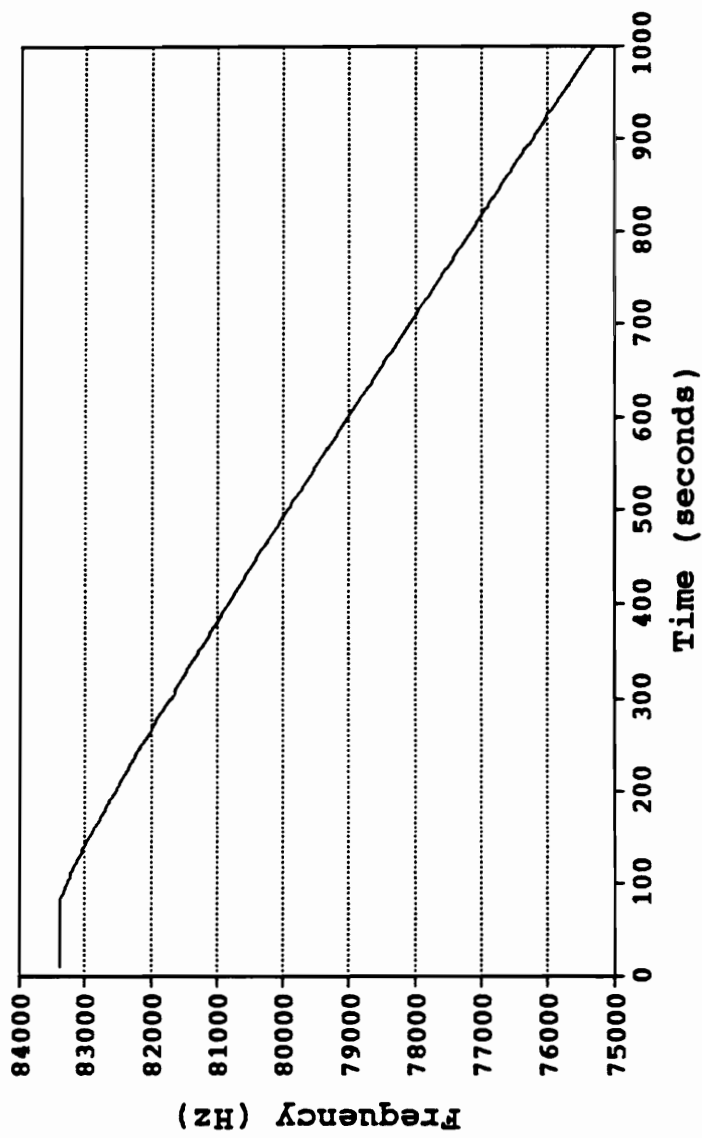


Figure 61. 4.96 ppm phosgene exposure.

50.05% NBP in poly(ethylene glycol) MW400
4.96 ppm Phosgene Exposure

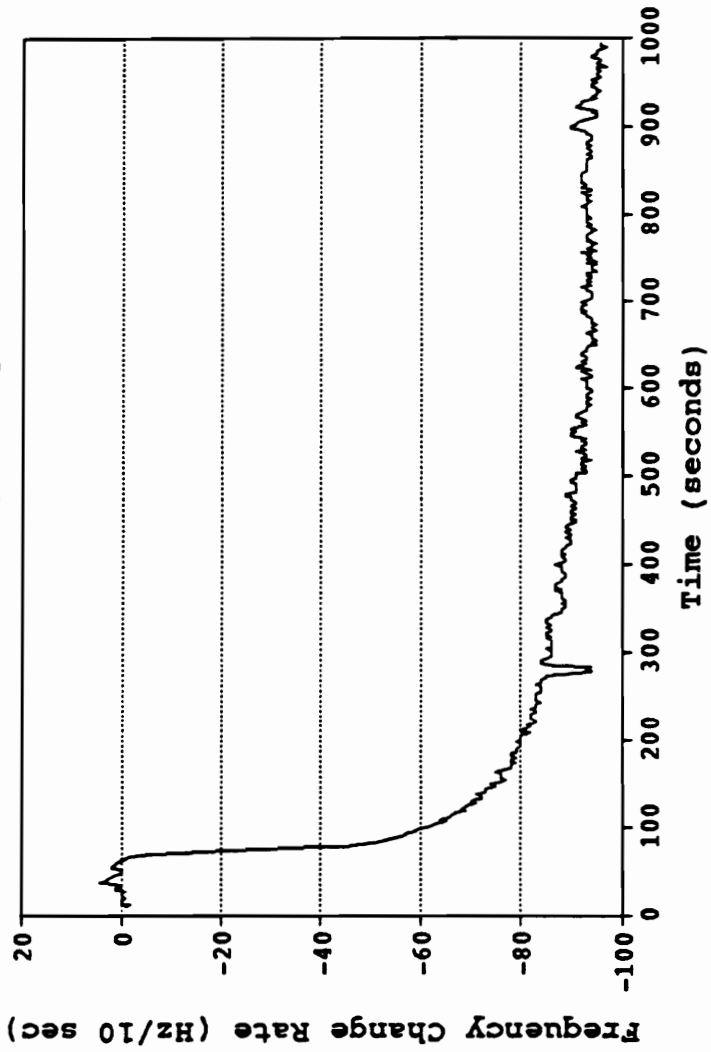


Figure 62. 4.96 ppm phosgene exposure - frequency change rate.

Table 2. Film exposure constants.

% NEP in Poly(Ethylene Glycol) MW 400
Calculation of Film Exposure Constants

Film Thickness (KHz)	%NEP Concentration	Time to Maximum (sec)	Phosgene		Film Constant (ppm-sec)/(KHz-%NEP)
			Concentration (ppm)	Concentration	
55.5	50.05	642	12.4		2.87
58.9	50.05	400	12.4		1.74
54.1	50.05	242	24.8		2.22
53.8	50.05	188	24.8		1.73
57.3	50.05	212	24.8		1.83
53.4	25.47	194	12.4		1.77
51.8	25.47	222	12.4		2.09
38.6	25.47	84	24.8		2.12
49.4	25.47	86	24.8		1.70
47.6	25.47	580	4.96		2.37
49.9	25.47	452	4.96		1.76
Average Exposure Constant				2.02	
Standard Deviation					0.24

calculating the film exposure constant was used for films with different film loads and phosgene exposure levels.

These results are found in Table 2 and will be compared to results obtained in the next series of experiments.

Experimental conditions:

Sample Film Composition: 25.47% 4-(4'-nitrobenzyl)pyridine in poly(ethylene glycol) MW 400

Reference Film Composition: 100% poly(ethylene glycol) MW 400, T_m 6°C.

Film Thickness: approximately 50 KHz

Flow Rate: 100 cc/min

Vapor being determined: phosgene

Concentrations: 24.8, 12.4 and 4.96 ppm

Films composed of a 4-(4'-nitrobenzyl)pyridine concentration approximately one-half of that used in the previous study were investigated for their response to phosgene exposure. As with the 50.05% 4-(4'-nitrobenzyl)pyridine films, exposure to these phosgene concentrations also lead to rapid mass loading of the sample SAW device and consumption of the 4-(4'-nitrobenzyl)pyridine before the frequency change rate could reach a constant value.

Film exposure constants for individual films can be determined using the same procedure demonstrated earlier for the 50.05% 4-(4'-nitrobenzyl)pyridine films. In the case of exposure to 4.96 ppm phosgene shown in Figures 63 and 64, the frequency change rate for a 47.6 KHz film load reaches a maximum of (75 Hz/10 seconds) before decreasing. The film lifetime for this particular film at this concentration was 580 seconds.

The film exposure constant for this particular film is therefore

25.47% NBP in poly(ethylene glycol) MW400
4.96 ppm Phosgene Exposure

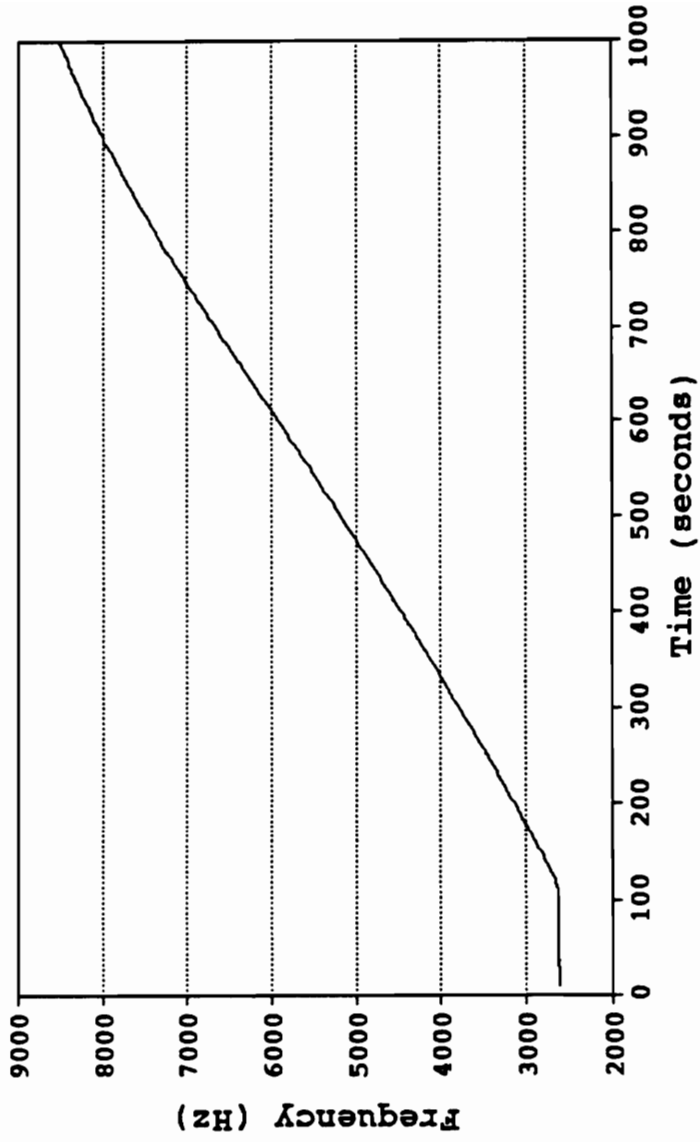


Figure 63. 4.96 ppm phosgene exposure.

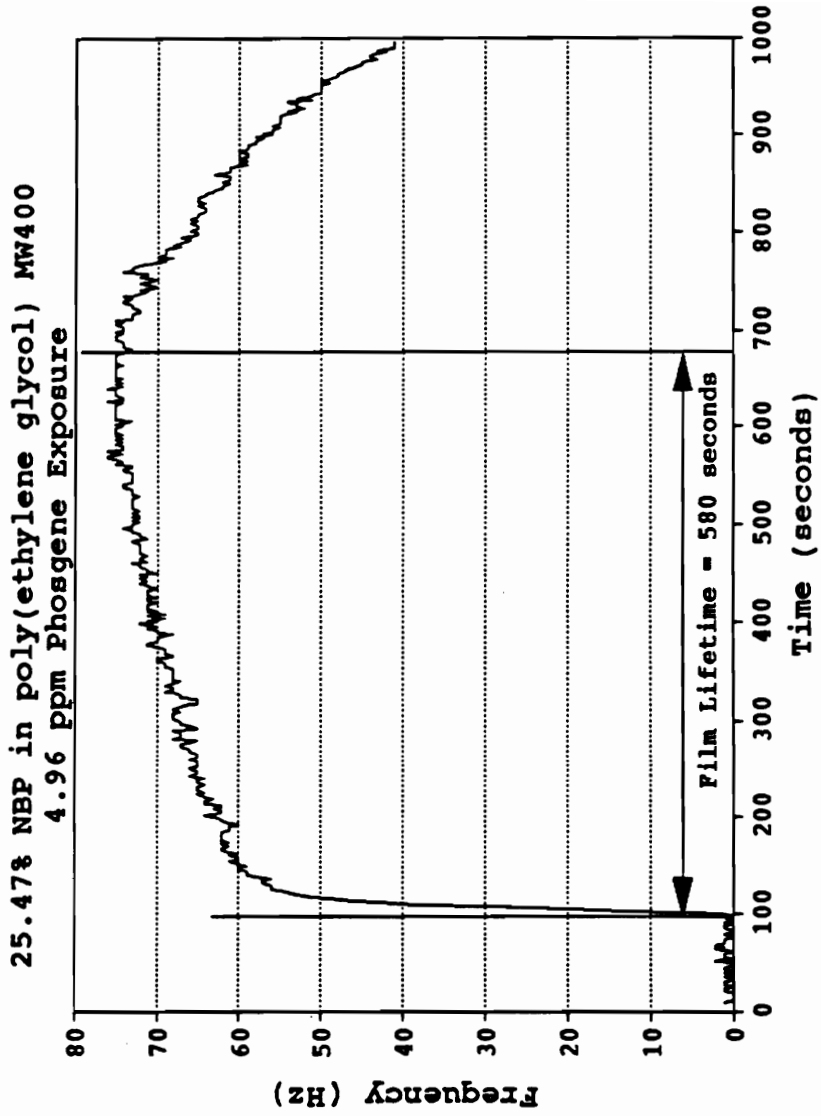


Figure 64. 4.96 ppm phosgene exposure - frequency change rate.

$$\text{Exposure} = (4.96 \text{ ppm} * 580 \text{ seconds}) / (47.6 \text{ KHz} * 25.47 \% \text{NBP}) \quad (71)$$

$$\text{Exposure} = 2.37 \text{ (ppm-seconds)} / (\text{KHz} - \% \text{NBP})$$

Calculations of film exposure constants for this film concentration with different film loads and phosgene exposure levels can also be found in Table 2 on page 141.

The use of a Wilcoxon rank sum test to determine if there is any statistical difference in the film exposure constants obtained for the 50.05% and 25.47% 4-(4'-nitrobenzyl)pyridine films shows that there is no difference. Based upon this observation, an estimate of general film lifetimes can be determined for different film compositions of 4-(4'-nitrobenzyl)pyridine in poly(ethylene glycol), MW 400, as

$$\text{Exposure} = 2.02 \pm 0.24 \text{ (ppm-seconds)} / (\text{KHz} - \% \text{NBP}). \quad (72)$$

The obvious question at this point is why does the film exposure constant remain the same for different phosgene vapor and 4-(4'-nitrobenzyl)pyridine film concentrations? What, if anything, does this indicate about the observed reaction order with respect to these species?

Since the exposure constant is defined as

$$\text{(ppm-seconds)} / ((\% \text{KHz})(\% \text{NBP})) \quad (73)$$

the results are consistent with a reaction rate that is first order dependent upon both the phosgene and 4-(4'-nitrobenzyl)pyridine concentrations. This conclusion can be reached based upon the following arguments.

First, using the same 4-(4'-nitrobenzyl)pyridine concentration, different concentrations of phosgene yield the same film exposure constant. While lower concentrations require longer times until the film is consumed, the time-concentration products when normalized for the specific film thickness used are the same. For this to occur, the reaction rate must be first order (ie. linear) with respect to the phosgene

concentration. This can be proven by examining what the results of the film exposure constants would be if the reaction rate was second order with respect to phosgene.

This is not to imply that the reaction is second order with respect to phosgene. The purpose of this examination of the film exposure constant calculation with respect to phosgene order is to demonstrate that the calculation is capable of differentiating between reaction orders.

As developed earlier, if the reaction rate was second order dependent upon the phosgene concentration, there would be an exponential relationship between reaction rate and phosgene concentration rather than a linear relationship. To demonstrate what the effect of a second order dependence upon the calculation of the film exposure constant would be, a film exposure constant from Table 2 on page 141 will be used.

A film thickness of 38.6 KHz containing 25.47% 4-(4'-nitrobenzyl)pyridine in poly(ethylene glycol), MW 400, when exposed to 24.8 ppm phosgene yielded a film exposure constant of 2.12 ppm-seconds/((KHz)(%NBP)). After 84 seconds of phosgene exposure to this film, enough of the 4-(4'-nitrobenzyl)pyridine in the film has reacted with the phosgene vapor so that the film no longer contains a flooded concentration of 4-(4'-nitrobenzyl)pyridine. As developed earlier, when the 4-(4'-nitrobenzyl)pyridine concentration also begins to affect the response of the film because it is no longer in a flooded state, the film is considered consumed. The reasonable assumption will be made that the amount of 4-(4'-nitrobenzyl)pyridine needed to be irreversibly reacted with in the film (and therefore the amount of product produced) before the film is considered consumed will be the same regardless of the phosgene concentration used for the exposure.

From the discussion of fixed time exposures, the amount of product produced for an exposure of a film containing reagent [B] at a constant concentration of vapor [A] for time t_1 is

$$[C] = k[A]^2[B]t_1 \quad (74)$$

For a fixed value of [C], exposure to phosgene concentrations of 24.8, 12.4 and 4.96 ppm will generate the following equalities

$$[C] = k[24.8]^2[B]t_1 = k[24.8/2]^2[B]t_2 = k[24.8/4]^2[B]t_3 \quad (75)$$

$$t_1 = t_2/4 = t_3/16$$

The calculation of film exposure constants for these three phosgene concentrations can be performed. These are

$$(24.8 \text{ ppm})(84 \text{ sec})/((38.6 \text{ KHz})(25.47\% \text{ NBP})) = 2.12 \quad (76)$$

$$(12.4 \text{ ppm})(84 \text{ sec})(4)/((38.6 \text{ KHz})(25.47\% \text{ NBP})) = 4.24 \quad (77)$$

$$(4.96 \text{ ppm})(84 \text{ sec})(16)/((38.6 \text{ KHz})(25.47\% \text{ NBP})) = 6.78 \quad (78)$$

The analysis conducted would be exact if the conditions assumed were rigorously correct. This is not the case, as it has been shown that the film concentration of phosgene increases with time at high concentrations. However the result of this analysis indicates that the variation encountered if the reaction rate were second order would be much greater than the 10% observed for the experiments conducted.

Based upon these results, the observed reaction rate order with respect to phosgene is first order.

Further analysis of the reaction rate order dependence for both phosgene and 4-(4'-nitrobenzyl)pyridine will be made in the short term fixed time exposure experiments that will be presented in later sections.

b) Low Phosgene Concentrations

Experimental Synopsis: With the rapid consumption of films by a phosgene concentration of 4.96 ppm and greater, the determination of the effect of phosgene exposure upon the frequency change rate of the dual SAW device detector for concentrations of 2.48, 1.24 and 0.496 ppm was deemed necessary.

Experimental conditions:

Sample Film Composition: 50.47% 4-(4'-nitrobenzyl)pyridine in poly(ethylene glycol) MW 400

Reference Film Composition: 100% poly(ethylene glycol) MW 400, T_m 6°C.

Film Thickness: approximately 50 KHz

Flow Rate: 100 cc/min

Vapor being determined: phosgene

Concentrations: 2.48, 1.24 and 0.496 ppm

Exposure to 2.48 ppm phosgene demonstrates what can be encountered in determining the frequency change rate for long term fixed concentration exposures. Over the 1800 seconds exposure represented in Figures 65, 66, 67, 68, the frequency change rate first levels at 16 Hz/10 seconds but continues to rise to 38 Hz/10 seconds. The conclusion is that the reaction rate (as measured by the frequency change rate) at this concentration is dependent upon the length of time of the exposure. This is indicative that the concentration of the adsorbed vapor in the film increases with time.

Not until the phosgene exposure level is reduced to 1.24 ppm does the frequency change rate reach a level which is constant for the lifetime of the exposure (Figure 70). For an exposure level of 1.24 ppm, a 41.4 KHz film load responds by attaining a frequency change rate of 15-17 Hz per 10 second increment within 300 seconds after initial exposure (Figure 70). For an exposure level of 0.496 ppm,

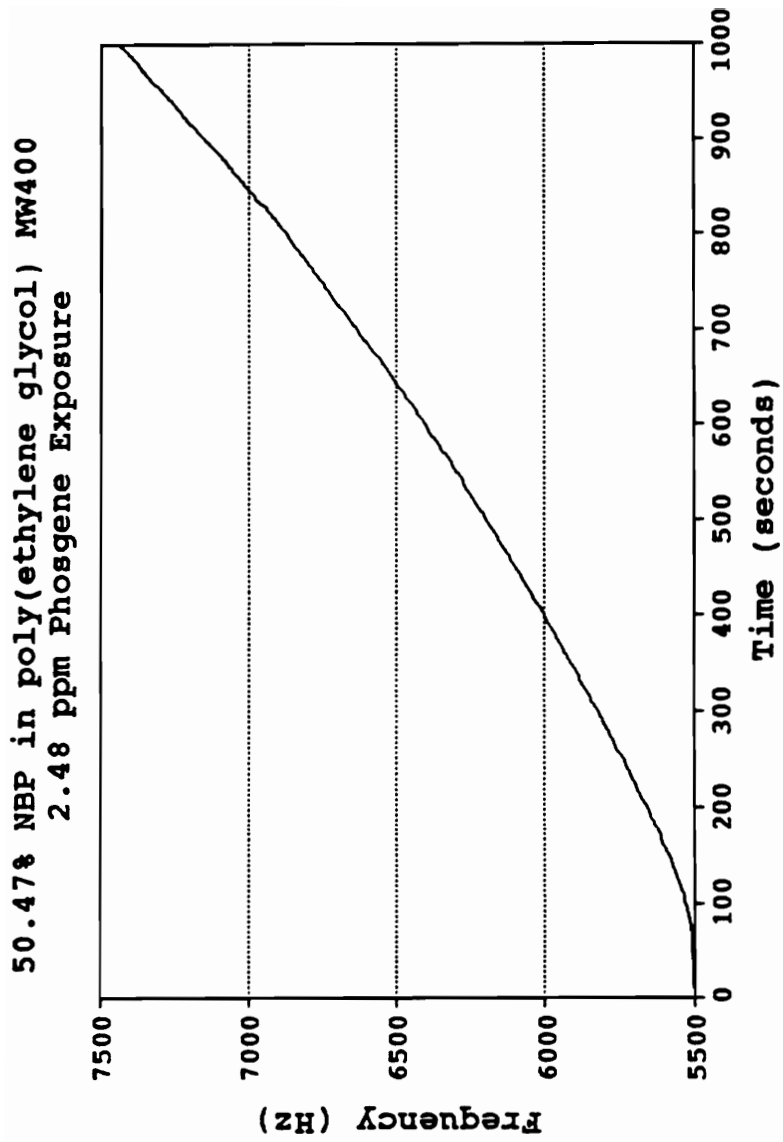


Figure 65. 2.48 ppm phosgene exposure.

50.47% NBP in poly(ethylene glycol) MW400
2.48 ppm Phosgene Exposure

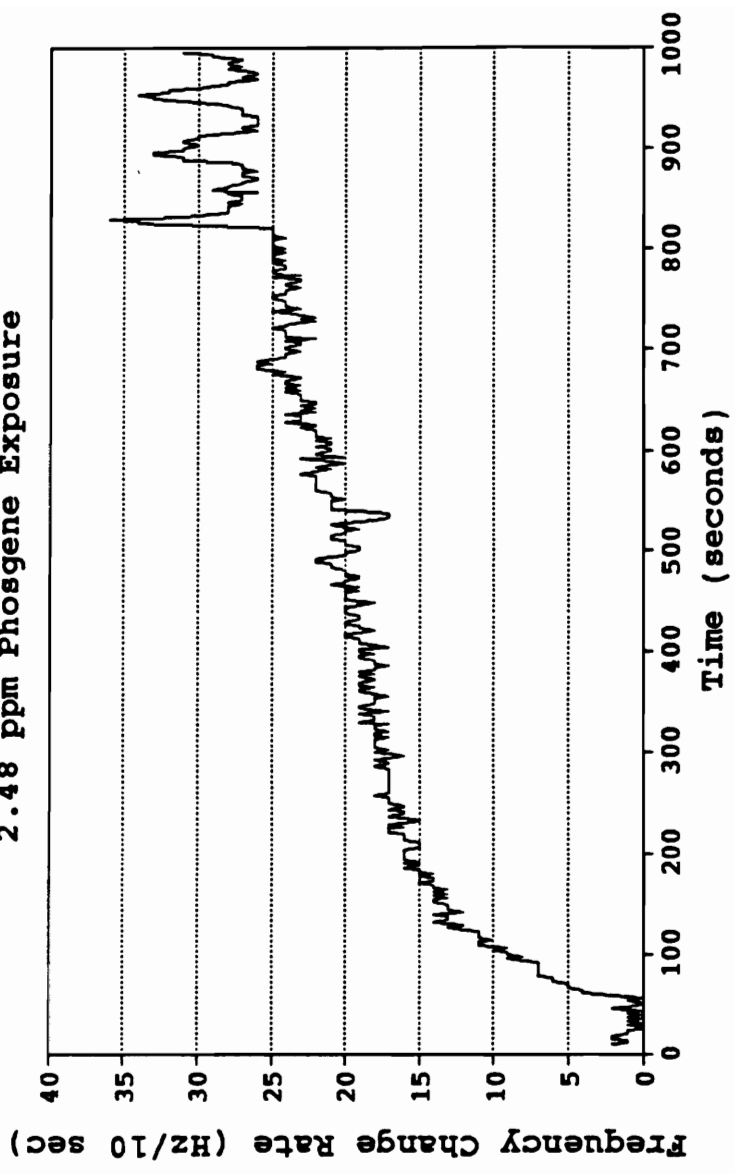


Figure 66. 2.48 ppm phosgene exposure - frequency change rate.

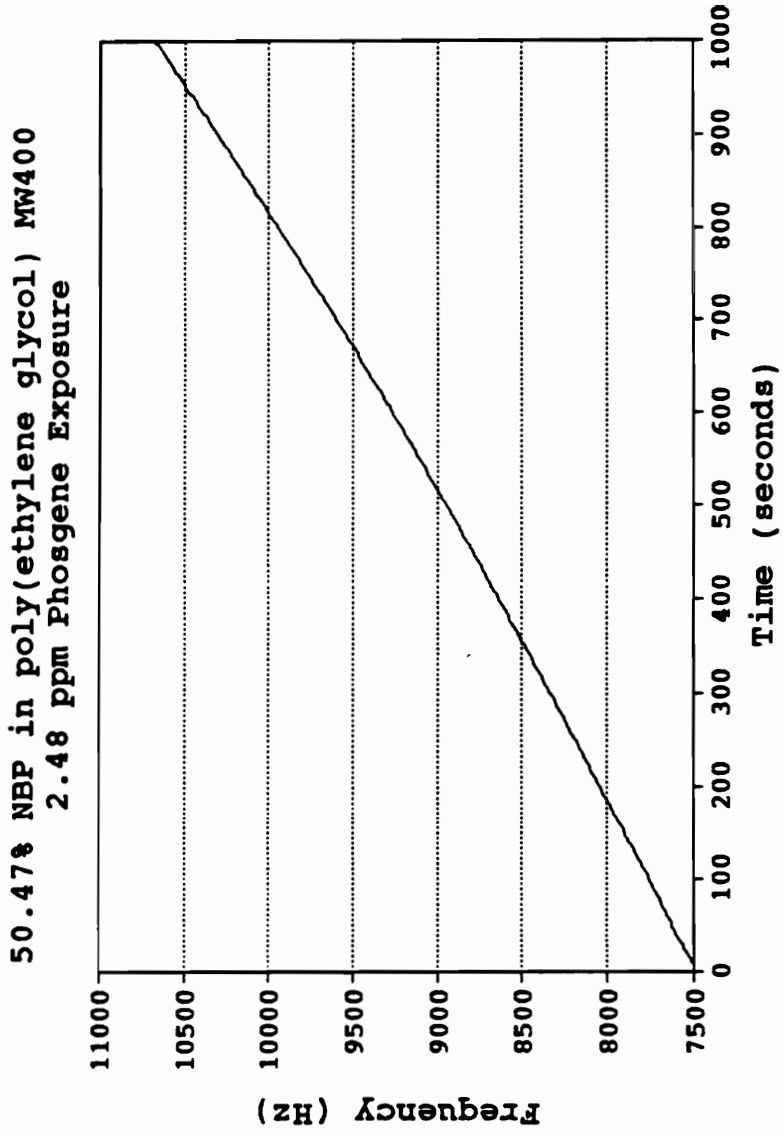


Figure 67. 2.48 ppm phosgene exposure.

50.47% NBP in poly(ethylene glycol) MW400
2.48 ppm Phosgene Exposure

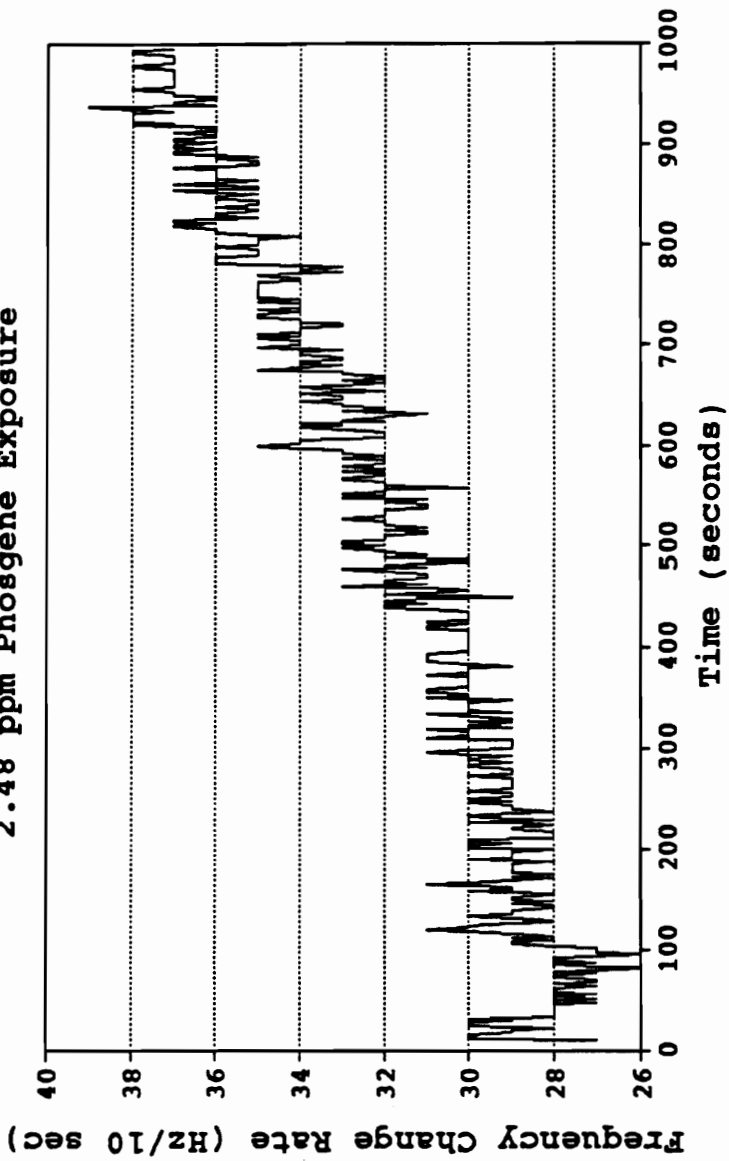


Figure 68. 2.48 ppm phosgene exposure - frequency change rate.

50.47% NBP in poly(ethylene glycol) MW400
1.24 ppm Phosgene Exposure

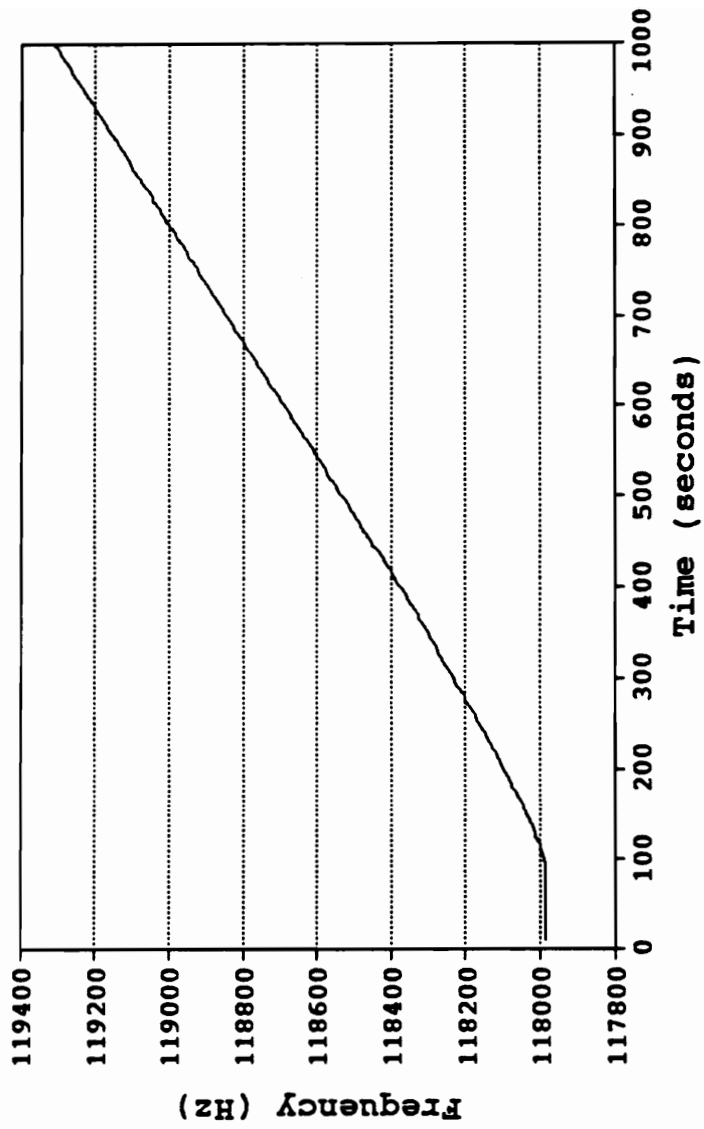


Figure 69. 1.24 ppm phosgene exposure.

50.47% NBP in poly(ethylene glycol) MW400
1.24 ppm Phosgene Exposure

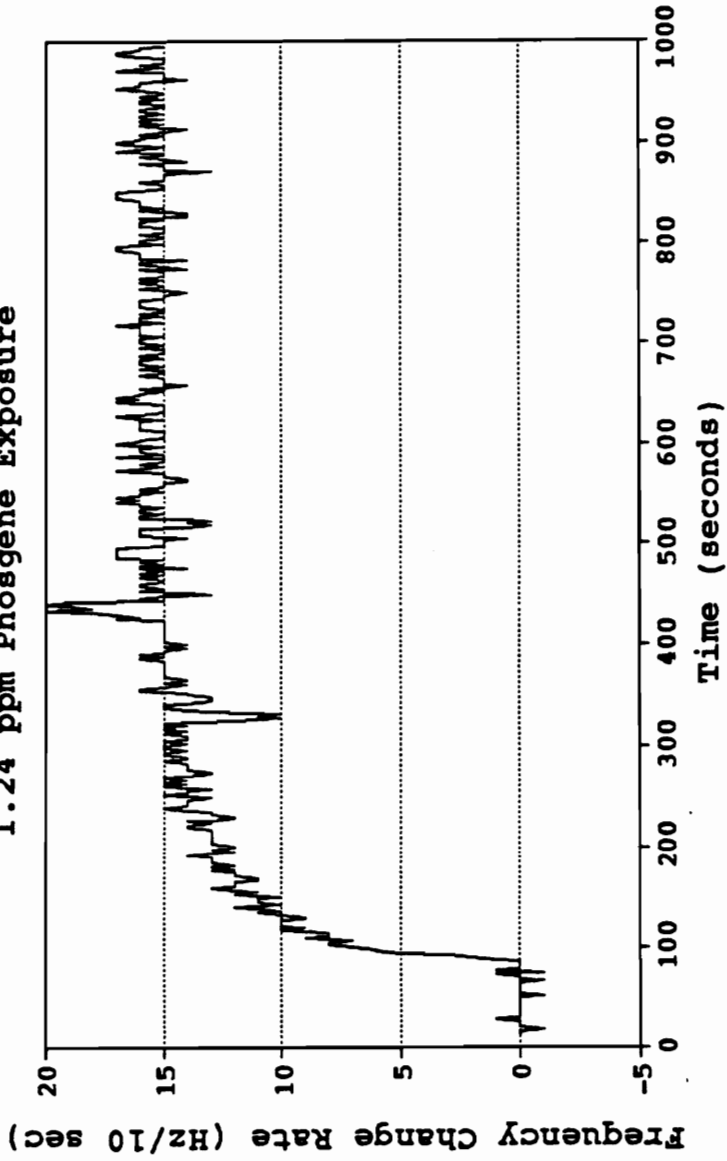


Figure 70. 1.24 ppm phosgene exposure - frequency change rate.

50.47% NBP in poly(ethylene glycol) MW400
0.496 ppm Phosgene Exposure

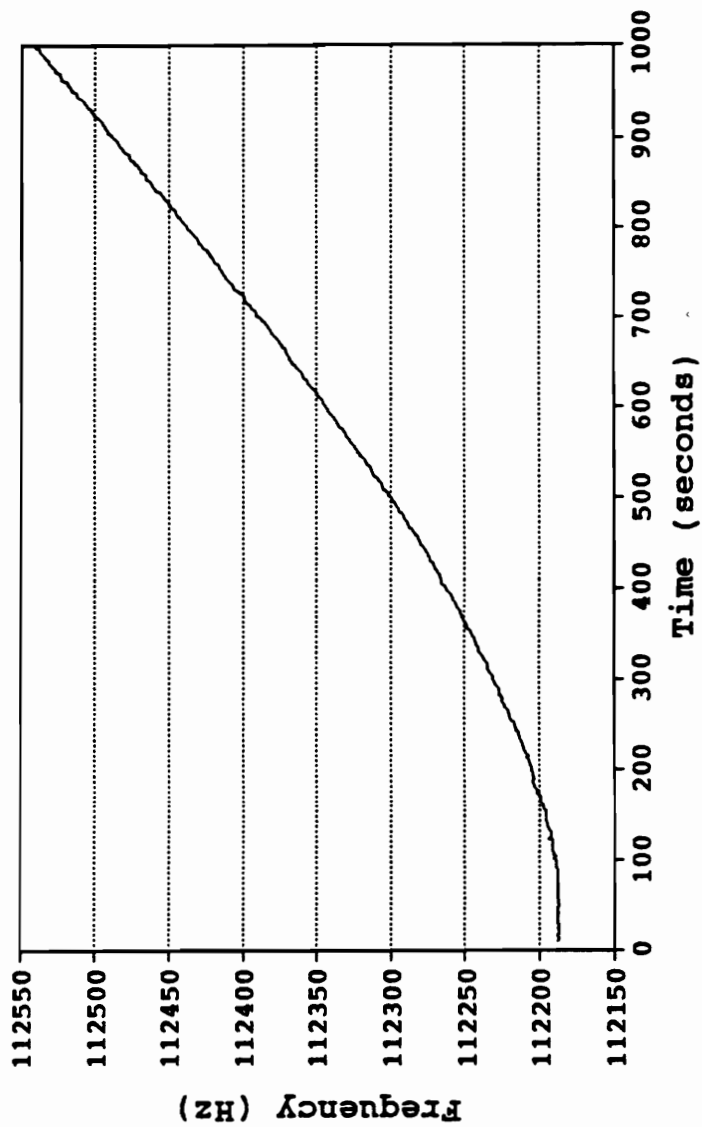


Figure 71. 0.496 ppm phosgene exposure.

50.47% NBP in poly(ethylene glycol) MW400
0.496 ppm Phosgene Exposure

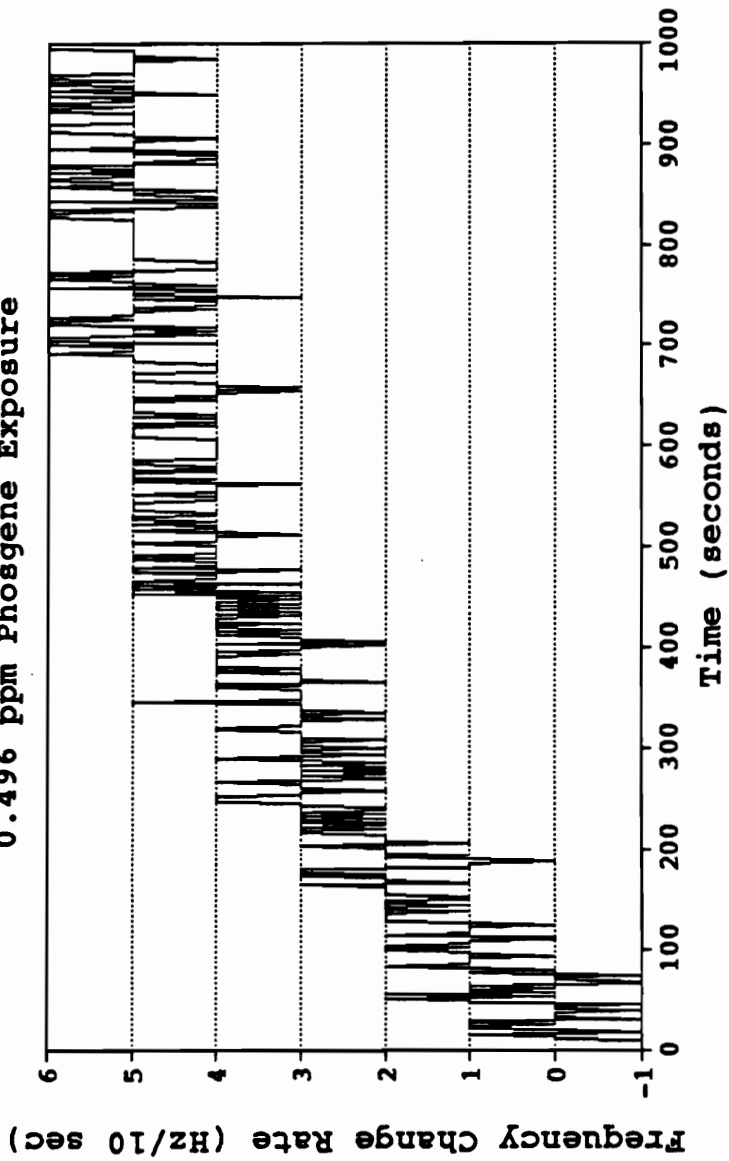


Figure 72. 0.496 ppm phosgene exposure - frequency change rate.

a 41.7 KHz film load responds by attaining a frequency change rate of 5-6 Hz per 10 second increment (Figure 72) . Using the previously determined film exposure constant of 2.02 ppm-seconds/(KHz- %NBP) for 4-(4'-nitrobenzyl)pyridine in poly(ethylene glycol) MW 400 and rearranging the equation used to calculated the film exposure constant to now determine a film lifetime, the expected film lifetimes for these two particular films exposed at these concentrations can be calculated. They are:

$$\text{Film Lifetime} = 2.02 \text{ (ppm-seconds)/(KHz- \%NBP)}(41.4 \text{ KHz} * 50.47 \% \text{NBP})/(1.24 \text{ ppm}) \quad (79)$$

$$\text{Film Lifetime} = 3404 \text{ seconds or } 56 \text{ minutes}$$

and

$$\text{Film Lifetime} = 2.02 \text{ (ppm-seconds)/(KHz- \%NBP)}(41.7 \text{ KHz} * 50.47 \% \text{NBP})/(0.496 \text{ ppm}) \quad (80)$$

$$\text{Film Lifetime} = 8571 \text{ seconds or } 143 \text{ minutes}$$

This information assumes that there is no change in response to different film thicknesses. In the short-term fixed-time exposure experiments to be reported later in this work, exposure of phosgene to different film thicknesses will demonstrate that this assumption is correct.

Due to the rapid rate at which phosgene reacts with the film, it became impossible to generate a calibration curve based on frequency change rates at the concentrations tested. Therefore short-term fixed-time exposure experiments were conducted later in this work to determine if a calibration curve would be developed based upon total frequency shift for a given concentration at a given time, measured in ppm-seconds of exposure.

3) 4-(4'-nitrobenzyl)pyridine in poly(ethylene glycol) MW 1500

Experimental Synopsis: With the rapid consumption of films using the liquid poly(ethylene glycol), MW 400 support matrix, a change to the waxy poly(ethylene glycol), MW 1500 was made in an attempt to slow the frequency change rate.

Experimental conditions:

Sample Film Composition: 50.00% 4-(4'-nitrobenzyl)pyridine in poly(ethylene glycol) MW 1500

Reference Film Composition: 100% poly(ethylene glycol) MW 1500, T_m 45°C.

Film Thickness: approximately 50 KHz

Flow Rate: 100 cc/min

Vapor being determined: phosgene

Concentrations: 24.8, 12.4 and 4.96 ppm

In a work environment, low level monitoring of toxic and harmful vapors is paramount to ensure the safety of personnel. However, high level monitoring is also needed for use in determining appropriate medical treatment for critical exposures. SAW devices are capable of real time monitoring generating data that will determine concentrations and exposure times. The time resolution is only dependent upon how often the frequency is measured. Most dosimeters are only capable of determining average exposure concentrations (the time weighed average) since the phenomena being used to determine the exposure level (ie. radiation level, transmittance, absorbance) is usually measured at the end of a user's shift. The intent is to provide more precise and immediate information for a more informed treatment.

With this in mind, an attempt was made to reduce the frequency change rate of the SAW devices upon phosgene exposure by using a higher molecular weight poly(ethylene glycol) with a T_m above the temperature of the detector cell. This

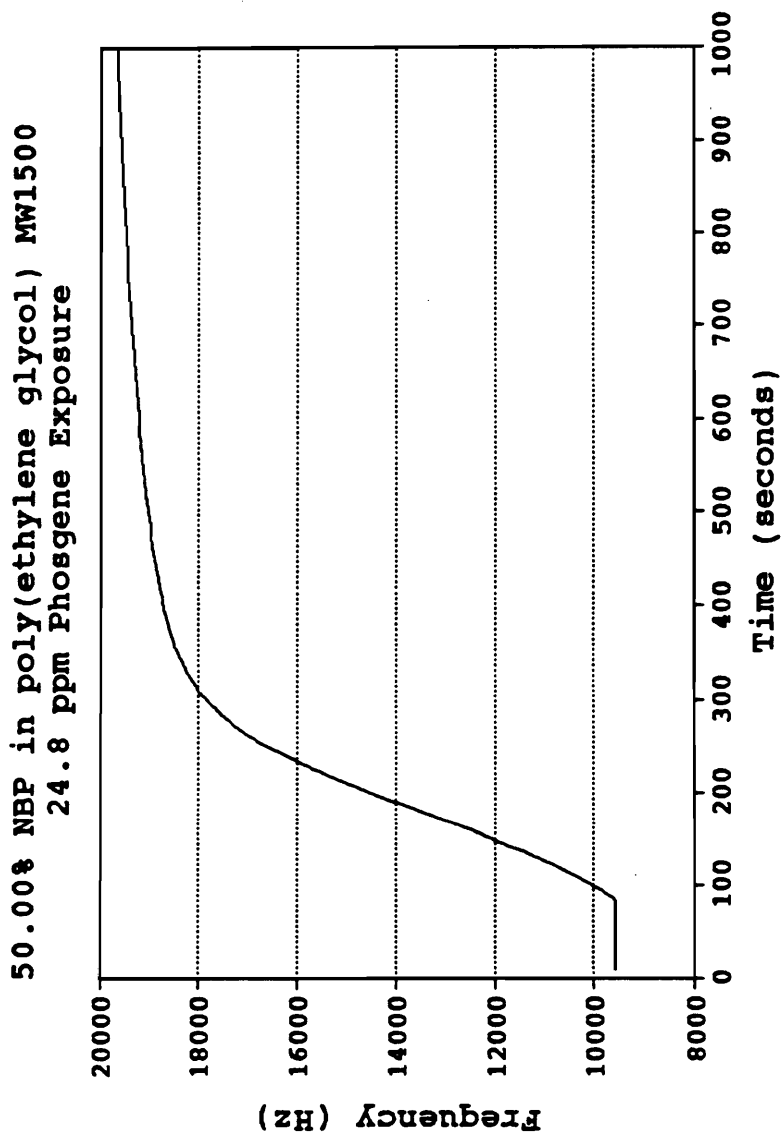


Figure 73. 24.8 ppm phosgene exposure.

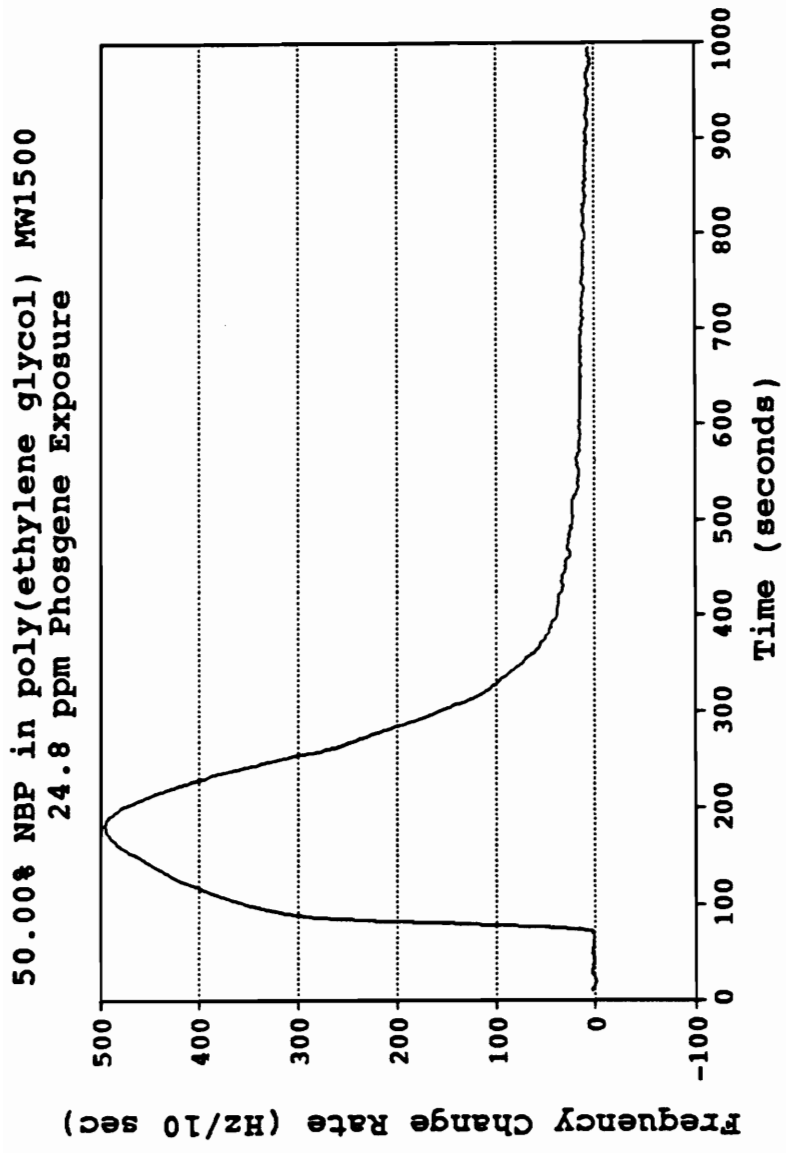


Figure 74. 24.8 ppm phosgene exposure - frequency change rate.

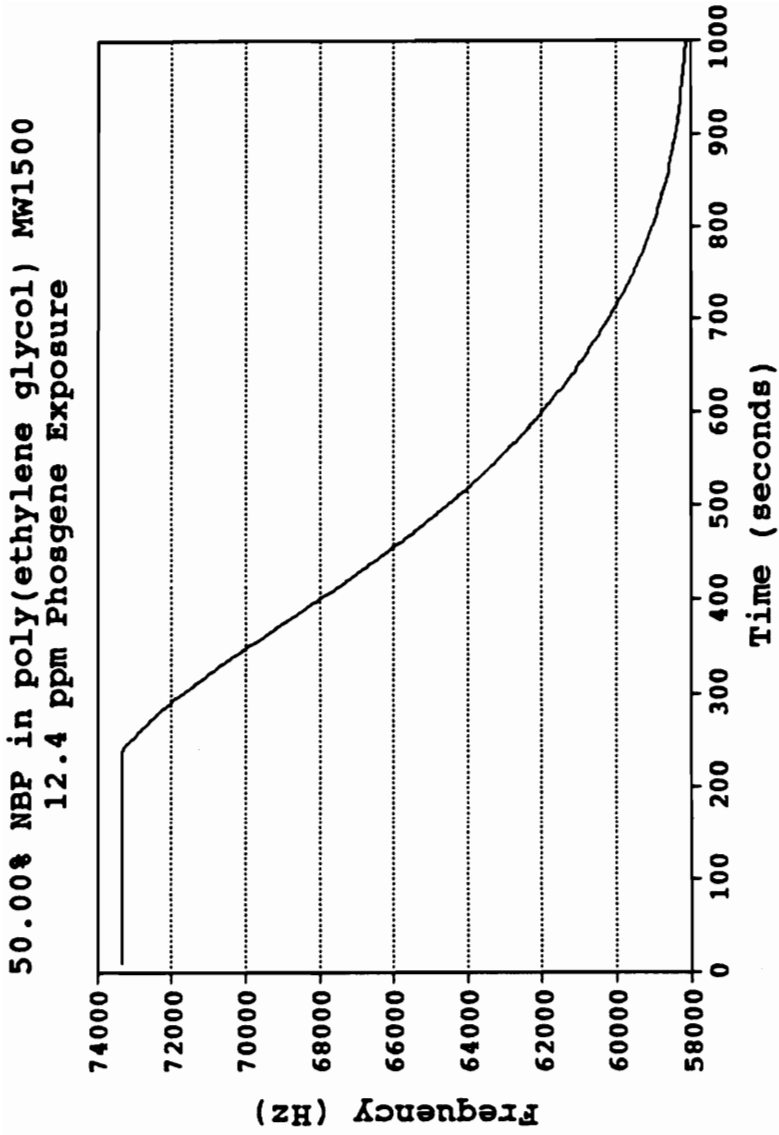


Figure 75. 12.4 ppm phosgene exposure.

50.00% NBP in poly(ethylene glycol) MW1500
12.4 ppm Phosgene Exposure

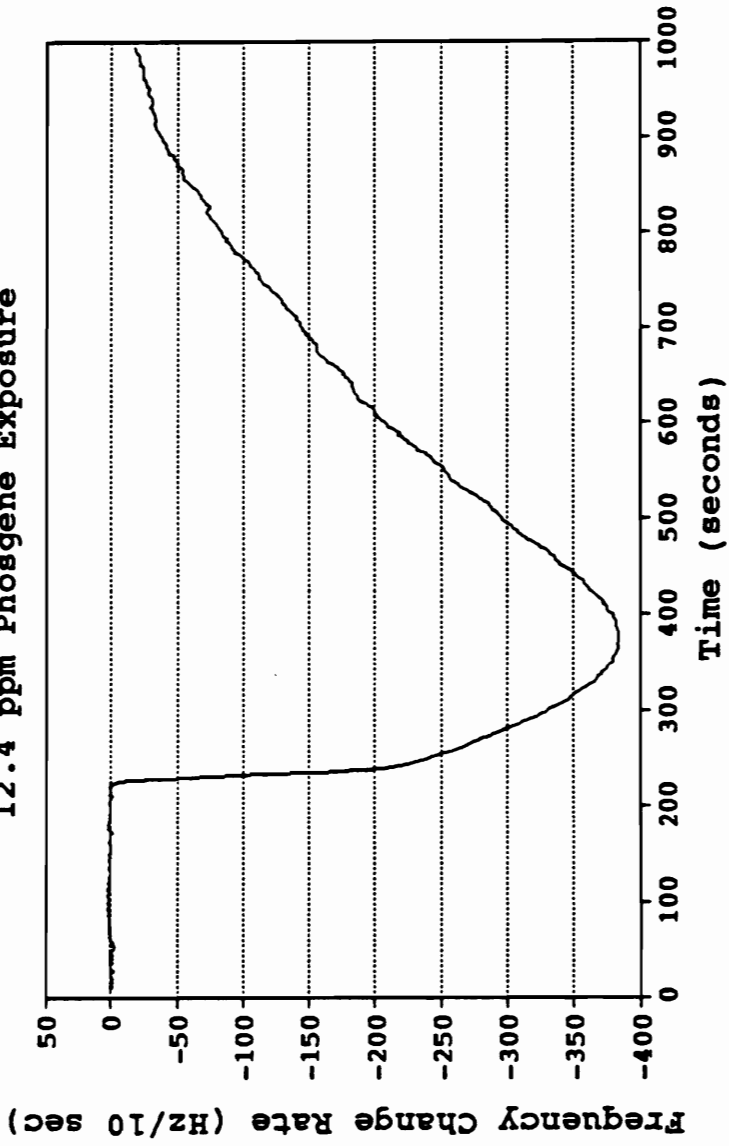


Figure 76. 12.4 ppm phosgene exposure - frequency change rate.

50.00% NBP in poly(ethylene glycol) MW1500
4.96 ppm Phosgene Exposure

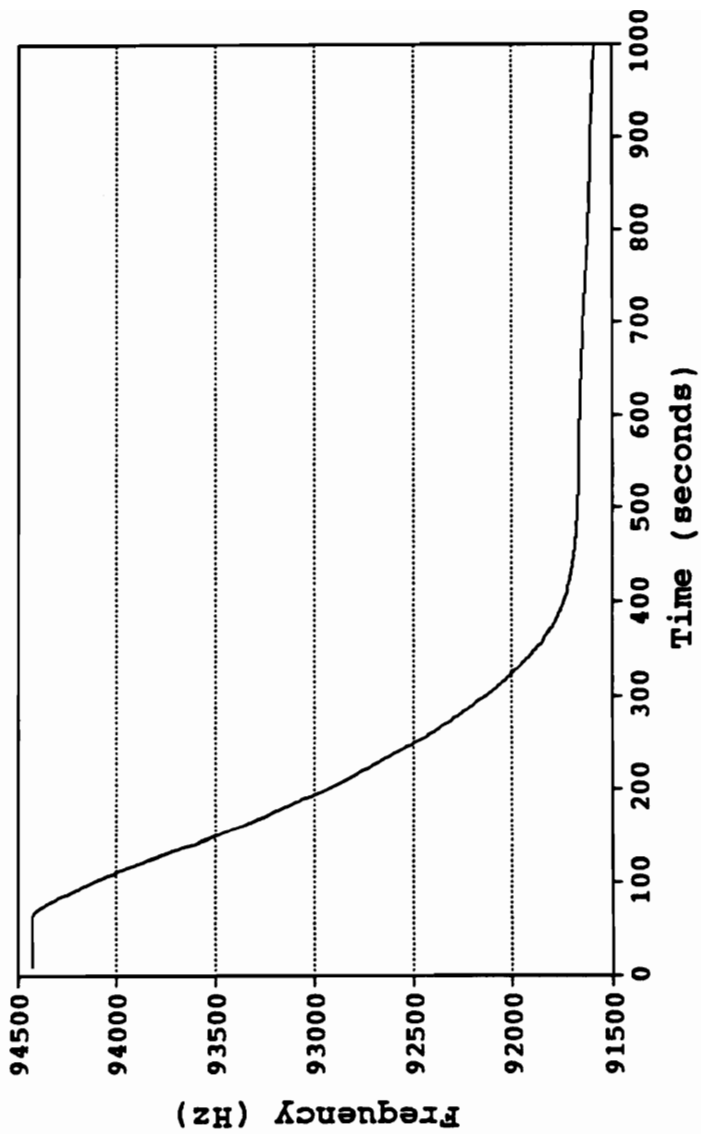


Figure 77. 4.96 ppm phosgene exposure.

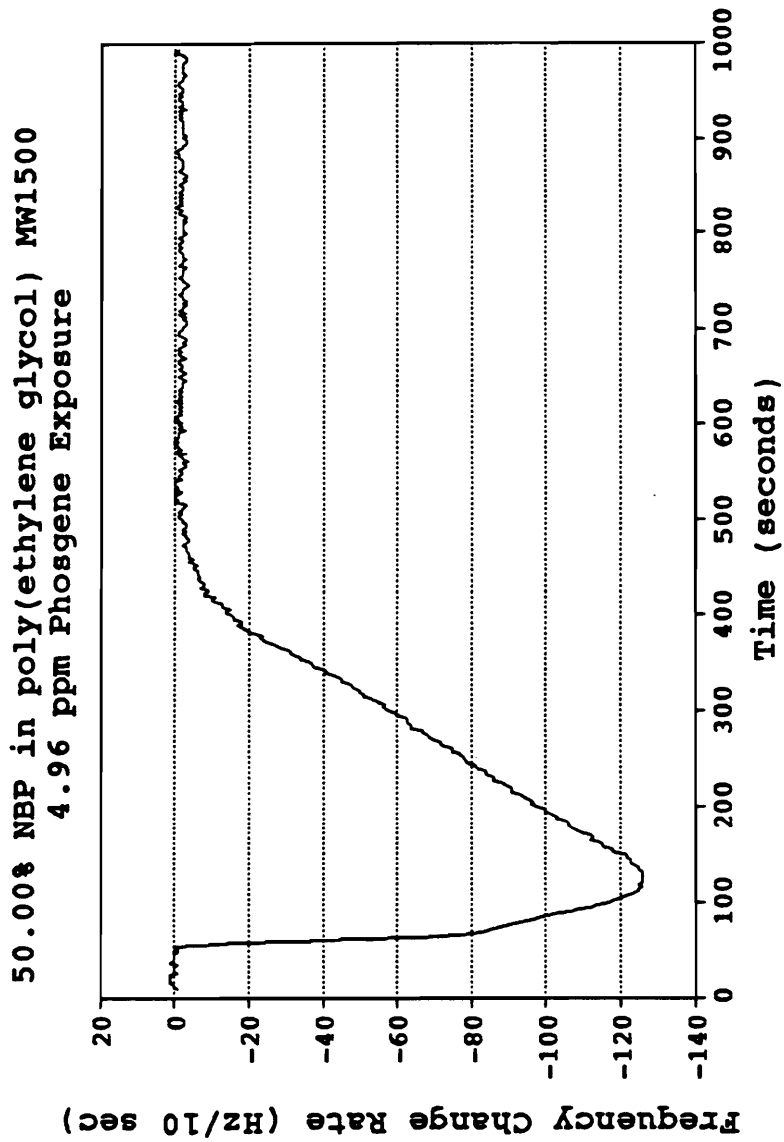


Figure 78. 4.96 ppm phosgene exposure - frequency change rate.

technique has been used successfully to vary the permeability rate of ethylene oxide for the development of colorimetric detector films⁸¹.

The rationale behind this approach is that if the polymer can slow down the rate of permeation of the vapor, the measured rate of reaction will be lowered as the permeability is now the rate determining step for the overall irreversible reaction. A crystalline material above its T_m will be less permeable than the same material in a viscous state as permeability for a particular polymer generally decreases with increasing crystallinity⁸².

While the SAW response will be less than that for a film which has a higher permeability, and therefore less sensitive, the film will be capable of measuring higher concentrations of phosgene than the more sensitive film. In this particular case, a film to accurately measure 12.4 and 24.8 ppm phosgene was pursued since the poly(ethylene glycol) MW 400 films were rapidly consumed and of no analytical use at these concentrations.

Unfortunately, exposure of 50.00% 4-(4'-nitrobenzyl)pyridine in poly(ethylene glycol) MW 1500 did not reduce the frequency rate of change for 24.8, 12.4 and 4.96 ppm phosgene from that obtained using poly(ethylene glycol) MW 400 (Figures 73, 74, 75, 76, 77, 78).

The results indicate that the extent of crystallinity of this polymer with dissolved 4-(4'-nitrobenzyl)pyridine is insufficient to reduce the film response to phosgene. In this application, there is no appreciable difference between the permeability of poly(ethylene glycol) films using a polymer matrix above the T_m and below the T_m .

Since the purpose of changing to the higher molecular weight poly(ethylene glycol) was to be able to successfully monitor the concentrations of phosgene that rapidly consumed the poly(ethylene glycol) MW 400 films (4.96, 12.4 and 24.8 ppm),

further long term experiments and short term exposures were not conducted with poly(ethylene glycol) MW 1500 as a support medium.

In order to reduce the permeation of phosgene into the film for phosgene analysis of concentrations that saturate poly(ethylene glycol), a more restrictive matrix needs to be utilized, and this is demonstrated in the next set of experiments.

4) 4-(4'-nitrobenzyl)pyridine in polystyrene MW 280,000

Experimental Synopsis: A change to a non-polar polymer below its T_g was made in an attempt to reduce the frequency change rate for analysis of high phosgene concentrations.

Experimental conditions:

Sample Film Composition: 49.90% 4-(4'-nitrobenzyl)pyridine in polystyrene, MW 280,000

Reference Film Composition: 100% polystyrene, MW 280,000, T_g 100°C, T_m 237.5°C

Film Thickness: approximately 50 KHz

Flow Rate: 100 cc/min

Vapor being determined: phosgene

Concentrations: 24.8 and 12.4 ppm

Since the reaction of phosgene with 4-(4'-nitrobenzyl)pyridine in poly(ethylene glycol) proved to be very rapid at high concentrations (ie. 4.96, 12.4, and 24.8 ppm), the choice of a non-polar glassy support matrix that would have a different permeability towards these polar alkylating agents seemed to be a reasonable direction to take towards developing a film for use at such high concentrations.

Exposure to 24.8 ppm phosgene yielded a frequency change rate of 3.5 to 4.5 Hz per 10 second increment (Figures 79, 80) while exposure to 12.4 ppm yielded a frequency change rate of 1.0 to 1.5 Hz per 10 second increment (Figures 81, 82) . The film lifetime and film exposure constant were not determined experimentally, but they can be approximated.

The frequency change rate for 24.8 ppm exposure was approximately the same as that determined for a 0.496 ppm phosgene exposure to 50.47% 4-(4'-nitrobenzyl)pyridine in polyethylene glycol MW 400 (Figure 72, 156). Assume that the film lifetimes are the same for a 0.496 ppm phosgene exposure to 50.47% 4-(4'-nitrobenzyl)pyridine in polyethylene glycol MW 400 and a 24.8 ppm phosgene exposure to 49.90% 4-(4'-nitrobenzyl)pyridine in polystyrene, MW 280,000 since the frequency change rates are approximately the same (it will be shown that this assumption does not have to be rigorously correct to explore the importance of the film). Then the film lifetime for a 40 KHz film load is:

$$((40 \text{ KHz})(50.47\% \text{ NBP in poly(ethylene glycol)})(2.02 \text{ ppm-sec}/(\text{KHz-}\% \text{NBP}))) / (0.496 \text{ ppm}) = 8222 \text{ seconds.} \quad (81)$$

This result leads to the determination of the film exposure constant for the polystyrene support matrix films as being:

$$((24.8 \text{ ppm})(8222 \text{ sec})) / ((40 \text{ KHz})(49.90\% \text{ NBP in polystyrene})) \quad (82)$$

$$102 \text{ (ppm-sec)/(KHz-}\% \text{NBP)}.$$

Although it might be argued that the assumption used to perform these calculations is not rigorously correct, the results of the calculations leads to an important conclusion about the usefulness of the polystyrene based film in a real world application.

The application of 4-(4'-nitrobenzyl)pyridine/polystyrene films would not require that the film be used to its film lifetime limit because this support matrix would be used in conjunction with another, more sensitive matrix such as poly(ethylene glycol). The more sensitive film would have been consumed long before the polystyrene film had reached its lifetime limit. In fact, the polystyrene based film will last longer in a phosgene environment than the person using the device.

To demonstrate these points, a configuration for a personal monitoring instrument can be examined. Monitoring in a real environment would require a minimum of four SAW devices, a sample and reference device pair utilizing two different support matrices. Using these studies as a guide, poly(ethylene glycol) MW 400 could be used as a support medium in one pair and polystyrene in the other. Since a four SAW device array detection system for pattern recognition analysis is presently available⁸³, simultaneous low level and high level phosgene vapor monitoring is possible in one microchip carrier.

Based upon the calculation of the film exposure constant for 4-(4'-nitrobenzyl)pyridine/polystyrene, a four SAW device array containing, for example, a 40 KHz film load of 50% 4-(4'-nitrobenzyl)pyridine in poly(ethylene glycol) MW 400 and a 40 KHz film load of 50% 4-(4'-nitrobenzyl)pyridine in polystyrene MW 280,000 continuously exposed to 25 ppm phosgene would have respective film lifetimes of

$$(2.02 \text{ ppm-seconds}/(\text{KHz} \cdot \% \text{NBP})) (40 \text{ KHz}) (50\% \text{ NBP}) / (25 \text{ ppm}) = 162 \text{ seconds (approximately 3 minutes)} \quad (83)$$

and

$$(100 \text{ ppm-seconds}/(\text{KHz} \cdot \% \text{NBP})) (40 \text{ KHz}) (50\% \text{ NBP}) / (25 \text{ ppm}) = 8000 \text{ seconds (approximately 133 minutes)}. \quad (84)$$

49.90% NBP in polystyrene MW 280,000
24.8 ppm Phosgene Exposure

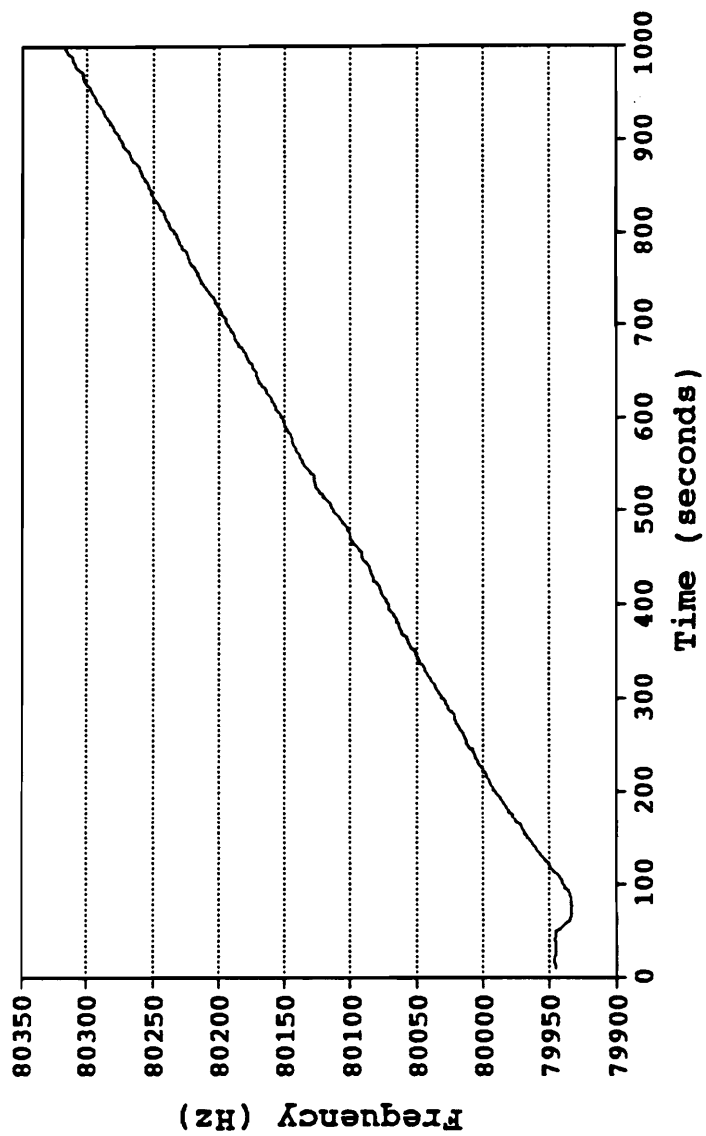


Figure 79. 24.8 ppm phosgene exposure.

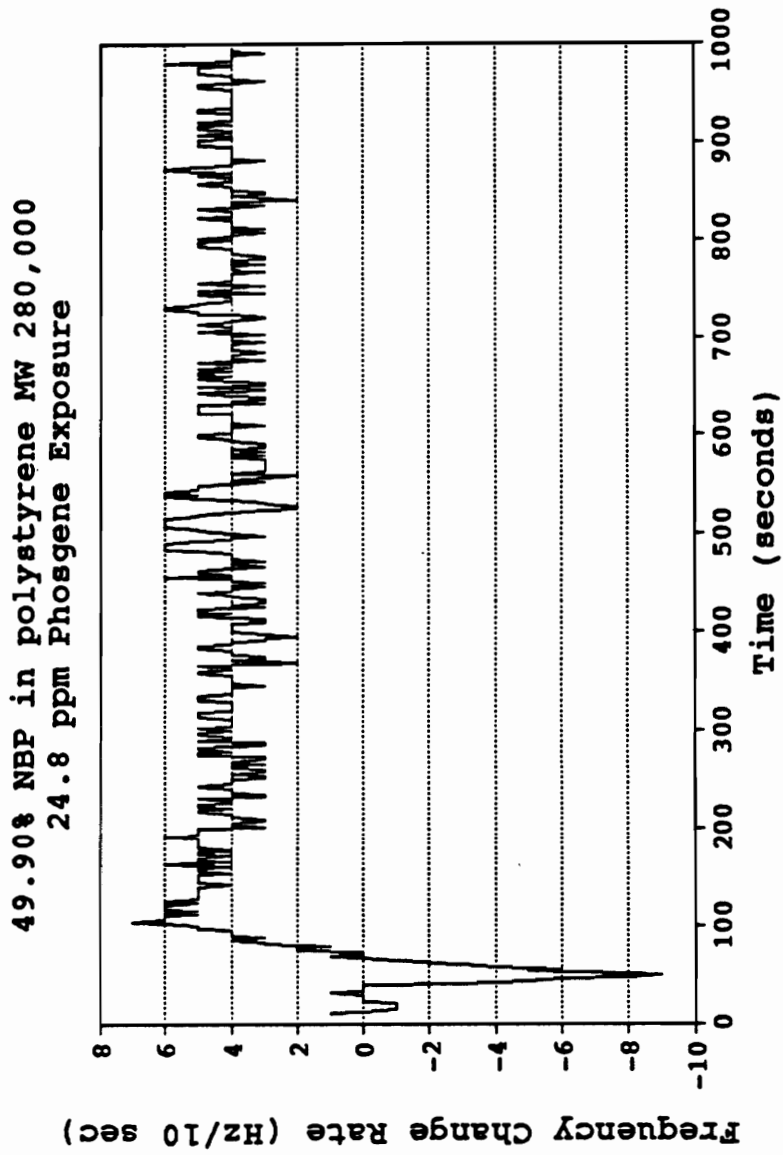


Figure 80. 24.8 ppm phosgene exposure - frequency change rate.

49.90% NBP in polystyrene MW 280,000
12.4 ppm Phosgene Exposure

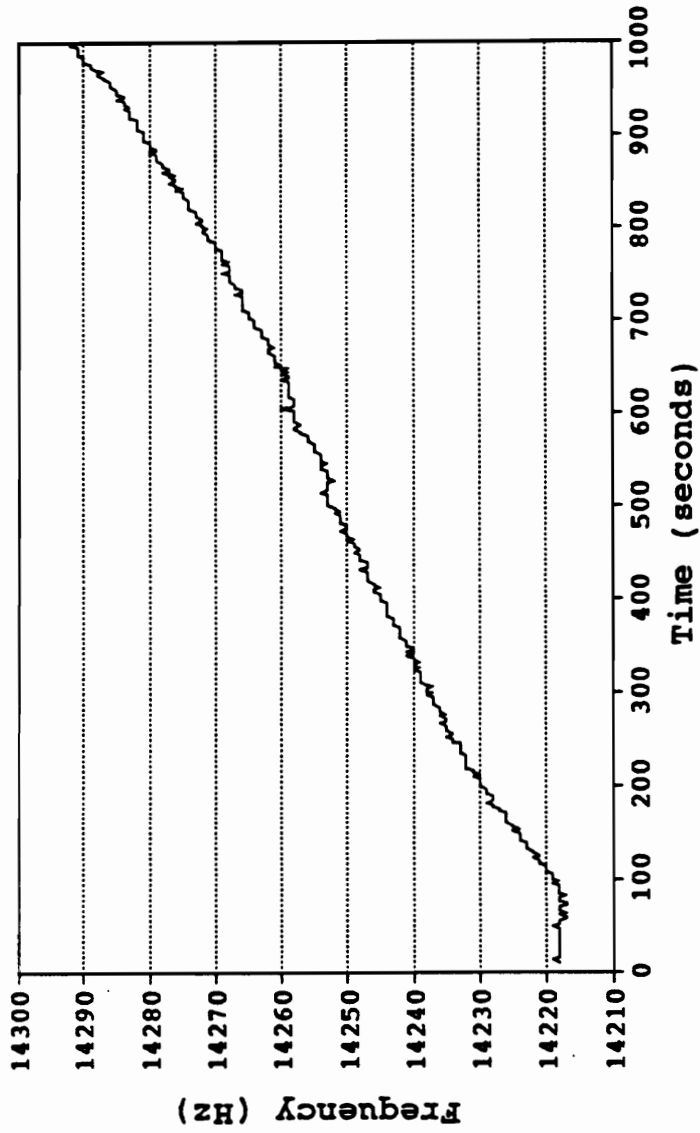


Figure 81. 12.4 ppm phosgene exposure.

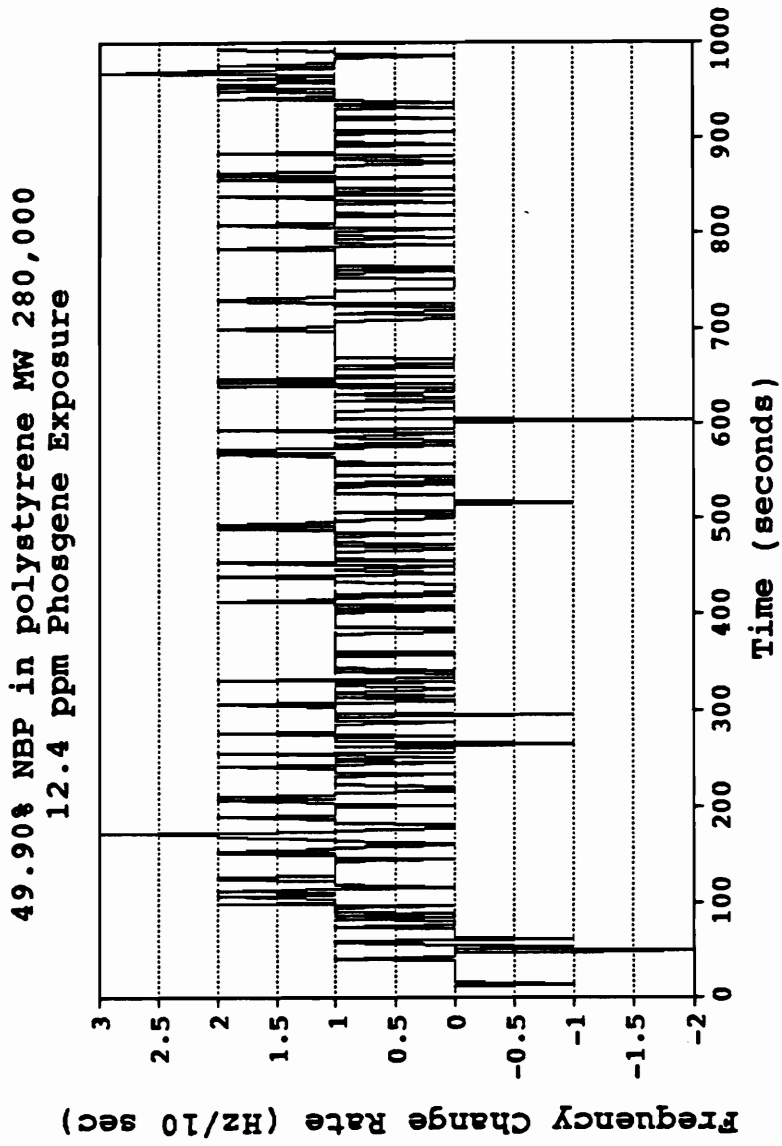


Figure 82. 12.4 ppm phosgene exposure - frequency change rate.

Two points can be made from this discussion. First, the more sensitive film (ie. poly(ethylene glycol) based film) is consumed more rapidly than the film with lower phosgene sensitivity (ie. polystyrene based film). The second and the more important point is that the polystyrene based film will still be analytically useful and not be consumed long after the user of the device succumbs to phosgene exposure.

Since the lethal phosgene exposure level is 500 ppm-minutes, the polystyrene film described above is capable of measuring an exposure of approximately 3300 ppm-minutes ($(8000 \text{ seconds} * 25 \text{ ppm}) / (60 \text{ sec/minute})$) or 6.5 times the lethal exposure level. Even if the polystyrene based film has a lifetime of only 4000 seconds (approximately 66.5 minutes), signifying an error in the assumption resulting in a 50% decrease in film lifetime, the film would still be capable of measuring greater than three times the lethal exposure level.

This configuration is similar in concept to that utilized by charcoal collection tubes but is much more useful. Charcoal collection tubes are composed of an analytical area and a breakthrough area, separated by a porous non-absorbing material. The purpose of the breakthrough area is to determine if the capacity of the analytical area had been exceeded, due either to an extremely high short term concentration saturating the absorbance capabilities of the tube or to an exposure of a concentration that over the sampling period consumes the absorbing sites of the analytical region. Any appearance of absorbed vapor in the breakthrough area is indicative of one of these situations occurring which voids the results. The four SAW array contains a film which will be capable of measuring high short term concentrations or long concentration exposures which saturate the more sensitive film, generating reliable real time information about exposure levels from both SAW pairs.

5) Background Exposures to Neat poly(ethylene glycol) MW 400

Experimental Synopsis: Determination of the effect of phosgene exposure upon the support matrix, poly(ethylene glycol), MW 400.

Experimental conditions:

Sample Film Composition: 100% poly(ethylene glycol), MW 400

Reference Film Composition: none

Film Thickness: approximately 50 KHz

Flow Rate: 100 cc/min

Vapor being determined: phosgene

Concentrations: 24.8, 12.4 and 4.96 ppm

Exposures generated an irreversible frequency shift which is apparently due to the presence of end chain hydroxyl groups on the polymer. Table 3 contains the results from these experiments.

When comparing the frequency change rate obtained for the (4-(4'-nitrobenzyl)pyridine in poly(ethylene glycol) films to that obtained for the neat poly(ethylene glycol) films, the frequency change rate of the neat poly(ethylene glycol) films is insignificant. As a comparison, for 24.8 ppm phosgene exposure, the frequency change rate for neat poly(ethylene glycol), MW 400, was 8 Hz per 10 seconds; while that obtained for 50.47% 4-(4'-nitrobenzyl)pyridine in poly(ethylene glycol), MW 400, reached a maximum of 511 Hz per 10 seconds, a rate difference of 639 percent.

The result of this comparison is the conclusion that the reaction rate of phosgene with polymer end group hydroxyls is insignificant when compared to the reaction rate of phosgene with 4-(4'-nitrobenzyl)pyridine. In the dual beam configuration of the instrument, phosgene will react with the polymer support matrix on both the sample and reference device. The common mode rejection of the dual beam configuration will

Table 3. Phosgene exposure to neat poly(ethylene glycol) MW 400.

% NBP in Poly(Ethylene Glycol) MW 400

Neat Polymer Phosgene Exposure

Phosgene Concentration (ppm)	Frequency Change Rate (Hz/10 sec)
24.8	8
12.4	2
4.96	1.5

reduce, if not eliminate, any effect that polymer reaction would have on the output of the detector.

Modifying the polymer so that the chain ending hydroxyl group is converted into a non-reactive functional group would be a solution that could be pursued to eliminate this effect. However since the rates of acylation of 4-(4'-nitrobenzyl)pyridine appear to be much greater than that for poly(ethylene glycol), the polymer was used as received with no attempt to correct for this effect.

c) Thionyl Chloride

Experimental Synopsis: The effect of changing from the carbonyl group to the less reactive thionyl group on the response of the dual SAW device detector was investigated.

Experimental conditions:

Sample Film Composition: 50.47% 4-(4'-nitrobenzyl)pyridine in poly(ethylene glycol) MW 400

Reference Film Composition: 100% poly(ethylene glycol) MW 400

Film Thickness: approximately 50 KHz

Flow Rate: 100 cc/min

Vapor being determined: thionyl chloride

Concentrations: 5.25 and 2.63 ppm

Using identical films with those used in the phosgene response experiments, long term exposures of thionyl chloride were investigated. These exposures generated responses that required an excessive amount of time to reach a steady frequency change rate. For example, an exposure of 5.25 ppm thionyl chloride for approximately 1900 seconds is exhibited in Figures 83, 84, 85, and 86. The response characteristics for this

50.47% NBP in poly(ethylene glycol) MW400
5.25 ppm Thionyl Chloride Exposure

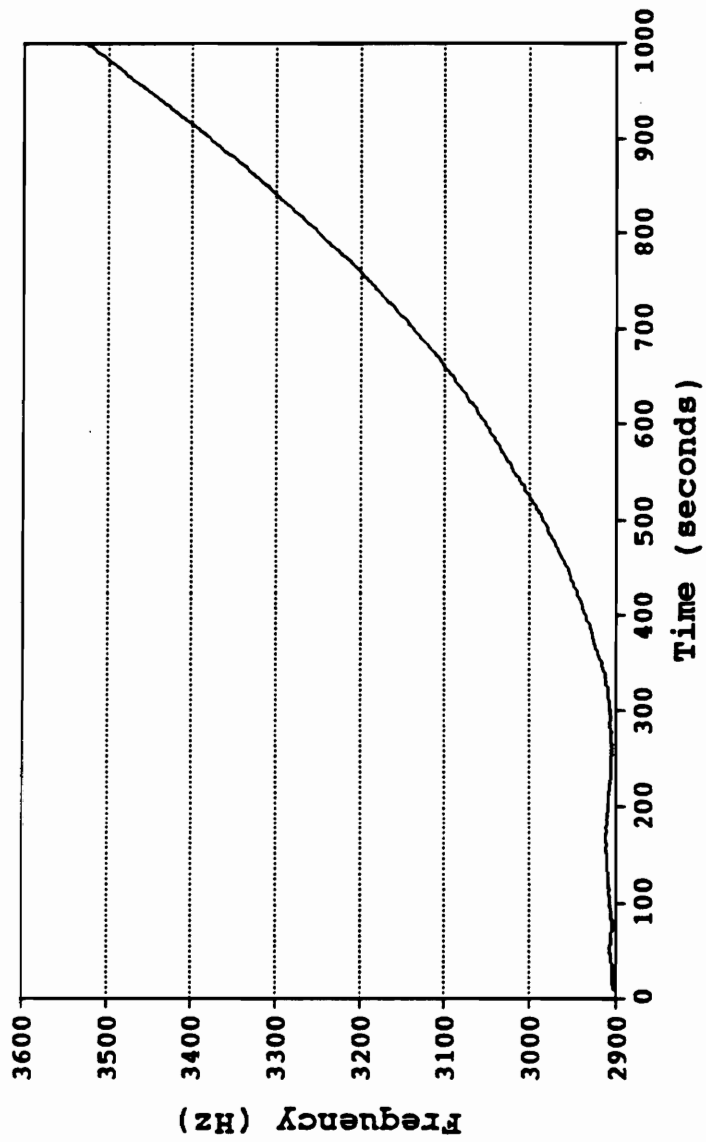


Figure 83. 5.25 ppm thionyl chloride exposure.

50.47% NBP in poly(ethylene glycol) MW400
5.25 ppm Thionyl Chloride Exposure

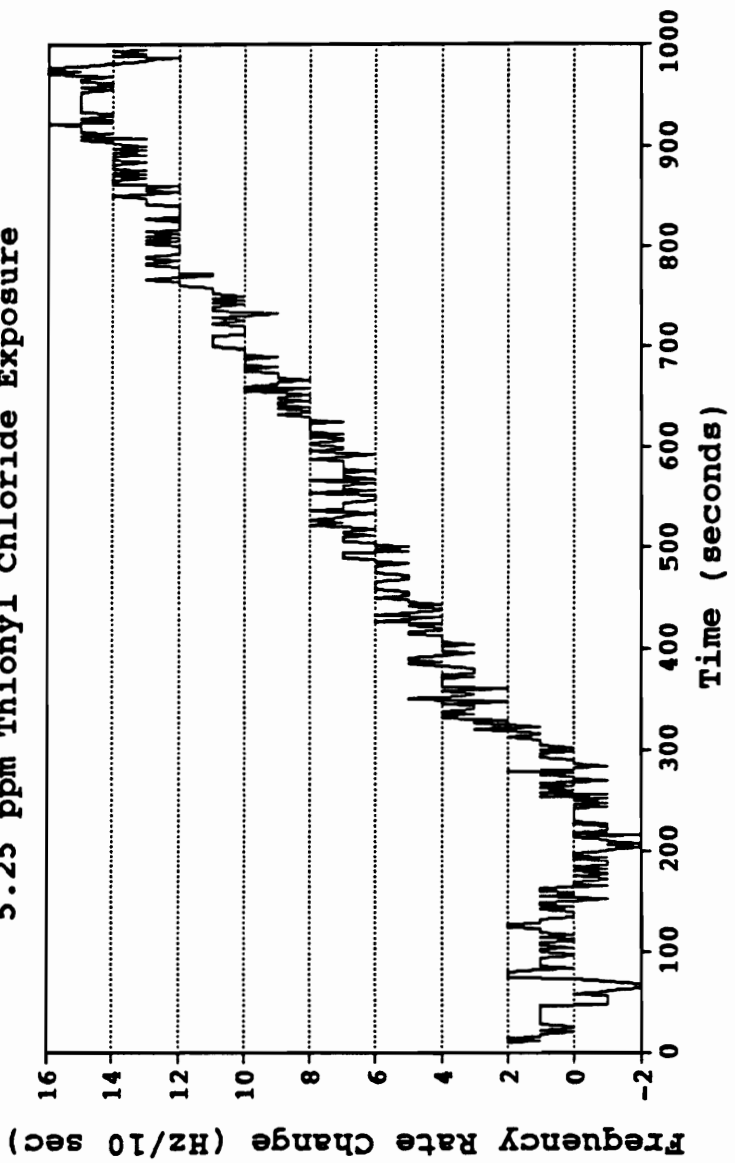


Figure 84. 5.25 ppm thionyl chloride exposure - frequency change rate.

50.47% NBP in poly(ethylene glycol) MW400
5.25 ppm Thionyl Chloride Exposure

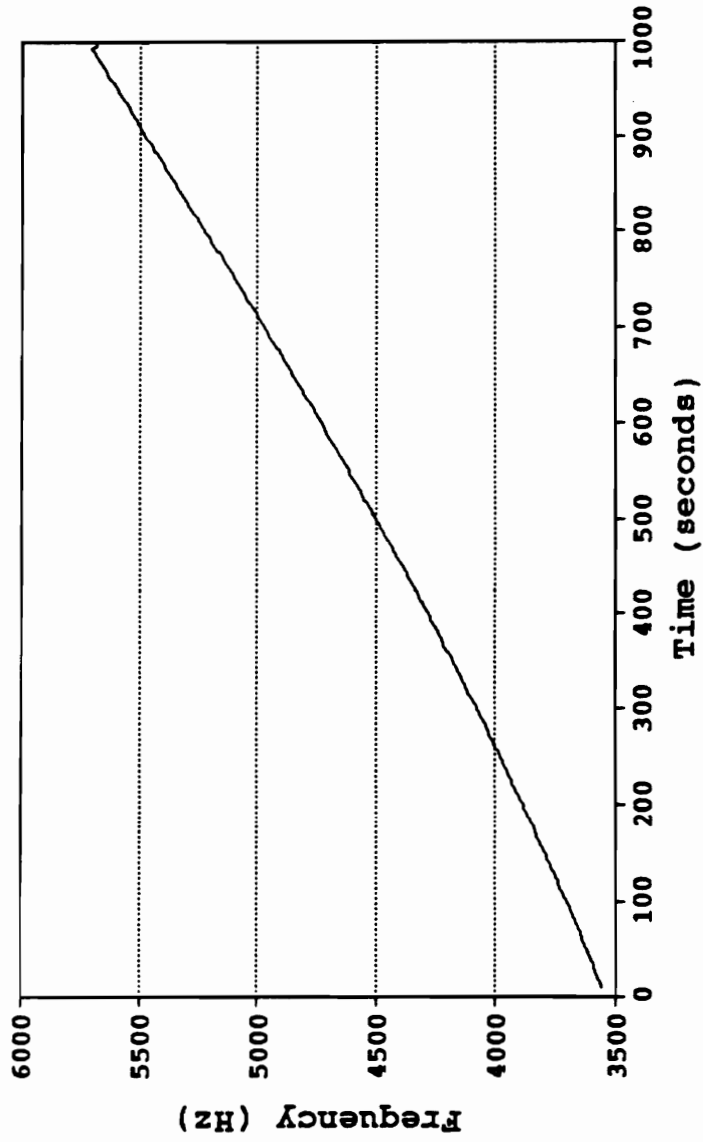


Figure 85. 5.25 ppm thionyl chloride exposure continued.

50.47% NBP in poly(ethylene glycol) MW400
5.25 ppm Thionyl Chloride Exposure

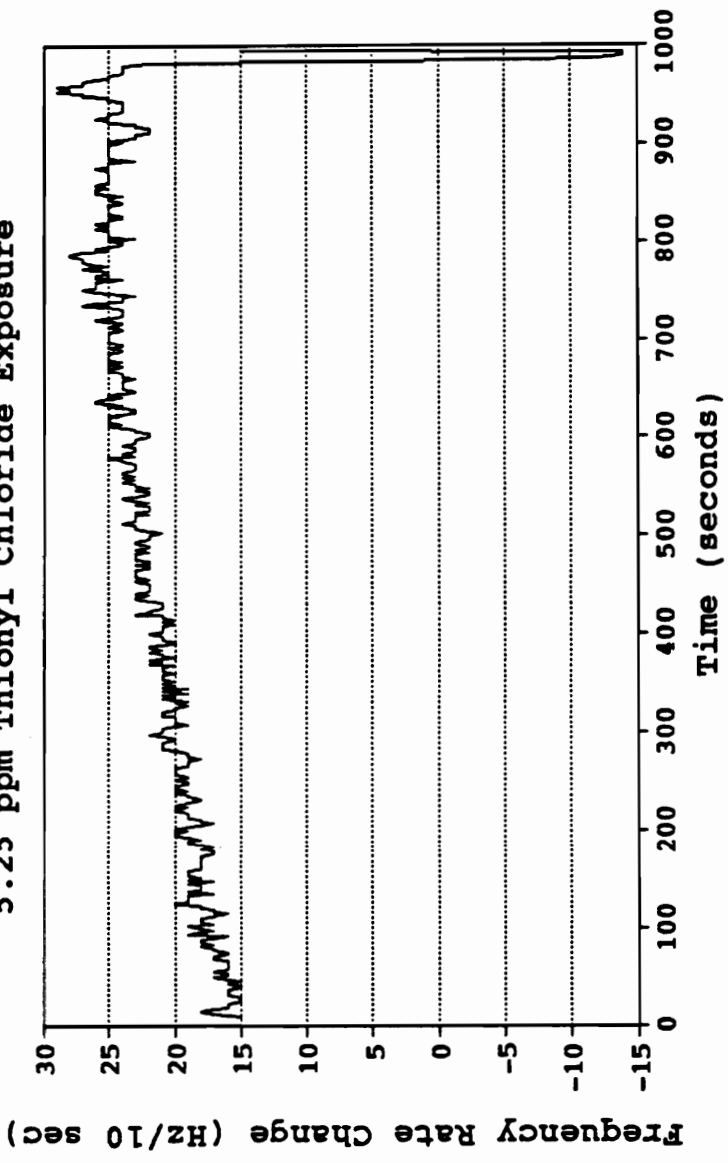


Figure 86. 5.25 ppm thionyl chloride exposure continued - frequency change rate.

vapor/film combination appears to indicate that the overall effect of permeability into the film and reactivity of thionyl chloride with 4-(4'-nitrobenzyl)pyridine presents a difficulty for its use as a long term exposure continuous monitoring tool.

Analysis of this SAW output leads to the interpretation that the thionyl chloride vapor concentration continually increases in the film over the time of the exposure and that the subsequent chemical reaction is slower than that of phosgene.

The phenomena of a slowly increasing frequency change rate during the time of the exposure was also discovered with 2.48 ppm phosgene (Figure 66, page 150). The main and important difference between the responses of the film to phosgene and thionyl chloride vapors can be found upon initial exposure of the film to each vapor.

For the exposure of 2.48 ppm phosgene, the frequency change rate reaches an initial plateau of 17 Hz/10 seconds within the first 200 seconds of exposure and then slowly increases. In the case of 5.25 ppm thionyl chloride, there is no initial plateau in the frequency change rate (as observed with the phosgene exposure). The response is simply a continuously increasing frequency change rate starting at zero upon initial exposure and increasing to 25 Hz/10 seconds after 1800 seconds of continuous exposure.

If the permeability is slow and the reactivity is slower, so that the concentration of the vapor in the film increases with time, the observed rate of reaction will slowly increase with time. The net result is that over a particular timeframe, the frequency change rate will slowly increase.

This explanation is consistent with the observation of the data collected for the 5.25 ppm exposure. To reach a constant frequency change rate, the exposure of this constant concentration needed to be maintained for approximately 1800 seconds (30 minutes). This would not be considered a reasonable response time for a device that is

advocated as a personal dosimeter and further experiments were conducted in a fixed time short term exposure mode. These results will be discussed in the short term thionyl chloride exposure section later in this work.

d) Long Term Exposure Summary

The results from the long term exposure studies conducted in this section can be summarized in a few paragraphs.

1) A film exposure constant for 4-(4'-nitrobenzyl)pyridine/poly(ethylene glycol) MW 400 films exposed to phosgene was determined for films using different 4-(4'-nitrobenzyl)pyridine film concentrations, phosgene exposure concentrations and film thicknesses.

2) 4-(4'-nitrobenzyl)pyridine/poly(ethylene glycol) films exposed to high concentration of phosgene (greater than 4.96 ppm) are consumed before a steady state can be achieved. Exposures between 4.96 and 1.24 ppm generate an initial frequency rate change upon exposure that increases with increasing exposure time length. Only at vapor concentration exposures of 1.24 ppm or less does a steady state condition occur resulting in a constant frequency change rate with increasing exposure time length.

3) Changing the matrix from a viscous liquid to a glassy film changes the response characteristics of the detector from a low level sensor (viscous liquid) to a less sensitive sensor (glassy film).

4) Neat 4-(4'-nitrobenzyl)pyridine films generate erratic response.

5) Thionyl chloride exposures do not generate an immediate response upon exposure but generate an ever increasing frequency change rate with increasing exposure time length.

6) The detection scheme used is incapable of measuring ethylene oxide concentrations of interest for personal monitoring purposes.

The results obtained are all dependent upon the relationship between equilibrium, permeability, reactivity and the rate at which they occur for the specific vapor/film systems investigated.

The ethylene oxide experiment demonstrates what transpires when a significant amount of reaction does not occur at the exposure concentrations used. With ethylene oxide, reversible loading without reaction is dependent upon the permeability and partition coefficient for the matrix film system. The amount of signal generated from simple absorption is minimized due to the dual mode configuration of the instrument.

With the phosgene experiments, the vapor will permeate into the film and attempt to reach an equilibrium concentration. However the consumption of dissolved vapor by the active agent, 4-(4'-nitrobenzyl)pyridine, is in direct competition with the drive to reach this dissolved vapor equilibrium concentration. If permeability is slower than reactivity, as is the case with the polystyrene films, the system resembles a permeation tube. In this scenario, the dissolved phosgene in the film is consumed faster than it can be replenished. With the vapor phase concentration above the film being constant, a constant permeation rate is predicted since the partial pressure of phosgene in the headspace and in the film is fixed. With this constant flux of phosgene into the film, a constant frequency change rate for the SAW output will be observed.

If the reactivity is less than the permeability, as in the case of high phosgene concentration exposures in poly(ethylene glycol) films, the concentration of the dissolved vapor in the film will increase with time in an attempt to establish an equilibrium concentration. With this increase in the dissolved phosgene concentration, the observed rate will also increase with time. If the concentration of the trapping

agent, 4-(4'-nitrobenzyl)pyridine, could be maintained constant to infinite time, a physical impossibility, the equilibrium concentration of the vapor in the film would eventually be reached. At this point, the frequency change rate would become constant as the amount of vapor removed from the film would be replaced by an equal amount of new vapor permeating into the film, reestablishing equilibrium. This does not occur because 4-(4'-nitrobenzyl)pyridine is eventually consumed, leading to a decrease in the frequency change rate. This phenomena is observed for phosgene concentrations greater than 2.48 ppm.

If the concentration of the vapor is reduced, eventually the constraints of equilibrium, permeability and reactivity lead to a condition in which the frequency change rate reaches a constant level. A change from 2.48 ppm to 1.24 ppm phosgene exposures using poly(ethylene glycol) substantiates this conclusion. Based upon this observation, it would appear that lower phosgene concentration levels could be analyzed in a long term mode with this support matrix.

While calibration curves could not be developed for the 4-(4'-nitrobenzyl)pyridine/poly(ethylene glycol) MW 400 exposures due to the fact the 1) high concentrations rapidly consumed the films and 2) concentrations above 1.24 ppm which do not rapidly consume the film do not attain a constant frequency change rate, the film exposure constant was developed from these studies.

The importance of this parameter is that knowing the 4-(4'-nitrobenzyl)pyridine film concentration and film thickness, the exposure measured in ppm-seconds necessary to analytically consume the film can be calculated. In the short term exposure studies discussed in the next section, each film deposited will be exposed to multiple fixed time exposures. The use of the film exposure constant is to guarantee that the total ppm-seconds of fixed time exposures does not exceed the maximum ppm-seconds of

exposure allowed for a film. To do so would be to use a film in which the 4-(4'-nitrobenzyl)pyridine would no longer be in a flooded condition, resulting in a response that will be less than the true response for a flooded film. This response would be unusable for the development of a calibration curve based on fixed time exposure responses.

The results from thionyl chloride detection displays what occurs when the apparent permeability is faster than the reaction rate but both are relatively slow compared to the time of analysis. As with the phosgene experiments, the solubilized vapor concentration increases with time. However, whereas films exposed to phosgene generate an initial rapid frequency change rate which slowly increases with increasing exposure time (Figure 66, page 150), films exposed to thionyl chloride generate very little if any initial response which slowly increases with increasing exposure time. This creates the problem, as found with the phosgene exposures, of being unable to generate a calibration curve due to the fact that the frequency change rate is changing continuously during the exposure of films to a constant vapor concentration.

The overall results of the long term exposure studies created distinct questions, necessitating the investigation of films exposed to short term fixed time vapor exposures. While a film exposure constant was developed for the 4-(4'-nitrobenzyl)pyridine/poly(ethylene glycol) MW 400 system, only qualitative information could be garnered from these investigations regarding the difference in phosgene response between poly(ethylene glycol) and polystyrene support matrices and the difference in detector response between phosgene and thionyl chloride vapor exposures. The goal of the short term fixed time exposure experiments will be to quantify the response of films used in these long term studies to phosgene and thionyl chloride vapor exposure. Quantification involves answering the following questions:

1) Can a calibration curve be developed for fixed time exposures measured in ppm-seconds of exposure versus the amount of frequency shift resulting from these exposures?

2) If calibration curves can be developed, is there any difference in detector response as a function of film thickness or film 4-(4'-nitrobenzyl)pyridine concentration? If a difference is determined, can it be quantified?

3) What is the minimum detectable quantity of phosgene for these systems?

4) What response occurs when the ppm-seconds of exposure for an individual exposure approaches the film lifetime for that particular film? For example, what frequency shift will occur when an exposure of 1500 ppm-seconds (such as 15 ppm for 100 seconds) if the film is analytically capable of measuring only 2000 ppm-seconds of exposure?

5) How does the differences in the long term response of films exposed to phosgene and thionyl chloride affect the short term fixed time exposure calibration curves for phosgene and thionyl chloride?

2) Short Term Exposure

The rapid reaction and consumption of the 4-(4'-nitrobenzyl)pyridine in poly(ethylene glycol) films used in the long term studies necessitated the investigation of short term exposures for fixed time increments of both poly(ethylene glycol), MW 400, and polystyrene, MW 280,000, films. In this mode, the short term exposure effects of higher concentrations of analyte upon the films could be investigated before the film was consumed, allowing the generation of calibration curves for different film thicknesses and film concentrations.

Exposure lengths of 10, 20, 40 and 60 seconds were used on films of 26.14% and 50.46% 4-(4'-nitrobenzyl)pyridine in poly(ethylene glycol) MW 400 and 50.22% 4-(4'-nitrobenzyl)pyridine in polystyrene MW 280,000.

The choice of these particular time increments is based upon factors previously introduced. The detector cell volume for this experimental configuration is 12 cc. A ten second bolus of 100 cc/min flow of vapor corresponds to 17 cc of volume. This sets the lower limit to ensure that the volume sampled is larger than the cell volume. The upper exposure limit of 60 seconds is based upon the toxicity of phosgene. One minute exposure of 400 to 500 ppm is sufficient to cause death.

Phosgene concentrations used for these investigations were the same as used in the long term exposure studies, namely 0.496, 1.24, 2.48 and 4.96 ppm. These concentrations and exposure times generated a range of phosgene exposures of 4.96 ppm-seconds to 297.6 ppm-seconds with duplication at certain ppm-second values (24.8 ppm-seconds = 1.24 ppm for 20 seconds or 2.48 ppm for 10 seconds). Flow rates used for these studies were 100 cc/min, 150 cc/min and 200 cc/min.

Fixed time exposures of thionyl chloride were conducted to investigate if a consistent response using the ppm-second exposure value could be obtained.

Concentrations of thionyl chloride used in the short term studies were 2.63 and 5.25 ppm. Using the same exposure time increments as those used for the phosgene studies (10, 20, 40 and 60 seconds), the ppm-second exposure levels ranged from 26.3 ppm-seconds to 315 ppm-seconds. A flow rate of 100 cc/min was used for these studies.

The particular parameters used for each investigation will be summarized as before and precede the discussion of the results of that investigation.

a) Phosgene

1) Poly(ethylene glycol) Exposures

a) 40 KHz film load exposures

Experimental Synopsis: Determination of the effect of phosgene exposure on the amount of frequency change (measured in Hz) of the dual SAW device detector. This response will be the benchmark by which results investigating other effects (ie. different film thicknesses, 4-(4'-nitrobenzyl)pyridine film concentrations, flow rates, support matrices) will be compared.

Experimental conditions:

Sample Film Composition: 50.46% 4-(4'-nitrobenzyl)pyridine in poly(ethylene glycol) MW 400

Reference Film Composition: 100% poly(ethylene glycol) MW 400

Film Thicknesses: approximately 40 KHz

Flow Rate: 100 cc/min

Vapor being determined: phosgene

Exposure levels: see Table 4

Table 4 contains data collected from multiple runs on multiple films. This table, and other tables generated for all of the short term fixed time exposure experiments, is composed of the concentration-time product used for the exposure, the average response from that exposure, the standard deviation for the multiple responses at the exposure, and the actual concentration used for the exposure.

The calibration curve generated from the data included in this table can be found in Figure 87.

b) 20 KHz film load exposures

Experimental Synopsis: To determine the effect of film thickness upon the response characteristics of the dual SAW device detector, 20 KHz film loads of the same film composition used in the 40 KHz film load study were exposed to phosgene. This corresponds to an average film thickness which is one-half of that used for the 40 KHz study.

Experimental conditions:

Sample Film Composition: 50.46% 4-(4'-nitrobenzyl)pyridine in poly(ethylene glycol) MW 400

Reference Film Composition: 100% poly(ethylene glycol) MW 400

Film Thickness: approximately 20 KHz

Flow Rate: 100 cc/min

Vapor being determined: phosgene

Exposure levels: see Table 5

Table 4. Concentration-time products and responses for phosgene exposure.

50.46% NBP in Poly(Ethylene Glycol) MW 400

Concentration Time products for Phosgene Exposure
40 KHz Film Load

Average for measured responses

CT Product (ppm-sec)	Average Response (Hz)	Standard Deviation	Exposure Level (ppm)
4.96	4.64	1.25	0.496
9.92	11.31	2.48	0.496
12.4	12.13	1.25	1.24
19.8	25.61	4.73	0.496
24.8	29.38	1.25	1.24
24.8	21.83	2.93	2.48
29.8	40.25	5.81	0.496
49.6	65.56	2.24	1.24
49.6	56.67	2.08	2.48
49.6	29.17	12.21	4.96
74.4	103.29	2.14	1.24
99.2	121.50	1.29	2.48
99.2	85.67	2.31	4.96
148.8	199.75	3.69	2.48
198.4	223.75	10.97	4.96
297.6	427.00	25.07	4.96

50.46% NBP in poly(ethylene glycol) MW 400 40KHZ

Phosgene response

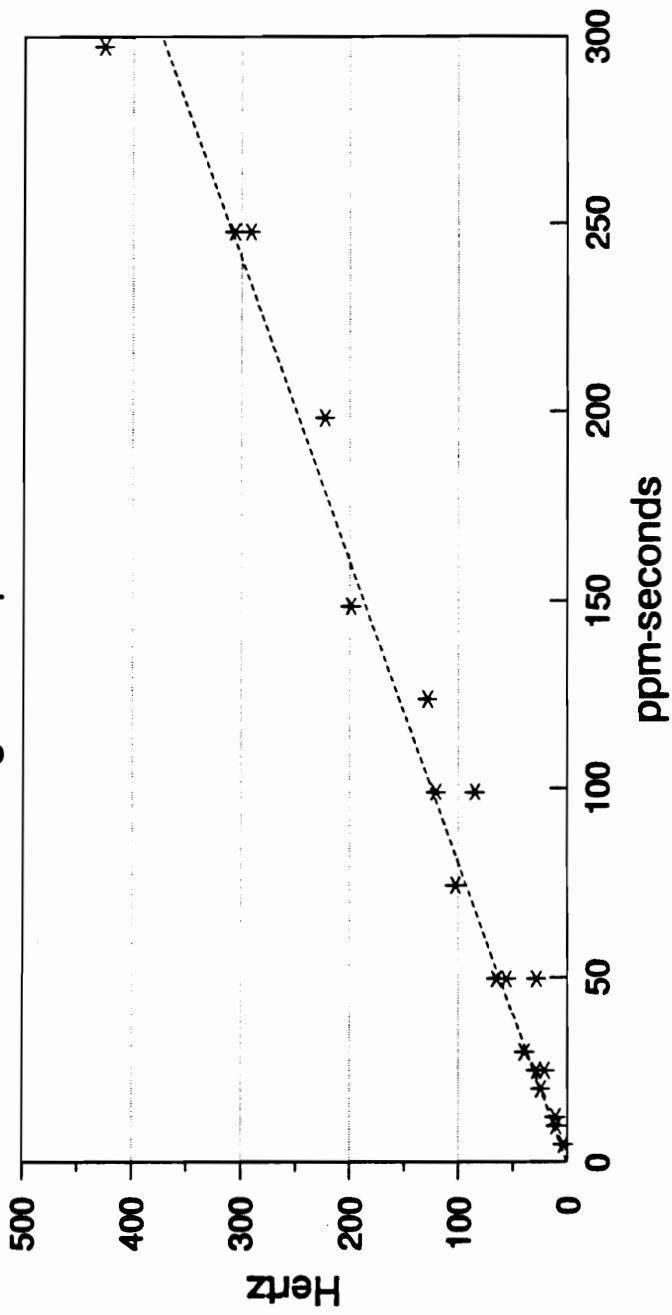


Figure 87. Calibration curve for phosgene exposure.

Table 5. Concentration-time products and responses for phosgene exposure.

50.46% NBP in Poly(Ethylene Glycol) MW 400

**Concentration Time products for Phosgene Exposure
20 KHz Film Load**

Average for measured responses

CT Product (ppm-sec)	Average Response (Hz)	Standard Deviation	Exposure Level (ppm)
4.96	3.70	0.97	0.496
9.92	9.50	1.84	0.496
12.4	10.40	1.85	1.24
19.8	23.60	3.05	0.496
24.8	23.30	1.48	1.24
24.8	16.30	1.20	2.48
29.8	35.25	2.99	0.496
49.6	57.20	1.79	1.24
49.6	41.22	6.41	2.48
49.6	40.00	3.86	4.96
74.4	86.00	3.16	1.24
99.2	132.00	5.94	2.48
99.2	105.00	5.15	4.96
148.8	227.00	9.35	2.48
198.4	279.29	37.72	4.96

50.46% NBP in poly(ethylene glycol) MW 400 20KHz

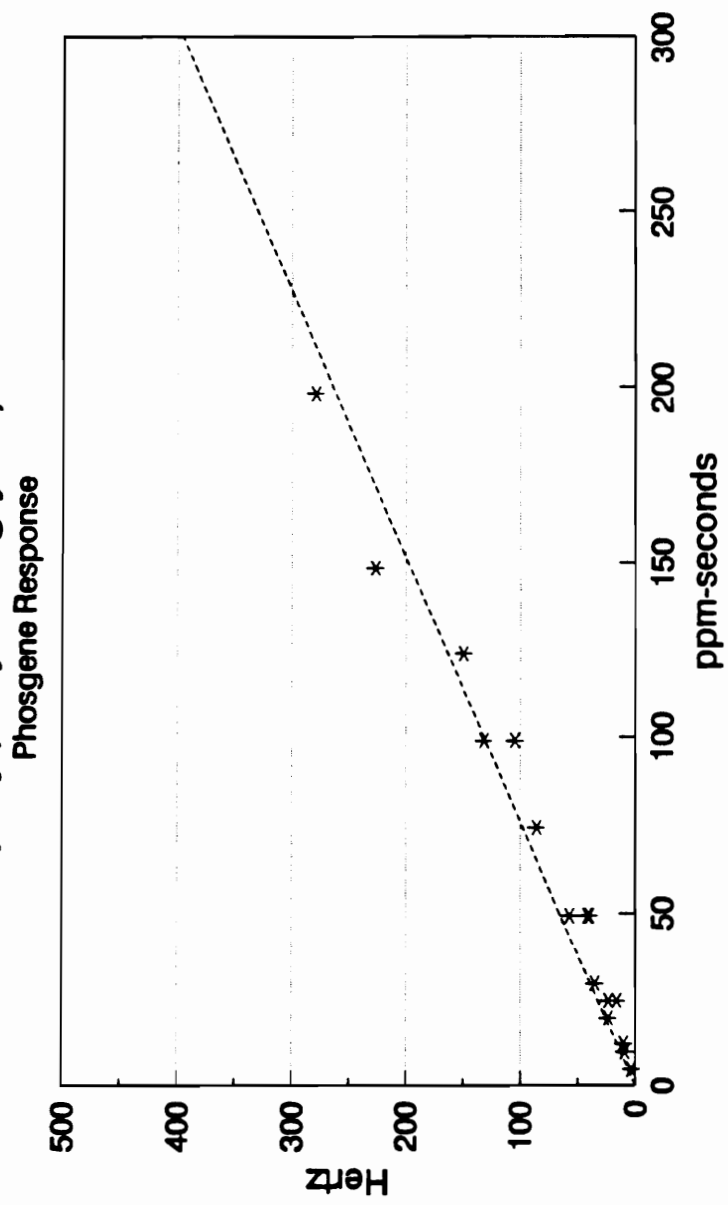


Figure 88. Calibration curve for phosgene exposure.

Film Response to Phosgene
50.46% NBP on poly(ethylene glycol) MW 400
20KHz and 40 KHz films

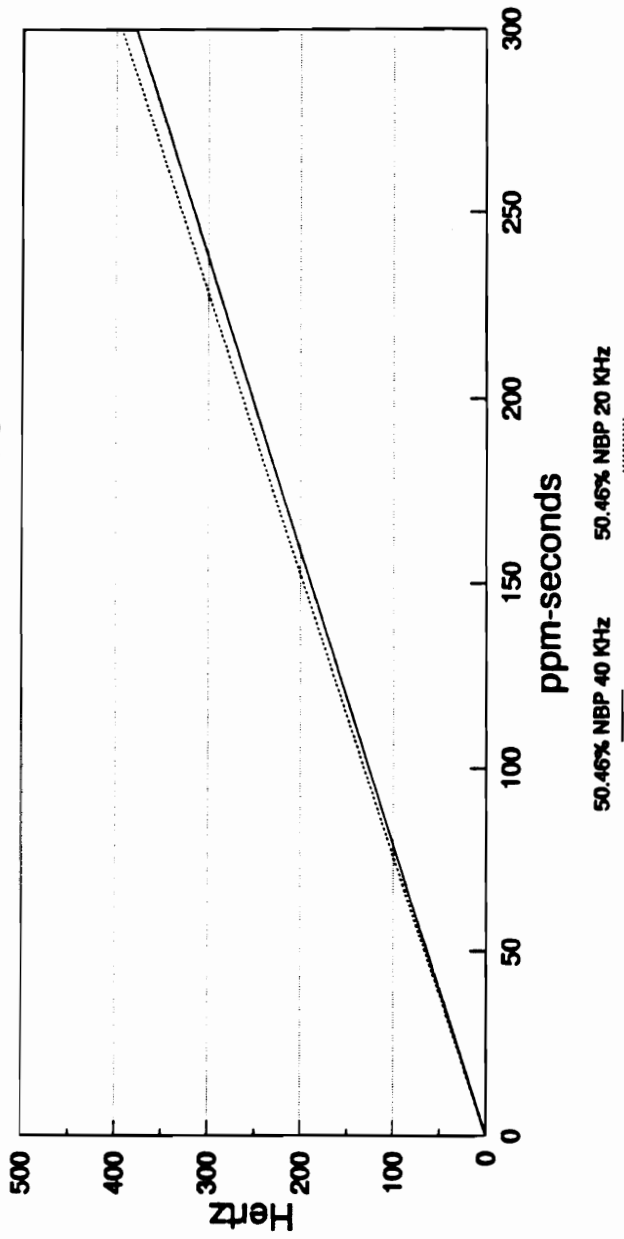


Figure 89. Calibration curves for phosgene exposure.

Table 6. Equations of the lines.

Equation of the Line - Calibration Curves

50.46% 4-(4'-nitrobenzyl)pyridine 40 KHz Films

Range (ppm)	slope	R squared
0 - 297.6	1.250	0.9710

50.46% 4-(4'-nitrobenzyl)pyridine 20 KHz Films

Range (ppm)	slope	R squared
0 - 297.6	1.312	0.9606

The calibration curve generated from the data obtained in this study can be found in Figure 88. To make the comparison between 20 KHz and 40 KHz film load responses, Figures 87 and 88 are combined into a new calibration curve, Figure 89.

Analysis of the two calibration curves contained in Figure 89 shows that film thickness for this dosimeter does not affect the frequency shift that occurs upon exposure, as the calibration curves are nearly identical. The results of a linear regression analysis for the approximately 40 KHz and 20 KHz films can be found in Table 6.

Previous investigations using SAW devices for fully reversible chemical systems were impaled on the horns of a dilemma. The choice was either to maximize the film thickness to increase the sensitivity of the device to the vapor being detected or decrease the film thickness in order to improve the response time. These factors were addressed by Wohltjen in his development of scaling laws for SAW devices⁵⁵.

The response for this dosimetric system is independent of film thickness. This can be explained by examining the fundamental difference between mass loading due to the fully reversible, simple solvation vapor detection schemes used previously and dosimetric, chemically reactive and irreversible schemes of which this application is an example.

For the reversible absorption of a vapor into a coating, Wohltjen has developed an analytical expression describing the SAW frequency change produced by a vapor forming a solution with a coating. Using the partition coefficient, the ideal gas law, Raoult's law and Henry's law, Wohltjen concluded that the frequency shift observed when a given coating of molecular weight M_S is exposed to a vapor of partial pressure P_V and molecular weight M_V can be described by the equation

$$\Delta f = \Delta f_S (M_V/M_S)(P_V/P_V^\circ)(1/\tau)$$

where Δf_s is the frequency shift produced by the coating alone, P_v° is the saturation vapor pressure at the system temperature and τ is the activity coefficient based on the pure liquid standard state⁸⁵. While this equation is only rigorously correct for liquid coatings, examination of the equation leads to the conclusion that the frequency response of a SAW device to reversible absorption of a chemical vapor into a coating is dependent upon the partition coefficient and the film thickness.

The implication of the equation is that in time a film will reach an equilibrium concentration of vapor phase reagent within it depending upon the concentration of that reagent above the film. The concentration of the vapor phase reagent dissolved in two different film thicknesses will be the same. The amount of material dissolved will be different. This condition is identical in concept to a solution of one molar sodium hydroxide in water completely filling a one liter beaker and a ten liter beaker. While the concentration of sodium hydroxide is the same in the two solutions, the total amount of material is not. Since a SAW device is mass sensitive, in an equilibrium driven detection scheme the film thickness (ie. "size of the beaker") is important in determining the amount of material dissolved.

In this dosimetric application, equilibrium and permeability of the film to the vapor are not the only factors that determine the response characteristics of the film. The kinetics of the reaction between the active agent and the vapor also enters into the equation. As discussed above, the concentration of the vapor in the film is determined by the same parameters affecting the equilibrium driven system. However, the ability of the system to reach an equilibrium film concentration is impeded by the reaction of the trapping agent contained in the film with the solubilized vapor. Since the concentration of the vapor in the film is reduced by reaction, more vapor permeates into the film. Therefore the amount of vapor mass that a film can support will be the

amount that reacts with the trapping agent and the amount that the support phase itself can reversibly solubilize.

The first factor will depend upon the reaction rate of the solubilized vapor with the trapping agent. The second factor will be determined by the support matrix and thickness of the film. However in the experimental configuration used (dual SAW devices - reference coated by support matrix material only), the mass loading due to reversible solubilization of vapor into the film is eliminated due to the common mode rejection of the dual device configuration. Therefore the only effect that will be measured by this detector system is that which affects the overall reaction rate of the vapor with the trapping agent.

Based upon this analysis, one of the most important parameters for the frequency response of the SAW device in a dosimetric application is the concentration of the active agent in the film. Depending upon the order of the reaction with respect to the trapping agent, the larger the concentration of the trapping agent in the film the faster the reaction and the larger the frequency shift per concentration-time unit. Using the beaker analogy from above, if phosgene is bubbled into the two solutions, the rate of reaction will be the same as long as the flooded concentrations of sodium hydroxide remains the same. The only difference will be in the amount of phosgene these solutions can consume before they are themselves consumed.

The only difference between the films investigated is the film thickness. The concentration of the active agent is the same. Based on this analysis, the concentration of 4-(4'-nitrobenzyl)pyridine in the support matrix will affect the response of the detector to phosgene vapor. This is investigated in the next series of experiments.

c) Reduced 4-(4'-nitrobenzyl)pyridine film concentration

Experimental Synopsis: Noting that the response of 20 KHz and 40 KHz film loads of 50.46% 4-(4'-nitrobenzyl)pyridine in poly(ethylene glycol) MW 400 to phosgene exposure were identical, 40 KHz film loads of 26.14% 4-(4'-nitrobenzyl)pyridine in poly(ethylene glycol) MW 400 were utilized to determine the effect of the 4-(4'-nitrobenzyl)pyridine film concentration upon the amount of frequency change observed.

Experimental conditions:

Sample Film Composition: 26.14% 4-(4'-nitrobenzyl)pyridine in poly(ethylene glycol) MW 400

Reference Film Composition: 100% poly(ethylene glycol) MW 400

Film Thickness: approximately 40 KHz

Flow Rate: 100 cc/min

Vapor being determined: phosgene

Exposure levels: see Table 6

Table 6 contains data collected from multiple runs on multiple films of 26.14% 4-(4'-nitrobenzyl)pyridine in poly(ethylene glycol) MW 400.

Examination of the calibration curve generated for the experimental results can be found in Figure 90. The regression analysis for this curve can be found in Table 8. Comparison of this curve with that obtained for the 20 KHz and 40 KHz film loads of 50.46% 4-(4'-nitrobenzyl)pyridine in poly(ethylene glycol) MW 400 reveals a significant difference in the response characteristics of the two films (Figure 91). The extent of the difference and the effect of the 4-(4'-nitrobenzyl)pyridine concentration can be determined from these results.

Table 7. Concentration-time products and responses for phosgene exposure.

26.14% NBP in Poly(Ethylene Glycol) MW 400

**Concentration Time products for Phosgene Exposure
40 KHz Film Load**

Average for measured responses

CT Product (ppm-sec)	Average Response (Hz)	Standard Deviation	Exposure Level (ppm)
4.96	0.00	0.00	0.496
9.92	2.50	0.71	0.496
12.4	7.00	1.41	1.24
19.8	9.75	0.35	0.496
24.8	12.50	2.12	1.24
24.8	5.75	2.47	2.48
29.8	16.00	2.12	0.496
49.6	31.25	2.47	1.24
49.6	23.25	1.06	2.48
49.6	11.17	5.25	4.96
74.4	59.00	8.49	1.24
99.2	60.50	4.95	2.48
99.2	49.50	2.12	4.96
148.8	106.33	1.53	2.48
198.4	129.00	4.24	4.96

26.14% NBP in poly(ethylene glycol) MW 400 40KHZ

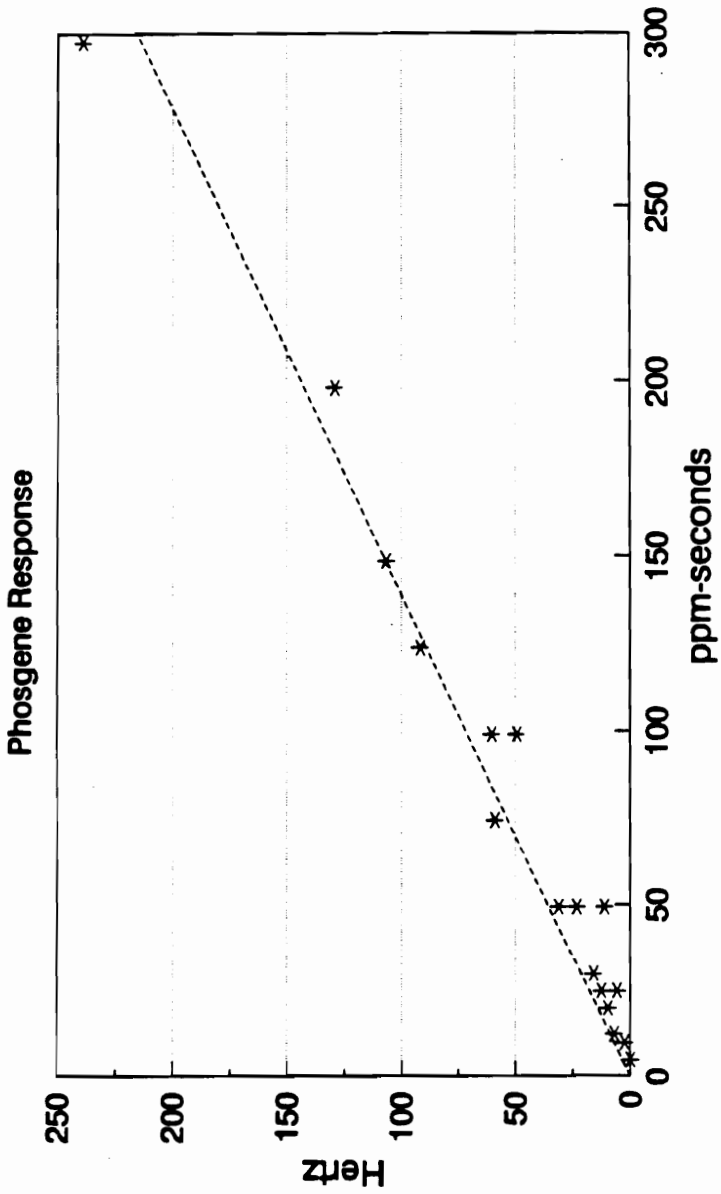


Figure 90. Calibration curve for phosgene exposure.

Table 8. Equations of the lines.

Equation of the Line - Calibration Curves

50.46% 4-(4'-nitrobenzyl)pyridine 40 KHz Films

Range (ppm)	slope	R squared
0 - 297.6	1.250	0.9710

50.46% 4-(4'-nitrobenzyl)pyridine 20 KHz Films

Range (ppm)	slope	R squared
0 - 297.6	1.312	0.9606

26.14% 4-(4'-nitrobenzyl)pyridine 40 KHz Films

Range (ppm)	slope	R squared
0 - 297.6	0.716	0.9603

Film Response to Phosgene
26.14% and 50.46% NBP on poly(ethylene glycol)
MW 400

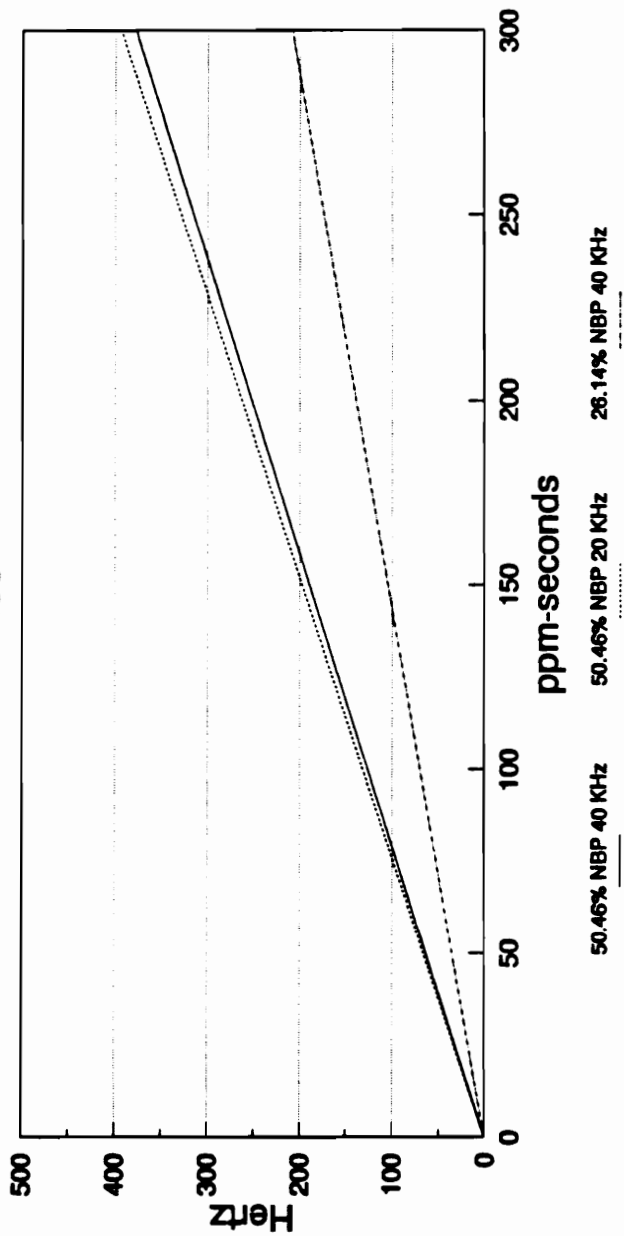


Figure 91. Calibration curves for phosgene exposure.

Normalized Film Response to Phosgene
26.14% and 50.46% NBP on poly(ethylene glycol)
MW 400

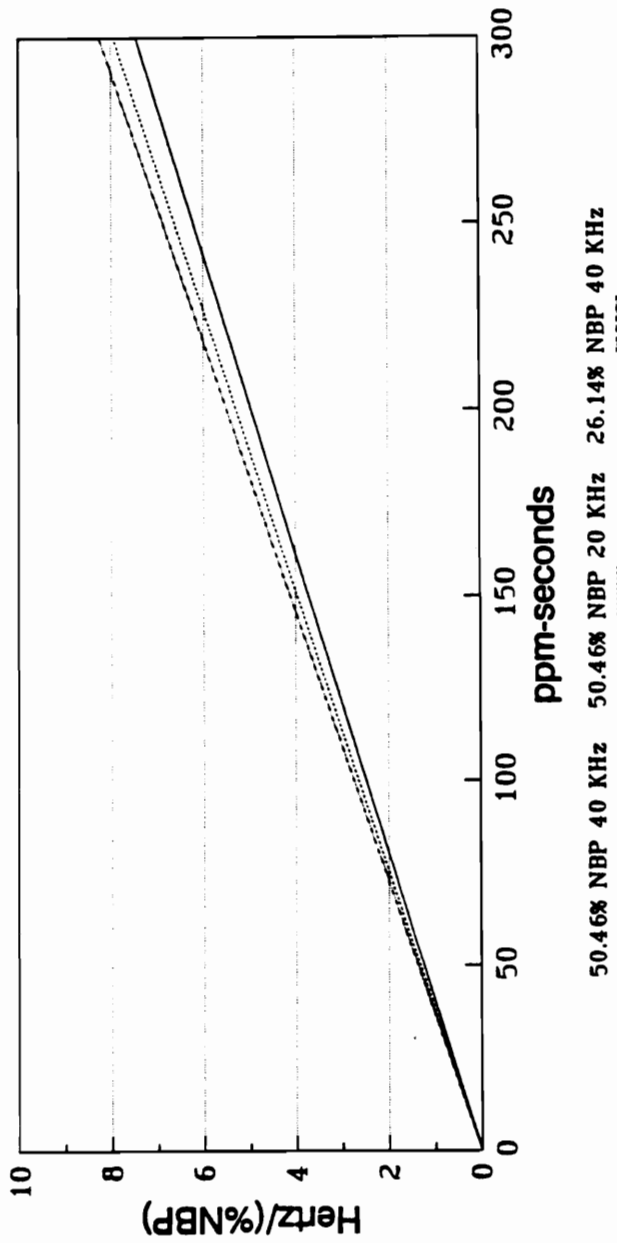


Figure 92. Normalized calibration curves for phosgene exposure.

Table 9. Normalized equations of the lines.
Equation of the Line - Normalized Calibration Curves

50.46% 4-(4'-nitrobenzyl)pyridine 40 KHz Films

Range (ppm)	slope	R squared
0 - 297.6	0.02478	0.9710

50.46% 4-(4'-nitrobenzyl)pyridine 20 KHz Films

Range (ppm)	slope	R squared
0 - 297.6	0.02600	0.9606

26.14% 4-(4'-nitrobenzyl)pyridine 40 KHz Films

Range (ppm)	slope	R squared
0 - 297.6	0.02737	0.9603

Since it is difficult to quantitatively compare the calibration curves for the 50.46% and 26.14% 4-(4'-nitrobenzyl)pyridine concentrations directly, normalization of the data [such that the ordinate is now defined as hertz/(percent 4-(4'-nitrobenzyl)pyridine)] was done to analyze the effect of the 4-(4'-nitrobenzyl)pyridine film concentration (Figure 92. Regression analysis for the normalized data can be found in Table 9 for the 20 and 40 KHz film loads of 50.46% 4-(4'-nitrobenzyl)pyridine and 26.14% 4-(4'-nitrobenzyl)pyridine in poly(ethylene glycol) MW 400. Examination of these normalized graphs leads to the conclusion that the observed effect of the concentration of 4-(4'-nitrobenzyl)pyridine upon the system is first order since the normalized calibration curves are independent of the 4-(4'-nitrobenzyl)pyridine concentration.

The frequency shifts used to generate the calibration curves also exhibit a first order dependence upon the phosgene concentration, in agreement with the calculations of film lifetime constants in the long term studies. This was not unexpected since previous studies cited in the literature using 4-(4'-nitrobenzyl)pyridine and a variety of alkylating and acylating agents showed first order dependence with both 4-(4'-nitrobenzyl)pyridine and the alkylating and acylating agents used. As discussed in the short term model SAW response, a second or third order rate dependence would yield calibration curves that would be scattered with no semblance to linearity, since a value of 200 ppm-seconds would have a response that would be appreciably different if the concentrations used were 10 ppm for 20 seconds or 2 ppm for 100 seconds.

d) Response to High Exposure Levels

Exposure of the films used in the short term exposure studies to high concentrations of phosgene (12.4 and 24.8 ppm) did not yield a calibration curve that

was linear (Figures 93,94). Examination of the curves generated from these high phosgene concentration exposures displays a upward "bend" in the calibration curve with a plateau developing at higher ppm-second exposures.

Recalling the long term differential response curves for 24.8 ppm and 12.4 ppm phosgene exposure, the reaction rate increases rapidly with increasing exposure time. The result of this increasing rate is that the frequency shift measured for 40 seconds of exposure will be greater than twice the frequency shift measured for 20 seconds, which is itself greater than twice the frequency shift measured for 10 seconds. The effect upon the calibration curve is that the curve will display an upward increasing slope rather than a linear slope.

A second factor that affects this high exposure calibration curve appears more prominently in the 26.14 % 4-(4'-nitrobenzyl)pyridine in poly(ethylene glycol) films.

Based upon long term results, the film exposure constants for the 4-(4'-nitrobenzyl)pyridine in poly(ethylene glycol) film was calculated to be 2.02 ppm-seconds/(KHz-%NBP). A 40 KHz film of 25 % 4-(4'-nitrobenzyl)pyridine in poly(ethylene glycol) will be considered expended for analytical usage at approximately 2000 ppm-seconds of exposure, the point at which the concentration of 4-(4'-nitrobenzyl)pyridine is no longer flooded and now affects the overall reactivity of the film. With an exposure of 24.8 ppm for 60 seconds (1488 ppm-seconds), 75 percent of the film is consumed with each exposure. This exposure level exceeds the capacity of the film to respond, leading to a levelling of the calibration curve. The overall effect is to generate an "S" shaped calibration curve, a very undesirable result.

With this in mind two limits are imposed upon the monitoring capabilities of these films in fixed exposure mode. The concentration of the vapor must be at 4.96 ppm or lower to generate a response which maintains a reasonable linearity. Second,

50.46% NBP in poly(ethylene glycol) MW 400 40KHZ

High Phosgene Exposure Response

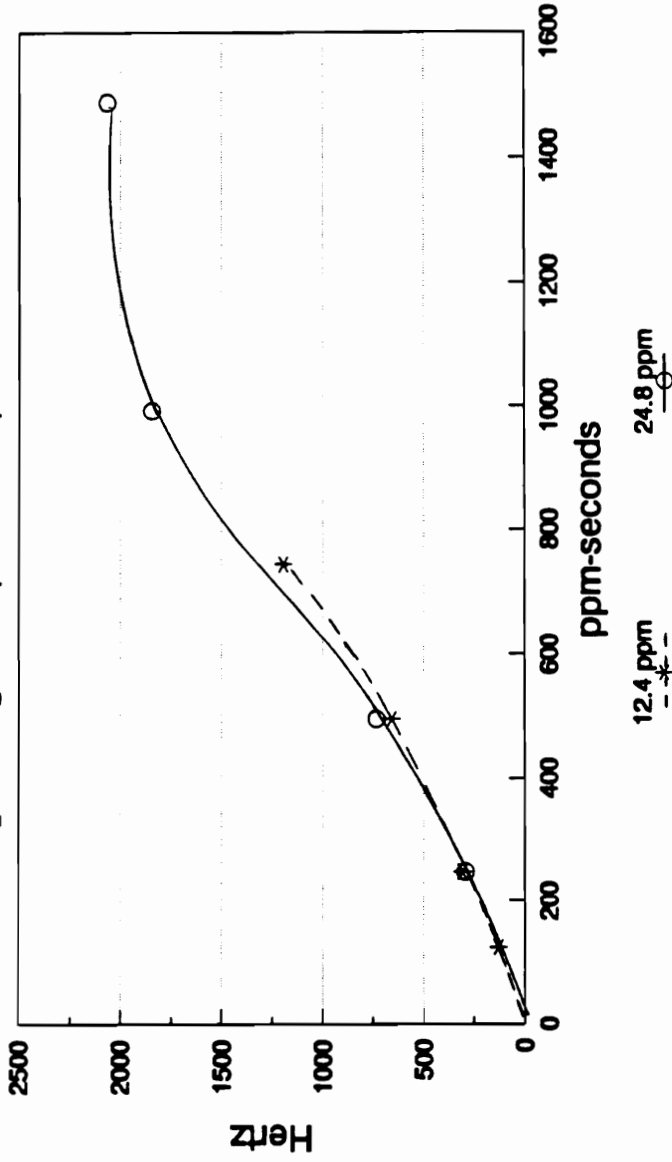


Figure 93. Exposure of high phosgene concentrations.

26.14% NBP in poly(ethylene glycol) MW 400 40KHz

High Phosgene Exposure Response

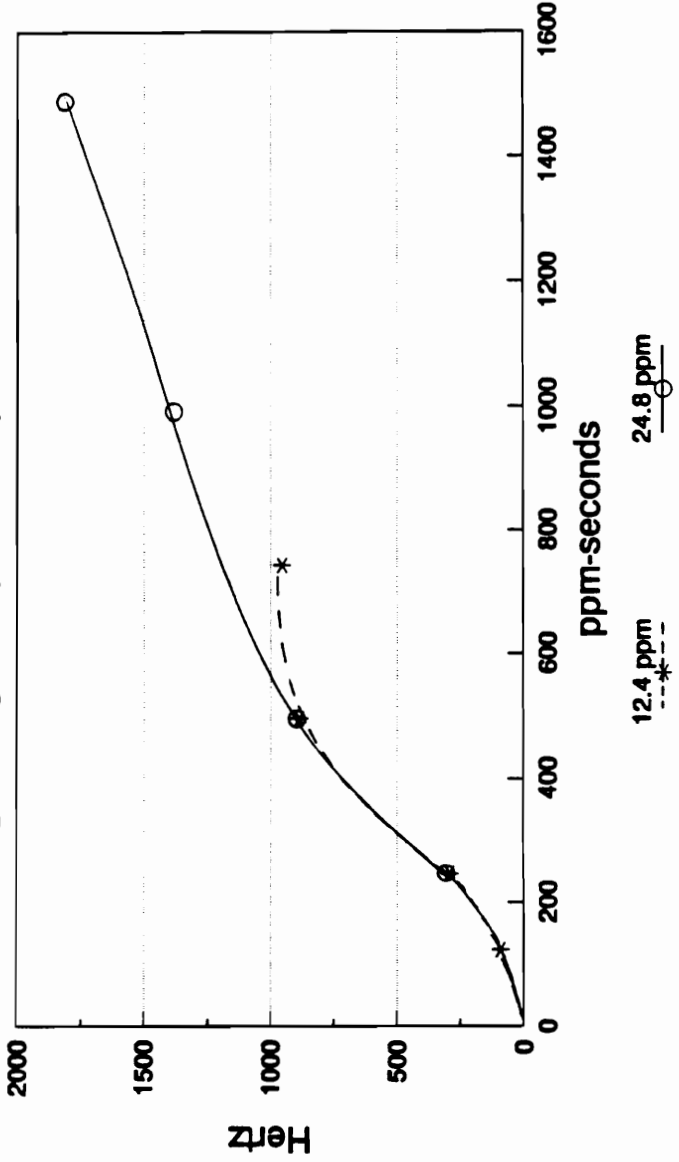


Figure 94. Exposure of high phosgene concentrations.

exposures which consume a relatively large proportion of the film creates a situation in which the film is incapable of responding proportionally to the exposure concentration.

With these limitations in mind, 20 KHz film loads composed of 50.46% 4-(4'-nitrobenzyl)pyridine in poly(ethylene glycol) were exposed to a maximum exposure of 300 ppm-seconds. This decision is based on the fact that the total amount of 4-(4'-nitrobenzyl)pyridine contained in a 20 KHz film load of 50.46% 4-(4'-nitrobenzyl)pyridine in poly(ethylene glycol) is less than the total amount of 4-(4'-nitrobenzyl)pyridine contained in a 40 KHz film load of 26.14% 4-(4'-nitrobenzyl)pyridine in poly(ethylene glycol). With less material, the observed effect would be much more pronounced. In fact, 20 KHz film loads of 50.46% 4-(4'-nitrobenzyl)pyridine in poly(ethylene glycol) exposed to 12.4 ppm phosgene for 20 seconds (248 ppm-seconds) generated very erratic results.

These limitations with high exposures led to the investigation of short term fixed exposure responses using polystyrene discussed later in this work.

e) Minimum Detectable Quantities

Minimum detectable quantities can be determined from background runs on unexposed films for the 50.46% and 26.14% 4-(4'-nitrobenzyl)pyridine in poly(ethylene glycol) mixtures. This value depends upon two factors, the inherent short term baseline noise in the frequency signal and long term frequency drift that occurs over time. Figure 95 displays both of these sources of noise.

Short term baseline noise is defined as the fluctuations that occur in the baseline frequency for short periods of time (0 to 10 seconds). The usual amount of fluctuation that occurs is on the order of 3 Hertz peak to peak. Previous work conducted has shown that the magnitude of this type of noise is typically one part in 10^7 of the

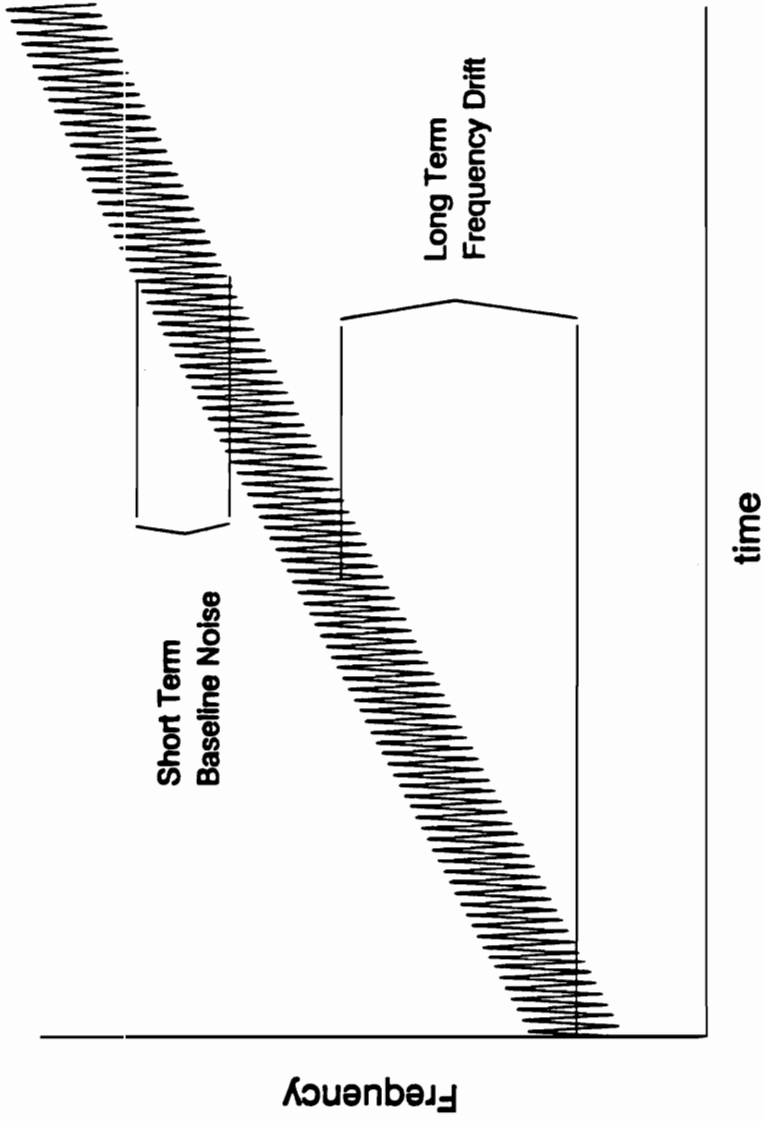


Figure 95. Short term baseline and long term frequency drift noise components.

resonant frequency of the device⁸⁶. Since the resonant frequency for the devices used in this investigation are 31 MHz, the short term baseline noise observed is compatible with this finding.

Long term frequency drift occurs when the film displays a tendency to wander to a different frequency over time. This type of noise is usually associated with evaporation of the solvent from the film and can be minimized by allowing a film to stabilize overnight. Ten Hz/hour at 30 MHz have been observed in other studies for films which have been thoroughly purged of solvent⁸⁷.

The important question is which noise level is the limiting factor in the determination of the minimum detectable quantity. If the experiment occurs during a timeframe where baseline noise is greater than drift, it will be the determining factor for the minimum detectable quantity. If the experiment occurs during a timeframe where drift is greater than baseline noise, it becomes the determining factor.

For example, a timeframe for exposure can be chosen in which the long term frequency drift is one hertz. The short term baseline noise is 3 hertz peak to peak. In this example the noise of concern is due to the baseline noise. However an exposure for a long period of time can be performed in which the long term frequency drift is 50 hertz. The short term baseline noise is 3 hertz peak to peak. In this case, the noise affecting the calculation of a minimum detectable quantity will be due to long term frequency drift

What is clear is that the minimum noise level for these experiments is the short term baseline noise, since it will always remain, even if there is no frequency drift. The noise level will never be better than three hertz for these particular devices.

Table 10 contains data and average frequency drifts for poly(ethylene glycol) MW 400 films used in the studies. The concept of a minimum detectable quantity using

frequency drift information is dependent upon the timeframe that is chosen for the analysis to occur. Using a signal to noise ratio of 3, the signal generated must be three times the frequency shift due to drift over the timeframe of interest. Minimum detectable quantities for timeframes of 200, 500 and 1000 second exposures were determined and are tabulated in Table 11.

Analysis of the drift noise associated with the three different 4-(4'-nitrobenzyl)pyridine in poly(ethylene glycol) MW 400 film types shows no appreciable difference with film thickness but a somewhat reduced drift with a film composed of 26.14% 4-(4'-nitrobenzyl)pyridine versus the films composed of 50.46% 4-(4'-nitrobenzyl)pyridine.

An analysis of the minimum detectable quantity for the three films investigated is as follows. Since the calibration curves for the 20 KHz and 40 KHz film loads of 50.46% 4-(4'-nitrobenzyl)pyridine in poly(ethylene glycol) MW 400 are nearly identical and the drift noise is nearly the same, the minimum detectable quantities for these films are comparable.

With the 40 KHz film loads of 26.14% 4-(4'-nitrobenzyl)pyridine in poly(ethylene glycol) MW 400, the calibration curve slope is roughly one-half that of the 50.46% 4-(4'-nitrobenzyl)pyridine in poly(ethylene glycol) MW 400 films due to the first order effect of 4-(4'-nitrobenzyl)pyridine upon the response of the detector (26.14%/50.46%). If the drift noise were the same, the minimum detectable quantity would be lower by a factor of 2. However, the drift noise for these films is less resulting in a minimum detectable quantity just slightly higher than those for the 50.46% 4-(4'-nitrobenzyl)pyridine in poly(ethylene glycol) MW 400 films.

Minimum detectable quantities for shorter timeframes could have been calculated, but the long term frequency drift that occurs during shorter time periods is

Table 10. Background run stability tests - long term frequency drifts.
Background Run Stability Tests
NBP in Poly(ethylene glycol) MW 400

Time (sec)	50.46% NBP 40 KHz load		50.46% NBP 20 KHz load		26.14% NBP 40 KHz load	
	Drift (Hz)	Time (sec)	Drift (Hz)	Time (sec)	Drift (Hz)	Time (sec)
10	18	1000	38	1000	13	900
60	28	835	42	1000	32	825
200	47	1000	13	1000	21	1000
1000	18	895	12	1000	18	750
	18	935			7	550
	37	1000			7	900
Total	166	5665	105	4000	115	5925
Average (Hz/sec)	0.0293		0.0263		0.0194	
Time (sec)		Drift (Hz)		Drift (Hz)		Drift (Hz)
10		0.29		0.26		0.19
60		1.76		1.58		1.16
200		5.86		5.25		3.88
1000		29.30		26.25		19.41

Table 11. Minimum detectable quantities.
Minimum Detectable Quantities
Poly(ethylene glycol) MW 400

50.46% 4-(4'-nitrobenzyl)pyridine 40 KHz Films

Time	Average Drift	3*(Drift)	ppm-sec	Minimum Detectable Quantity
200	5.86	17.58	12	60 ppb
500	14.65	43.95	28	56 ppb
1000	29.30	87.90	58	58 ppb

50.46% 4-(4'-nitrobenzyl)pyridine 20 KHz Films

Time	Average Drift	3*(Drift)	ppm-sec	Minimum Detectable Quantity
200	5.25	15.75	10	50 ppb
500	13.13	39.39	25	50 ppb
1000	26.25	78.75	49	49 ppb

26.14% 4-(4'-nitrobenzyl)pyridine 40 KHz Films

Time	Average Drift	3*(Drift)	ppm-sec	Minimum Detectable Quantity
200	3.88	11.64	18	90 ppb
500	9.70	29.10	44	88 ppb
1000	19.40	58.20	88	88 ppb

less than the short term baseline noise. Therefore at shorter timeframes, the short term noise will be the limiting factor in the calculation of minimum detectable quantities. As an example, the minimum detectable quantity for the 40 KHz film load of 50.46% 4-(4'-nitrobenzyl)pyridine in poly(ethylene glycol), MW 400 film for a 60 second period can be calculated.

The frequency drift associated with 100 seconds is 1.76 Hz. The short term noise level is 3 Hz. The limiting noise level is therefore short term noise for this timeframe. Using a signal to noise ratio of 3, the minimum signal that can be identified as a signal is 9 Hz. From the calibration curve, 9 Hz corresponds to 7.2 ppm-seconds of exposure. For a 100 second period, this corresponds to a 120 ppb (7.2 ppm-seconds/60 seconds) minimum detectable quantity.

If the timeframe chosen had been 30 instead of 60 seconds, the numbers would have been the same except for the time used. This affects the minimum detectable quantity calculated. The limiting noise level would still be 3 Hz. The minimum identifiable signal would be 9 Hz, and this would still correspond to 7.2 ppm-seconds. However for a period of 30 seconds, the minimum detectable quantity would be 240 ppb. The conclusion that is reached is that the use of shorter timeframes will worsen the minimum detectable quantity since the noise level is fixed by the short term noise.

Background runs on the films were performed within 1 to 2 hours after stabilization in the detector cell chamber. Improvement can be attained if the films are allowed to stabilize overnight leading to frequency drifts previously cited as being approximately 10 Hz per hour⁸⁷. If this level of stability is obtained for such films, the drift occurring during 500 seconds would be 1.39 Hz. As demonstrated in the previous paragraphs, short term baseline noise would limit the minimum detectable quantity. Three times this noise is 9 Hz. For a 50.46% 4-(4'-nitrobenzyl)pyridine in

poly(ethylene glycol) 40 KHz film load this corresponds to 7.2 ppm-seconds of exposure. Therefore the minimum detectable quantity for 500 seconds is approximately 15 ppb (7.2 ppm-seconds/500 seconds).

2) Flow Rate Effects on Poly(ethylene glycol) Films

Experimental Synopsis: Determination of the effect of different flow rates upon the amount of frequency change of the dual SAW device detector for exposure levels ranging from 4.96 ppm-seconds to 74.4 ppm-seconds of phosgene.

Experimental conditions:

Sample Film Composition: 50.46% 4-(4'-nitrobenzyl)pyridine in poly(ethylene glycol) MW 400

Reference Film Composition: 100% poly(ethylene glycol) MW 400

Film Thickness: approximately 40 KHz

Flow Rates: 100, 150 and 200 cc/min

Vapor being determined: phosgene

Exposure levels: see Table 12

Flow rates have an effect upon the amount of frequency shift observed upon exposure of the films. Figure 96 shows the calibration curve for 100, 150 and 200 cc/min flow rates. While there is an appreciable difference between the 100 and 150 cc/min flow rates, the difference between 150 and 200 cc/min is much reduced. A comparison of the calibration curve slopes for the different flow rates can be found in Table 13.

The overall effect appears to be due to mass transfer versus permeability and reactivity effects. The parameters that will affect the response characteristics of the SAW device are, the amount and rate of vapor transferred to the headspace above the

Table 12. Concentration-time products and responses for phosgene exposure - flow rate effects.

50.46% NBP in Poly(Ethylene Glycol) MW 400 40KHz Load

Concentration Time products for Phosgene Exposure

CT Product (ppm-sec)	100 cc/min		150 cc/min		200 cc/min		Exposure Level (ppm)
	Average Response (Hz)	Standard Deviation (Hz)	Average Response (Hz)	Standard Deviation (Hz)	Average Response (Hz)	Standard Deviation (Hz)	
4.96	4.64	1.25	9.60	0.42			0.496
9.92	11.31	2.48	20.40	0.55			0.496
12.4	12.13	1.25	22.50	1.27	22.90	1.67	1.24
19.8	25.61	4.73	44.20	1.48	51.40	2.07	0.496
24.8	29.38	1.25	48.50	1.32			1.24
29.8	40.25	5.81	69.00	0.82	115.80	3.83	0.496
49.6	65.56	2.24	108.20	3.19			1.24
74.4	103.29	2.14	172.50	3.32	182.50	3.70	1.24

50.46% NBP in poly(ethylene glycol) MW 400 40KHZ

Phosgene response -- flowrate effects

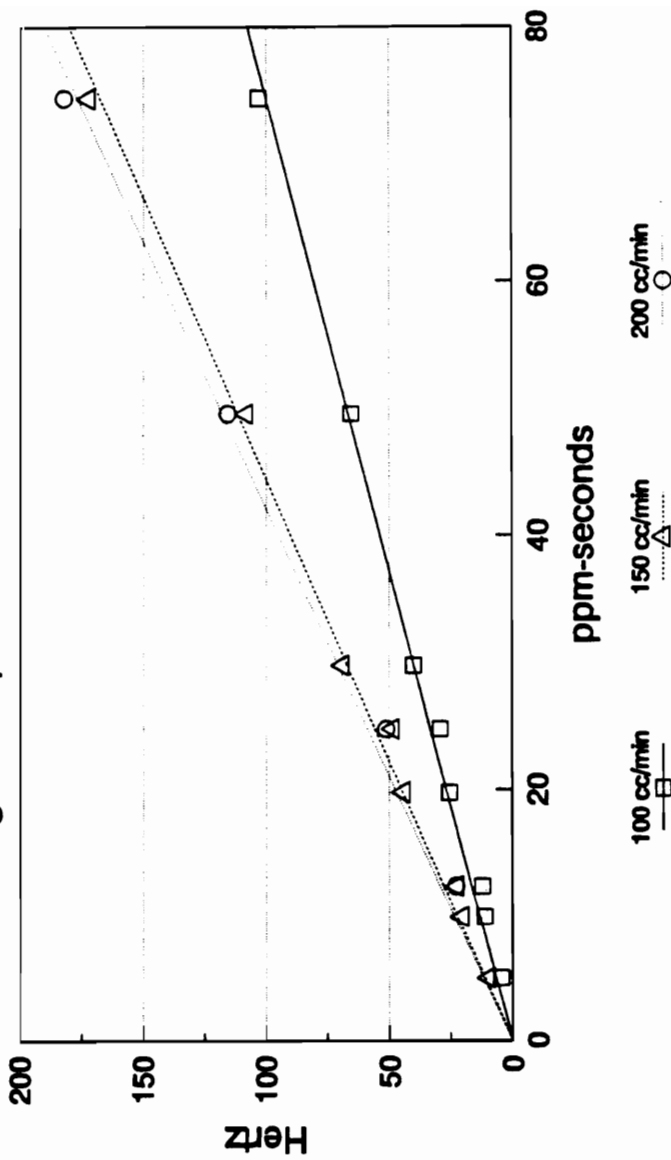


Figure 96. Calibration curves for phosgene exposure - flow rate effects.

Table 13. Equations of the lines - flow rate effects.

Equation of the Line - Calibration Curves

50.46% 4-(4'-nitrobenzyl)pyridine 40 KHz Films
Flow rate effects

100 cc/min flow rate

Range (ppm)	slope	R squared
0 - 74.4	1.343	0.9926

150 cc/min flow rate

Range (ppm)	slope	R squared
0 - 74.4	2.249	0.9938

200 cc/min flow rate

Range (ppm)	slope	R squared
0 - 74.4	2.382	0.9910

device, the permeability of the vapor into the film and finally the reactivity of the solubilized vapor with the trapping reagent. The results of the flow rate experiments indicate that at 100 cc/min, the mass of vapor transferred to the headspace above the device affects the response of the device, acting as a bottleneck to the amount of phosgene that is allowed to flow across the film per unit time. By increasing the flow rate, the amount of vapor that will appear above the surface of the device will increase, until the point is reached where mass transfer will no longer have an affect upon the response of the film. This appears to be the case when the flow rate is increased from 150 cc/min to 200 cc/min. This same flow rate effect has been noted with dosimeters being developed in other laboratories⁸⁸.

A visualization of the process involved in the response of the detector at different flow rates can be attempted. As the vapor enters the detector chamber, the partition coefficient for the vapor/film system will determine the equilibrium concentrations of the vapor in the headspace above the film and the vapor dissolved in the film. If mass transfer is a bottleneck, the amount of vapor entering the detector cell will be insufficient to ensure that the headspace vapor concentration remains constant. For example, if a 5 ppm vapor concentration enters the detector chamber at a flow rate of 100 cc/min, upon contact with the film the headspace vapor concentration may drop to 2.5 ppm as the headspace vapor begins to permeate into the film. At a 150 cc/min flow rate, this headspace vapor concentration may drop to 4.5 ppm. Eventually a flow rate may be reached where the amount of mass entering the detector chamber per unit time is sufficient to ensure that a minimum concentration drop occurs in the headspace above the film. At this point any increase in the flow rate will not affect the headspace concentration and mass transfer is no longer a bottleneck.

The higher the concentration of the headspace vapor above the film, the greater the amount of vapor permeating into the film in an attempt to establish equilibrium. Therefore if the headspace concentration above the film approaches a constant value with increasing flow rate, the response of the device will also approach a constant value for a given vapor concentration.

To continue with the example presented, a 10 second injection of 5 ppm at 100 cc/min flow will result in a 10 Hz signal while a 150 cc/min flow of the same 5 ppm at 10 seconds of exposure will result in a 15 Hz signal. Increasing the flow rate further will only increase the response slightly as the headspace vapor concentration above the film increases only slightly.

The overall effect is demonstrated in figure 96. The slope of a calibration curve for the low flow rate will be less than that for a higher flow rate. Increasing the flow rate will increase the response for each individual concentration-time exposure, thereby increasing the slope of the calibration curve. However as the flow rate is increased to the point where it no longer affects the response, the slope of the calibration curve will reach a maximum.

A separate study investigating flow rate effects upon the response of the device, involving parameters such as device size and cell volume, should be investigated. The goal would be to determine an ideal configuration that will minimize flow rate effects. The use of a gas chromatograph to measure the vapor concentration before exposure and after exposure to the film would determine the amount of vapor removed by the film at different flow rates. Based upon the above analysis, it would be expected that as the head space concentration approaches the true vapor concentration before it enters the detector chamber, the calibration curves generated from these conditions would approach a maximum constant slope response.

3) Polystyrene Films

Experimental Synopsis: Recognizing the rapid consumption of films using the poly(ethylene glycol) support matrices at phosgene concentrations greater than 5 ppm, a change to an entirely different polymer was made in an attempt to reduce the frequency change rate. This would enable analysis of concentrations that poly(ethylene glycol) films are incapable of accurately measuring.

Experimental conditions:

Sample Film Composition: 50.22% 4-(4'-nitrobenzyl)pyridine in polystyrene, MW 280,000

Reference Film Composition: 100% polystyrene, MW 280,000

Film Thickness: approximately 50 KHz

Flow Rate: 100 cc/min

Vapor being determined: phosgene

Concentrations: see Table 14

Changing the support matrix from poly(ethylene glycol) MW 400 to polystyrene MW 280,000 had a drastic effect upon the response of the detector to phosgene concentrations. As could be expected from the results obtained in the long term studies, the sensitivity of polystyrene based films to phosgene is much less than that obtained from poly(ethylene glycol) MW 400 (Figure 97). The film does not generate a measurable response to phosgene until exposed to 12.4 ppm for 20 seconds (248 ppm-seconds). Normalizing the response of 50.22% 4-(4'-nitrobenzyl)pyridine in polystyrene [as was done with the polyethylene glycol studies] allows a plot comparing polystyrene (Figure 99) and polyethylene glycol matrices directly (Figure 98). This shows a difference in response factor of 200 when measured at the 300 ppm-seconds exposure level.

Table 14. Concentration-time products and responses for phosgene exposure.

50.22% NBP in Polystyrene MW 280,000

**Concentration Time products for Phosgene Exposure
40 KHz Film Load**

Average for measured responses

CT Product (ppm-sec)	Average Response (Hz)	Standard Deviation	Exposure Level (ppm)
24.8	0.00	0.00	2.48
49.6	0.00	0.00	2.48
49.6	0.00	0.00	4.96
99.2	0.00	0.00	2.48
99.2	0.00	0.00	2.48
124	0.00	0.00	12.4
148.8	0.00	0.00	2.48
198.4	0.00	0.00	4.96
248	4.00	0.94	12.4
248	0.40	0.55	24.8
297.6	0.00	0.00	4.96
496	6.50	0.41	12.4
496	3.10	0.55	24.8
744	8.50	0.50	12.4
992	6.50	1.06	24.8
1488	9.75	0.87	24.8

50.22% NBP in polystyrene MW 280,000
24.8 ppm Phosgene Response

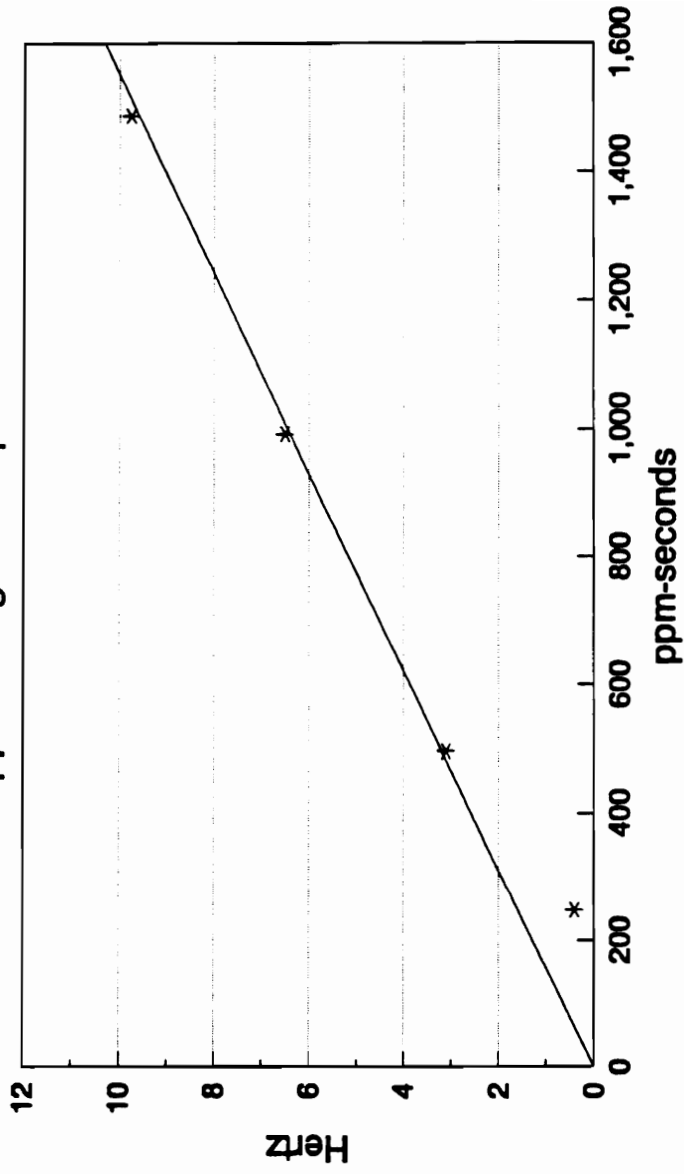


Figure 97. Calibration curve for phosgene exposure.

**Normalized Film Response to Phosgene
26.14% and 50.46% NBP on poly(ethylene glycol)
MW 400**

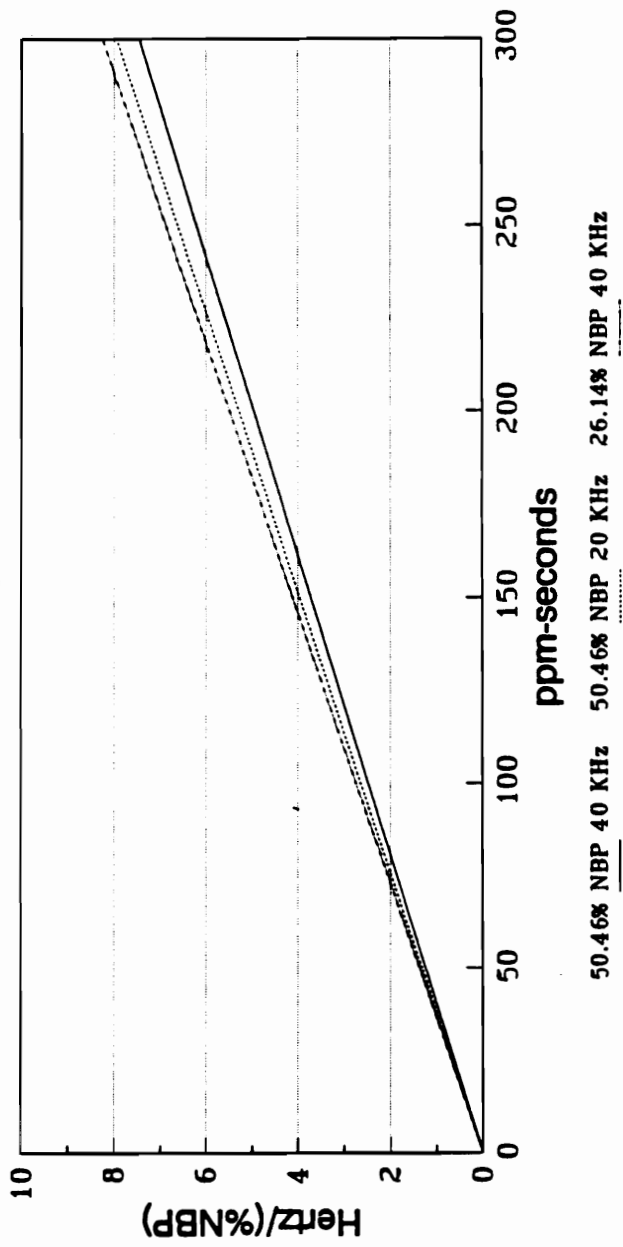


Figure 98. Normalized calibration curves for 4-(4'-nitrobenzyl)pyridine in poly(ethylene glycol), MW 400.

Normalized Film Response to Phosgene
50.22% NBP in polystyrene MW 280,000
24.8 ppm Phosgene Exposure

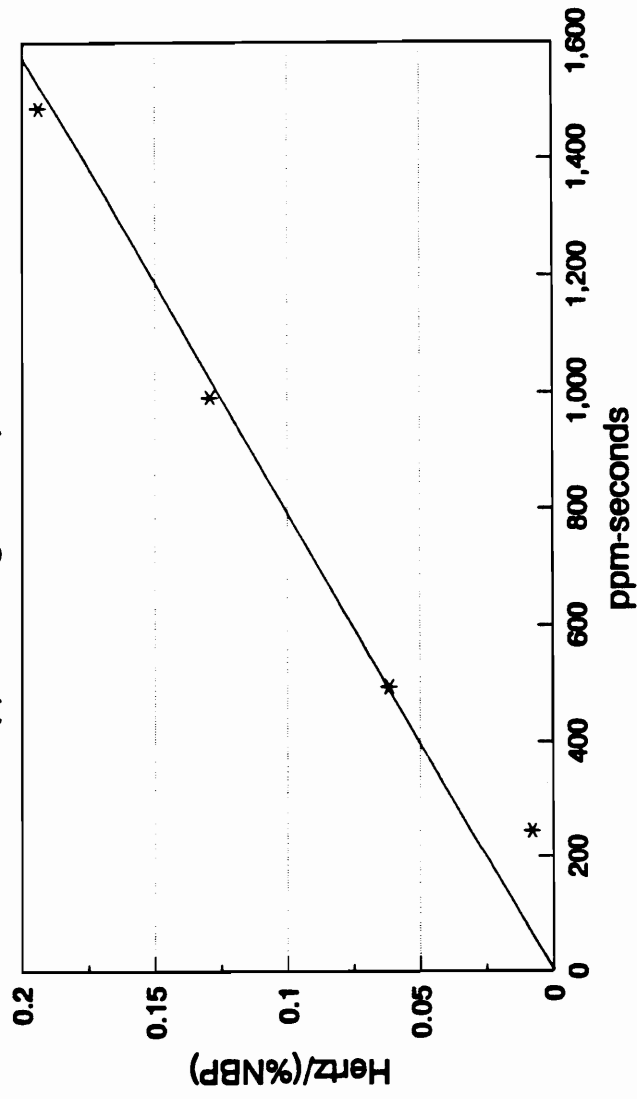


Figure 99. Normalized calibration curve for 4-(4'-nitrobenzyl)pyridine in polystyrene MW 280,000.

While this may be considered a serious limitation if the goal is low level detection of phosgene, the value of this film is in monitoring fatal levels of phosgene. As demonstrated in the long term exposure experiments, the very sensitive films are consumed before the concentration of the vapor can be determined. Also the length of exposure to fatal concentrations cannot be ascertained by a film with a lifetime measured in seconds at a high concentration.

The important result of this investigation is the observation that by changing the support matrix for the active agent the analytical range of the detector system can be extended to higher concentrations.

The development of a "universal" equation for the solubility of gaseous solutes in polymers has been reported by Taft and his coworkers⁶⁹ with an improvement in this model resulting in the linear solvation energy relationship as introduced by Grate and Abraham⁷¹. The information provided by these two models will lead to the optimal implementation of particular films for selectivity and sensitivity to target vapors. This has been the goal of previous research using SAW devices, focusing on the development of highly sensitive films to target vapors. What has not been the focus of previous research until this investigation, but is equally important, is the attempt to reduce the sensitivity of the film to the vapor of interest.

As discovered with the high phosgene concentration exposures of the poly(ethylene glycol) films, the analytical capabilities of those highly sensitive films were exceeded. To ensure accurate measurement of high concentrations, a change to a less permeable film was necessary. The results of these investigations suggest that a deliberate mismatch of the solvation parameters of the models for the vapor/polymer system will lead to a reduced sensitivity, increasing the analytical range of the detector system to the target vapor. The use of the glassy polystyrene demonstrates that reduced

permeability does indeed reduce the sensitivity of the device to the target vapor, thereby increasing the analytical range of the device. Therefore, either the introduction of a less permeable glass support matrix or the mismatching of solvation parameters will prove to be an effective tool for expanding the analytical range of SAW devices to target vapors.

b) Thionyl Chloride

Experimental Synopsis: Changing from the carbonyl group to the less reactive thionyl group allowed determination of the response of the dual SAW device detector to thionyl chloride.

Experimental conditions:

Sample Film Composition: 50.46% 4-(4'-nitrobenzyl)pyridine in poly(ethylene glycol) MW 400

Reference Film Composition: 100% poly(ethylene glycol) MW 400

Film Thickness: approximately 40 KHz

Flow Rate: 100 cc/min

Vapor being determined: thionyl chloride

Concentrations: see Table 15

Film loads of approximately 40 KHz were exposed to 2.63 and 5.26 ppm thionyl chloride for 10 to 60 second injection intervals. Table 15 contains data for these exposures. The frequency responses from exposure of 50.46% 4-(4'-nitrobenzyl)pyridine in poly(ethylene glycol) MW400 to 2.63 ppm and 5.26 ppm thionyl chloride for 10, 20, 40 and 60 second intervals were used for the development of the calibration chart in figure 101. Normalizing the response as in previous experiments, the response of the film to phosgene is approximately 20 times greater

than the response to thionyl chloride as measured at 300 ppm-second exposure (Figure 102).

This difference in the amount of frequency change is attributed to the chemical nature of the vapors. Since the rate of loading is dependent upon the reactivity of the vapor with the active agent 4-(4'-nitrobenzyl)pyridine, a higher reactivity is expected for phosgene due to the larger polarity of the carbonyl group versus that of the thionyl group. This manifests itself in a more rapid nucleophilic attack by 4-(4'-nitrobenzyl)pyridine.

The non-linearity that is noted in the calibration curve can be explained by using the results obtained from the long term exposure experiments. Examination of the frequency change rates for the long term exposure experiments shows that the frequency change rate at fixed concentration is time dependent, with larger changes occurring at times later in the exposure (Figure 84, page 178). The result is that a calibration curve generated for the responses of the detector to thionyl chloride will literally be a curve whose slope increases with increasing ppm-seconds of exposure. This same effect was noted at high concentrations of phosgene. The response characteristics of this film to thionyl chloride are undesirable, and for this reason the use of this particular system for the measurement of thionyl chloride is questionable.

The difference noted in the response of the detector to two different vapors, phosgene and thionyl chloride, can be used as a selectivity parameter for a dosimetric film.

Table 15. Concentration-time products and responses for thionyl chloride exposure.

50.46% NBP in Poly(Ethylene Glycol) MW 400

**Concentration Time products for Thionyl Chloride Exposure
40 KHz Film Load**

Average for measured responses

CT Product (ppm-sec)	Average Response (Hz)	Standard Deviation	Exposure Level (ppm)
26.3	0.00	0.00	2.63
52.6	0.00	0.00	2.63
52.6	0.00	0.00	5.26
105.2	0.00	0.00	2.63
105.2	2.30	0.27	5.26
157.8	3.25	0.96	2.63
210.4	9.10	1.82	5.26
315.6	24.00	1.35	5.26

50.46% NBP in poly(ethylene glycol) MW 400 40KHz

Thionyl Chloride Response

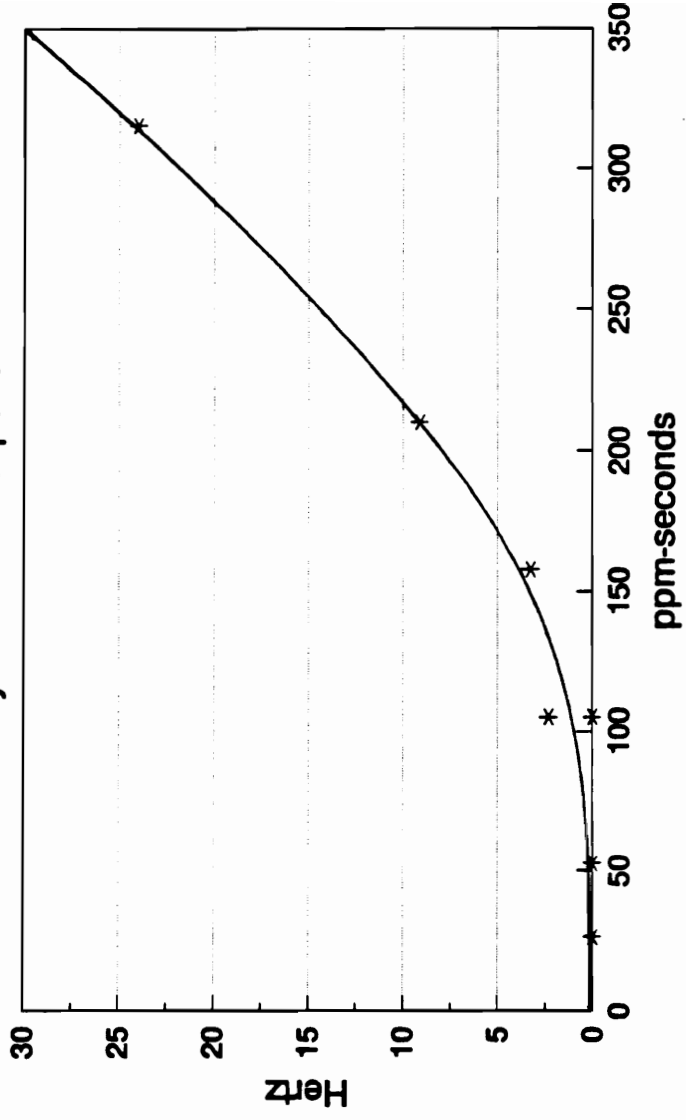


Figure 101. Calibration curve for thionyl chloride exposure.

Normalized Film Response to Thionyl Chloride
50.46% NBP in poly(ethylene glycol) MW 400 40 KHz

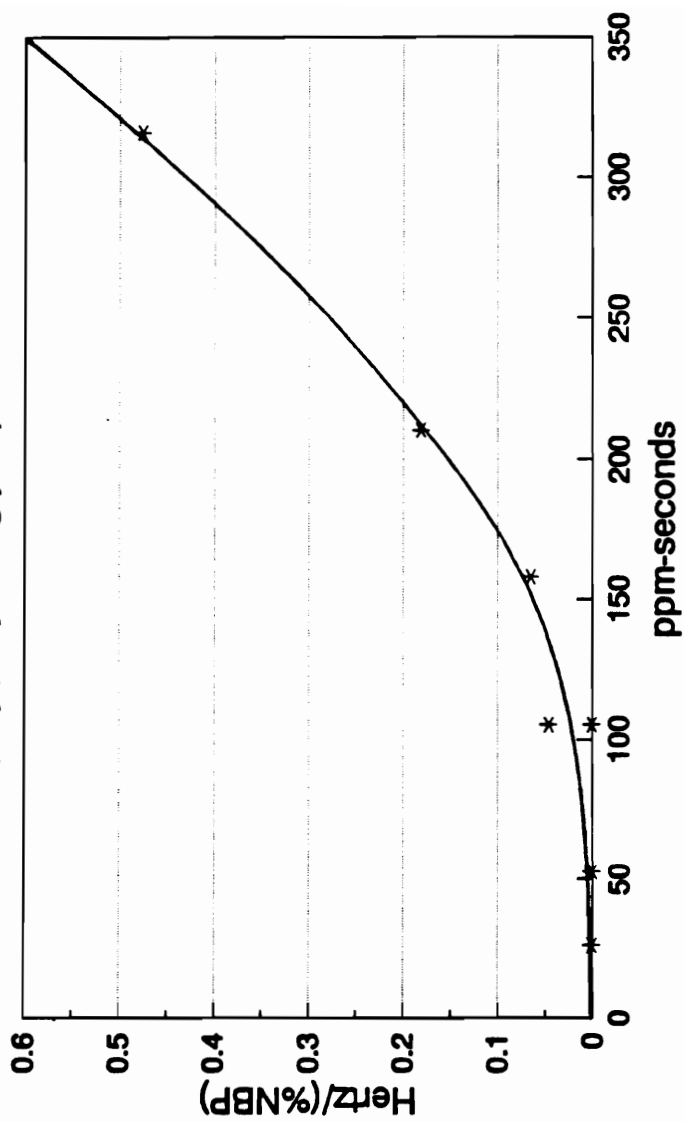


Figure 102. Normalized calibration curve for thionyl chloride exposure.

C) Infrared and Visible Results

To determine the structural makeup and stability of the resulting reaction product, infrared studies were undertaken to examine this product. The experiments included 1) infrared spectrum of 50.46% 4-(4'-nitrobenzyl)pyridine in poly(ethylene glycol) MW400 applied to NaCl window, 2) IR spectrum of the same film after exposure to 24.8 ppm phosgene for 922 seconds, 3) IR spectrum of this same film after 5 days aeration. Since neither of the materials composing the sensing film, 4-(4'-nitrobenzyl)pyridine or poly(ethylene glycol), contained a carbonyl functional group, this portion of the infrared spectrum was monitored for an indication of the irreversible incorporation of phosgene into the film.

The differences between the unexposed and exposed films produces development of bands in the carbonyl region at 1690 and 1760 cm^{-1} . Upon aeration for 5 days these bands remained.

This result is interpreted as the creation of a stable product. While the band at 1760 cm^{-1} is interpreted as due to the reaction of phosgene with poly(ethylene glycol) end chain hydroxyl groups, the creation of the band at 1690 cm^{-1} can be attributed to the existence of a carbonyl group in the resulting product. This is not surprising since nucleophilic attack of the carbonyl group by the pyridine moiety of 4-(4'-nitrobenzyl)pyridine is involved in the detection scheme. Cockerill determined that the carbonyl peak for the dihydroquinone structure appears at 1658 cm^{-1} .

To further determine if this carbonyl band was characteristic of phosgene reaction with 4-(4'-nitrobenzyl)pyridine, a mixture of 50.22% 4-(4'-nitrobenzyl)pyridine in polystyrene, MW 280,000, was exposed to phosgene. The development of a single carbonyl band at 1660 cm^{-1} is further evidence for the irreversible reaction of phosgene with 4-(4'-nitrobenzyl)pyridine.

The visible spectra obtained on the 50.46% 4-(4'-nitrobenzyl)pyridine in poly(ethylene glycol), MW400, film showed the development of an absorption maximum upon phosgene exposure at 450 nm. This is in close agreement with that determined by Cockerill (440 nm)⁸⁹.

Quantization of this peak was not attempted, since a chromophoric generating species and stabilizing agent, such as NaOH and N-benzylamine respectively, were not incorporated into the sensing film. Because the measurement of phosgene by a SAW device relies upon mass loading of the film, the incorporation of these agents adds nothing to the amount of active agent in the film, in fact appearing as useless mass. With the film load capacity of the device being fixed, these agents will reduce the relative amount of 4-(4'-nitrobenzyl)pyridine in the film, thereby reducing the response of the device to phosgene.

CONCLUSIONS AND FUTURE INVESTIGATIONS

The development of chemical systems for detecting hazardous vapors using SAW devices can be expanded beyond simple physisorption processes for detecting these vapors. By incorporating an active agent in a film, the film can be targeted to vapors that specifically react with the agent.

The advantage of the systems studied in this work is in the development of the concept that by changing the support matrix a change in the analytical range for the sensor can occur. Previous studies focused strictly on achieving the highest sensitivity towards the vapor being targeted. This in itself is an important undertaking; but as discussed earlier, it is not in itself the total story. What differentiates this work from previous studies is the realization that besides maximizing the minimum detectable quantities for vapors being investigated, for the first higher vapor concentrations which will saturate a very sensitive film can be investigated using a matrix that will limit the permeability of the vapor to the trapping agent. By the judicious choice of support phases, using either a solvatochromic or linear solvation energy relationship model, or using different phases or crystallinities, the analytical range for the particular trapping agent employed can be changed. This would allow monitoring at concentrations not available with very sensitive films. Therefore this investigation, developing both a highly sensitive film and a less sensitive film, can be used as a template in the development of films for the purpose of monitoring other target vapors.

The discovery that device response is independent of film thickness for irreversible dosimetric applications is important in the pursuit of increased sensitivity of SAW devices to target vapors.

SAW devices, in order to oscillate, require that the average film thickness does not exceed one percent of the SAW wavelength. Thicker films lead to greater attenuation and eventually cause cessation in oscillation of the circuit. Since 40 KHz film loads were required for the 31 MHz devices used in this study, 20 KHz loads (ie. one-half the film thickness) would be required for 62 MHz devices. Since the films respond identically, going to a higher frequency device increases the signal generated with exposure by a factor of four, since the frequency shift for each mass per unit area increase is dependent upon the frequency squared. Wohltjen's scaling laws show that the signal to noise ratio improves linearly with frequency. The net result is that increasing the frequency of the device will improve the signal to noise ratio linearly, producing a sensor with greater sensitivity to the vapor. The higher the oscillating frequency, the greater the sensitivity.

The only tradeoff is the film lifetime. Since the film exposure constant, previously defined as:

$$\text{Exposure} = (\text{ppm-second})/(\text{KHz} \cdot \%[\text{NBP}]) \quad (85)$$

is independent of film thickness, reducing the film thickness linearly reduces the lifetime of the film. The question that needs to be answered for each application is which is most important, film lifetime or sensitivity. The answer will dictate the frequency of the device to be used.

The use of a reference device coated with the neat support matrix reduces effects due simply to solvation. As shown by the use of ethylene oxide, a vapor which does not react with the trapping agent during the time of analysis will simply solvate both the sample and reference device films. Since the beat frequency is the signal being measured, the common mode rejection capabilities of this dual beam configuration results in a minimal false signal generation.

Finally, the characteristic of all SAW device sensors is their ability for immediate response to the presence of the target vapor. Colorometric badges may require minutes of exposure to generate a sufficient amount of color indicating the presence of the vapor being monitored.⁹⁰ With exposure of SAW devices to vapors, the response is immediate due to their extreme sensitivity to mass changes, as is evident in the exposure of films to 0.496 ppm phosgene. This immediate and sensitive response to vapors has been, and continues to be, the driving force behind the investigation of SAW device chemical sensors.

With their compact size, personal monitors can be designed for real time response to targeted vapors, generating an immediate signal which can be recorded and which allows the user of the device ample warning for the presence of a dangerous environment.

The result of this work demonstrates that the chemistry of the film will determine their usefulness in real world situations. To those who wish to delve into this arena, the chemistry occurring upon the surface of these devices will determine, in the long run, whether they will play a major role in ambient monitoring.

REFERENCES

- 1 Carey, W. P.; Beebe, K. R.; Kowalski, B. R.; Illman, D. L.; Hirshfeld, T.; Anal. Chem. 1986, 58, 149.
- 2 Wilson, B. E.; Kowalski, B. R.; Anal. Chem. 1989, 61, 2277.
- 3 King, W. H., Jr.; Anal. Chem. 1964, 36, 1735.
- 4 Hlavay, J.; Guilbault, G. G.; Anal. Chem. 1977, 49, 1890.
- 5 Edmunds, T. E.; West, T. S.; Anal. Chim. Acta 1980, 117, 147.
- 6 White, R. M.; Volltmer, F. W.; Appl. Phys. Lett. 1965, 7, 314.
- 7 Slobodnik, A. J.; J. Appl. Phys. 1972, 43(6), 2565.
- 8 Wohltjen, H.; Dessy, R. E.; Anal. Chem. 1979, 51, 1458.
- 9 D'Amico, A.; Palma, A.; Verona, E.; Proc. IEEE Ultrason. Symp.- 1982, 308.
- 10 Nieuwenhuizen, M. S.; Nederlof, A. J.; Anal. Chem. 1988, 60, 236.
- 11 Brace, J. G.; Sanfelippo, T. S.; Joshi, S. G.; Sens. Actuators 1988, 14, 47.
- 12 D'Amico, A.; Petri, A.; Verardi, P.; Verona, E.; Proc. IEEE Ultrason. Symp.- 1987, 633.

- 13 Ballantine, D.; Wohltjen, H.; *Chemical Sensors and Microinstrumentation*, ACS Symposium series 403; American Chemical Society: Washington, DC, 1989, 222.
- 14 Ricco, A. J.; Martin, S. J.; Zipperian, T. E.; *Sens. Actuators* 1985, 8, 319.
- 15 D'Amico, A.; Palma, A.; Verona, E.; *Sens. Actuators* 1982, 3, 31.
- 16 D'Amico, A.; Petri, A.; Verardi, P.; Verona, E.; *Proc. IEEE Ultrason. Symp.*- 1987, 633.
- 17 Vetelino, J. F.; Lade, R. K.; Falconer, R. S.; *IEEE Trans.* 1987, UFFC-34(2), 156.
- 18 Snow, A.; Wohltjen, H.; *Anal. Chem.* 1984, 56, 1411.
- 19 Zellers, E. T.; *Chemical Sensors and Microinstrumentation*, ACS Symposium series 403; American Chemical Society: Washington, DC, 1989, 176.
- 20 Roederer, J. E.; Bastiaans, G. J.; *Anal. Chem.* 1983, 55, 2333.
- 21 Calabrese, G. S.; Wohltjen, H.; Roy, M. K.; *Anal. Chem.* 1987, 59, 833.
- 22 Ricco, A. J.; Martin, S. J.; *Appl. Phys. Lett.* 1987, 50(21), 1474.
- 23 White, R.M.; Wenzel, S.W. *Appl. Phys. Lett.* 1988, 52(20), 1653.
- 24 Brown, W. G.; Wilzbach, K. E.; Ballweber, E. G.; *Library of Congress*, PB No. 5945, September, 1945

- 25 Liddell, H. F.; *Analyst* 1957, 82, 375.
- 26 Witten, B.; Prostack, A.; *Anal. Chem.* 1957, 29, 885.
- 27 Dixon, B. E.; Hands, G. C.; *Analyst* 1959, 84, 463.
- 28 Linch, A. L.; Lord, Jr, S. S.; Kubitz, K. A.; De Brunner, M. R.; *American Ind. Hyg. Ass. J.* 1965, 26, 465.
- 29 Noweir, M. D.; Pfitzer, E. A.; *American Ind. Hyg. Ass. J.* 1971, 32(3), 163.
- 30 Tuggle, R. M.; Esposito, G. G.; Guinivan, T. L.; Hess, T. L.; Lillian, D.; Podolak, G. E.; Sexton, K. G.; Smith, N. V.; *American Ind. Hyg. Ass. J.* 1979, 40, 387.
- 31 Matherne, R. N.; Lubs, P. L.; Kerfoot, E. J.; *American Ind. Hyg. Ass. J.* 1981, 42(9), 681.
- 32 Dick, K. F.; Ham, G. E.; Gross, J. R.; U.S. Patent #4,378,454, 1983.
- 33 Suleiman, A.; Guilbault, G. G.; *Anal. Chim. Acta* 1984, 162, 97.
- 34 Friedman, O. M.; Boger, E.; *Anal. Chem.* 1961, 33, 906.
- 35 Agree, A. M.; Meeker, R. L.; *Talanta* 1966, 13, 1151.
- 36 *Threshold Limit Values and Biological Exposure Indices for 1986-1987*, American Conference of Governmental Industrial Hygienists: Cincinnati, OH.

- 37 Brewer, J. H.; Arnsberger, R. J.; *Journal of Pharmaceutical Sciences* 1966, 55(1), 57.
- 38 Cheng, S.; U.S. Patent 3,738,811, 1973
- 39 Whitbourne, J. E.; Eastman, C. A.; U.S. Patent 3,992,154, 1976
- 40 Sumimoto, M.; Kohama, H.; U.S. Patent 4,094,642, 1978
- 41 Manning, C. R.; U.S. Patent 4,426,819, 1984
- 42 Gonzalez, L. A.; Sefton, M. V.; *American Ind. Hyg. Ass. J.* 1985, 46(10), 591.
- 43 Dobinson, B.; Hofmann, W.; Stark, B. P.; *The Determination of Epoxide Groups*; Pergamon Press: New York, 1969; 56.
- 44 Kring, E.; Damrell, D.; Basilio, A.; McGibney, P.; Douglas, J.; Henry, T.; Ansul, G.; *American Ind. Hyg. Ass. J.* 1984, 45(10), 697.
- 45 Lord Rayleigh, *Proc. London Math. Soc.* 1885, 17, 4.
- 46 White, R. M.; Voltmer, F. W.; *Appl. Phys. Lett.* 1965, 7, 314.
- 47 Morgan, D.P., *Ultrasonics*, 1973, 121.
- 48 Dieulesaint, E.; *Elastic Waves in Solids*, Applications to Signal Processing; John Wiley: New York, 1980; 334.
- 49 Wohltjen, H.; *Sens. Actuators* 1984, 5, 307.

- 50 Auld, B. A.; *Acoustic Fields and Waves in Solids, Vol. II*; Wiley-Interscience: New York, 1973; Chapter 12.
- 51 Venema, A.; Nieuwkoop, E.; Vellekoop, M. J.; Nieuwenhuizen, M. S.; Barendsz, A. W.; *Sens. Actuators* 1986, 10, 47.
- 52 Dransfeld, K.; Salzmann, E.; *Physical Acoustics Vol VII*, Mason and Thurston eds.; Academic Press: New York, 1970; 219.
- 53 Calabrese, G. S.; Wohltjen, H.; Roy, M.K.; *Anal. Chem.* 1987, 59, 833.
- 54 Snider, D. R.; Fredrickson, H. P.; Scheider, S. C.; *J. Appl. Phys.* 1981, 52.
- 55 Wohltjen, H.; Snow, A.; Ballantine, D.; *Proceedings of the International Conference on Solid State Sensors and Actuators - Transducers '85*, Boston, MA, June 11-14, 1985, 66.
- 56 Goldschmidt, B. M.; Van Duuren, B. L.; Goldstein, R. C.; *J. Heterocyclic Chem.* 1976, 13, 517.
- 57 Cockerill, A. F.; Davies, G. L. O.; Rackham, D. M.; *Tetrahedron Lett.* 1972, 1, 27.
- 58 Morrill, T. C.; Friedrich, L. E.; Machonkin, M. A.; Whitbourne, J. E.; Eastman, C. A.; *J. Heterocyclic Chem.* 1981, 18, 1645.
- 59 Bardos, T. J.; Datta-Gupta, N.; Hebborn, P.; Triggle, D. J.; *J. Med. Chem.* 1965, 8, 167.

- 60 Wohltjen, H.; Snow, A. W.; Barger, W. R.; Ballantine, D. S.; IEEE Transactions of Ultrasonics, Ferroelectrics, and Frequency Control, vol. UFFC-34 1987, 2, 172.
- 61 Tuck, B.; *Introduction to Diffusion in Semiconductors*; Peter Peregrinus Ltd.: Stevenage, England, 1974; 35.
- 62 Brandrup, J.; Immergut, E. H.; *Polymer Handbook*, 3rd ed.; John Wiley and Sons Inc.: New York, 1989; VI435.
- 63 Barendsz, A. W.; Van der Linden-Tak, G.; Z. Anal. Chem. 1975, 274, 207.
- 64 McNair, H. M.; Bonelli, E. J.; *Basic Gas Chromatography*; Varian: Palo Alto, CA, 1969; 32.
- 65 McNair, H. M.; Bonelli, E. J.; *Basic Gas Chromatography*; Varian, Palo Alto, CA, 1969; 44
- 66 Demertzis, P. G.; Kontominas, M. G.; *Inverse Gas Chromatography, Characterization of Polymers and Other Materials*; Lloyd, D. R.; Ward, T.C.; Schreiber, H. P.; eds.; ACS Symposium series 391, American Chemical Society: Washington, DC, 1989, 78.
- 67 Grate, J. W.; Snow, A.; Ballantine, D. S.; Wohltjen, H.; Abraham, M. H.; McGill, R. A.; Sasson, P.; Anal. Chem. 1988, 60, 869.
- 68 Kamlet, M. J.; Doherty, R. M.; Abboud, J.-L. M.; Abraham, M. H.; Taft, R. W.; CHEMTECH 1986, 16, 566.

- 69 Abraham, M. H.; Grellier, P. L.; McGill, R. A.; Doherty, R. M.; Kamlet, M. J.; Hall, T. M.; Taft, R. W.; Carr, P. W.; Koros, W. J.; *Polymer* 1987, 28, 1363.
- 70 Abraham, M. H.; Grellier, P. L.; McGill, R. A.; *J. Chem. Soc., Perkin Trans.* 1987, 2, 797.
- 71 Grate, J. W.; Abraham, M. H.; *Sens. Actuators B*, 3, 85, 1991.
- 72 Espenson, J. H.; *Chemical Kinetics and Reaction Mechanisms*; McGraw-Hill: New York, NY, 1981; 2.
- 73 Witten, B.; Probst, A.; *Anal. Chem.* 1957, 29, 885.
- 74 Rudin, A.; *The Elements of Polymer Science and Engineering*; Academic Press: New York, NY, 1982; 395.
- 75 Snow, A.; Wohltjen, H.; *Anal. Chem.* 1984, 56, 1411.
- 76 Zellers, E. T.; White, R. M.; Rappaport, S. M.; *Anal. Chem.* 1990, 62, 1222.
- 77 Wohltjen, H.; Snow, A. W.; Barger, W. R.; Ballantine, D. S.; *IEEE Trans. Ultrasonics, Ferroelectrics, Freq. Control*, Vol. UFFC-34 1987, 2, 172.
- 78 Morgan, D.P., *Ultrasonics*, May 1973, 121.
- 79 Carey, W. P.; Beebe, K. R.; Kowalski, B. R.; Illman, D. L.; Hirshfeld, T.; *Anal. Chem.* 1986, 58, 149.

- 80 Zellers, E. T.; *Chemical Sensors and Microinstrumentation*, ACS Symposium series 403; American Chemical Society: Washington, DC, 1989; 176.
- 81 Whitbourne, J. E. Eastman, C. A.; US Patent #3,992,154, 1976.
- 82 Hall, Christopher; *Polymer Materials*, Second Edition; John Wiley and Sons: New York, 1989; 127.
- 83 Microsensor Systems, Inc., P.O.Box 8, Springfield, VA 22150, Catalog 102, 13.
- 84 Wohltjen, H. personal communication.
- 85 Wohltjen, H.; Snow, A.; Ballantine, D.; Proceedings of the International Conference on Solid-State Sensors and Actuators - Transducers '85 1985, 66.
- 86 Wohltjen, H.; Snow, A. W.; Barger, W. R.; Ballantine, D. S.; IEEE Transactions on Ultrasonics, Ferroelectrics, and Frequency Control, Vol. UFFC-34 1987, 2, 172.
- 87 Wohltjen, H.; Snow, A. W.; Jarvis, N. L.; *Surface Acoustic Wave Devices as Chemical Vapor Microsensors*, NRL Memorandum Report 5530; Naval Research Laboratory: Washington, DC, 1985; 13.
- 88 Wohltjen, H.; personal communication.
- 89 Cockerill, A. F.; Davies, G. L. O.; Rackham, D. M.; *Tetrahedron Lett.* 1972, 1, 27.

- 90 Matherne, R. N.; Lubs, P. L.; Kerfoot, E. J.; American Ind. Hyg. Ass. J. 1981, 42(9), 681.
- 91 Aeissen, H.; Wöhrle, D.; Makromol. Chem. 1981, 182, 2961.
- 92 Gillis, J. N.; Sievers, R. E.; Pollock, G. E.; Anal. Chem. 1985, 57, 1572.
- 93 Tsuchida, E.; Nishide, H.; Manshi Ohyanagi, M.; Kawakami, H.; Macromolecules 1987, 20, 1907.

APPENDIX A - FORTH SOFTWARE LISTINGS.

200 LIST

```
0 ( DOER AND MAKE FROM LEO BRODIE -- EVENT LINE VAPOR CODE)
1 : NULL ;
2 : DOER ( -- ) CREATE ['] NULL , DOES> @ >R ;
3 : MAKE ( -- ) R> DUP 2+ SWAP @ 2+ ! ;
4 DOER ON    DOER OFF
5
6 : (ON) MAKE ON ;
7 : (OFF) MAKE OFF ;
8 : DISABLES (ON) (OFF) ;
9
10 : (ON) MAKE ON SWAP 64 + SWAP ! DISABLES ;
11 : (OFF) MAKE OFF 0 SWAP ! DISABLES ;
12 : CLOCK CONSTANT DOES> @ (ON) (OFF) ;
13
14 201 207 THRU
15
```

201 LIST

```
0 ( CLOCK DETERMINATIONS AND SET-UPS )  OCTAL
1 2  CONSTANT  TEN.KHZ
2 3  CONSTANT  1KHZ
3 4  CONSTANT  HUNDRED.HZ
4 5  CONSTANT  TEN.HZ
5 6  CONSTANT  1HZ
6 7  CONSTANT  ONE.TENTH.HZ
7 170000 CLOCK A-CLOCK
8 170002 CLOCK B-CLOCK
9 170004 CLOCK EVENT
10 170006 CLOCK A/D-CLOCK
11
12
13 ( HUNDRED.HZ EVENT ON    ( Enable the WATCHDOG timer )
14
15 DECIMAL
```

202 LIST

```
0 ( SAW DEVICE ADDRESSES )
1 OCTAL
2 176770 CONSTANT ADCSR          176772 CONSTANT ADBUF
3 167770 CONSTANT CSR.PARALLEL  167772 CONSTANT PARALLEL.OUT
4 167774 CONSTANT PARALLEL.IN
5 CODE ADC_DONE? BEGIN ADCSR TST B      ( is conversion done? )
6     0 < END S -) ADBUF MOV NEXT      ( leave it on the stack )
7 CODE ADC@ ( # of AtoD -- )
8     0 400 # MOV 1 S )+ MOV      ( determine AtoD to be used )
9     0 1 MUL ADCSR 1 MOV NEXT      ( and set select bits in CSR )
10 : AtoD ADC@ ADC_DONE? ;
11 CODE 0CSR.ON CSR.PARALLEL 1 # BIS NEXT
12 CODE 0CSR.OFF CSR.PARALLEL 1 # BIC NEXT
13 CODE 1CSR.ON CSR.PARALLEL 2 # BIS NEXT
14 CODE 1CSR.OFF CSR.PARALLEL 2 # BIC NEXT
15 DECIMAL
```

203 LIST

```
0 ( TIME AND FREQUENCY BACKGROUND TASK FOR UV IRRADIATION )
1 VARIABLE TIME.ARRAY 1022 ALLOT      TIME.ARRAY 1024 ERASE
2 2VARIABLE FREQUENCY.ARRAY 2044 ALLOT
3     FREQUENCY.ARRAY 2048 ERASE
4 VARIABLE POINTS 0 POINTS !
5 VARIABLE #POINTS 0 #POINTS !
6 VARIABLE DELAY 2 DELAY !
7 : PTS POINTS ? ." Points taken " ;
8 : 2+! DUP @ 2+ SWAP ! ;
9
10
11 ( TURN OFF THE VALVES FOR INJECTION PURPOSES )
12 ( : 1CSR.ON ;      : 1CSR.OFF ;      )
13
14
15
```

204 LIST

```
0 ( PERMEATION TUBE SOFTWARE )
1 VARIABLE INJECT.TIME 0 INJECT.TIME !
2 VARIABLE INJECTION 0 INJECTION !
3 : ?INJECT ( n -- n )
4     INJECTION @ IF DUP 1CSR.ON INJECT.TIME !
5     0 INJECTION ! THEN ;
6 VARIABLE CEASE.TIME 0 CEASE.TIME !
7 VARIABLE CEASE.INJECT 0 CEASE.INJECT !
8 : ?CEASE ( n -- n )
9     CEASE.INJECT @ IF DUP 1CSR.OFF
10    CEASE.TIME ! 0 CEASE.INJECT ! THEN ;
11 : INJECT 1 INJECTION ! ;
12 : CEASE 1 CEASE.INJECT ! ;
13 : RESET.TIME 0 INJECT.TIME ! 0 CEASE.TIME ! ;
14 : SAVE.INJECT TIME.ARRAY 1010 + DUP INJECT.TIME @ SWAP !
15    2+ CEASE.TIME @ SWAP ! ;
```

205 LIST

```
0 ( VECTORED EXECUTION ROUTINE FOR UV IRRADIATION CONTROL )
1 VARIABLE INTERVAL 10 INTERVAL !
2 VARIABLE (?UV.ON) VARIABLE (?UV.OFF)
3 VARIABLE (EXPOSURE)
4 : NO-OP ; ( Dummy definition for no operation )
5
6 ' NO-OP (?UV.ON) !
7 ' NO-OP (?UV.OFF) !
8 ' NO-OP (EXPOSURE) !
9 : ?UV.ON (?UV.ON) @ EXECUTE ;
10 : ?UV.OFF (?UV.OFF) @ EXECUTE ;
11 : EXPOSURE (EXPOSURE) @ EXECUTE ;
12 217 LOAD
13 : MANUAL.EXPOSURE ['] MANUAL (EXPOSURE) ! ;
14 : AUTO.EXPOSURE ['] AUTOMATIC (EXPOSURE) ! ;
15
```

206 LIST

```
0 ( PARALLEL FLUKE FREQUENCY ACQ. AND DOUBLE LENGTH DUMP )
1 : FREQUENCY
2     0.180 DO PARALLEL.IN C@ 15 AND *DIGIT LOOP DROP ;
3 : IS  <##### 46 HOLD #S #> TYPE ." Khz " ;
4
5 VARIABLE TRACKER  0 TRACKER !
6
7 : DDUMP ( address count --- )
8     OVER + SWAP DO TRACKER @ 4 MOD 0= IF CR I . THEN
9         I 2@ 14 D.R TRACKER 1+! 4 +LOOP 0 TRACKER ! ;
10
11 : HZDUMP  FREQUENCY.ARRAY 2048 DDUMP ;
12 : QW  HZDUMP ;
13 : QWE  TIME.ARRAY 1024 DUMP ;
14
15
```

207 LIST

```
0 ( EVENT INTERRUPT SERVICE AND MODE SELECTION)
1 BASE @
2 VARIABLE LTC          0 LTC !
3 A-CLOCK OFF
4 OCTAL
5 ASSEMBLER BEGIN  LTC TST 0= NOT IF
6     R -) 0 MOV  0 LTC MOV 10 0 )) TST 0=
7     IF 10 0 )) DELAY MOV  LTC I) WAKE # MOV
8     THEN 10 0 )) DEC
9     0 R )+ MOV THEN  240 200 INTERRUPT
10 FORTH
11 BASE !
12 : FREQUENCY_ONLY 208 LOAD 209 LOAD ;
13 : FREQUENCY_AND_TEMPERATURE 210 212 THRU ;
14 : SUPERACID 213 LOAD ;
15 FREQUENCY_ONLY MANUAL.EXPOSURE
```


208 LIST

```

0 ( TIME AND FREQUENCY BACKGROUND TASK - BACKGROUND TASK )
1 : VAPOR TASK ; <CONSIGN> VAPOR      OCTAL
2 CODE TASKCLEAR 0 R -) MOV 0 VAPOR MOV 10 0 )) CLR
3   R )+ 0 MOV NEXT          DECIMAL
4 : CLEAR.ARRAYS  #POINTS @ DUP TIME.ARRAY SWAP 2* ERASE
5   FREQUENCY.ARRAY SWAP 2* 2* ERASE 0 POINTS !
6   0 DUP INJECT.TIME ! CEASE.TIME ! ;
7 : ACQUIRE      #POINTS ! CLEAR.ARRAYS 1HZ A-CLOCK ON
8   TASKCLEAR VAPOR ACTIVATE DECIMAL LTC GET
9   #POINTS @ 0 DO STOP POINTS 1+!
10  FREQUENCY FREQUENCY.ARRAY I 4 * + 2!
11  DELAY @ I * EXPOSURE ?UV.ON ?UV.OFF
12  TIME.ARRAY I 2* + !
13  LOOP LTC RELEASE  SAVE.INJECT A-CLOCK OFF  STOP ;
14
15

```

209 LIST

```

0 ( STORE ROUTINE FOR SAVING FREQ. AND TIME DATA -- 3 BLOCKS)
1 : STORE_BLOCK ( address blk# #of.blocks --- last blk stored)
2   2DUP + 1- >R          ( put block# on ret. stack)
3   0 DO 2DUP I +        ( which block? )
4   SWAP I 1024 * +      ( which array add.?)
5   SWAP BLOCK 1024 MOVE ( get block buffer add.)
6   UPDATE LOOP          ( move 512 pts and update blk)
7   2DROP R> ;          ( drop add. and leave last blk)
8 : (DATE) ( block# -- )
9   BLOCK 1000 + DAY 2@ ROT 2! UPDATE ;
10 : SAVER ( array.address block #of.blocks )
11   STORE_BLOCK (DATE) ;
12 : SAVE.DATA ( block # -- )
13   DUP FREQUENCY.ARRAY SWAP 2 SAVER
14   TIME.ARRAY SWAP 2 + 1 SAVER ;
15

```

210 LIST

```

0 ( Temperature calculation for RTD probe on SAW chamber)
1 .141127 2CONSTANT SLOPE
2 -39.47222 2CONSTANT Y_INTERCEPT
3
4 : AD+ 0 AtoD 2560 + ; ( Offset added to prevent neg. numbers)
5
6 : ?TEMP ( AtoD conv. -- temp * 10 in Kelvin )
7     SLOPE ROT 10 M*/ ( scale slope calc )
8     Y_INTERCEPT D+ 1 10000 M*/ ( add offset and scale)
9     D̄ROP ; ( make single prec. number)
10 : CALC_TEMP AD+ ?TEMP ;
11 : TEMP_PRINT 0 <## 46 HOLD #S #> TYPE SPACE ." K " ;
12 : T CALC_TEMP TEMP_PRINT ;
13 VARIABLE TEMPERATURE.ARRAY 1022 ALLOT
14     TEMPERATURE.ARRAY 1024 ERASE
15 : Q TEMPERATURE.ARRAY 1024 DUMP ;

```

211 LIST

```

0 ( TIME, TEMPERATURE AND FREQUENCY BACKGROUND TASK )
1 : DUAL TASK ; <CONSIGN> DUAL OCTAL
2 CODE TASKCLEAR 0 R -) MOV 0 DUAL MOV 10 0 )) CLR
3     R )+ 0 MOV NEXT DECIMAL
4 : CLEAR.ARRAYS #POINTS @ DUP DUP TIME.ARRAY SWAP 2* ERASE
5     FREQUENCY.ARRAY SWAP 2* 2* ERASE
6     TEMPERATURE.ARRAY SWAP 2* ERASE 0 POINTS !
7     0 DUP INJECT.TIME ! CEASE.TIME ! ;
8 : ACQUIRE #POINTS ! CLEAR.ARRAYS 1HZ A-CLOCK ON
9     TASKCLEAR DUAL ACTIVATE DECIMAL LTC GET
10    #POINTS @ 0 DO STOP POINTS 1+!
11    FREQUENCY FREQUENCY.ARRAY I 4 * + 2!
12    CALC_TEMP TEMPERATURE.ARRAY I 2* + !
13    DELAY @ I * EXPOSURE ?UV.ON ?UV.OFF
14    TIME.ARRAY I 2* + !
15    LOOP LTC RELEASE SAVE.INJECT A-CLOCK OFF STOP ;

```

212 LIST

```
0 ( STORE ROUTINE FOR FREQ., TIME AND TEMP. RUN -- 4 BLOCKS)
1 : STORE_BLOCK ( address blk# #of.blocks --- last blk stored)
2     2DUP + 1- >R      ( put block# on ret. stack)
3     0 DO 2DUP I +    ( which block? )
4     SWAP I 1024 * +  ( which array add.?)
5     SWAP BLOCK 1024 MOVE ( get block buffer add.)
6     UPDATE LOOP      ( move 512 pts and update blk)
7     2DROP R> ;      ( drop add. and leave last blk)
8 : (DATE) ( block# -- )
9     BLOCK 1000 + DAY 2@ ROT 2! UPDATE ;
10 : SAVER ( array.address block #of.blocks )
11     STORE_BLOCK (DATE) ;
12 : SAVE.DATA ( block # -- )
13     DUP DUP FREQUENCY.ARRAY SWAP 2 SAVER
14     TIME.ARRAY SWAP 2 + 1 SAVER
15     TEMPERATURE.ARRAY SWAP 3 + 1 SAVER ;
```

213 LIST

```
0 ( PERMEATION TUBE SOFTWARE SAVING UV IRRADIATION TIMES)
1 VARIABLE UV.ON.TIME 0 UV.ON.TIME !
2 VARIABLE UV?ON 0 UV?ON !
3 VARIABLE UV.OFF.TIME 0 UV.OFF.TIME !
4 VARIABLE UV?OFF 0 UV?OFF !
5
6 : UVON 1 UV?ON ! ;
7 : UVOFF 1 UV?OFF ! ;
8 : SAVE.UV TIME.ARRAY 1014 + DUP UV.ON.TIME @ SWAP !
9     2+ UV.OFF.TIME @ SWAP ! ;
10 : RESET.UV 0 UV.ON.TIME ! 0 UV.OFF.TIME ! SAVE.UV ;
11 : SAVE.DATA SAVE.UV SAVE.DATA ;
12 : ACQUIRE RESET.UV ACQUIRE ;
13 : REMOTE.LAMP 215 LOAD ;
14 : OPERATOR.LAMP 214 LOAD ;
15 REMOTE.LAMP
```

214 LIST

```
0 ( UV irradiation by operator control)
1
2 : LAMP.ON  UV?ON @ IF DUP 0CSR.ON
3           UV.ON.TIME ! 0 UV?ON ! THEN ;
4
5 : LAMP.OFF UV?OFF @ IF DUP 0CSR.OFF
6           UV.OFF.TIME ! 0 UV?OFF ! THEN ;
7
8 ' LAMP.ON (?UV.ON) !
9 ' LAMP.OFF (?UV.OFF) !
10
11
12
13
14
15
```

215 LIST

```
0 ( UV irradiation by preset times)
1 VARIABLE START.IRRADIATION 30 START.IRRADIATION !
2 VARIABLE STOP.IRRADIATION 50 STOP.IRRADIATION !
3 : LAMP UVON UVOFF ;
4
5 : LAMP.ON
6     UV?ON @ IF
7         DUP START.IRRADIATION @ < NOT IF 0 UV?ON !
8         0CSR.ON DUP UV.ON.TIME ! THEN THEN ;
9
10 : LAMP.OFF
11     UV?OFF @ IF
12         DUP STOP.IRRADIATION @ < NOT IF 0 UV?OFF !
13         0CSR.OFF DUP UV.OFF.TIME ! THEN THEN ;
14 ' LAMP.ON (?UV.ON) !
15 ' LAMP.OFF (?UV.OFF) !
```

216 LIST

```
0 ( TEST BLOCK FOR SAVER SOFTWARE )
1 : STORE_BLOCK ( address blk# #of.blocks --- last blk stored)
2     2DUP + 1- >R      ( put block# on ret. stack)
3     0 DO 2DUP I +     ( which block? )
4     SWAP I 1024 * +   ( which array add.?)
5     SWAP BLOCK 1024 MOVE ( get block buffer add.)
6     UPDATE LOOP      ( move 512 pts and update blk)
7     2DROP R> ;      ( drop add. and leave last blk)
8 : (DATE) ( block# -- )
9     BLOCK 1000 + DAY 2@ ROT 2! UPDATE ;
10 : SAVER ( array.address block #of.blocks )
11     STORE_BLOCK (DATE) ;
12 : SAVE.DATA ( block # -- )
13     DUP FREQUENCY.ARRAY SWAP 2 SAVER
14     TIME.ARRAY SWAP 2 + 1 SAVER ;
15
```

217 LIST

```
0 ( VECTORED EXECUTION FOR PERM. TUBE INJECTION ROUTINES )
1
2 : MANUAL ?INJECT ?CEASE ;
3
4 : ?AUTO.INJECT ( n - n )
5     INJECTION @ IF DUP DUP INJECT.TIME ! INTERVAL @ +
6     CEASE.TIME ! 1CSR.ON 0 INJECTION !
7     1 CEASE.INJECT ! THEN ;
8
9 : ?AUTO.CEASE ( n - n )
10    CEASE.INJECT @ IF DUP CEASE.TIME @ < NOT IF
11    1CSR.OFF 0 CEASE.INJECT ! DUP CEASE.TIME !
12    THEN THEN ;
13
14 : AUTOMATIC ?AUTO.INJECT ?AUTO.CEASE ;
15
```

APPENDIX B - REVERSIBLE DETECTOR USING COBALT SCHIFF BASE COMPLEXES.

Investigations of reversible systems that rely on more than simple solubility parameters remains a worthwhile pursuit. In this laboratory the development of a film selective to oxygen has been pursued. The investigation involves the incorporation of a cobalt-schiff base complex in a polymer matrix, first as a simple mixture and later as an incorporation of the cobalt-schiff base complex into the backbone of the polymer⁹¹. The deposition of the polymer upon the reference device will be used for the common mode rejection of reversible polymer solvation by vapors other than oxygen. This investigation holds promise due to the development of a cobalt-schiff base complex as the active site in the chromatographic stationary phase developed for the separation of oxygen in a gas mixture⁹² and the enhanced permeability of oxygen over nitrogen in polymer films incorporating a cobalt-schiff base complex⁹³. The equilibrium constants as measured in solution for some of these complexes indicated that the partial pressure of oxygen needed to create an appreciable amount of oxygenated complex is in the region of 20% oxygen in nitrogen. While it is not rigorously correct to extrapolate solution conditions to solid-vapor interactions, the use of this information would indicate that this film would probably have use in the personnel monitoring range, 15% to 22% oxygen in nitrogen.

Since the equilibrium constant will determine the extent of mass loading for this system, the expected response of a SAW device with this reversible heterogeneous system should be discussed.

Using the fundamental SAW device mass loading equation,

$$\Delta f_{\text{base}} = (k_1 + k_2)f_{\text{O}}^2 h p$$

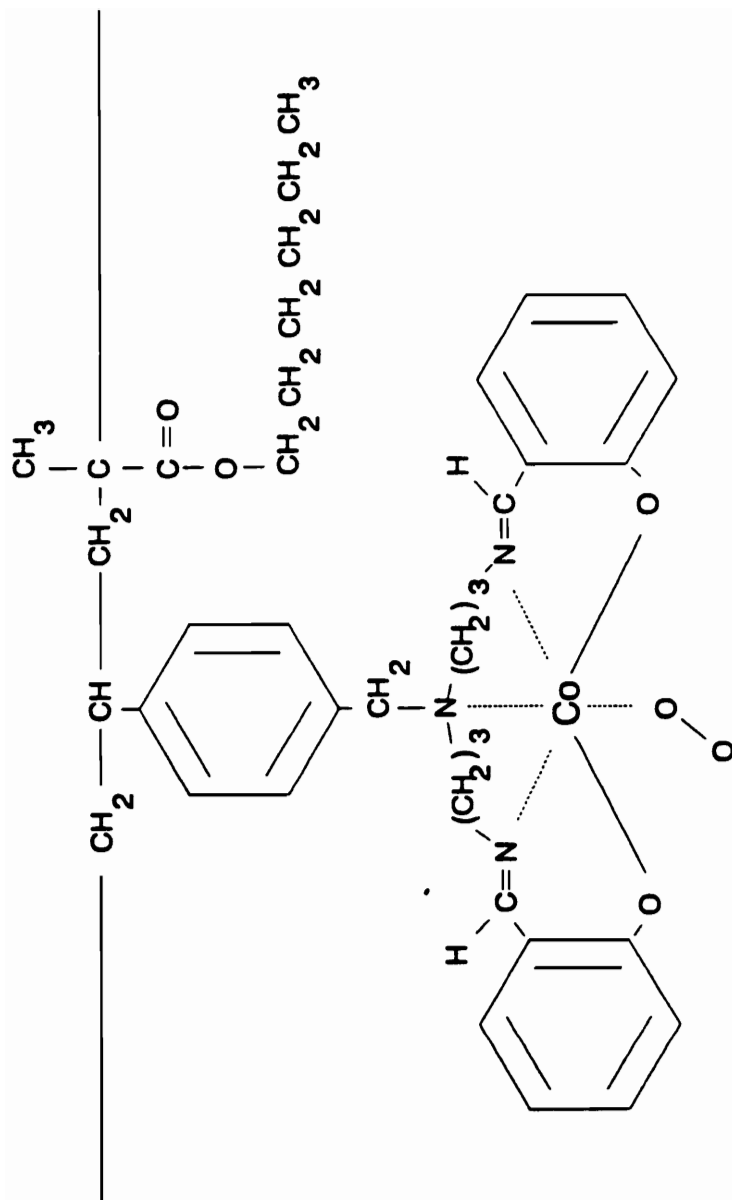


Figure 103. Copolymer of p-chloromethylstyrene and n-hexyl methacrylate incorporating oxygenated Co(salDPT).

a film deposited upon the surface of a device will generate a frequency shift of Δf_{base} Hz for a mass per unit area of $h_p \text{ g/cm}^2$.

As developed earlier, the ratio of the molecular weights of the resulting product with that of the trapping agent in the film will determine the frequency shift that results from exposure of the film to the vapor to be monitored. An specific example describing a possible oxygen sensor system should help to clarify this point.

A copolymer composed of a 20 mole % p-chloromethylstyrene in n-hexyl methacrylate will undergo an amine alkylation of bis(salicylaldehyde)dipropylenetriamine with later reaction of Co(II)-acetateH₂O to produce the Cobalt Schiff-base (Co(salDPT)) bound complex (Figure 103). The overall molecular weight for one reactive unit, defined as the molecular structure that will react with one mole of oxygen, is:

- four monomer units of n-hexyl methacrylate (4 * 170 AMU)
- one monomer unit of p-chloromethylstyrene (117 AMU)
- one monomer unit of Co(salDPT) (395 AMU)

1192 AMU. Since oxygen has a molecular weight of 32 AMU's, the molecular weight of the oxygenated reactive unit will be 1224 AMU, resulting in a 2.68 percent increase in the weight of the film.

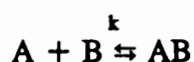
Since the frequency shift of a SAW device is linearly dependent with mass, this would increase the frequency by only 0.0268hp from that of the coated but unexposed device. The basis SAW device mass loading equation can now be modified to show the maximum frequency shift of the device upon exposure to oxygen:

$$\Delta f_{\text{oxy}} = (k_1 + k_2)f_o^2 h_p (MW_{\text{complex}} / MW_{\text{free}})$$

This assumes that all of the reactive sites undergo an irreversible reaction with oxygen. This is not the case. Since the reaction is reversible, the equilibrium constant

for the reaction will determine the amount of cobalt Schiff-base converted into the oxygenated form.

If the reaction proceeds as follows:



the equilibrium constant for the reaction is:

$$k = \frac{[AB]}{[A][B]}$$

or

$$k[B] = \frac{[AB]}{[A]} = \frac{Y}{1-Y}$$

The equilibrium constant needs to be converted from a ratio of [AB] to [A] to the amount of conversion of [A] to [AB]. The reason for this is that the increase in the mass of the film will be determined by the amount of [A] that is converted to [AB]. The amount of conversion is expressed as follows:

$$\text{conversion} = Y = \frac{[AB]}{[A] + [AB]}$$

Rearrangement of the equilibrium constant equation yields:

$$k[B] = \frac{[AB]}{[A]} = \frac{Y}{1-Y}$$

$$\frac{1}{k[B]} = \frac{1-Y}{Y}$$

$$\frac{1}{k[B]} = \frac{1}{Y} - 1$$

$$\frac{1}{Y} = \frac{1}{k[B]} + 1$$

$$\frac{1}{Y} = \frac{k[B] + 1}{k[B]}$$

$$Y = \frac{k[B]}{k[B] + 1}$$

$$Y = \frac{[AB]/[A]}{1 + [AB]/[A]}$$

$$Y = \frac{[AB]}{[A] + [AB]}$$

Using this information, the equation can now be constructed that can be used to determine the maximum shift in frequency for an equilibrium driven reversible reaction:

$$\Delta f_{\text{oxy}} = (k_1 + k_2)f_o^2 \text{hp}(MW_{\text{complex}}/ MW_{\text{free}}) \frac{(k[B])}{(k[B] + 1)}$$

Since the signal to be measured is the difference between the film unexposed to oxygen and the film exposed to oxygen, this signal is:

$$\Delta f_{\text{diff}} = \Delta f_{\text{oxy}} - \Delta f_{\text{base}}$$

$$\Delta f_{\text{diff}} = \{(MW_{\text{complex}}/ MW_{\text{free}})(k[B]/(k[B]+1)) - 1\} \Delta f_{\text{base}}$$

There are two important factors that can be discerned from an analysis of this equation.

The ratio of the molecular weights of the complexed species with that of the free species will affect the size of the signal that can be measured. If the species being detected contributes very little to the mass of the complex created, then the signal frequency range capabilities of the SAW will be limited due to the fact that the net change in weight of the film is very small. From the oxygen sensor example, the

maximum weight percent change that can occur do to oxygenation of the cobalt Schiff base is 2.68 percent. If the film deposited generates a 40 KHz shift film, the maximum shift will only be 1072 Hz if every site is complexed.

The maximum mass change is unattainable in an analytical mode because the amount of conversion of the free species to the complexed species is based upon the concentration of the vapor being monitored and the equilibrium constant for the reaction. If k is large, then $[B]$ can be small to yield a sufficient conversion. If k is small, then $[B]$ must be large in order to get sufficient conversion of the free to the complexed species. Therefore the equilibrium constant will determine if the film will be useful as a part per million or percent detector.

Finally one item that the equation does not address is the time it takes for the system to reach equilibrium. This will be dependent upon the permeability of the vapor in the polymer. The incorporation of n-hexyl methacrylate into the polymer backbone was a technique used by Nishide to increase the permeability of oxygen through a film containing a cobalt Schiff-base complex. As demonstrated in the phosgene studies using polystyrene, a polymer which is impermeable or slightly permeable to the vapor will affect the rate at which the vapor will react with the active agent in the film. The choice of the wrong polymer could prevent this system from ever reaching equilibrium.

VITA

Glen Wollenberg was born on August 7, 1955 in Buffalo, New York. He attended Canisius College and received his B.S. degree in Chemistry in 1977. After graduation, he worked for Union Carbide Corporation - Linde Division for four years, first as a chemist in Tonawanda, New York. then as a Technical Representative for Specialty Gases in Cleveland, Ohio. In August, 1981 he entered Virginia Polytechnic Institute and State University and began his graduate studies with Dr. R. E. Dessy. In January, 1992, he accepted a job offer as a senior research chemist with Merck, Sharpe and Dohme Research Laboratories in West Point, Pennsylvania.

Glen Wollenberg was married to Kelly Sanderson on May 23, 1987. They now have a son named Andrew who was born on Thanksgiving Day, November 28, 1991.